Practical Rock Engineering

Evert Hoek

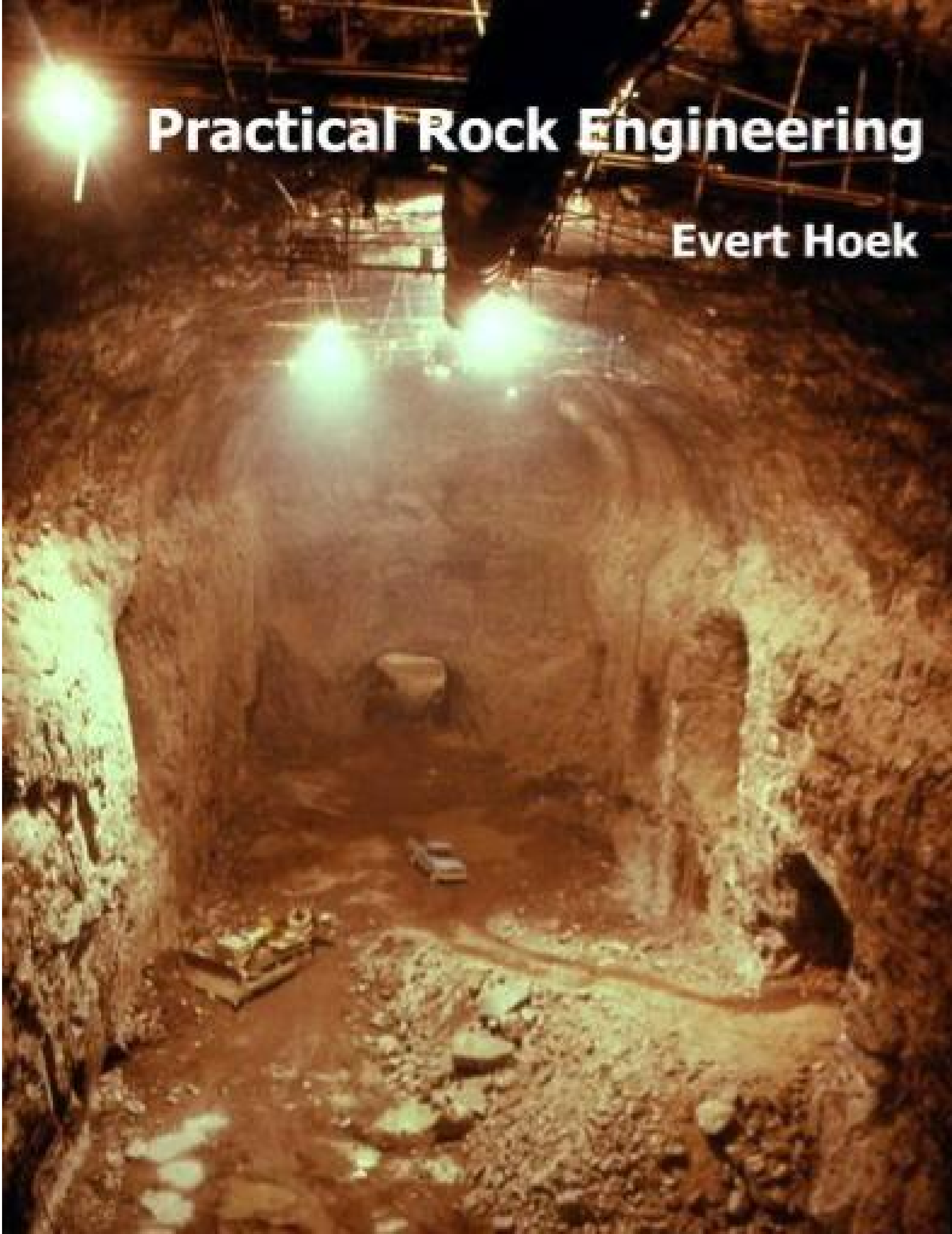

Preface

These notes were originally prepared during the period 1987 to 1993 for undergraduate and graduate courses in rock engineering at the University of Toronto. While some revisions were made in 2000 these were difficult because the notes had been formatted as a book with sequential chapter and page numbering. Any changes required reformatting the entire set of notes and this made it impractical to carry out regular updates.

In 2006 it was decided that a major revision was required in order to incorporate significant developments in rock engineering during the 20 years since the notes were originally written. The existing document was broken into a series of completely self-contained chapters, each with its own page numbering and references. This means that individual chapters can be updated at any time and that new chapters can be inserted as required.

The notes are intended to provide an insight into practical rock engineering to students, geotechnical engineers and engineering geologists. Case histories are used, wherever possible, to illustrate the methods currently used by practicing engineers. No attempt has been made to include recent research findings which have not yet found their way into everyday practical application. These research findings are adequately covered in conference proceedings, journals and on the Internet.

It is emphasised that these are notes are not a formal text. They have not been and will not be published in their present form and the contents will be revised from time to time to meet the needs of particular audiences.

Readers are encouraged to send their comments, corrections, criticisms and suggestions to me at the address given below. These contributions will help me to improve the notes for the future.

Dr Evert Hoek
Evert Hoek Consulting Engineer Inc.
3034 Edgemont Boulevard
P.O. Box 75516
North Vancouver, B.C.
Canada V7R 4X1

Email: ehoek@mailas.com

Evert Hoek

Evert Hoek was born in Zimbabwe and graduated in mechanical engineering from the University of Cape Town with a B.Sc in 1955 and an M.Sc in 1958.

He became involved in rock mechanics in 1958 when he joined the South African Council for Scientific and Industrial Research and worked on problems of rock fracture in very deep level gold mines. He was awarded a Ph.D in 1965 by the University of Cape Town for his research on brittle rock failure.

In 1966 he was appointed Reader and, in 1970, Professor of Rock Mechanics at the Imperial College of Science and Technology in London. He was responsible for establishing an inter-departmental group for teaching and research in rock mechanics. He ran two major research projects, sponsored by a number of international mining companies, that provided practical training for graduate students. These research projects also resulted in the publication of *Rock Slope Engineering* (with J.W. Bray) in 1974 and *Underground Excavations in Rock* (with E.T. Brown) in 1980. These books have been translated into several languages and are still used as text books in a number of university programs.

In 1975 he moved to Vancouver in Canada as a Principal of Golder Associates, an international geotechnical consulting organization. During his 12 years with this company he worked as a consultant on major civil and mining projects in over 20 countries around the world.

In 1987 he returned to academia as NSERC Industrial Research Professor of Rock Engineering in the Department of Civil Engineering in the University of Toronto. Here he was involved in another industry sponsored research project which resulted in the publication of a book entitled *Support of Underground Excavations in Hard Rock* (with P.K. Kaiser and W.F. Bawden) in 1995. During this time he continued to work on consulting boards and panels of experts on a number of international projects.

In 1993 he returned to Vancouver to devote his full time to consulting as an independent specialist, working exclusively on consulting and review boards and panels of experts on civil and mining projects around the world. He has maintained his research interests and continues to write papers with friends and colleagues associated with these consulting projects.

His contributions to rock engineering have been recognized by the award of an honorary D.Sc in Engineering by the University of Waterloo in 1994 and an honorary D.Eng in Engineering by the University of Toronto in 2004 and by his election as a Fellow of the Royal Academy of Engineering (UK) in 1982, a Fellow of the Canadian

Academy of Engineering in 2001 and as a Foreign Associate of the US National Academy of Engineering in 2006.

He has also received many awards and presented several named lectures including the Consolidated Goldfields Gold Medal, UK (1970), the AIME Rock Mechanics Award, US (1975), the E. Burwell Award from the Geological Society of America (1979), the Sir Julius Werhner Memorial Lecture, UK (1982), the Rankine Lecture, British Geotechnical Society (1983), the Gold Medal of the Institution of Mining and Metallurgy, UK (1985), the Müller Award, International Society of Rock Mechanics (1991), the William Smith Medal, Geological Society, UK (1993), the Glossop Lecture, Geological Society, UK (1998), the Terzaghi Lecturer, American Society of Civil Engineers (2000).

The development of rock engineering

Introduction

We tend to think of rock engineering as a modern discipline and yet, as early as 1773, Coulomb included results of tests on rocks from Bordeaux in a paper read before the French Academy in Paris (Coulomb, 1776, Heyman, 1972). French engineers started construction of the Panama Canal in 1884 and this task was taken over by the US Army Corps of Engineers in 1908. In the half century between 1910 and 1964, 60 slides were recorded in cuts along the canal and, although these slides were not analysed in rock mechanics terms, recent work by the US Corps of Engineers (Lutton et al, 1979) shows that these slides were predominantly controlled by structural discontinuities and that modern rock mechanics concepts are fully applicable to the analysis of these failures. In discussing the Panama Canal slides in his Presidential Address to the first international conference on Soil Mechanics and Foundation Engineering in 1936, Karl Terzaghi (Terzaghi, 1936, Terzaghi and Voight, 1979) said 'The catastrophic descent of the slopes of the deepest cut of the Panama Canal issued a warning that we were overstepping the limits of our ability to predict the consequences of our actions ....'.

In 1920 Josef Stini started teaching 'Technical Geology' at the Vienna Technical University and before he died in 1958 he had published 333 papers and books (Müller, 1979). He founded the journal Geologie und Bauwesen, the forerunner of today's journal *Rock Mechanics*, and was probably the first to emphasise the importance of structural discontinuities on the engineering behaviour of rock masses.

Other notable scientists and engineers from a variety of disciplines did some interesting work on rock behaviour during the early part of this century. von Karman (1911), King (1912), Griggs (1936), Ide (1936), and Terzaghi (1945) all worked on the failure of rock materials. In 1921 Griffith proposed his theory of brittle material failure and, in 1931 Bucky started using a centrifuge to study the failure of mine models under simulated gravity loading.

None of these persons would have classified themselves as rock engineers or rock mechanics engineers - the title had not been invented at that time - but all of them made significant contributions to the fundamental basis of the subject as we know it today. I have made no attempt to provide an exhaustive list of papers related to rock mechanics which were published before 1960 but the references given above will show that important developments in the subject were taking place well before that date.

The early 1960s were very important in the general development of rock engineering world-wide because a number of catastrophic failures occurred which clearly demonstrated that, in rock as well as in soil, 'we were over-stepping the limits of our ability to predict the consequences of our actions' (Terzaghi and Voight, 1979).

In December 1959 the foundation of the Malpasset concrete arch dam in France failed and the resulting flood killed about 450 people (Figure 1). In October 1963 about 2500 people in the Italian town of Longarone were killed as a result of a landslide generated wave which overtopped the Vajont dam (Figure 2). These two disasters had a major impact on rock mechanics in civil engineering and a large number of papers were written on the possible causes of the failures (Jaeger, 1972).

Figure 1: Remains of the Malpasset Dam as seen today. Photograph by Mark Diederichs, 2003.

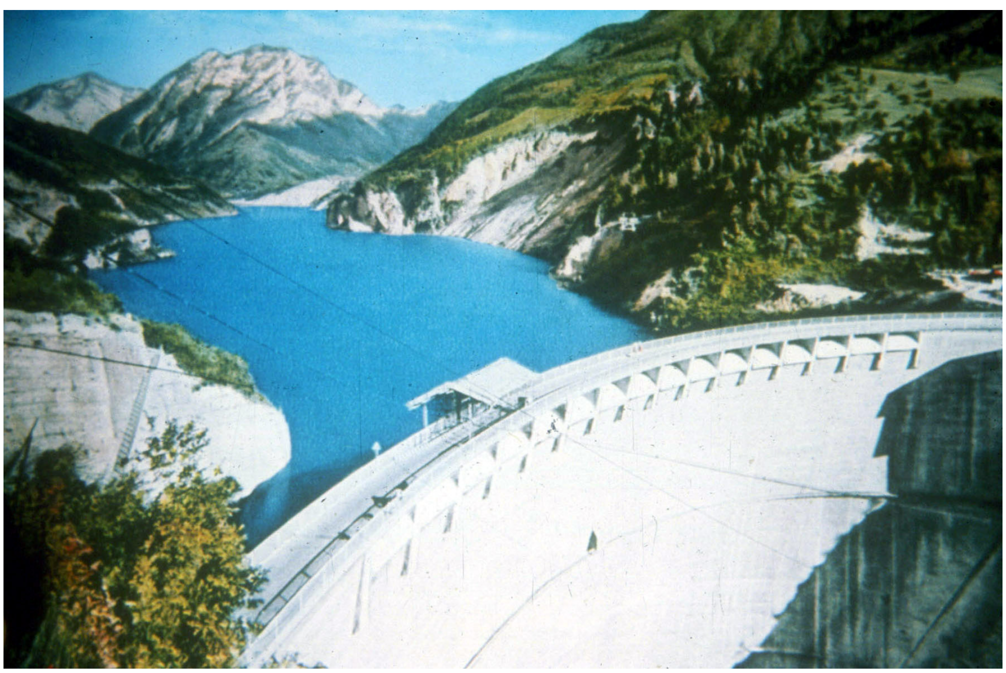

Figure 2a: The Vajont dam during impounding of the reservoir. In the middle distance, in the centre of the picture, is Mount Toc with the unstable slope visible as a white scar on the mountain side above the waterline.

Figure 2b: During the filling of the Vajont reservoir the toe of the slope on Mount Toc was submerged and this precipitated a slide. The mound of debris from the slide is visible in the central part of the photograph. The very rapid descent of the slide material displaced the water in the reservoir causing a 100 m high wave to overtop the dam wall. The dam itself, visible in the foreground, was largely undamaged.

Figure 2c: The town of Longarone, located downstream of the Vajont dam, before the Mount Toc failure in October 1963.

Figure 2d: The remains of the town of Longarone after the flood caused by the overtopping of the Vajont dam as a result of the Mount Toc failure. More than 2000 persons were killed in this flood.

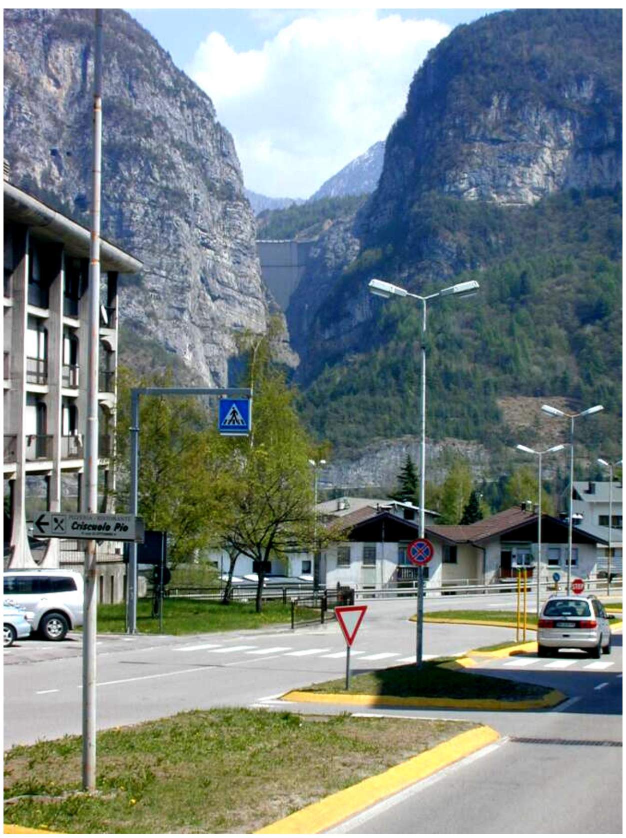

Figure 2e: The remains of the Vajont dam perched above the present town of Longarone. Photograph by Mark Diederichs, 2003.

In 1960 a coal mine at Coalbrook in South Africa collapsed with the loss of 432 lives. This event was responsible for the initiation of an intensive research programme which resulted in major advances in the methods used for designing coal pillars (Salamon and Munro, 1967).

The formal development of rock engineering or rock mechanics, as it was originally known, as an engineering discipline in its own right dates from this period in the early 1960s and I will attempt to review these developments in the following chapters of these notes. I consider myself extremely fortunate to have been intimately involved in the subject since 1958. I have also been fortunate to have been in positions which required extensive travel and which have brought me into personal contact with most of the persons with whom the development of modern rock engineering is associated.

Rockbursts and elastic theory

Rockbursts are explosive failures of rock which occur when very high stress concentrations are induced around underground openings. The problem is particularly acute in deep level mining in hard brittle rock. Figure 3 shows the damage resulting from a rockburst in an underground mine. The deep level gold mines in the Witwatersrand area in South Africa, the Kolar gold mines in India, the nickel mines centred on Sudbury in Canada, the mines in the Coeur d'Alene area in Idaho in the USA and the gold mines in the Kalgoorlie area in Australia, are amongst the mines which have suffered from rockburst problems.

Figure 3: The results of a rockburst in an underground mine in brittle rock subjected to very high stresses.

As early as 1935 the deep level nickel mines near Sudbury were experiencing rockburst problems and a report on these problems was prepared by Morrison in 1942. Morrison also worked on rockburst problems in the Kolar gold fields in India and describes some of these problems in his book, A Philosophy of Ground Control (1976).

Early work on rockbursts in South African gold mines was reported by Gane et al (1946) and a summary of rockburst research up to 1966 was presented by Cook et al (1966). Work on the seismic location of rockbursts by Cook (1963) resulted in a significant improvement of our understanding of the mechanics of rockbursting and laid the foundations for the microseismic monitoring systems which are now common in mines with rockburst problems.

A characteristic of almost all rockbursts is that they occur in highly stressed, brittle rock. Consequently, the analysis of stresses induced around underground mining excavations, a key in the generation of rockbursts, can be dealt with by means of the theory of elasticity. Much of the early work in rock mechanics applied to mining was focused on the problem of rockbursts and this work is dominated by theoretical solutions which assume isotropic elastic rock and which make no provision for the role of structural discontinuities. In the first edition of Jaeger and Cook's book, Fundamentals of Rock Mechanics (1969), mention of structural discontinuities occurs on about a dozen of the 500 pages of the book. This comment does not imply criticism of this outstanding book but it illustrates the dominance of elastic theory in the approach to rock mechanics associated with deep-level mining problems. Books by Coates (1966) and by Obert and Duvall (1967) reflect the same emphasis on elastic theory.

This emphasis on the use of elastic theory for the study of rock mechanics problems was particularly strong in the English speaking world and it had both advantages and disadvantages. The disadvantage was that it ignored the critical role of structural features. The advantage was that the tremendous concentration of effort on this approach resulted in advances which may not have occurred if the approach had been more general.

Many mines and large civil engineering projects have benefited from this early work in the application of elastic theory and most of the modern underground excavation design methods have their origins in this work.

Discontinuous rock masses

Stini was one of the pioneers of rock mechanics in Europe and he emphasised the importance of structural discontinuities in controlling the behaviour of rock masses (Müller, 1979). Stini was involved in a wide range of near-surface civil engineering works and it is not surprising that his emphasis was on the role of discontinuities since this was obviously the dominant problem in all his work. Similarly, the text book by Talobre (1957), reflecting the French approach to rock mechanics, recognised the role of structure to a much greater extent than did the texts of Jaeger and Cook, Coates and Obert and Duvall.

A major impetus was given to this work by the Malpasset dam failure and the Vajont disaster mentioned earlier. The outstanding work by Londe and his co-workers in France (Londe, 1965, Londe et al, 1969, 1970) and by Wittke (1965) and John (1968) in Germany laid the foundation for the three-dimensional structural analyses which we have available today. Figure 4 shows a wedge failure controlled by two intersecting structural features in the bench of an open pit mine.

Figure 4: A wedge failure controlled by intersecting structural features in the rock mass forming the bench of an open pit mine.

Rock Engineering

Civil and mining engineers have been building structures on or in rock for centuries (Figure 5) and the principles of rock engineering have been understood for a long time. Rock mechanics is merely a formal expression of some of these principles and it is only during the past few decades that the theory and practice in this subject have come together in the discipline which we know today as rock engineering. A particularly important event in the development of the subject was the merging of elastic theory, which dominated the English language literature on the subject, with the discontinuum approach of the Europeans. The gradual recognition that rock could act both as an elastic material and a discontinuous mass resulted in a much more mature approach to the subject than had previously been the case. At the same time, the subject borrowed techniques for dealing with soft rocks and clays from soil mechanics and recognised the importance of viscoelastic and rheological behaviour in materials such as salt and potash.

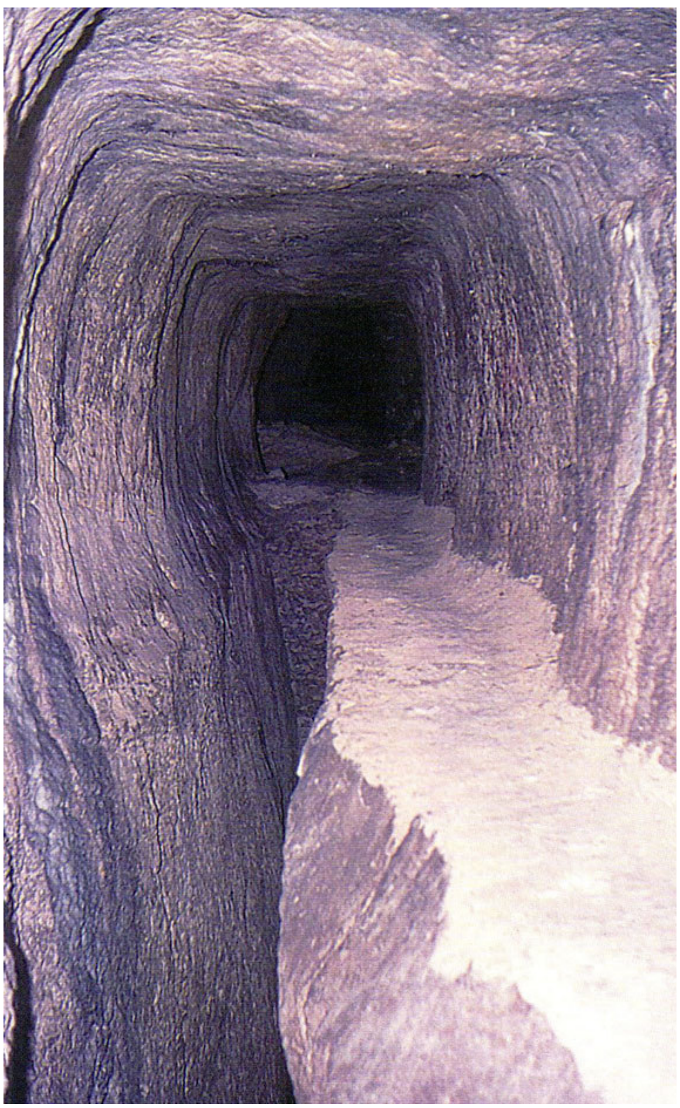

Figure 5: The 1036 m long Eupalinos water supply tunnel was built in 530 BC on the Greek island of Samos. This is the first known tunnel to have been built from two portals and the two drives met with a very small error.

The photograph was provided by Professor Paul Marinos of the National Technical University of Athens.

I should point out that significant work on rock mechanics was being carried out in countries such as Russia, Japan and China during the 25 years covered by this review but, due to language differences, this work was almost unknown in the English language and European rock mechanics centres and almost none of it was incorporated into the literature produced by these centres.

Geological data collection

The corner-stone of any practical rock mechanics analysis is the geological model and the geological data base upon which the definition of rock types, structural discontinuities and material properties is based. Even the most sophisticated analysis can become a meaningless exercise if the geological model upon which it is based is inadequate or inaccurate.

Methods for the collection of geological data have not changed a great deal over the past 25 years and there is still no acceptable substitute for the field mapping and core logging. There have been some advances in the equipment used for such logging and a typical example is the electronic compass illustrated in Figure 6. The emergence of geological engineering or engineering geology as recognised university degree courses has been an important step in the development of rock engineering. These courses train geologists to be specialists in the recognition and interpretation of geological information which is significant in engineering design. These geological engineers, following in the tradition started by Stini in the 1920s, play an increasingly important role in modern rock engineering.

Figure 6: A Clar electronic geological compass manufactured by F.W. Breihapt in Germany.

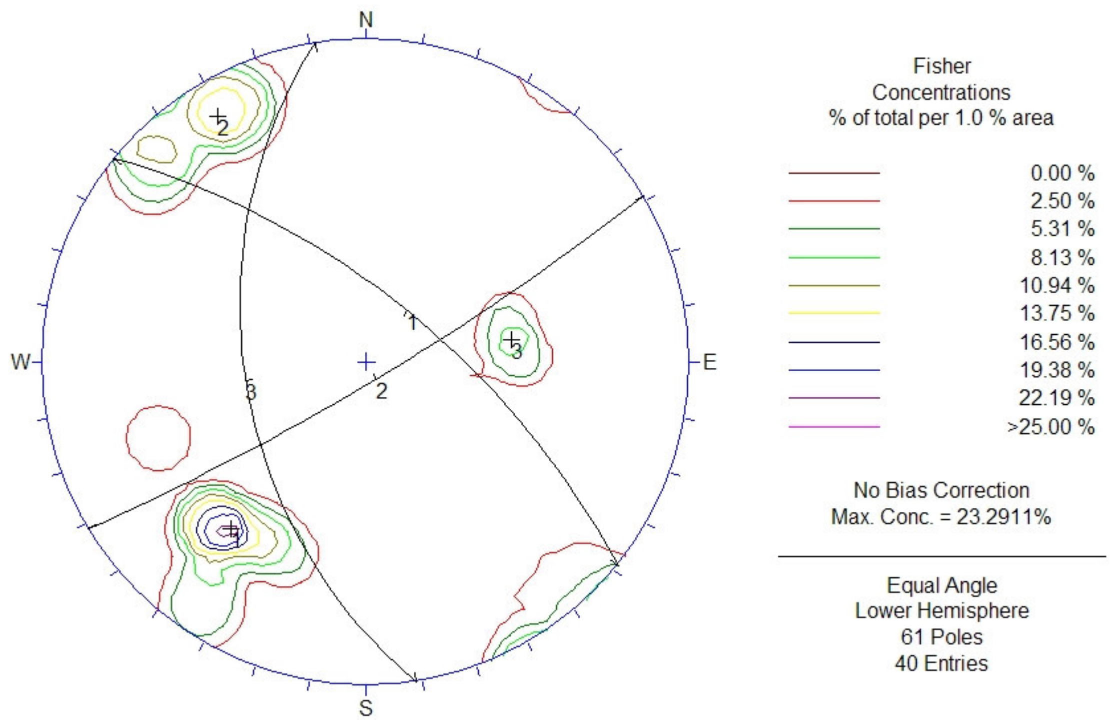

Figure 7: Plot of structural features using the program DIPS.

Once the geological data have been collected, computer processing of this data can be of considerable assistance in plotting the information and in the interpretation of statistically significant trends. Figure 7 illustrates a plot of contoured pole concentrations and corresponding great circles produced by the program DIPS developed at the University of Toronto and now available from Rocscience Inc.

Surface and down-hole geophysical tools and devices such as borehole cameras have been available for several years and their reliability and usefulness has gradually improved as electronic components and manufacturing techniques have advanced. However, current capital and operating costs of these tools are high and these factors, together with uncertainties associated with the interpretation of the information obtained from them, have tended to restrict their use in rock engineering. It is probable that the use of these tools will become more widespread in years to come as further developments occur.

Laboratory testing of rock

There has always been a tendency to equate rock mechanics with laboratory testing of rock specimens and hence laboratory testing has played a disproportionately large role in the subject. This does not imply that laboratory testing is not important but I would suggest that only about 10 percent of a well balanced rock mechanics program should be allocated to laboratory testing.

Laboratory testing techniques have been borrowed from civil and mechanical engineering and have remained largely unaltered for the past 25 years. An exception has been the development of servo-controlled stiff testing machines which permit the determination of the complete stress-strain curve for rocks. This information is important in the design of underground excavations since the properties of the failed rock surrounding the excavations have a significant influence upon the stability of the excavations.

Rock mass classification

A major deficiency of laboratory testing of rock specimens is that the specimens are limited in size and therefore represent a very small and highly selective sample of the rock mass from which they were removed. In a typical engineering project, the samples tested in the laboratory represent only a very small fraction of one percent of the volume of the rock mass. In addition, since only those specimens which survive the collection and preparation process are tested, the results of these tests represent a highly biased sample. How then can these results be used to estimate the properties of the in situ rock mass?

In an attempt to provide guidance on the properties of rock masses a number of rock mass classification systems have been developed. In Japan, for example, there are 7 rock mass classification systems, each one developed to meet a particular set of needs.

Probably the most widely known classifications, at least in the English speaking world, are the RMR system of Bieniawski (1973, 1974) and the Q system of Barton, Lien and Lunde (1974). The classifications include information on the strength of the intact rock material, the spacing, number and surface properties of the structural discontinuities as well as allowances for the influence of subsurface groundwater, in situ stresses and the orientation and inclination of dominant discontinuities. These classifications were developed primarily for the estimation of the support requirements in tunnels but their use has been expanded to cover many other fields.

Provided that they are used within the limits within which they were developed, as discussed by Palmstrom and Broch (2006), these rock mass classification systems can be very useful practical engineering tools, not only because they provide a starting point for the design of tunnel support but also because they force users to examine the properties of the rock mass in a very systematic manner.

Rock mass strength

One of the major problems confronting designers of engineering structures in rock is that of estimating the strength of the rock mass. This rock mass is usually made up of an interlocking matrix of discrete blocks. These blocks may have been weathered or altered to varying degrees and the contact surfaces between the blocks may vary from clean and fresh to clay covered and slickensided.

Determination of the strength of an in situ rock mass by laboratory type testing is generally not practical. Hence this strength must be estimated from geological observations and from test results on individual rock pieces or rock surfaces which have been removed from the rock mass. This question has been discussed extensively by Hoek and Brown (1980) who used the results of theoretical (Hoek, 1968) and model studies (Brown, 1970, Ladanyi and Archambault, 1970) and the limited amount of available strength data, to develop an empirical failure criterion for jointed rock masses. Hoek (1983) also proposed that the rock mass classification system of Bieniawski could be used for estimating the rock mass constants required for this empirical failure criterion. This classification proved to be adequate for better quality rock masses but it soon became obvious that a new classification was required for the very weak tectonically disturbed rock masses associated with the major mountain chains of the Alps, the Himalayas and the Andes.

The Geological Strength Index (GSI) was introduced by Hoek in 1994 and this Index was subsequently modified and expanded as experience was gained on its application to practical rock engineering problems. Marinos and Hoek (2000, 2001) published the chart reproduced in Figure 8 for use in estimating the properties of heterogeneous rock masses such as flysch (Figure 9).

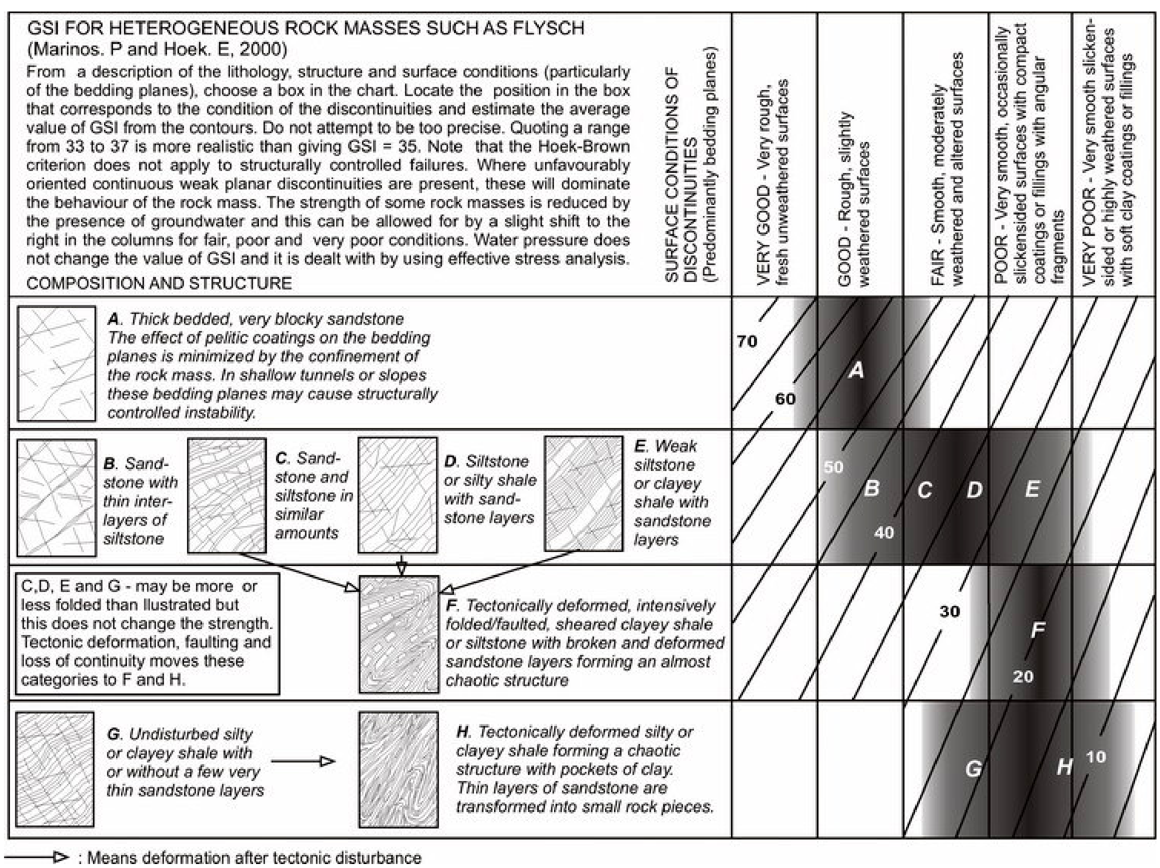

Figure 8: Geological Strength Index for heterogeneous rock masses such as flysch from Marinos and Hoek 2000.

Figure 9: Various grades of flysch in an exposure in the Pindos mountains of northern Greece.

Practical application of the GSI system and the Hoek-Brown failure criterion in a number of engineering projects around the world have shown that the system gives reasonable estimates of the strength of a wide variety of rock masses. These estimates have to be refined and adjusted for individual conditions, usually based upon back analysis of tunnel or slope behaviour, but they provide a sound basis for design analyses. The most recent version of the Hoek-Brown criterion has been published by Hoek, Carranza-Torres and Corkum (2002) and this paper, together with a program called RocLab for implementing the criterion, can be downloaded from the Internet at www.rocscience.com.

In situ stress measurements

The stability of deep underground excavations depends upon the strength of the rock mass surrounding the excavations and upon the stresses induced in this rock. These induced stresses are a function of the shape of the excavations and the in situ stresses which existed before the creation of the excavations. The magnitudes of pre-existing in situ stresses have been found to vary widely, depending upon the geological history of the rock mass in which they are measured (Hoek and Brown, 1980). Theoretical predictions of these stresses are considered to be unreliable and, hence, measurement of the actual in situ stresses is necessary for major underground excavation design. A phenomenon which is frequently observed in massive rock subjected to high in situ stresses is ‘core disking’, illustrated in Figure 10.

Figure 10: Disking of a 150 mm core of granite as a result of high in situ stresses.

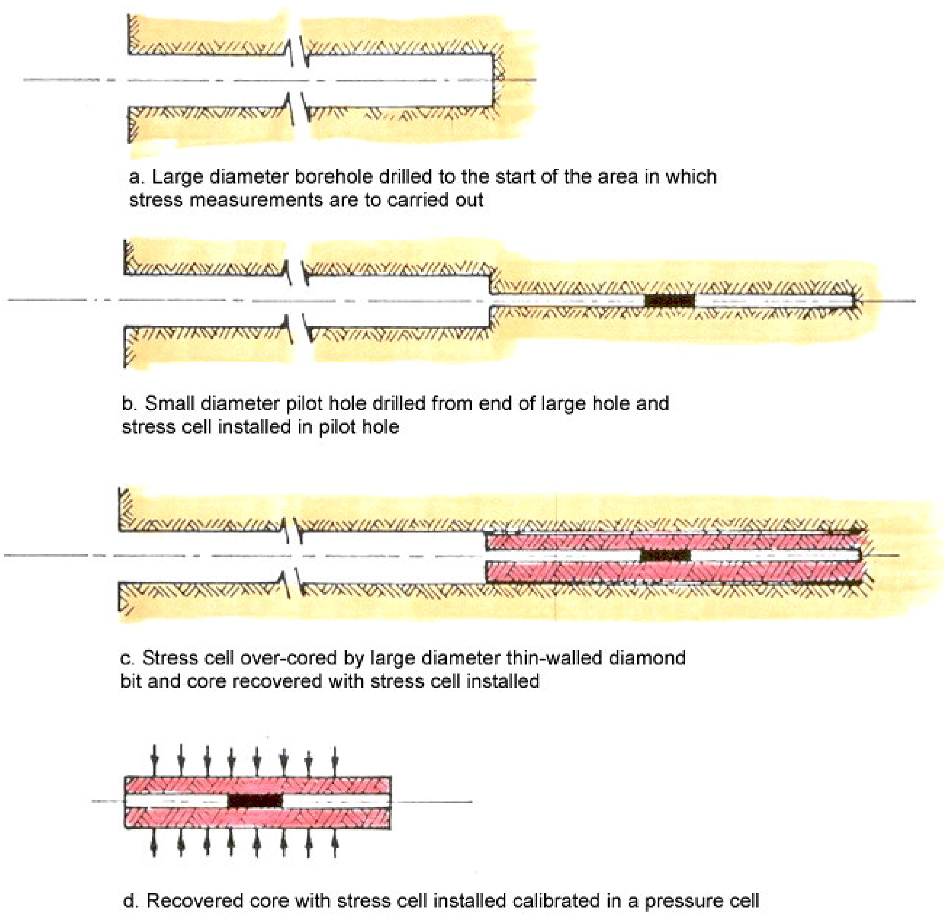

Figure 11: Typical sequence of over-coring stress measurements.

Figure 12: A cell for measuring the in situ triaxial stress field in a rock mass, developed in Australia (Worotnicki and Walton 1976). The hollow cylinder (on the left) is filled with adhesive which is extruded when the piston (on the right) is forced into the cylinder.

During early site investigations, when no underground access is available, the only practical method for measuring in situ stresses is by hydrofracturing (Haimson, 1978) in which the hydraulic pressure required to open existing cracks is used to estimate in situ stress levels. Once underground access is available, over-coring techniques for in situ stress measurement (Leeman and Hayes, 1966, Worotnicki and Walton, 1976) can be used and, provided that sufficient care is taken in executing the measurements, the results are usually adequate for design purposes. A typical over-coring sequence for in situ stress measurement is illustrated in Figure 11 and one of the instruments used for such measurement is illustrated in Figure 12.

Groundwater problems

The presence of large volumes of groundwater is an operational problem in tunnelling but water pressures are generally not too serious a problem in underground excavation engineering. Exceptions are pressure tunnels associated with hydroelectric projects. In these cases, inadequate confining stresses due to insufficient depth of burial of the tunnel can cause serious problems in the tunnel and in the adjacent slopes. The steel linings for these tunnels can cost several thousand dollars per metre and are frequently a critical factor in the design of a hydroelectric project. The installation of a steel tunnel lining is illustrated in Figure 13.

Figure 13: Installation of steel lining in a pressure tunnel in a hydroelectric project.

Groundwater pressures are a major factor in all slope stability problems and an understanding of the role of subsurface groundwater is an essential requirement for any meaningful slope design (Hoek and Bray, 1981, Brown, 1982).

While the actual distributions of water pressures in rock slopes are probably much more complex than the simple distributions normally assumed in slope stability analyses (Freeze and Cherry, 1979), sensitivity studies based upon these simple assumptions are generally adequate for the design of drainage systems (Masur and Kaufman, 1962). Monitoring of groundwater pressures by means of piezometers (Brown, 1982) is the most reliable means of establishing the input parameters for these groundwater models and for checking upon the effectiveness of drainage measures.

In the case of dams, forces generated by the water acting on the upstream face of the dam and water pressures generated in the foundations are critical in the assessment of the stability of the dam. Estimates of the water pressure distribution in the foundations and of the influence of grout and drainage curtains upon this distribution have to be made with care since they have a significant impact upon the overall dam and foundation design (Soos, 1979).

The major advances that have been made in the groundwater field during the past decades have been in the understanding of the transport of pollutants by groundwater. Because of the urgency associated with nuclear and toxic waste disposal in industrialised countries, there has been a concentration of research effort in this field and advances have been impressive. The results of this research do not have a direct impact on conventional geotechnical engineering but there have been many indirect benefits from the development of instrumentation and computer software which can be applied to both waste disposal and geotechnical problems.

Rock reinforcement and support design

Safety during construction and long term stability are factors that have to be considered by the designers of excavations in rock. It is not unusual for these requirements to lead to a need for the installation of some form of rock reinforcement or support. Fortunately, practical developments in this field have been significant during the past 25 years and today's rock engineer has a wide choice of reinforcement systems and tunnel lining techniques. In particular, the development of shotcrete has made a major contribution to modern underground construction.

There has been considerable confusion in the use of the terms "reinforcement" and "support" in rock engineering and it is important for the reader to understand the different roles of these two important systems.

Rock reinforcement, as the name implies, is used to improve the strength and/or deformational behaviour of a rock mass in much the same way that steel bars are used to improve the performance of reinforced concrete. The reinforcement generally consists of bolts or cables that are placed in the rock mass in such a way that they provide confinement or restraint to counteract loosening and movement of the rock blocks. They may or may not be tensioned, depending upon the sequence of installation, and they may or may not be grouted, depending upon whether they are temporary or permanent. In general, rock reinforcement is only fully effective in reasonably frictional rock masses of moderate to high strength. Such rock masses permit effective anchoring of the reinforcement and they also develop the interlocking required to benefit from the confinement provided by the reinforcement. In reinforced rock masses, mesh and/or shotcrete play an important role in bridging the gap between adjacent bolt or anchor heads and in preventing progressive ravelling of small pieces of rock that are not confined by the reinforcement.

For weak to very weak rock masses that are more cohesive than frictional, reinforcement is less effective and, in the case of extremely weak materials, may not work at all. In these cases it is more appropriate to use support rather than reinforcement. This support, which generally consists of steel sets and shotcrete or concrete linings in different combinations, must act as a load bearing structural shell to be fully effective in failing weak ground. The primary function of the support is to limit deformation of the rock or soil mass surrounding the tunnel and the sequence of installation, in relation to the advance of the tunnel face, is critically important. The capacity of the structural shell must be calculated on the basis of the bending moments and axial thrusts that are generated in the support elements and connections. In the case of large tunnels in very weak, highly stressed ground, where top heading and bench or multiple headings are used, temporary internal support shells may be required in order to prevent collapse of the temporary excavation boundaries. The development of shotcrete has been extremely important in weak ground tunnelling since it permits the rapid installation of a temporary or permanent load bearing lining with embedded reinforcement as required.

The use of long untensioned grouted cables in underground hard rock mining (Clifford, 1974, Fuller, 1983, Hunt and Askew, 1977, Brady and Brown, 1985) has been a particularly important innovation which has resulted in significant improvements in safety and mining costs in massive ore bodies. The lessons learned from these mining systems have been applied with considerable success in civil engineering and the use of untensioned dowels, installed as close as possible to the advancing face, has many advantages in high speed tunnel construction. The use of untensioned grouted cables or reinforcing bars has also proved to be a very effective and economical technique in rock slope stabilisation. This reinforcement is installed progressively as the slope is benched downward and it is very effective in knitting the rock mass together and preventing the initiation of ravelling.

The design of both rock reinforcement and support have benefited greatly from the evolution of personal computers and the development of very powerful and user-friendly software. Whereas, in the past, these designs were based on empirical rules or classification schemes derived from experience, it is now possible to study a wide range of excavation geometries, excavation sequences, rock mass properties and reinforcement or support options by means of numerical models. This does not imply that every metre of every excavation has to be subjected to such analyses but it does mean that, once a reliable geological model has been established, the designer can choose a few reinforcement or support systems and optimize these for the typical conditions anticipated.

Excavation methods in rock

As pointed out earlier, the strength of jointed rock masses is very dependent upon the interlocking between individual rock pieces. This interlocking is easily destroyed and careless blasting during excavation is one of the most common causes of underground excavation instability. The following quotation is taken from a paper by Holmberg and Persson (1980):

The innocent rock mass is often blamed for insufficient stability that is actually the result of rough and careless blasting. Where no precautions have been taken to avoid blasting damage, no knowledge of the real stability of the undisturbed rock can be gained from looking at the remaining rock wall. What one sees are the sad remains of what could have been a perfectly safe and stable rock face.

Techniques for controlling blast damage in rock are well-known (Svanholm et al, 1977, Langefors and Kihlstrom, 1963, Hagan, 1980) but it is sometimes difficult to persuade owners and contractors that the application of these techniques is worthwhile. Experience in projects in which carefully controlled blasting has been used generally shows that the amount of reinforcement can be reduced significantly and that the overall cost of excavation and support is lower than in the case of poorly blasted excavations (Hoek, 1982). Examples of poor and good quality blasting in tunnels are illustrated in Figures 1.10 and 1.11.

Machine excavation is a technique which causes very little disturbance to the rock surrounding an underground excavation. A wide range of tunnelling machines have been developed over the past 25 years and these machines are now capable of working in almost all rock types (Robbins, 1976, McFeat-Smith, 1982). Further development of these machines can be expected and it is probable that machine excavation will play a much more important role in future tunnelling than it does today.

Analytical tools

Analytical models have always played an important role in rock mechanics. The earliest models date back to closed form solutions such as that for calculating the stresses surrounding a circular hole in a stressed plate published by Kirsch in 1898. The development of the computer in the early 1960s made possible the use of iterative numerical techniques such as finite element (Clough, 1960), boundary element (Crouch and Starfield, 1983), discrete element (Cundall, 1971) and combinations of these methods (von Kimmelmann et al, 1984, Lorig and Brady, 1984). These have become almost universal tools in rock mechanics.

The computer has also made it much more convenient to use powerful limit equilibrium methods (Sarma, 1979, Brown and Ferguson, 1979, Shi and Goodman, 1981, Warburton, 1981) and probabilistic approaches (McMahon, 1971, Morriss and Stoter, 1983, Priest and Brown, 1982, Read and Lye, 1983) for rock mechanics studies.

The advent of the micro-computer and the rapid developments which have taken place in inexpensive hardware have brought us to the era of a computer on every professional's desk. The power of these machines is transforming our approach to rock mechanics analysis since it is now possible to perform a large number of sensitivity or probabilistic studies in a fraction of the time which was required for a single analysis a few years ago. Given the inherently inhomogeneous nature of rock masses, such sensitivity studies enable us to explore the influence of variations in the value of each input parameter and to base our engineering judgements upon the rate of change in the calculated value rather than on a single answer.

Figure 1.10: An example of poor blasting in a tunnel.

Figure 1.11: An example of good blasting in a tunnel.

Conclusions

Over the past 25 years, rock mechanics has developed into a mature subject which is built on a solid foundation of geology and engineering mechanics. Individuals drawn from many different disciplines have contributed to this subject and have developed a wide range of practical tools and techniques. There is still a great deal of room for development, innovation and improvement in almost every aspect of the subject and it is a field which will continue to provide exciting challenges for many years to come.

References

Barton, N.R., Lien, R. and Lunde, J. 1974. Engineering classification of rock masses for the design of tunnel support. *Rock Mech.* **6**(4), 189-239.

Bieniawski, Z.T. 1973. Engineering classification of jointed rock masses. *Trans S. Afr. Inst. Civ. Engrs* **15**, 335-344.

Bieniawski, Z.T. 1974. Geomechanics classification of rock masses and its application in tunnelling. In *Advances in Rock Mechanics* **2** , part A: pp.27-32. Washington, D.C.: National Academy of Sciences.

Brown, A. 1982. The influence and control of groundwater in large slopes. In *Stability in Surface Mining* (ed. C.O. Brawner), pp. 19-41. New York: Society of Mining Engineers, AIME.

Bucky, P.B. 1931. Use of models for the study of mining problems. Am. Inst. Min. Metall. Engrs , Technical Publication 425.

Coates, D. 1966. *Rock Mechanics Principles*. Ottawa: Dept. Mines and Technical Surveys.

Cook, N.G.W., Hoek, E., Pretorius, J.P.G., Ortlepp, W.D. and Salamon, M.D.G. 1966. Rock mechanics applied to the study of rockbursts. *J. S. Afr. Inst. Min. Metall.* **66,** 436-528.

Cook, N.G.W. 1965. The failure of rock. *Int. J. Rock Mech. Min. Sci. Geomech. Abstr.* **2**, 389-403.

Coulomb, C.A. 1776. Essai sur une application des regles de maximis et minimis a quelques problemes de statique, relatifs a l'architecture. *Memoires de Mathematique & de Physique* **7**, 343- 82.

Freeze, A.R. and Cherry, J.A. 1979. *Groundwater*. Englewood Cliffs, NJ: Prentice-Hall 604 pages

Gane, P.G., Hales, A.L. and Oliver, H.A. 1946. A seismic investigation of Witwatersrand earth tremors. *Bull. Seism. Soc. Am.* **36** , 49-80.

Griffith, A.A. 1921. The phenomenon of rupture and flow in solids. *Phil. Trans. Roy. Soc., London* **A221** , 163-198.

Griffith, A.A. 1924. Theory of rupture. *Proc. 1st congr. applied mechanics*, Delft, 55-63. Delft: Technische Bockhandel en Drukkerij.

Griggs, D.T. 1936. Deformation of rocks under high confining pressures. *J. Geol.* **44** , 541-577.

Haimson, B.C. 1978. The hydrofracturing stress measuring method and recent field results. *Int. J. Rock Mech. Min. Sci. & Geomech. Abstr.* **15** , 167-178.

Heyman, J. 1972. *Coulomb's Memoir on Statics* . Cambridge: at the University Press.

Hoek E. and Brown E.T. 1980. *Underground Excavations in Rock* . London: Instn Min. Metall. 527 pages

Hoek, E. 1994. Strength of rock and rock masses, *ISRM News Journal,* **2**(2), 4-16.

Hoek, E., Carranza-Torres, C. and Corkum, B. 2002. The Hoek-Brown failure criterion – 2002 Edition. *Proc. 5th North American Rock Mechanics Sym. and 17th Tunneling Assn of Canada conf.* pp.267-271. Toronto:NARMS-TAC.

Ide, J.M. 1936. Comparison of statically and dynamically determined Young's modulus of rock. *Proc. Nat. Acad. Sci.* **22** , 81- 92.

Jaeger, C. 1972. *Rock Mechanics and Engineering* . Cambridge: at the University Press. 417 pages.

Jaeger, J.C. and Cook, N.G.W. 1969. *Fundamentals of Rock Mechanics* . London: Chapman and Hall.

John, K.W. 1968. Graphical stability analyses of slopes in jointed rock. *Proc. Soil Mech. Fndn Div*., ASCE , SM2, paper no. 5865.

King, L.V. 1912. On the limiting strength of rocks under conditions of stress existing in the earth's interior. *J. Geol*. **20** , 119- 138.

Leeman, E.R. and Hayes, D.J. 1966. A technique for determining the complete state of stress in rock using a single borehole. *Proc. 1st Cong. Int. Soc. Rock Mech, Lisbon* **2** , 17-24.

Londe, P. 1965. Une méthode d'analyse à trois dimensions de la stabilité d'une rive rocheuse. *Annales des Ponts et Chaussees* **135** (1), 37-60.

Londe, P., Vigier, G. and Vormeringer, R. 1969. The stability of rock slopes, a three-dimensional study. *J. Soil Mech. Foundns Div., ASCE* **95** (SM 1), 235-262.

Londe, P., Vigier, G. and Vormeringer, R. 1970. Stability of slopes - graphical methods. *J. Soil Mech. Fndns Div., ASCE* **96** (SM 4), 1411-1434.

Lutton, R.J., Banks, D.C. and Strohm, W.E. 1979. Slides in the Gaillard Cut, Panama Canal Zone. In *Rockslides and Avalanches* (ed. B. Voight) **2**,151-224. New York: Elsevier.

Masur, C.I. and Kaufman, R.I. 1962. Dewatering. In *Foundation Engineering* (ed. G.A. Leonards), pp. 241-350. New York: McGraw- Hill.

Marinos, P. and Hoek, E. 2000. GSI – A geologically friendly tool for rock mass strength estimation. *Proc. GeoEng2000 Conf., Melbourne.*

Marinos, P. and Hoek, E. 2001. Estimating the geotechnical properties of heterogeneous rock masses such as Flysch. *Bull. Engng. Geol. Env*. **60,** 85-92,

Morrison, R.G.K. 1942. Report on the rockburst situation in Ontario mines. *Trans. Can. Inst. Min. Metall.* **45** .

Morrison, R.G.K. 1976. *A philosophy of ground control: a bridge between theory and practice* . rev. edn. Montreal: Dept.Min. Metall. Engng, McGill University . 182 pages.

Muller, J. 1979. Josef Stini. Contributions to engineering geology and slope movement investigations. In *Rockslides and Avalanches* (ed. B. Voight), Part 2,. 95-109. New York: Elsevier.

Obert, L. and Duvall, W.I. 1967. *Rock Mechanics and the Design of Structures in Rock* . New York: Wiley. 65 pages.

Palmstrom, A. and Broch, E. 2006. Use and misuse of rock mass classification systems with particular reference to the Q-system. *Tunnels and Underground Space Technology,* **21**, 575-593.

Salamon, M.D.G. and Munro, A.H. 1967. A study of the strength of coal pillars. *J. S. Afr. Inst. Min. Metall.* **65** , 55- 67.

Soos, I.G.K. 1979. Uplift pressures in hydraulic structures. *Water Power and Dam Construction.* **31**(5) 21-24.

Talobre, J. 1957. *La mecanique des roches* . Paris: Dunod.

Terzaghi, K. 1936. Presidential Address. *Proc. 1st Int. Conf. for Soil Mechanics and Foundations Engineering, Cambridge, Mass*. **1** , 22-3.

Terzaghi, K. 1945. Stress conditions for the failure of saturated concrete and rock. *Proc. Am. Soc. Test. Mater.* **45** , 777-801.

Terzaghi, R. and Voight, B. 1979. Karl Terzaghi on rockslides: the perspective of a half-century. In *Rockslides and Avalanches* (ed. B. Voight), Part 2, 111-131. New York: Elsevier.

von Karman. Th. 1911. Festigkeitsversuche unter allseitigem Druck. *Zeit d Ver Deutscher Ing.* **55** , 1749-1757.

Wittke, W.W. 1965. Method to analyse the stability of rock slopes with and without additional loading. (in German) *Felsmechanik und Ingerieurgeologie* , Supp. 11, **30** , 52-79. English translation in Imperial College Rock Mechanics Research Report.

Worotnicki, G. and Walton, R.J. 1976. Triaxial 'hollow inclusion' gauges for determination of rock stresses in situ. *Proc symp. ISRM on Investigation of Stress in Rock, Sydney*. Supplement 1-8. Sydney, Australia: Instn Engrs.

When is a rock engineering design acceptable

Introduction

When is a design in rock engineering acceptable? The aim of the following text[1] is to demonstrate that there are no simple universal rules for acceptability nor are there standard factors of safety which can be used to guarantee that a rock structure will be safe and that it will perform adequately. Each design is unique and the acceptability of the structure has to be considered in terms of the particular set of circumstances, rock types, design loads and end uses for which it is intended. The responsibility of the geotechnical engineer is to find a safe and economical solution which is compatible with all the constraints which apply to the project. Such a solution should be based upon engineering judgement guided by practical and theoretical studies such as stability or deformation analyses, if and when these analyses are applicable.

Tables 1 to 4 summarise some of the typical problems, critical parameters, analysis methods and acceptability criteria which apply to a number of different rock engineering structures. These examples have been drawn from my own consulting experience and I make no claims that this is a complete list nor do I expect readers to agree with all of the items which I have included under the various headings. The purpose of presenting these tables is to demonstrate the diversity of problems and criteria which have to be considered and to emphasise the dangers of attempting to use standard factors of safety or other acceptability criteria.

In order to amplify some of the items included in Tables 1 to 4, several case histories will be discussed in terms of the factors which were considered and the acceptability criteria which were used.

Landslides in reservoirs

The presence of unstable slopes in reservoirs is a major concern for the designers of dams for hydroelectric and irrigation projects. The Vajont failure in 1963 alerted the engineering community of the danger of underestimating the potential for the mobilisation of existing landslides as a result of submergence of the slide toe during impounding of the reservoir.

---

[1]Based upon the text of the Müller lecture presented at the 7th Congress of the International Society for Rock Mechanics held in Aachen, Germany, in September 1991.

Table 1 : Typical problems, critical parameters, methods of analysis and acceptability criteria for slopes.

STRUCTURE	TYPICAL PROBLEMS	CRITICAL PARAMETERS	ANALYSIS METHODS	ACCEPTABILITY CRITERIA
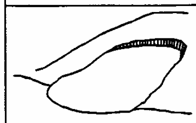 Landslides.	Complex failure along a circular or near circular failure surface involving sliding on faults and other structural features as well as failure of intact materials.	• Presence of regional faults. • Shear strength of materials along failure surface. • Groundwater distribution in slope, particularly in response to rainfall or to submergence of slope toe. • Potential earthquake loading.	Limit equilibrium methods which allow for non-circular failure surfaces can be used to estimate changes in factor of safety as a result of drainage or slope profile changes. Numerical methods such as finite element or discrete element analysis can be used to investigate failure mechanisms and history of slope displacement.	Absolute value of factor of safety has little meaning but rate of change of factor of safety can be used to judge effectiveness of remedial measures. Long term monitoring of surface and subsurface displacements in slope is the only practical means of evaluating slope behaviour and effectiveness of remedial action.
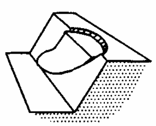 Soil or heavily jointed rock slopes.	Circular failure along a spoon-shaped surface through soil or heavily jointed rock masses.	• Height and angle of slope face. • Shear strength of materials along failure surface. • Groundwater distribution in slope. • Potential surcharge or earthquake loading.	Two-dimensional limit equilibrium methods which include automatic searching for the critical failure surface are used for parametric studies of factor of safety. Probability analyses, three-dimensional limit equilibrium analyses or numerical stress analyses are occasionally used to investigate unusual slope problems.	Factor of safety > 1.3 for "temporary" slopes with minimal risk of damage. Factor of safety > 1.5 for "permanent" slopes with significant risk of damage. Where displacements are critical, numerical analyses of slope deformation may be required and higher factors of safety will generally apply in these cases.
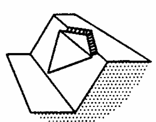 Jointed rock slopes.	Planar or wedge sliding on one structural feature or along the line of intersection of two structural features.	• Slope height, angle and orientation. • Dip and strike of structural features. • Groundwater distribution in slope. • Potential earthquake loading. • Sequence of excavation and support installation.	Limit equilibrium analyses which determine three-dimensional sliding modes are used for parametric studies on factor of safety. Failure probability analyses, based upon distribution of structural orientations and shear strengths, are useful for some applications.	Factor of safety > 1.3 for "temporary" slopes with minimal risk of damage. Factor of safety > 1.5 for "permanent" slopes with significant risk of damage. Probability of failure of 10 to 15% may be acceptable for open pit mine slopes where cost of clean up is less than cost of stabilization.
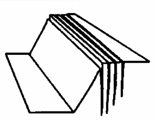 Vertically jointed rock slopes .	Toppling of columns separated from the rock mass by steeply dipping structural features which are parallel or nearly parallel to the slope face.	• Slope height, angle and orientation. • Dip and strike of structural features. • Groundwater distribution in slope. • Potential earthquake loading.	Crude limit equilibrium analyses of simplified block models are useful for estimating potential for toppling and sliding. Discrete element models of simplified slope geometry can be used for exploring toppling failure mechanisms.	No generally acceptable criterion for toppling failure is available although potential for toppling is usually obvious. Monitoring of slope displacements is the only practical means of determining slope behaviour and effectiveness of remedial measures.
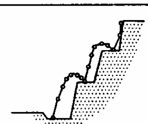 Loose boulders on rock slopes.	Sliding, rolling, falling and bouncing of loose rocks and boulders on the slope.	• Geometry of slope. • Presence of loose boulders. • Coefficients of restitution of materials forming slope. • Presence of structures to arrest falling and bouncing rocks.	Calculation of trajectories of falling or bouncing rocks based upon velocity changes at each impact is generally adequate. Monte Carlo analyses of many trajectories based upon variation of slope geometry and surface properties give useful information on distribution of fallen rocks.	Location of fallen rock or distribution of a large number of fallen rocks will give an indication of the magnitude of the potential rockfall problem and of the effectiveness of remedial measures such as draped mesh, catch fences and ditches at the toe of the slope.

Table 2 : Typical problems, critical parameters, methods of analysis and acceptability criteria for dams and foundations.

STRUCTURE	TYPICAL PROBLEMS	CRITICAL PARAMETERS	ANALYSIS METHODS	ACCEPTABILITY CRITERIA
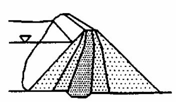 Zoned fill dams.	Circular or near-circular failure of dam, particularly during rapid drawdown. Foundation failure on weak seams. Piping and erosion of core.	• Presence of weak or permeable zones in foundation. • Shear strength, durability, gradation and placement of dam construction materials, particularly filters. • Effectiveness of grout curtain and drainage system. • Stability of reservoir slopes.	Seepage analyses are required to determine water pressure and velocity distribution through dam and abutments. Limit equilibrium methods should be used for parametric studies of stability. Numerical methods can be used to investigate dynamic response of dam during earthquakes.	**Safety factor >1.5 for full pool with steady state seepage; >1.3 for end of construction with no reservoir loading and undissipated foundation porewater pressures; >1.2 for probable maximum flood with steady state seepage and >1.0 for full pool with steady state seepage and maximum credible horizontal psuedo-static seismic loading.**
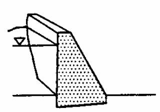 Gravity dams.	Shear failure of interface between concrete and rock or of foundation rock. Tension crack formation at heel of dam. Leakage through foundation and abutments.	• Presence of weak or permeable zones in rock mass. • Shear strength of interface between concrete and rock. • Shear strength of rock mass. • Effectiveness of grout curtain and drainage system. • Stability of reservoir slopes.	Parametric studies using limit equilibrium methods should be used to investigate sliding on the interface between concrete and rock and sliding on weak seams in the foundation. A large number of trial failure surfaces are required unless a non-circular failure analysis with automatic detection of critical failure surfaces is available.	**Safety factor against foundation failure should exceed 1.5 for normal full pool operating conditions provided that conservative shear strength values are used ($c' \approx 0$). Safety factor > 1.3 for probable mximum food (PMF). Safety factor > 1 for extreme loading - maximum credible earthquake and PMF.**
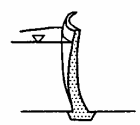 Arch dams.	Shear failure in foundation or abutments. Cracking of arch due to differential settlements of foundation. Leakage through foundations or abutments.	• Presence of weak, deformable or permeable zones in rock mass. • Orientation, inclination and shear strength of structural features. • Effectiveness of grout curtain and drainage system. • Stability of reservoir slopes.	Limit equilibrium methods are used for parametric studies of three-dimensional sliding modes in the foundation and abutments, including the influence of water pressures and reinforcement. Three-dimensional numerical analyses are required to determine stresses and displacements in the concrete arch.	**Safety factor against foundation failure >1.5 for normal full pool operating conditions and >1.3 for probable maximum flood conditions provided that conservative shear strength values are used ($c' \approx 0$). Stresses and deformations in concrete arch should be within allowable working levels defined in concrete specifications.**
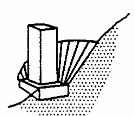 Foundations on rock slopes.	Slope failure resulting from excessive foundation loading. Differential settlement due to anisotropic deformation properties of foundation rocks.	• Orientation, inclination and shear strength of structural features in rock mass forming foundation. • Presence of inclined layers with significantly different deformation properties. • Groundwater distribution in slope.	Limit equilibrium analyses of potential planar or wedge failures in the foundation or in adjacent slopes are used for parametric studies of factor of safety. Numerical analyses can be used to determine foundation deformation, particularly for anisotropic rock masses.	Factor of safety against sliding of any potential foundation wedges or blocks should exceed 1.5 for normal operating conditions. Differential settlement should be within limits specified by structural engineers.
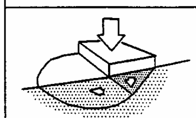 Foundations on soft rock or soil.	Bearing capacity failure resulting from shear failure of soils or weak rocks underlying foundation slab.	• Shear strength of soil or jointed rock materials. • Groundwater distribution in soil or rock foundation. • Foundation loading conditions and potential for earthquake loading.	Limit equilibrium analyses using inclined slices and non-circular failure surfaces are used for parametric studies of factor of safety. Numerical analyses may be required to determine deformations, particularly for anisotropic foundation materials.	**Bearing capacity failure should not be permitted for normal loading conditions. Differential settlement should be within limits specified by structural engineers.**

Table 3 : Typical problems, critical parameters, methods of analysis and acceptability criteria for underground civil engineering excavations.

STRUCTURE	TYPICAL PROBLEMS	CRITICAL PARAMETERS	ANALYSIS METHODS	ACCEPTABILITY CRITERIA
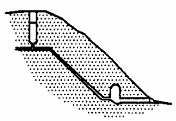 Pressure tunnels in hydro-power projects.	Excessive leakage from unlined or concrete lined tunnels. Rupture or buckling of steel lining due to rock deformation or external pressure.	• Ratio of maximum hydraulic pressure in tunnel to minimum principal stress in the surrounding rock. • Length of steel lining and effectiveness of grouting. • Groundwater levels in the rock mass.	Determination of minimum cover depths along pressure tunnel route from accurate topographic maps. Stress analyses of sections along and across tunnel axis. Comparison between minimum principal stresses and maximum dynamic hydraulic pressure to determine steel lining lengths.	Steel lining is required where the minimum principal stress in the rock is less than 1.3 times the maximum static head for typical hydroelectric operations or 1.15 for operations with very low dynamic pressures. Hydraulic pressure testing in boreholes at the calculated ends of the steel lining is essential to check the design assumptions.
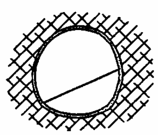 Soft rock tunnels.	Rock failure where strength is exceeded by induced stresses. Swelling, squeezing or excessive closure if support is inadequate.	• Strength of rock mass and of individual structural features. • Swelling potential, particularly of sedimentary rocks. • Excavation method and sequence. • Capacity and installation sequence of support systems.	Stress analyses using numerical methods to determine extent of failure zones and probable displacements in the rock mass. Rock-support interaction analyses using closed-form or numerical methods to determine capacity and installation sequence for support and to estimate displacements in the rock mass.	Capacity of installed support should be sufficient to stabilize the rock mass and to limit closure to an acceptable level. Tunnelling machines and internal structures must be designed for closure of the tunnel as a result of swelling or time-dependent deformation. Monitoring of deformations is an important aspect of construction control.
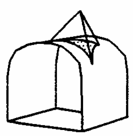 Shallow tunnels in jointed rock.	Gravity driven falling or sliding wedges or blocks defined by intersecting structural features. Unravelling of inadequately supported surface material.	• Orientation, inclination and shear strength of structural features in the rock mass. • Shape and orientation of excavation. • Quality of drilling and blasting during excavation. • Capacity and installation sequence of support systems.	Spherical projection techniques or analytical methods are used for the determination and visualization of all potential wedges in the rock mass surrounding the tunnel. Limit equilibrium analyses of critical wedges are used for parametric studies on the mode of failure, factor of safety and support requirements.	Factor of safety, including the effects of reinforcement, should exceed 1.5 for sliding and 2.0 for falling wedges and blocks. Support installation sequence is critical and wedges or blocks should be identified and supported before they are fully exposed by excavation. Displacement monitoring is of little value.
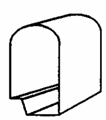 Large caverns in jointed rock.	Gravity driven falling or sliding wedges or tensile and shear failure of rock mass, depending upon spacing of structural features and magnitude of in situ stresses.	• Shape and orientation of cavern in relation to orientation, inclination and shear strength of structural features in the rock mass. • In situ stresses in the rock mass. • Excavation and support sequence and quality of drilling and blasting.	Spherical projection techniques or analytical methods are used for the determination and visualization of all potential wedges in the rock mass. Stresses and displacements induced by each stage of cavern excavation are determined by numerical analyses and are used to estimate support requirements for the cavern roof and walls.	An acceptable design is achieved when numerical models indicate that the extent of failure has been controlled by installed support, that the support is not overstressed and that the displacements in the rock mass stabilize. Monitoring of displacements is essential to confirm design predictions.
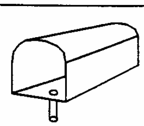 Underground nuclear waste disposal.	Stress and/or thermally induced spalling of the rock surrounding the excavations resulting in increased permeability and higher probability of radioactive leakage.	• Orientation, inclination, permeability and shear strength of structural features in the rock mass. • In situ and thermal stresses in the rock surrounding the excavations. • Groundwater distribution in the rock mass.	Numerical analyses are used to calculate stresses and displacements induced by excavation and by thermal loading from waste canisters. Groundwater flow patterns and velocities, particularly through blast damaged zones, fissures in the rock and shaft seals are calculated using numerical methods.	An acceptable design requires extremely low rates of groundwater movement through the waste canister containment area in order to limit transport of radioactive material. Shafts, tunnels and canister holes must remain stable for approximately 50 years to permit retrieval of waste if necessary.

Table 4 : Typical problems, critical parameters, methods of analysis and acceptability criteria for underground hard rock mining excavations.

STRUCTURE	TYPICAL PROBLEMS	CRITICAL PARAMETERS	ANALYSIS METHODS	ACCEPTABILITY CRITERIA
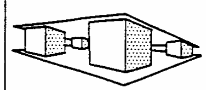 Pillars.	Progressive spalling and slabbing of the rock mass leading to eventual pillar collapse or rockbursting.	• Strength of the rock mass forming the pillars. • Presence of unfavourably oriented structural features. • Pillar geometry, particularly width to height ratio. • Overall mine geometry including extraction ratio.	For horizontally bedded deposits, pillar strength from empirical relationships based upon width to height ratios and average pillar stress based on tributary area calculations are compared to give a factor of safety. For more complex mining geometry, numerical analyses including progressive pillar failure may be required.	Factor of safety for simple pillar layouts in horizontally bedded deposits should exceed 1.6 for "permanent" pillars. In cases where progressive failure of complex pillar layouts is modelled, individual pillar failures can be tolerated provided that they do not initiate "domino" failure of adjacent pillars.
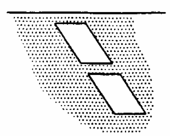 Crown pillars.	Caving of surface crown pillars for which the ratio of pillar depth to stope span is inadequate. Rockbursting or gradual spalling of overstressed internal crown pillars.	• Strength of the rock mass forming the pillars. • Depth of weathering and presence of steeply dipping structural features in the case of surface crown pillars. • In situ stress levels and geometry of internal crown pillars.	Rock mass classification and limit equilibrium analyses can give useful guidance on surface crown pillar dimensions for different rock masses. Numerical analyses, including discrete element studies, can give approximate stress levels and indications of zones of potential failure.	Surface crown pillar depth to span ratio should be large enough to ensure very low probability of failure. Internal crown pillars may require extensive support to ensure stability during mining of adjacent stopes. Careful planning of mining sequence may be necessary to avoid high stress levels and rockburst problems.
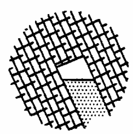 Cut and fill stopes.	Falls of structurally defined wedges and blocks from stope backs and hanging walls. Stress induced failures and rockbursting in high stress environments.	• Orientation, inclination and shear strength of structural features in the rock mass. • In situ stresses in the rock mass. • Shape and orientation of stope. • Quality, placement and drainage of fill.	Numerical analyses of stresses and displacements for each excavation stage will give some indication of potential problems. Some of the more sophisticated numerical models will permit inclusion of the support provided by fill or the reinforcement of the rock by means of grouted cables.	Local instability should be controlled by the installation of rockbolts or grouted cables to improve safety and to minimize dilution. Overall stability is controlled by the geometry and excavation sequence of the stopes and the quality and sequence of filling. Acceptable mining conditions are achieved when all the ore is recovered safely.
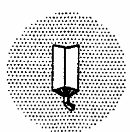 Non-entry stopes.	Ore dilution resulting from rockfalls from stope back and walls. Rockbursting or progressive failure induced by high stresses in pillars between stopes.	• Quality and strength of the rock. • In situ and induced stresses in the rock surrounding the excavations. • Quality of drilling and blasting in excavation of the stope.	Some empirical rules, based on rock mass classification, are available for estimating safe stope dimensions. Numerical analyses of stope layout and mining sequence, using three-dimensional analyses for complex orebody shapes, will provide indications of potential problems and estimates of support requirements.	A design of this type can be considered acceptable when safe and low cost recovery of a large proportion of the orebody has been achieved. Rockfalls in shafts and haulages are an unacceptable safety hazard and pattern support may be required. In high stress environments, local destressing may be used to reduce rockbursting.
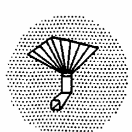 Drawpoints and orepasses.	Local rock mass failure resulting from abrasion and wear of poorly supported drawpoints or orepasses. In extreme cases this may lead to loss of stopes or orepasses.	• Quality and strength of the rock. • In situ and induced stresses and stress changes in the rock surrounding the excavations. • Selection and installation sequence of support.	Limit equilibrium or numerical analyses are not particularly useful since the processes of wear and abrasion are not included in these models. Empirical designs based upon previous experience or trial and error methods are generally used.	The shape of the opening should be maintained for the design life of the drawpoint or orepass. Loss of control can result in serious dilution of the ore or abandonment of the excavation. Wear resistant flexible reinforcement such as grouted cables, installed during excavation of the opening, may be successful in controlling instability.

During the construction of the Mica and Revelstoke dams on the Columbia River in British Columbia, Canada, several potential slides were investigated. Two of these, the Downie Slide, a 1.4 billion cubic metre ancient rock slide, and Dutchman's Ridge, a 115 million cubic metre potential rock slide, were given special attention because of the serious consequences which could have resulted from failure of these slides (Imrie, 1983, Lewis and Moore, 1989, Imrie, Moore and Enegren, 1992).

The Downie Slide and Dutchman's Ridge are located in steep, narrow, V-shaped sections of the Columbia River valley which has been subjected to several episodes of glaciation. The bedrock at these sites consists mainly of Pre-Cambrian para-gneisses and schists within or on the fringe of the Shuswap Metamorphic Complex. In both cases, the potential slide planes, determined by diamond drilling and slope displacement monitoring, are relatively flat-lying outward-dipping tectonic faults or shears which daylight in the base of the river valley.

Based on thorough investigation and monitoring programs, British Columbia Hydro and Power Authority (BC Hydro) decided that remedial measures had to be taken to improve the stability of both the Downie Slide and Dutchman's Ridge. These remedial measures consisted of drainage adits extending within and/or behind the failure surfaces and supplemented by drainholes drilled from chambers excavated along the adits. Work on the Downie Slide was carried out in the period 1977 to 1982 (which included a 3 year observation period) and work on Dutchman's Ridge was carried out from 1986 to 1988.

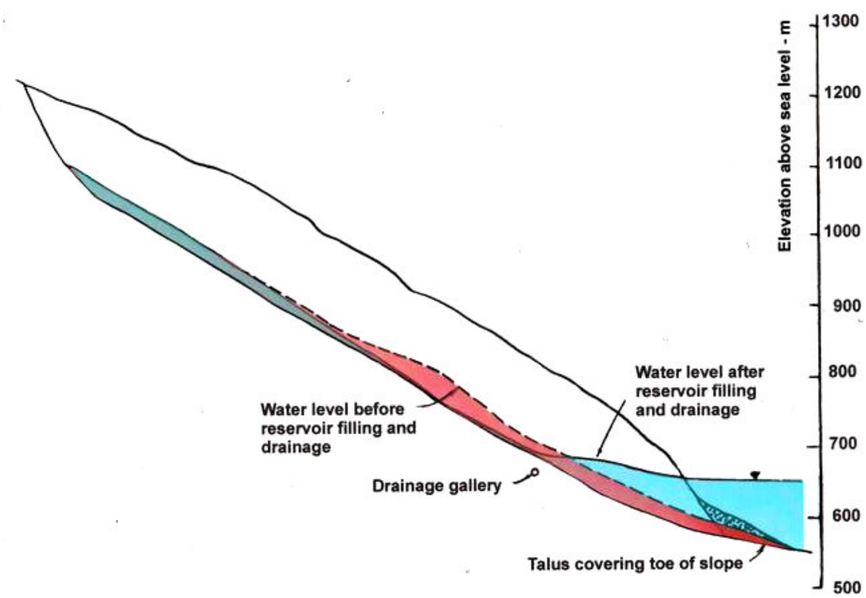

Figure 1: Section through Dutchman's Ridge showing potential slide surface and water levels before and after drainage.

A section through Dutchman's Ridge is given in Figure 1 and this shows the water levels in the slope before reservoir filling and after reservoir filling and the construction of the drainage system. Figure 2 shows contours of reduction in water levels as a result of the installation of the drainage system which consisted of 872 m of adit and 12,000 m of drainhole drilling. Note that the drawdown area on the right hand side of the potential slide was achieved by long boreholes from the end of the drainage adit branch.

Comparative studies of the stability of the slope section shown in Figure 1, based upon a factor of safety of 1.00 for the slope after reservoir filling but before implementation of the drainage system, gave a factor of safety of 1.06 for the drained slope. This 6% improvement in factor of safety may not seem very significant to the designer of small scale rock and soil slopes but it was considered acceptable in this case for a number of reasons:

1. The factor of safety of 1.00 calculated for the undrained slope is based upon a 'back-analysis' of observed slope behaviour. Provided that the same method of analysis and shear strength parameters are used for the stability analysis of the same slope with different groundwater conditions, the ratio of the factors of safety is a very reliable indicator of the change in slope stability, even if the absolute values of the factor of safety are not accurate. Consequently, the degree of uncertainty, which has to be allowed for in slope designs where no back-analyses have been performed, can be eliminated and a lower factor of safety accepted.

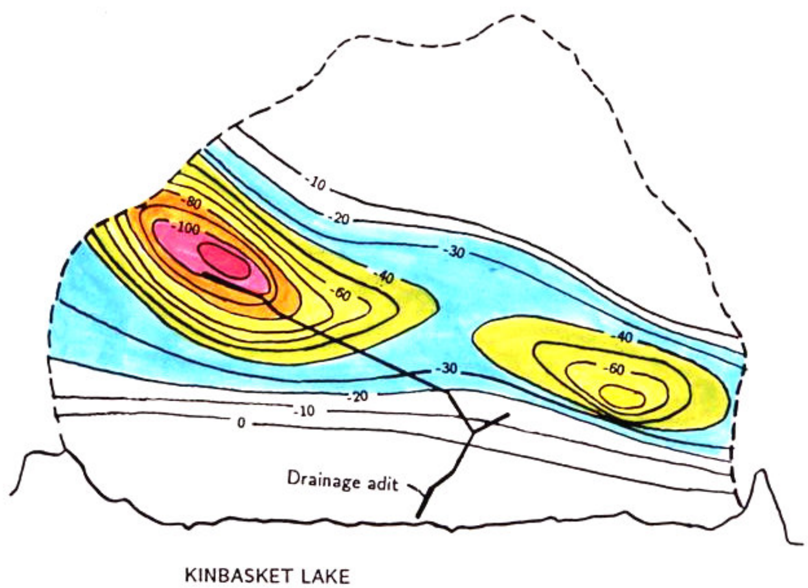

Figure 2: Contours of water level reduction (in metres) as a result of the implementation of drainage in Dutchman's Ridge.

2. The groundwater levels in the slope were reduced by drainage to lower than the pre-reservoir conditions and the stability of the slope is at least as good if not better than these pre-reservoir conditions. This particular slope is considered to have withstood several significant earthquakes during the 10,000 years since the last episode of glaciation which is responsible for the present valley shape.
3. Possibly the most significant indicator of an improvement in stability, for both the Downie Slide and Dutchman's Ridge, has been a significant reduction in the rate of down-slope movement which has been monitored for the past 25 years. In the case of the Downie Slide, this movement has practically ceased. At Dutchman's Ridge, the movements are significantly slower and it is anticipated that they will stabilize when the drainage system has been in operation for a few more years.

Deformation of rock slopes

In a slope in which the rock is jointed but where there are no significant discontinuities dipping out of the slope which could cause sliding, deformation and failure of the slope is controlled by a complex process of block rotation, tilting and sliding. In an extreme case, where the rock mass consists of near vertical joints separating columns of massive rock, toppling movement and failure may occur.

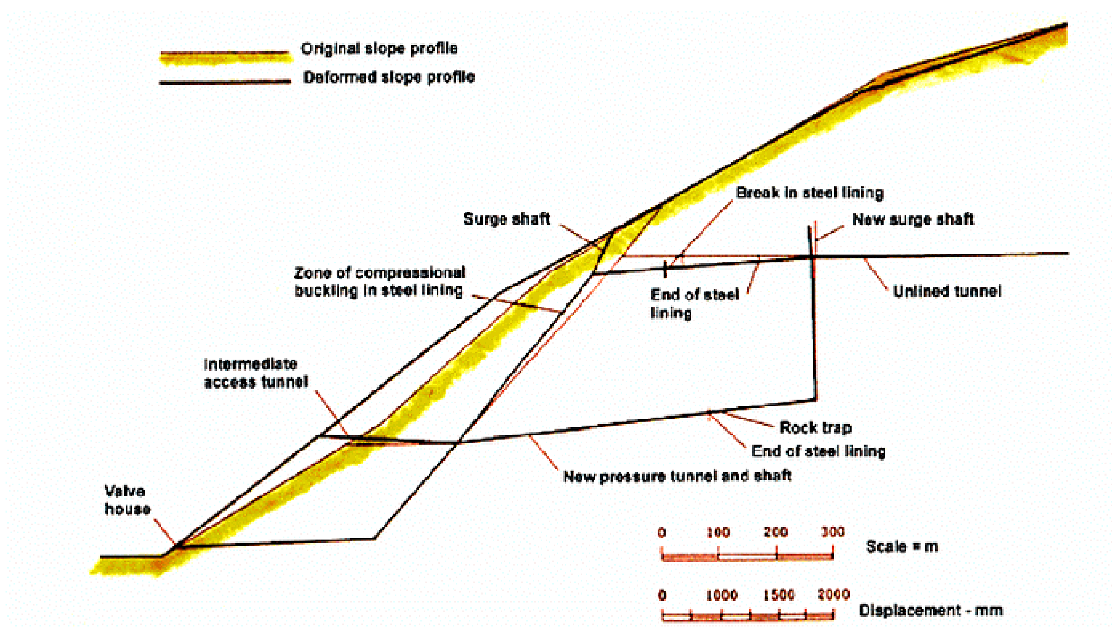

Figure 3: Cross-section through a section of the Wahleach power tunnel showing the original tunnel alignment and the location of the replacement conduit. The dashed line is the approximate location of a gradational boundary between loosened, fractured and weathered rock and more intact rock. Down-slope movement currently being monitored is well above this boundary.

Figure 3 is a section through part of the power tunnel for the Wahleach hydroelectric project in British Columbia, Canada. A break in the steel lining in this power tunnel occurred in January 1989 and it is thought this break was caused by a slow down-slope gravitational movement caused by block rotations within a near-surface zone of loosened jointed rock.

The Wahleach project is located 120 km east of Vancouver and power is generated from 620 m of head between Wahleach Lake and a surface powerhouse located adjacent to the Fraser River. Water flows through a 3500 m long three metre diameter unlined upper tunnel, a rock trap, a 600 m two metre diameter concrete encased steel lined shaft inclined at 48° to the horizontal, a 300 m long lower tunnel and a 485 m long surface penstock to the powerhouse.

The tunnels were excavated mainly in granodiorite which varies from highly fractured and moderately weathered in the upper portions of the slope to moderately fractured and fresh in both the lower portions of the slope and below the highly fractured mass. Two main joint sets occur in the rock mass, one set striking parallel to the slope and the other perpendicular to it. Both dip very steeply. Average joint spacings range from 0.5 to 1 m. A few joints occur sub-parallel to the ground surface and these joints are most well developed in the ground surface adjacent to the inclined shaft. Thorough investigations failed to reveal any significant shear zones or faults conducive to sliding.

The toe of the slope is buried beneath colluvial and fan deposits from two creeks which have incised the Fraser Valley slope to form the prominence in which the inclined shaft was excavated. This prominence is crossed by several linear troughs which trend along the ground surface contours and are evidence of previous down-slope movement of the prominence. Mature trees growing in these troughs indicate a history of movement of at least several hundred years (Moore, Imrie and Baker, 1991).

The water conduit operated without incident between the initial filling in 1952 and May 1981 when leakage was first noted from the upper access adit located near the intersection of the inclined shaft and the upper tunnel (see Figure 3). This leakage stopped when two drain pipes embedded in the concrete backfill beneath the steel lining were plugged at their upstream ends. Large holes had been eroded in these drainage pipes where they were not encased in concrete and it was concluded that this corrosion was responsible for the leakage. This conclusion appeared to be valid until 25 January, 1989 when a much larger water flow occurred.

Investigations in the dewatered tunnel revealed a 150 mm wide circumferential tension crack in the steel lining of the upper tunnel, about 55 m from its intersection with the inclined shaft. In addition, eight compressional buckle zones were found in the upper portion of the inclined shaft. Subsequent investigations revealed that approximately 20 million cubic metres of rock are involved in down-slope creep which, during 1989-90, amounted to several centimetres per year and which appears to be ongoing. This down-slope creep appears to be related to a process of block rotation rather than to any deep seated sliding as was the case at both the Downie Slide and Dutchman's Ridge.

While discrete element models may give some indication of the overall mechanics of this type of slope deformation, there is no way in which a factor of safety, equivalent to that for sliding failure, can be calculated. Consequently, in deciding upon the remedial measures to be implemented, other factors have to be taken into consideration.

After thorough study by the BC Hydro and their consultants, it was decided to construct a replacement conduit consisting of an unlined shaft and tunnel section and a steel lined section where the rock cover is insufficient to contain the internal pressure in the tunnel. This replacement conduit, illustrated in Figure 3, will remove the steel lined portions of the system from zones in which large displacements are likely to occur in the future. This in turn will minimise the risk of a rupture of the steel lining which would inject high pressure water into the slope. It was agreed that such high pressure water leakage could be a cause for instability of the overall slope. Further studies are being undertaken to determine whether additional drainage is required in order to provide further safeguards.

Careful measurements of the displacements in the inclined shaft, the length of the steel lining cans as compared with the original specified lengths and the opening of the tensile crack in the upper portion of the steel lined tunnel, provided an overall picture of the displacements in the rock mass. These observed displacements were compared with displacement patterns computed by means of a number of numerical studies using both continuum and discrete element models and the results of these studies were used in deciding upon the location of the replacement conduit.

In addition to the construction of this replacement conduit to re-route the water away from the upper and potentially unstable part of the slope, a comprehensive displacement and water pressure monitoring system has been installed and is being monitored by BC Hydro (Baker, 1991, Tatchell, 1991).

Structural failures in rock masses

In slopes, foundations and shallow underground excavations in hard rock, failure is frequently controlled by the presence of discontinuities such as faults, shear zones, bedding planes and joints. The intersection of these structural features can release blocks or wedges which can fall or slide from the surface of the excavation. Failure of the intact rock is seldom a problem in these cases where deformation and failure are caused by sliding along individual discontinuity surfaces or along lines of intersection of surfaces. Separation of planes and rotation of blocks and wedges can also play a role in the deformation and failure process.

An analysis of the stability of these excavations depends primarily upon a correct interpretation of the structural geological conditions in the rock mass followed by a study of the blocks and wedges which can be released by the creation of the excavation. Identification and visualisation of these blocks and wedges is by far the most important part of this analysis. Analysis of the stability of the blocks and wedges, and of the reinforcing forces required to stabilize them, is a relatively simple process once this identification has been carried out.

The Río Grande Pumped Storage Project is located in the Province of Córdoba in the Republic of Argentina. Four reversible pump-turbines operating at an average head of 170 m give the project a total installed capacity of 750 MW. These turbines are installed in a 25 m span, 50 m high, 105 m long cavern at an average depth of 160 m .

The rock in which the underground excavations are situated is a massive tonalitic gneiss of excellent quality (Amos et al, 1981). The gneiss has an average uniaxial compressive strength of 140 MPa. The maximum principal stress, determined by overcoring tests, is 9.4 MPa and is almost horizontal and oriented approximately normal to the cavern axis. In massive rocks, this 15:1 ratio of uniaxial strength to maximum principal stress is unlikely to result in any significant failure in the rock and this was confirmed by numerical stress analyses (Moretto, 1982). The principal type of instability which had to be dealt with in the underground excavations was that of potentially unstable blocks and wedges defined by intersecting structural features (Hammett and Hoek, 1981). In one section of the cavern, the axis of which is oriented in the direction 158-338, four joint sets were mapped and were found to have the following dip/dip direction values:

Table 5. Dip and dip direction values for joints in one location in the Río Grande cavern

N.	Dip	Dip dir.	Comments
1	50	131	infrequently occurring joints
2	85	264	shear joint set
3	70	226	shear joint set
4	50	345	tension joint set

Figure 4 is a perspective view of the Río Grande power cavern showing typical wedges which can be formed in the roof, sidewalls, bench and floor by joint sets 2, 3 and 4. These figures represent the maximum possible sizes of wedges which can be formed and, during construction, the sizes of the wedges were scaled down in accordance with average joint trace lengths measured in the excavation faces. In Figure 4 it is evident that the roof and the two sidewall wedges were potentially unstable and that they needed to be stabilised. This stabilisation was achieved by the placement of tensioned and grouted rockbolts which were installed at each stage of the cavern excavation. Decisions on the number, length and capacity of the rockbolts were made by on-site geotechnical staff using limit equilibrium calculations based upon the volume of the wedges defined by the measured trace lengths. For those wedges which involved sliding on one plane or along the line of intersection of two planes, rockbolts were installed across these planes to bring the sliding factor of safety of the wedge up to 1.5. For wedges which were free to fall from the roof, a factor of safety of 2 was used. This factor was calculated as the ratio

of the total capacity of the bolts to the weight of the wedge and was intended to account for uncertainties associated with the bolt installation.
The floor wedge was of no significance while the wedges in the bench at the base of the upstream wall were stabilised by dowels placed in grout-filled vertical holes before excavation of the lower benches.

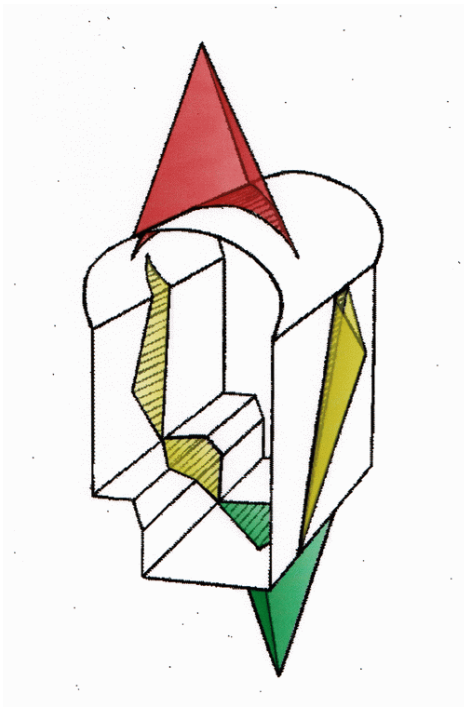

Figure 4: Perspective view of Río Grande power cavern showing potentially unstable wedges in the roof, sidewalls, bench and floor.

Early recognition of the potential instability problems, identification and visualization of the wedges which could be released and the installation of support at each stage of excavation, before the wedge bases were fully exposed, resulted in a very effective stabilisation program. Apart from a minimal amount of mesh and shotcrete applied to areas of intense jointing, no other support was used in the power cavern which has operated without any signs of instability since its completion in 1982.

Excavations in weak rock

In contrast to the structurally controlled failures in strong rock discussed in the previous section, there are many cases where tunnels and caverns are excavated in rock masses which are weak as a result of intense jointing or because the rock material itself has a low strength. Rocks such as shales, mudstones, siltstones, phyllites and tuffs are typical weak rocks in which even moderate in situ stresses are likely to induce failure in the rock surrounding underground excavations.

Progressive failure of this type, which can occur in the rock surrounding an underground excavation in a weak rock mass, is a difficult analytical problem and there are no simple numerical models nor factor of safety calculations which can be used to define acceptable limits to this failure process. Judgement on the adequacy of a support design has to be based upon an evaluation of a number of factors such as the magnitude and distribution of deformations in the rock and the stresses induced in support elements such as grouted cables, steel sets or concrete linings. This design process is illustrated by means of an example.

The Mingtan pumped storage project is located in the central region of the island of Taiwan and utilizes the 400 m head difference between the Sun Moon Lake and the Shuili River to generate up to 1600 MW at times of peak demand. The power cavern is 22 m wide, 46 m high and 158 m long and a parallel transformer hall is 13 m wide, 20 m high and 17 m long. The caverns are 45 m apart and are located at a depth of 30 m below surface in the steep left bank of the Shuili river (Liu, Cheng and Chang, 1988).

The rock mass consists of weathered, interbedded sandstones, siltstones and shales dipping at about 35° to the horizontal. The Rock Mass Ratings (RMR) (Bieniawski, 1974) and Tunnelling Quality Index Q (Barton, Lien and Lunde, 1974) and approximate shear strength values for the various components of the rock mass are given in Table 6 below.

Table 6. Rock mass classifications and approximate friction angles ϕ and cohesive strengths c for the rock mass in which the Mingtan power cavern is excavated

Rock type	RMR	Q	ϕ' degrees	c' MPa
Jointed sandstone	63-75	12-39	50	1.0
Bedded sandstone	56-60	7-31	45	0.8
Faults or shears	10-33	0.1-1.1	30-40	0.15-0.3

Weak beds of siltstone, up to 2 m thick, appear to have caused a concentration of shear movements during tectonic activity so that fault zones have developed parallel to the bedding. The common feature observed for all these faults is the presence of continuous clay filling with a thickness varying from a few mm to 200 mm. The cavern axis is intentionally oriented at right angles to the strike of these faults.

The measured in situ stresses in the rock mass surrounding the cavern are approximately

Maximum principal stress (horizontal) $\sigma_{max} = 10.9$ MPa

Minimum principal stress (vertical) $\sigma_{min} = 7.5$ MPa

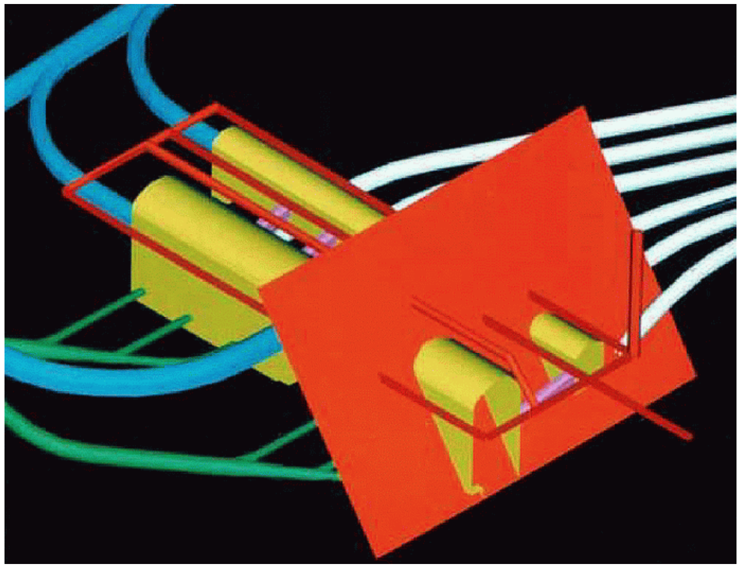

Figure 5: Orientation of the underground excavations in relation to the faults in the bedded sandstone surrounding the power cavern and transformer hall of the Mingtan Project. The red plane indicates the dip and strike of the faults.

Bedding faults of significant thickness which were intersected in the roof of the cavern were treated by using high pressure water jets to remove the clay and then filling the cavities with non shrink cementitious mortar (Cheng, 1987, Moy and Hoek, 1989). This was followed by the installation of 50 tonne capacity untensioned grouted cables from a drainage gallery 10 m above the cavern roof in order to create a pre-reinforced rock mass above the cavern. All of this work was carried out from construction adits before the main contract for the cavern excavation commenced.

The initial design of the reinforcing cables was based upon experience and precedent practice. Figures 6 and 7 give the lengths of rockbolts and cables in the roof and sidewalls of some typical large powerhouse caverns in weak rock masses. Plotted on the same graphs are empirical relationships suggested by Barton (1989) for bolt and cable lengths for underground powerhouses.

During benching down in the cavern, 112 tonne capacity tensioned and grouted cables were installed on a 3 m x 3 m grid in the sidewalls. The final layout of the cables in the rock surrounding the power cavern and the transformer hall is illustrated in Figure 8. Five metre long grouted rockbolts were installed as required at the centre of the squares formed by the cable face plates A 50 mm layer of steel fibre reinforced microsilica shotcrete was applied within 5 to 10 m of the face. This shotcrete was later built up to a thickness of 150 mm on the roof and upper sidewalls and 50 mm on the lower sidewalls where it would eventually be incorporated into the concrete foundations.

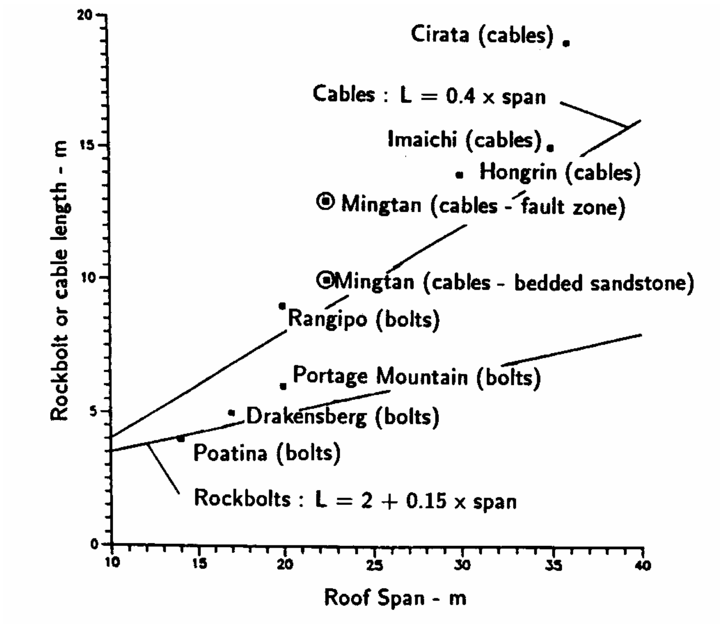

Figure 6: Lengths of rockbolts and cables used for roof support in some large caverns in weak rock. Equations defining trend lines were suggested by Barton (1989).

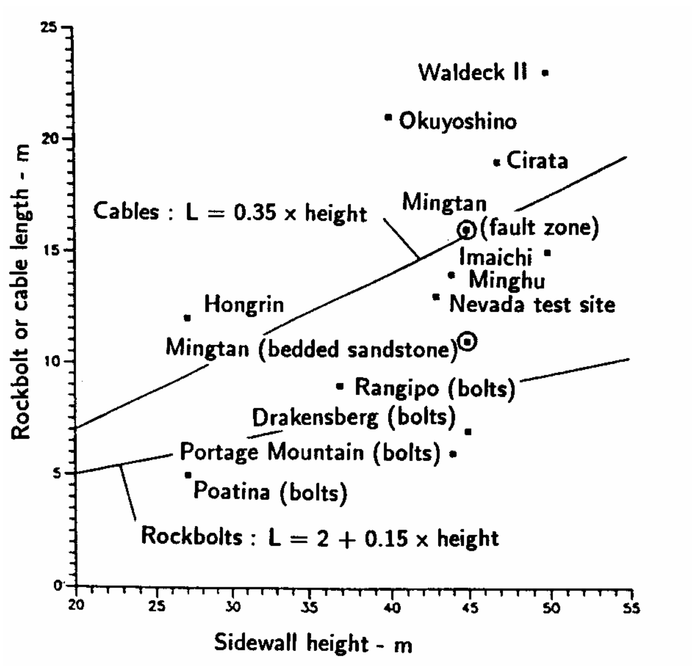

Figure 7: Lengths of rockbolts and cables used for sidewall support in some large caverns in weak rock. Equations defining trend lines were suggested by Barton (1989).

A key element in the decision making process on the adequacy of the support system was a monitoring and analysis process which involved the following steps :

1. Displacements in the rock surrounding the excavations monitored by means of convergence arrays and extensometers, some of which had been installed from construction galleries before excavation of the caverns commenced.

2. Numerical modelling of each excavation stage using non-linear multiple-material models. The material properties used in the models of the early excavation stages were adjusted to obtain the best match between predicted and measured displacements.

3. Prediction of displacements and support loads during future excavation stages and adjustment of support capacity, installation and pre-tensioning to control displacements and cable loads.

4. Measurement of displacements and cable loads (using load cells on selected cables which had been de-bonded) and comparison between measured and predicted displacements and cable loads.

5. Installation of additional cables or adjustment of cable loads to control unusual displacements or support loads.

The aim of this program was to maintain as uniform a displacement pattern around the excavations as possible and to keep the loads on the cables at less than 45% of their yield load. The intermediate rockbolts and the shotcrete were not accounted for in the numerical modelling since it was assumed that their role was confined to supporting the rock immediately adjacent to the excavations and that the overall stability was controlled by the 10 to 15 m long grouted cables.

Figure 8 shows the combination of materials used in analysing one section of the cavern, assuming that the bedding faults could be represented by horizontal layers in the two-dimensional model. In order to match the measured and predicted displacements in the rock mass, it was found that a 2.5 m thick zone of softened and weakened material had to be wrapped around the excavations to account for blast damaged material (achieving good blasting results was difficult in this interbedded rock).

In Figure 9, the predicted and measured displacements along six extensometers installed in the power cavern sidewalls are compared. The overall agreement is considered to be acceptable. Maximum sidewall displacements were of the order of 100 mm at the mid-height of the upstream wall, adjacent to one of the major faults. Elsewhere, displacements were of the order to 25 to 46 mm.

Figure 10 shows the results of monitoring at seven stations along the axis of the power cavern. Before excavation of the cavern commenced, extensometers were installed at each of these stations from a drainage gallery above the roof arch and from construction galleries as shown in the upper part of Figure 10. In addition, load cells were installed on cables adjacent to some of the extensometers.

Rapid responses were recorded in all extensometers and load cells as the top heading passed underneath them. Further responses occurred as the haunches of the cavern arch were excavated and as the first bench was removed. As can be seen from the plots, after this rapid response to the initial excavation stages, the displacements and cable loads became stable and showed very little tendency to increase with time. The difference in the magnitudes of the displacements and cable loads at different stations can be related to the proximity of the monitoring instruments to faults in the rock above the cavern arch.

The rapid load acceptance and the modest loading of the cables together with the control of the displacements in the rock mass were the goals of the support design. Measurements obtained from the extensometers and cable load cells indicate that these goals have been met.

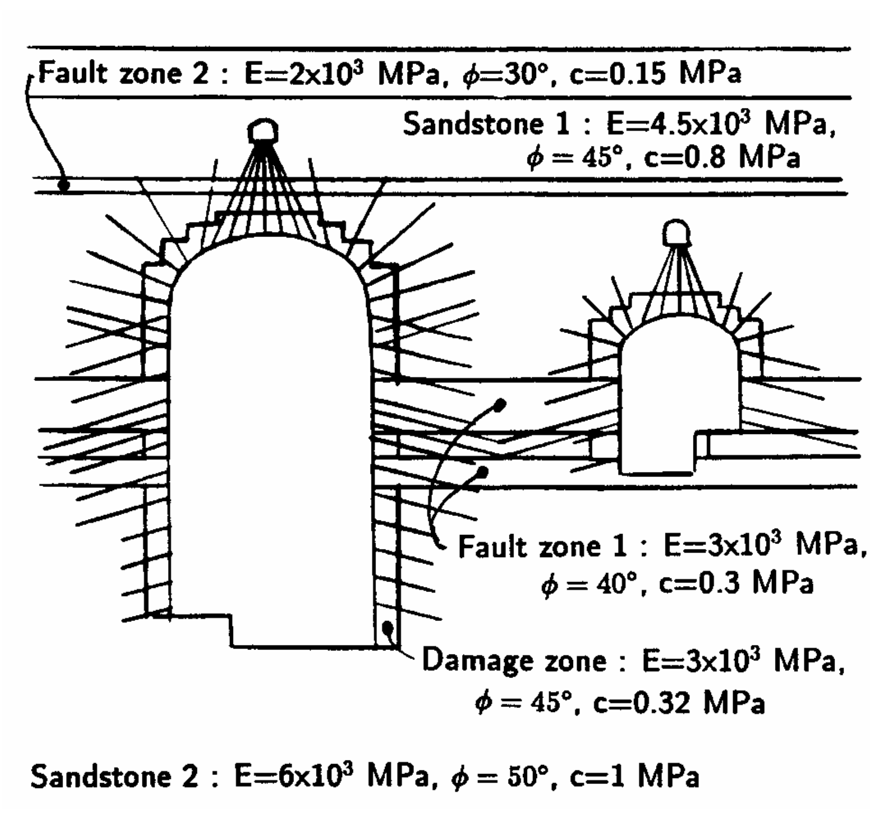

Figure 8: Layout of cables used to support the rock surrounding the power cavern and the transformer hall in the Mingtan pumped storage project. The location and properties of the rock units represent those used in the numerical analysis of failure, deformation and cable loading in a typical vertical section.

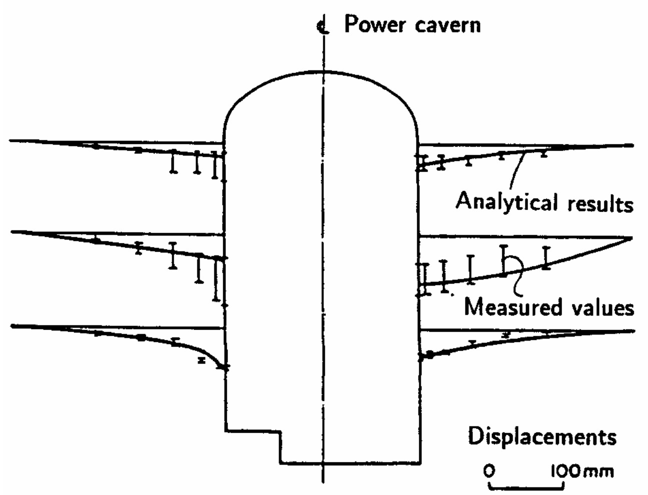

Figure 9: Comparison between calculated and measured displacements along six extensometers installed in the sidewalls of the Mingtan power cavern.

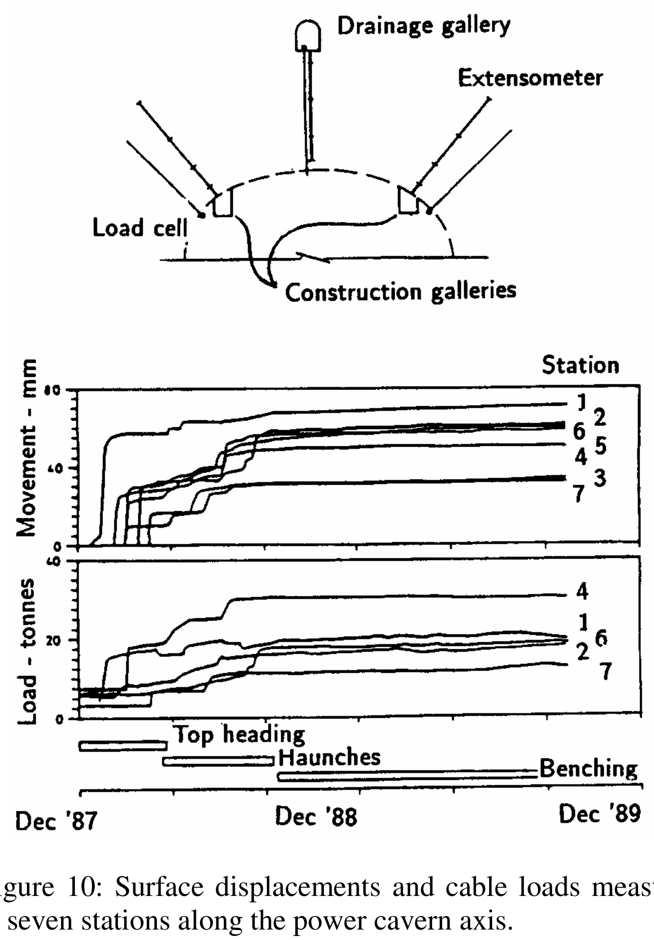

Figure 10: Surface displacements and cable loads measured at seven stations along the power cavern axis.

Factor of safety

The four case histories, discussed in previous sections, have been presented to demonstrate that a variety of criteria have to be considered in deciding upon the adequacy of a rock structure to perform its design objectives. This is true for any design in rock since the performance of each structure will be uniquely dependent upon the particular set of rock conditions, design loads and intended end use.

In one group of structures, traditional designs have been based upon a `factor of safety' against sliding. These structures, which include gravity and fill dams as well as rock and soil slopes, all involve the potential for sliding along well defined failure surfaces. The factor of safety is defined as the factor by which the shear strength parameters may be reduced in order to bring the slope (or dam foundation) into a state of limiting equilibrium (Morgenstern, 1991). The numerical value of the factor of safety chosen for a particular design depends upon the level of confidence which the designer has in the shear strength parameters, the groundwater pressures, the location of the critical failure surface and the magnitude of the external driving forces acting upon the structure.

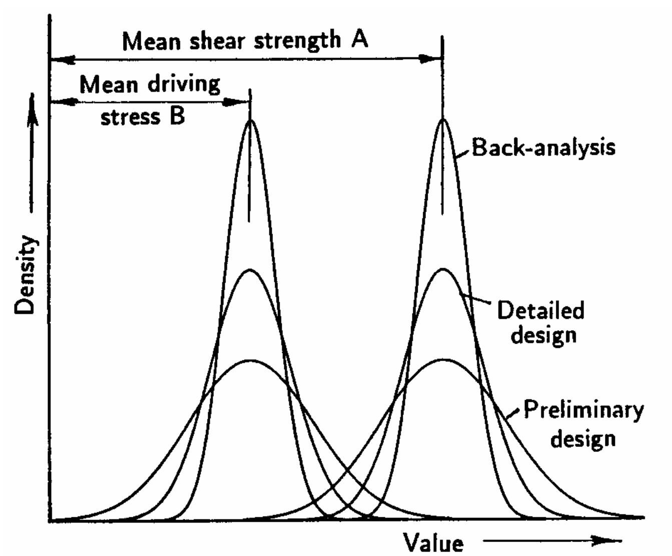

Figure 11: Hypothetical distribution curves representing the degree of uncertainty associated with information on driving stresses and shear strengths at different stages in the design of a structure such as a dam foundation.

Figure 11 illustrates a set of hypothetical distribution curves representing the degree of uncertainty associated with available information on shear strength parameters and disturbing stresses for different stages in the design of a rock or soil structure. The factor of safety is defined as A/B where A is the mean of the distribution of shear strength values and B is the mean of the distribution of driving stresses. For the purpose of this discussion, the same factor of safety has been assumed for all three cases illustrated.

During preliminary design studies, the amount of information available is usually very limited. Estimates of the shear strength of the rock or soil are generally based upon the judgement of an experienced engineer or geologist which may be supplemented, in some cases, by estimates based upon rock mass classifications or simple index tests. Similarly, the disturbing forces are not known with very much certainty since the location of the critical failure surface will not have been well defined and the magnitude of externally applied loads may not have been established. In the case of dam design, the magnitude of the probable maximum flood, which is usually based upon probabilistic analysis, frequently remains ill defined until very late in the design process.

For this case, the range of both available shear strength and disturbing stresses, which have to be considered, is large. If too low a factor of safety is used, there may be a significant probability of failure, represented by the section where the distribution curves overlap in Figure 11. In order to minimise this failure probability, a high value for the factor of safety is sometimes used. For example, in the 1977 edition of the US Bureau of Reclamation Engineering Monograph on Design Criteria for Concrete Arch and Gravity Dams, a factor of safety of 3.0 is recommended for normal loading conditions when 'only limited information is available on the strength parameters'. This value can be reduced to 2.0 when the strength parameters are 'determined by testing of core samples from a field investigation program or by past experience'.

During detailed design studies, the amount of information available is usually significantly greater than in the preliminary design stage discussed above. A comprehensive program of site investigations and laboratory or in situ shear strength tests will normally have been carried out and the external loads acting on the structure will have been better defined. In addition, studies of the groundwater flow and pressure distributions in the rock mass, together with modifications of these distributions by grouting and drainage, will usually have been carried out. Consequently, the ranges of shear strength and driving stress values, which have to be considered in the design, are smaller and the distribution curves are more tightly constrained.

The case histories of the Downie Slide and Dutchman's Ridge, discussed earlier, are good examples of designs based upon back-analyses. In both of these cases, very extensive site investigations and displacement monitoring had established the location of the critical failure surfaces with a high degree of certainty. Careful monitoring of the groundwater in the slopes (256 piezometer measuring points were installed in Dutchman's Ridge) had defined the water pressures in the slopes and their fluctuations over several years. Some shear testing on fault material recovered from cores was carried out but, more importantly, the mobilized shear strength along the potential failure surfaces was calculated by back-analysis, assuming a factor of safety of 1.00 for existing conditions.

Figure 11 illustrates the hypothetical distribution curves for the range of values for shear strength and driving stresses for the case of a structure in which an existing failure has been carefully back-analyzed. Depending upon the degree of care which has been taken with this back-analysis, these curves will be very tightly constrained and a low factor of safety can be used for the design of the remedial works.

This discussion illustrates the point that different factors of safety may be appropriate for different stages in the design of a rock structure. This difference is primarily dependent upon the level of confidence which the designer has in the values of shear strength to be included in the analysis. Hence, a critical question which arises in all of these cases is the determination or estimation of the shear strength along the potential sliding surface. In a paper on the strength of rockfill materials, Marachi, Chan and Seed (1972) summarize this problem as follows: 'No stability analysis, regardless of how intricate and theoretically exact it may be, can be useful for design if an incorrect estimation of the shearing strength of the construction material has been made'.

Except in simple cases involving homogeneous soils or planar continuous weak seams, determination of the shear strength along potential sliding surfaces is a notoriously difficult problem. This is particularly true of the determination of the cohesive component, *c'*, of the commonly used Mohr-Coulomb failure criterion. Laboratory test specimens tend to be too small to give representative results while in situ tests are difficult and expensive and, unless carried out with very great care, are liable to give unreliable results.

Table 7: Factors of safety for different loading in the design of earth and rockfill dams.

Loading condition	S.F.	Remarks
End of construction porewater pressures in the dam and undissipated porewater pressures in the foundation. No reservoir loading.	1.3	
Reservoir at full supply level with steady state seepage in the dam and undissipated end-of-construction porewater pressures in the foundation.	1.3	Possibly the most critical (even if rare) condition.
Reservoir at full supply level with steady state seepage.	1.5	Critical to design.
Reservoir at probable maximum flood level with steady state seepage conditions.	1.2	
Rapid reservoir drawdown from full supply level to minimum supply level	1.3	Not significant in design. Failures very rare and, if they occur, usually shallow.

For failure surfaces which involve sliding on rough or undulating rock surfaces such as joints or bedding planes, the methodology proposed by Barton (1976) is appropriate for estimating the overall shear strength of the potential sliding surface. This involves adding a measured or estimated roughness component to the basic frictional strength which can be determined on sawn and polished laboratory shear test specimens.

For heavily jointed rock masses in which there are no dominant weakness zones such as faults or shear zones, a crude estimate of the shear strength of the rock mass can be obtained by means of the use of rock mass classification systems as proposed by Hoek and Brown (1988).

In all cases, a greater reliance can be placed upon the frictional component, ϕ, of the Mohr-Coulomb shear strength equation and extreme care has to be taken in the estimation of the cohesive strength, c'. Where no reliable estimates of this value are available from carefully conducted shear tests or from back-analysis of existing failures, it is prudent to assume a cohesive strength of zero for any stability analysis involving structures such as dam foundations.

In the design of fill and gravity dams there is a tendency to move away from the high factors of safety of 2 or 3 which have been used in the past, provided that care is taken in choosing sensible conservative shear strength parameters, particularly for continuous weak seams in the foundations. An example of the range of factors of safety which can be used in the design of earth or rockfill dams is given in Table 7.

Probabilistic analyses

The uncertainty associated with the properties of geotechnical materials and the great care which has to be taken in selecting appropriate values for analyses has prompted several authors to suggest that the traditional deterministic methods of slope stability analyses should be replaced by probabilistic methods (Priest and Brown, 1983, McMahon, 1975, Vanmarcke, 1980, Morriss and Stoter, 1983, Read and Lye, 1983).

One branch of rock mechanics in which probabilistic analyses have been accepted for many years is that of the design of open pit mine slopes. This is because open pit planners are familiar with the concepts of risk analysis applied to ore grade and metal price fluctuations. Probabilistic methods are used in estimating the economic viability of various options in developing an open pit mine and so it is a small step to incorporate the probability of a geotechnical failure into the overall risk assessment of the mine. The mine planner has the choice of reducing the probability of failure by the installation of reinforcement, reducing the angle of the slope or accepting that failure will occur and providing for extra equipment which may be needed to clean up the failure. Since the mine is usually owned and operated by a single company and access to the mine benches is restricted to trained personnel, accepting a risk of failure and dealing with the consequences on a routine basis is a viable option.

On the other hand, the emotional impact of suggesting to the public that there is a finite risk of failure attached to a dam design is such that it is difficult to suggest the replacement of the standard factor of safety design approach with one which explicitly states a probability of failure or a coefficient of reliability. The current perception is that the factor of safety is more meaningful than the probability of failure. Even if this were not so, there is still the problem of deciding what probability of failure is acceptable for a rock structure to which the general public has access.

In spite of these difficulties, there does appear to be a slow but steady trend in society to accept the concepts of risk analysis more readily than has been the case in the past. The geotechnical community has an obligation to take note of these developments and to encourage the teaching and practical use of probabilistic as well as deterministic techniques with the aim of removing the cloak of mystery which surrounds the use of these methods.

Fortunately, there is a compromise solution which is a form of risk analysis used intuitively by most experienced engineers. This is a parametric analysis in which a wide range of possibilities are considered in a conventional deterministic analysis in order to gain a 'feel' for the sensitivity of the design. Hence, the factor of safety for a slope would be calculated for both fully drained and fully saturated groundwater conditions, for a range of friction angles and cohesive strengths covering the full spectrum which could be anticipated for the geological conditions existing on the site, for external forces ranging from zero to the maximum possible for that slope. The availability of user-friendly microcomputer software for most forms of limit equilibrium analysis means that these parametric studies can be carried out quickly and easily for most designs.

References

Amos, A.J., Granero Hernandez, A. and Rocca, R.J. 1981. Problemas de meteorizacion del geneis en la Presa Principal del complejo hidroeléctrico Río Grande I. *Proc. VIII Cong. Geol. Arg. Actas* **2,** 123-135.

Baker, D.G. 1991. Wahleach power tunnel monitoring. *Proc. 3rd Int. Symp. on Field Measurements in Geomechanics,* Oslo, Norway.

Barton, N. 1976. The shear strength of rock and rock joints. *Int. J. Rock Mech. Min. Sci. & Geomech. Abstr.* **13,** 1-24.

Barton, N. 1989. Cavern design for Hong Kong rocks. *Proc. Rock Cavern Seminar - Hong Kong* (eds A.W. Malone and P.G.D. Whiteside), 179-202. London: Instn Min. Metall.

Barton, N.R. 1976. The shear strength of rock and rock joints. *Int. J. Mech. Min. Sci. & Geomech. Abstr*. **13**(10), 1-24.

Barton, N.R., Lien, R. and Lunde, J. 1974. Engineering classification of rock masses for the design of tunnel support. *Rock Mech.* **6**(4), 189-239.

Bieniawski, Z.T. 1974. Estimating the strength of rock materials. *J. S. African Inst. Min. Metall* . **74** (8), 312-320.

Bieniawski, Z.T. 1974. Geomechanics classification of rock masses and its application in tunnelling. In *Advances in Rock Mechanics*, **2**, part A:27-32. Washington, D.C.: Nat. Acad. of Sciences.

Cheng, Y. 1987. New development in seam treatment of Feitsui arch dam foundation. *Proc. 6th Cong. ISRM, Montreal*, 319-326.

Hammett, R.D. and Hoek, E. 1981. Design of large underground caverns for hydroelectric projects, with reference to structurally controlled failure mechanisms. *Proc. American Soc. Civil Engrs. Int. Conf. on Recent Developments in Geotechnical Engineering for Hydro Projects.* 192-206. New York: ASCE.

Hoek E and Brown E.T. 1988. The Hoek-Brown failure criterion - a 1988 update. *Proc. 15th Canadian Rock Mech. Symp.* (ed. J.H. Curran), 31-38. Toronto: Civil Engineering Dept., University of Toronto.

Imrie, A.S. 1983. Taming the Downie Slide. *Canadian Geographic* **103**.

Imrie, A.S., Moore, D.P. and Enegren,E.G. 1992. Performance and maintenance of the drainage system at Downie Slide. *Proc. 6th Int. Symp. on Landslides,* Christchurch, New Zealand.

Lewis, M.R. and Moore, D.P. 1989. Construction of the Downie Slide and Dutchman's Ridge drainage adits. *Canadian Tunnelling* (ed. Z. Eisenstein), 163-172. Vancouver: Bi-Tech.

Liu, S.C., Cheng, Y. and Chang, C.T. 1988. Design of the Mingtan cavern. *Proc .symp. ISRM. on Rock Mech. and Power Plants, Madrid*, 199-208.

Marachi, N.D., Chan, C.K. and Seed, H.B. 1972. Evaluation of properties of rockfill materials. *J. Soil Mechs. Fdns. Div. ASCE* **98** (SM4), 95-114.

McMahon, B.K. 1975. Probability of failure and expected volume of failure in high rock slopes. *Proc. 2nd Aust.-New Zealand Conf. on Geomech., Brisbane*.

Moore, D.P., Imrie, A.S. and Baker, D.G.. 1991. Rockslide risk reduction using monitoring. *Proc. Can. Dam Safety Assn. Annual Meeting,* Whistler, British Columbia.

Moretto, O. 1982. Mecánica de rocas en el complejo hidroeléectrico Río Grande No. 1. *Proc. Primer. Cong. Sudamericano de Mecánica de Rocas, Bogotá, Colombia*.

Morgenstern, N.R. 1991. Limitations of stability analysis in geo-technical practice. *Geotecnia* **61**: 5-19.

Morriss, P. and Stoter, H.J. 1983. Open-cut slope design using probabilistic methods. *Proc. 5th. Cong. ISRM., Melbourne* **1** , C107-C113. Rotterdam: Balkema.

Moy, D. and Hoek, E. 1989. Progress with the excavation and support of the Mingtan power cavern roof. *Proc. Rock Cavern Seminar - Hong Kong* (eds A.W. Malone and P.G.D. Whiteside), 235-245. London: Instn Min. Metall.

Priest, S.D. and Brown, E.T. 1983. Probabilistic stability analysis of variable rock slopes. *Trans. Inst. Min. Metall.*(Sect. A) **92**: 1-12.

Read, J.R.L. and Lye, G.N. 1983. Pit slope design methods, Bougainville Copper Limited open cut. *Proc. 5th Cong. ISRM., Melbourne*, C93-C98. Rotterdam: Balkema.

Tatchell, G.E. 1991. Automatic data acquisition systems for monitoring dams and landslides. *Proc. 3rd Int. symp. on Field Measurements in Geomechanics,* Oslo, Norway.

Vanmarcke, E.H. 1980. Probabilistic analysis of earth slopes. *Engineering Geology* **16**: 29-50.

Rock mass classification

Introduction

During the feasibility and preliminary design stages of a project, when very little detailed information is available on the rock mass and its stress and hydrologic characteristics, the use of a rock mass classification scheme can be of considerable benefit. At its simplest, this may involve using the classification scheme as a check-list to ensure that all relevant information has been considered. At the other end of the spectrum, one or more rock mass classification schemes can be used to build up a picture of the composition and characteristics of a rock mass to provide initial estimates of support requirements, and to provide estimates of the strength and deformation properties of the rock mass.

It is important to understand the limitations of rock mass classification schemes (Palmstrom and Broch, 2006) and that their use does not (and cannot) replace some of the more elaborate design procedures. However, the use of these design procedures requires access to relatively detailed information on in situ stresses, rock mass properties and planned excavation sequence, none of which may be available at an early stage in the project. As this information becomes available, the use of the rock mass classification schemes should be updated and used in conjunction with site specific analyses.

Engineering rock mass classification

Rock mass classification schemes have been developing for over 100 years since Ritter (1879) attempted to formalise an empirical approach to tunnel design, in particular for determining support requirements. While the classification schemes are appropriate for their original application, especially if used within the bounds of the case histories from which they were developed, considerable caution must be exercised in applying rock mass classifications to other rock engineering problems.

Summaries of some important classification systems are presented in this chapter, and although every attempt has been made to present all of the pertinent data from the original texts, there are numerous notes and comments which cannot be included. The interested reader should make every effort to read the cited references for a full appreciation of the use, applicability and limitations of each system.

Most of the multi-parameter classification schemes (Wickham et al (1972) Bieniawski (1973, 1989) and Barton et al (1974)) were developed from civil engineering case histories in which all of the components of the engineering geological character of the rock mass were included. In underground hard rock mining, however, especially at deep levels, rock mass weathering and the influence of water usually are not significant and may be ignored. Different classification systems place different emphases on the various parameters, and it is recommended that at least two methods be used at any site during the early stages of a project.

Terzaghi's rock mass classification

The earliest reference to the use of rock mass classification for the design of tunnel support is in a paper by Terzaghi (1946) in which the rock loads, carried by steel sets, are estimated on the basis of a descriptive classification. While no useful purpose would be served by including details of Terzaghi's classification in this discussion on the design of support, it is interesting to examine the rock mass descriptions included in his original paper, because he draws attention to those characteristics that dominate rock mass behaviour, particularly in situations where gravity constitutes the dominant driving force. The clear and concise definitions and the practical comments included in these descriptions are good examples of the type of engineering geology information, which is most useful for engineering design.

Terzaghi's descriptions (quoted directly from his paper) are:

- *Intact* rock contains neither joints nor hair cracks. Hence, if it breaks, it breaks across sound rock. On account of the injury to the rock due to blasting, spalls may drop off the roof several hours or days after blasting. This is known as a *spalling* condition. Hard, intact rock may also be encountered in the *popping* condition involving the spontaneous and violent detachment of rock slabs from the sides or roof.
- *Stratified* rock consists of individual strata with little or no resistance against separation along the boundaries between the strata. The strata may or may not be weakened by transverse joints. In such rock the spalling condition is quite common.
- *Moderately jointed* rock contains joints and hair cracks, but the blocks between joints are locally grown together or so intimately interlocked that vertical walls do not require lateral support. In rocks of this type, both spalling and popping conditions may be encountered.
- *Blocky and seamy* rock consists of chemically intact or almost intact rock fragments which are entirely separated from each other and imperfectly interlocked. In such rock, vertical walls may require lateral support.
- *Crushed* but chemically intact rock has the character of crusher run. If most or all of the fragments are as small as fine sand grains and no recementation has taken place, crushed rock below the water table exhibits the properties of a water-bearing sand.
- *Squeezing* rock slowly advances into the tunnel without perceptible volume increase. A prerequisite for squeeze is a high percentage of microscopic and sub-microscopic particles of micaceous minerals or clay minerals with a low swelling capacity.
- *Swelling* rock advances into the tunnel chiefly on account of expansion. The capacity to swell seems to be limited to those rocks that contain clay minerals such as montmorillonite, with a high swelling capacity.

Classifications involving stand-up time

Lauffer (1958) proposed that the stand-up time for an unsupported span is related to the quality of the rock mass in which the span is excavated. In a tunnel, the unsupported span is defined as the span of the tunnel or the distance between the face and the nearest support, if this is greater than the tunnel span. Lauffer's original classification has since been modified by a number of authors, notably Pacher et al (1974), and now forms part of the general tunnelling approach known as the New Austrian Tunnelling Method.

The significance of the stand-up time concept is that an increase in the span of the tunnel leads to a significant reduction in the time available for the installation of support. For example, a small pilot tunnel may be successfully constructed with minimal support, while a larger span tunnel in the same rock mass may not be stable without the immediate installation of substantial support.

The New Austrian Tunnelling Method includes a number of techniques for safe tunnelling in rock conditions in which the stand-up time is limited before failure occurs. These techniques include the use of smaller headings and benching or the use of multiple drifts to form a reinforced ring inside which the bulk of the tunnel can be excavated. These techniques are applicable in soft rocks such as shales, phyllites and mudstones in which the squeezing and swelling problems, described by Terzaghi (see previous section), are likely to occur. The techniques are also applicable when tunnelling in excessively broken rock, but great care should be taken in attempting to apply these techniques to excavations in hard rocks in which different failure mechanisms occur.

In designing support for hard rock excavations it is prudent to assume that the stability of the rock mass surrounding the excavation is not time-dependent. Hence, if a structurally defined wedge is exposed in the roof of an excavation, it will fall as soon as the rock supporting it is removed. This can occur at the time of the blast or during the subsequent scaling operation. If it is required to keep such a wedge in place, or to enhance the margin of safety, it is essential that the support be installed as early as possible, preferably before the rock supporting the full wedge is removed. On the other hand, in a highly stressed rock, failure will generally be induced by some change in the stress field surrounding the excavation. The failure may occur gradually and manifest itself as spalling or slabbing or it may occur suddenly in the form of a rock burst. In either case, the support design must take into account the change in the stress field rather than the ‘stand-up’ time of the excavation.

Rock quality designation index (RQD)

The Rock Quality Designation index (*RQD*) was developed by Deere (Deere et al 1967) to provide a quantitative estimate of rock mass quality from drill core logs. RQD is defined as the percentage of intact core pieces longer than 100 mm (4 inches) in the total length of core. The core should be at least NW size (54.7 mm or 2.15 inches in diameter) and should be drilled with a double-tube core barrel. The correct procedures for measurement of the length of core pieces and the calculation of *RQD* are summarised in Figure 1.

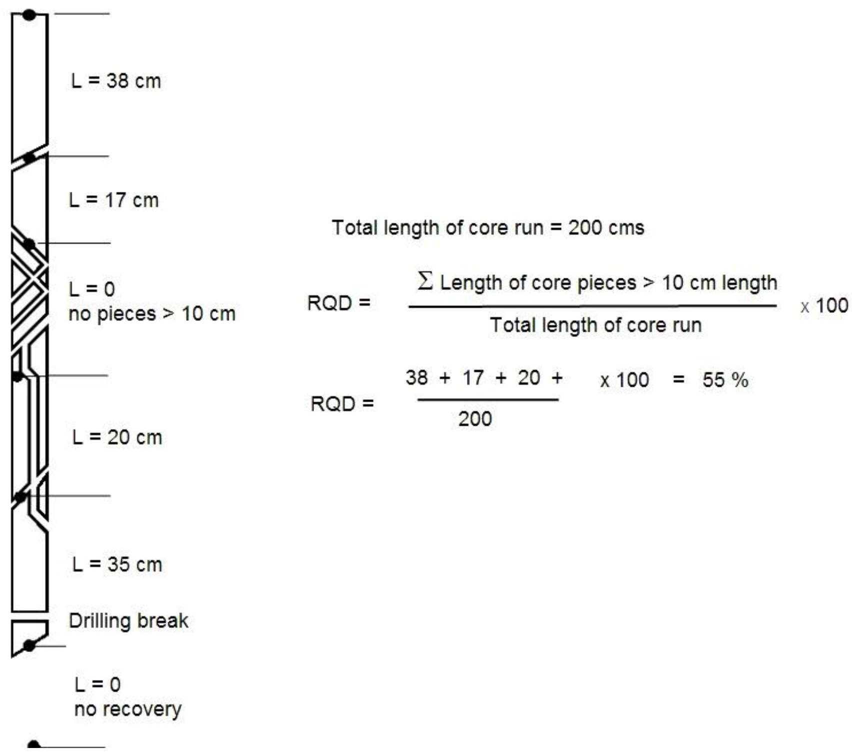

Figure 1: Procedure for measurement and calculation of *RQD* (After Deere, 1989).

Palmström (1982) suggested that, when no core is available but discontinuity traces are visible in surface exposures or exploration adits, the *RQD* may be estimated from the number of discontinuities per unit volume. The suggested relationship for clay-free rock masses is:

$$RQD = 115 - 3.3\, J_V \qquad (1)$$

where J_V is the sum of the number of joints per unit length for all joint (discontinuity) sets known as the volumetric joint count.

RQD is a directionally dependent parameter and its value may change significantly, depending upon the borehole orientation. The use of the volumetric joint count can be quite useful in reducing this directional dependence.

RQD is intended to represent the rock mass quality in situ. When using diamond drill core, care must be taken to ensure that fractures, which have been caused by handling or the drilling process, are identified and ignored when determining the value of *RQD*.

When using Palmström's relationship for exposure mapping, blast induced fractures should not be included when estimating J_V.

Deere's *RQD* was widely used, particularly in North America, after its introduction. Cording and Deere (1972), Merritt (1972) and Deere and Deere (1988) attempted to relate *RQD* to Terzaghi's rock load factors and to rockbolt requirements in tunnels. In the context of this discussion, the most important use of *RQD* is as a component of the *RMR* and *Q* rock mass classifications covered later in this chapter.

Rock Structure Rating (RSR)

Wickham et al (1972) described a quantitative method for describing the quality of a rock mass and for selecting appropriate support on the basis of their Rock Structure Rating (*RSR*) classification. Most of the case histories, used in the development of this system, were for relatively small tunnels supported by means of steel sets, although historically this system was the first to make reference to shotcrete support. In spite of this limitation, it is worth examining the *RSR* system in some detail since it demonstrates the logic involved in developing a quasi-quantitative rock mass classification system.

The significance of the *RSR* system, in the context of this discussion, is that it introduced the concept of rating each of the components listed below to arrive at a numerical value of $RSR = A + B + C$.

1. *Parameter A, Geology:* General appraisal of geological structure on the basis of:
   a. Rock type origin (igneous, metamorphic, sedimentary).
   b. Rock hardness (hard, medium, soft, decomposed).
   c. Geologic structure (massive, slightly faulted/folded, moderately faulted/folded, intensely faulted/folded).
2. *Parameter B, Geometry*: Effect of discontinuity pattern with respect to the direction of the tunnel drive on the basis of:
   a. Joint spacing.
   b. Joint orientation (strike and dip).
   c. Direction of tunnel drive.
3. *Parameter C*: Effect of groundwater inflow and joint condition on the basis of:
   a. Overall rock mass quality on the basis of A and B combined.
   b. Joint condition (good, fair, poor).
   c. Amount of water inflow (in gallons per minute per 1000 feet of tunnel).

Note that the *RSR* classification used Imperial units and that these units have been retained in this discussion.

Three tables from Wickham et al's 1972 paper are reproduced in Tables 1, 2 and 3. These tables can be used to evaluate the rating of each of these parameters to arrive at the *RSR* value (maximum *RSR* = 100).

Table 1: Rock Structure Rating: Parameter A: General area geology

	Basic Rock Type				Geological Structure			
	Hard	Medium	Soft	Decomposed				
Igneous	1	2	3	4		Slightly Folded or Faulted	Moderately Folded or Faulted	Intensively Folded or Faulted
Metamorphic	1	2	3	4				
Sedimentary	2	3	4	4	Massive			
Type 1					30	22	15	9
Type 2					27	20	13	8
Type 3					24	18	12	7
Type 4					19	15	10	6

Table 2: Rock Structure Rating: Parameter *B*: Joint pattern, direction of drive

	Strike ⊥ to Axis					Strike || to Axis		
	Direction of Drive					Direction of Drive		
	Both	With Dip		Against Dip		Either direction		
	Dip of Prominent Joints [a]					Dip of Prominent Joints		
Average joint spacing	Flat	Dipping	Vertical	Dipping	Vertical	Flat	Dipping	Vertical
1. Very closely jointed, < 2 in	9	11	13	10	12	9	9	7
2. Closely jointed, 2-6 in	13	16	19	15	17	14	14	11
3. Moderately jointed, 6-12 in	23	24	28	19	22	23	23	19
4. Moderate to blocky, 1-2 ft	30	32	36	25	28	30	28	24
5. Blocky to massive, 2-4 ft	36	38	40	33	35	36	24	28
6. Massive, > 4 ft	40	43	45	37	40	40	38	34

Table 3: Rock Structure Rating: Parameter *C*: Groundwater, joint condition

	Sum of Parameters *A* + *B*					
	13 - 44			45 - 75		
Anticipated water inflow	Joint Condition [b]					
gpm/1000 ft of tunnel	Good	Fair	Poor	Good	Fair	Poor
None	22	18	12	25	22	18
Slight, < 200 gpm	19	15	9	23	19	14
Moderate, 200-1000 gpm	15	22	7	21	16	12
Heavy, > 1000 gp	10	8	6	18	14	10

[a] Dip: flat: 0-20°; dipping: 20-50°; and vertical: 50-90°

[b] Joint condition: good = tight or cemented; fair = slightly weathered or altered; poor = severely weathered, altered or open

For example, a hard metamorphic rock which is slightly folded or faulted has a rating of *A* = 22 (from Table 1). The rock mass is moderately jointed, with joints striking perpendicular to the tunnel axis which is being driven east-west, and dipping at between 20° and 50°.

Table 2 gives the rating for *B* = 24 for driving with dip (defined below).

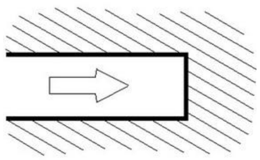

Drive with dip

The value of *A* + *B* = 46 and this means that, for joints of fair condition (slightly weathered and altered) and a moderate water inflow of between 200 and 1,000 gallons per minute, Table 3 gives the rating for *C* = 16. Hence, the final value of the rock structure rating *RSR* = *A* + *B* + *C* = 62.

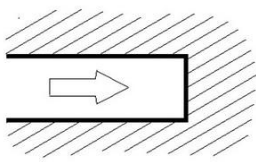

Drive against dip

A typical set of prediction curves for a 24 foot diameter tunnel are given in Figure 2 which shows that, for the *RSR* value of 62 derived above, the predicted support would be 2 inches of shotcrete and 1 inch diameter rockbolts spaced at 5 foot centres. As indicated in the figure, steel sets would be spaced at more than 7 feet apart and would not be considered a practical solution for the support of this tunnel.

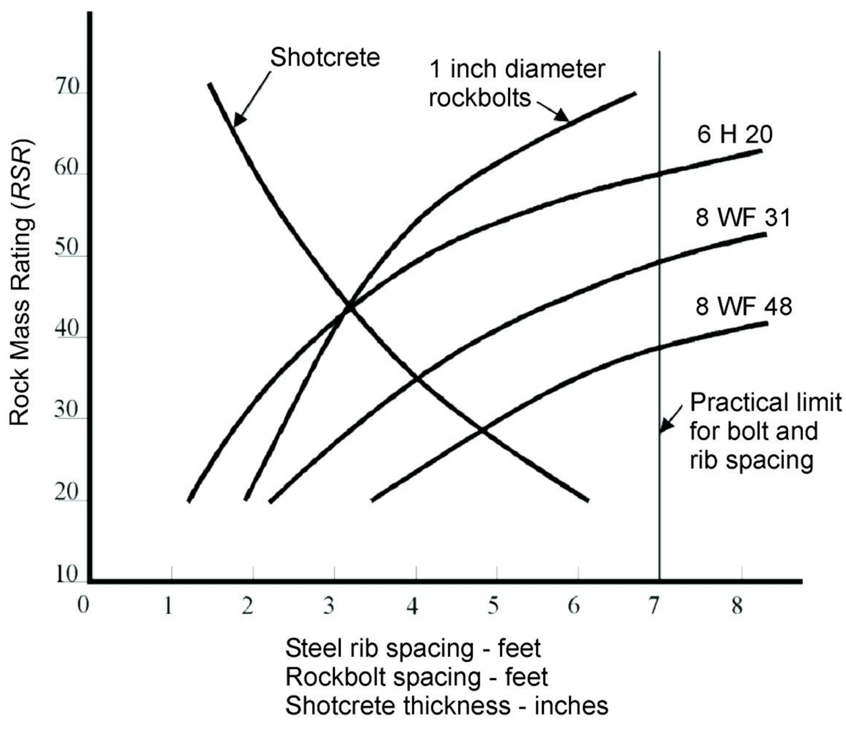

Figure 2: *RSR* support estimates for a 24 ft. (7.3 m) diameter circular tunnel. Note that rockbolts and shotcrete are generally used together. (After Wickham et al 1972).

For the same size tunnel in a rock mass with *RSR* = 30, the support could be provided by 8 WF 31 steel sets (8 inch deep wide flange I section weighing 31 lb per foot) spaced 3 feet apart, or by 5 inches of shotcrete and 1 inch diameter rockbolts spaced at 2.5 feet centres. In this case it is probable that the steel set solution would be cheaper and more effective than the use of rockbolts and shotcrete.

Although the *RSR* classification system is not widely used today, Wickham et al's work played a significant role in the development of the classification schemes discussed in the remaining sections of this chapter.

Geomechanics Classification

Bieniawski (1976) published the details of a rock mass classification called the Geomechanics Classification or the Rock Mass Rating (*RMR*) system. Over the years, this system has been successively refined as more case records have been examined and the reader should be aware that Bieniawski has made significant changes in the ratings assigned to different parameters. The discussion which follows is based upon the 1989 version of the classification (Bieniawski, 1989). Both this version and the 1976 version deal with estimating the strength of rock masses. The following six parameters are used to classify a rock mass using the *RMR* system:

1. Uniaxial compressive strength of rock material.
2. Rock Quality Designation (*RQD*).
3. Spacing of discontinuities.
4. Condition of discontinuities.
5. Groundwater conditions.
6. Orientation of discontinuities.

In applying this classification system, the rock mass is divided into a number of structural regions and each region is classified separately. The boundaries of the structural regions usually coincide with a major structural feature such as a fault or with a change in rock type. In some cases, significant changes in discontinuity spacing or characteristics, within the same rock type, may necessitate the division of the rock mass into a number of small structural regions.

The Rock Mass Rating system is presented in Table 4, giving the ratings for each of the six parameters listed above. These ratings are summed to give a value of *RMR*. The following example illustrates the use of these tables to arrive at an *RMR* value.

A tunnel is to be driven through slightly weathered granite with a dominant joint set dipping at 60^{o} against the direction of the drive. Index testing and logging of diamond drilled core give typical Point-load strength index values of 8 MPa and average *RQD* values of 70%. The slightly rough and slightly weathered joints with a separation of < 1 mm, are spaced at 300 mm. Tunnelling conditions are anticipated to be wet.

Table 4: Rock Mass Rating System (After Bieniawski 1989).

A. CLASSIFICATION PARAMETERS AND THEIR RATINGS									
	Parameter		Range of values						
1	Strength of intact rock material	Point-load strength index	>10 MPa	4 - 10 MPa	2 - 4 MPa	1 - 2 MPa	For this low range - uniaxial compressive test is preferred		
		Uniaxial comp. strength	>250 MPa	100 - 250 MPa	50 - 100 MPa	25 - 50 MPa	5 - 25 MPa	1 - 5 MPa	< 1 MPa
	Rating		15	12	7	4	2	1	0
2	Drill core Quality *RQD*		90% - 100%	75% - 90%	50% - 75%	25% - 50%	< 25%		
	Rating		20	17	13	8	3		
3	Spacing of discontinuities		> 2 m	0.6 - 2 . m	200 - 600 mm	60 - 200 mm	< 60 mm		
	Rating		20	15	10	8	5		
4	Condition of discontinuities (See E)		Very rough surfaces Not continuous No separation Unweathered wall rock	Slightly rough surfaces Separation < 1 mm Slightly weathered walls	Slightly rough surfaces Separation < 1 mm Highly weathered walls	Slickensided surfaces or Gouge < 5 mm thick or Separation 1-5 mm Continuous	Soft gouge >5 mm thick or Separation > 5 mm Continuous		
	Rating		30	25	20	10	0		
5	Groundwater	Inflow per 10 m tunnel length (l/m)	None	< 10	10 - 25	25 - 125	> 125		
		(Joint water press)/ (Major principal σ)	0	< 0.1	0.1, - 0.2	0.2 - 0.5	> 0.5		
		General conditions	Completely dry	Damp	Wet	Dripping	Flowing		
	Rating		15	10	7	4	0		

B. RATING ADJUSTMENT FOR DISCONTINUITY ORIENTATIONS (See F)						
Strike and dip orientations		Very favourable	Favourable	Fair	Unfavourable	Very Unfavourable
Ratings	Tunnels & mines	0	-2	-5	-10	-12
	Foundations	0	-2	-7	-15	-25
	Slopes	0	-5	-25	-50	
C. ROCK MASS CLASSES DETERMINED FROM TOTAL RATINGS						
Rating		100 ← 81	80 ← 61	60 ← 41	40 ← 21	< 21
Class number		I	II	III	IV	V
Description		Very good rock	Good rock	Fair rock	Poor rock	Very poor rock
D. MEANING OF ROCK CLASSES						
Class number		I	II	III	IV	V
Average stand-up time		20 yrs for 15 m span	1 year for 10 m span	1 week for 5 m span	10 hrs for 2.5 m span	30 min for 1 m span
Cohesion of rock mass (kPa)		> 400	300 - 400	200 - 300	100 - 200	< 100
Friction angle of rock mass (deg)		> 45	35 - 45	25 - 35	15 - 25	< 15
E. GUIDELINES FOR CLASSIFICATION OF DISCONTINUITY conditions						
Discontinuity length (persistence)		< 1 m	1 - 3 m	3 - 10 m	10 - 20 m	> 20 m
Rating		6	4	2	1	0
Separation (aperture)		None	< 0.1 mm	0.1 - 1.0 mm	1 - 5 mm	> 5 mm
Rating		6	5	4	1	0
Roughness		Very rough	Rough	Slightly rough	Smooth	Slickensided
Rating		6	5	3	1	0
Infilling (gouge)		None	Hard filling < 5 mm	Hard filling > 5 mm	Soft filling < 5 mm	Soft filling > 5 mm
Rating		6	4	2	2	0
Weathering		Unweathered	Slightly weathered	Moderately weathered	Highly weathered	Decomposed
Ratings		6	5	3	1	0

F. EFFECT OF DISCONTINUITY STRIKE AND DIP ORIENTATION IN TUNNELLING**			
Strike perpendicular to tunnel axis		Strike parallel to tunnel axis	
Drive with dip - Dip 45 - 90°	Drive with dip - Dip 20 - 45°	Dip 45 - 90°	Dip 20 - 45°
Very favourable	Favourable	Very unfavourable	Fair
Drive against dip - Dip 45-90°	Drive against dip - Dip 20-45°	Dip 0-20 - Irrespective of strike°	
Fair	Unfavourable	Fair	

* Some conditions are mutually exclusive . For example, if infilling is present, the roughness of the surface will be overshadowed by the influence of the gouge. In such cases use A.4 directly.

** Modified after Wickham et al (1972).

The *RMR* value for the example under consideration is determined as follows:

Table	*Item*	*Value*	*Rating*
4: A.1	Point load index	8 MPa	12
4: A.2	*RQD*	70%	13
4: A.3	Spacing of discontinuities	300 mm	10
4: E.4	Condition of discontinuities	Note 1	22
4: A.5	Groundwater	Wet	7
4: B	Adjustment for joint orientation	Note 2	-5
		Total	59

Note 1. For slightly rough and altered discontinuity surfaces with a separation of < 1 mm, Table 4.A.4 gives a rating of 25. When more detailed information is available, Table 4.E can be used to obtain a more refined rating. Hence, in this case, the rating is the sum of: 4 (1-3 m discontinuity length), 4 (separation 0.1-1.0 mm), 3 (slightly rough), 6 (no infilling) and 5 (slightly weathered) = 22.

Note 2. Table 4.F gives a description of 'Fair' for the conditions assumed where the tunnel is to be driven against the dip of a set of joints dipping at 60^{o}. Using this description for 'Tunnels and Mines' in Table 4.B gives an adjustment rating of -5.

Bieniawski (1989) published a set of guidelines for the selection of support in tunnels in rock for which the value of *RMR* has been determined. These guidelines are reproduced in Table 4. Note that these guidelines have been published for a 10 m span horseshoe shaped tunnel, constructed using drill and blast methods, in a rock mass subjected to a vertical stress < 25 MPa (equivalent to a depth below surface of <900 m).

For the case considered earlier, with *RMR* = 59, Table 4 suggests that a tunnel could be excavated by top heading and bench, with a 1.5 to 3 m advance in the top heading. Support should be installed after each blast and the support should be placed at a maximum distance of 10 m from the face. Systematic rock bolting, using 4 m long 20 mm diameter fully grouted bolts spaced at 1.5 to 2 m in the crown and walls, is recommended. Wire mesh, with 50 to 100 mm of shotcrete for the crown and 30 mm of shotcrete for the walls, is recommended.

The value of *RMR* of 59 indicates that the rock mass is on the boundary between the 'Fair rock' and 'Good rock' categories. In the initial stages of design and construction, it is advisable to utilise the support suggested for fair rock. If the construction is progressing well with no stability problems, and the support is performing very well, then it should be possible to gradually reduce the support requirements to those indicated for a good rock mass. In addition, if the excavation is required to be stable for a short amount of time, then it is advisable to try the less expensive and extensive support suggested for good rock. However, if the rock mass surrounding the excavation is expected to undergo large mining induced stress changes, then more substantial support appropriate for fair rock should be installed. This example indicates that a great deal of judgement is needed in the application of rock mass classification to support design.

Table 5: Guidelines for excavation and support of 10 m span rock tunnels in accordance with the *RMR* system (After Bieniawski 1989).

Rock mass class	Excavation	Rock bolts (20 mm diameter, fully grouted)	Shotcrete	Steel sets
I - Very good rock *RMR*: 81-100	Full face, 3 m advance.	Generally no support required except spot bolting.		
II - Good rock *RMR*: 61-80	Full face , 1-1.5 m advance. Complete support 20 m from face.	Locally, bolts in crown 3 m long, spaced 2.5 m with occasional wire mesh.	50 mm in crown where required.	None.
III - Fair rock *RMR*: 41-60	Top heading and bench 1.5-3 m advance in top heading. Commence support after each blast. Complete support 10 m from face.	Systematic bolts 4 m long, spaced 1.5 - 2 m in crown and walls with wire mesh in crown.	50-100 mm in crown and 30 mm in sides.	None.
IV - Poor rock *RMR*: 21-40	Top heading and bench 1.0-1.5 m advance in top heading. Install support concurrently with excavation, 10 m from face.	Systematic bolts 4-5 m long, spaced 1-1.5 m in crown and walls with wire mesh.	100-150 mm in crown and 100 mm in sides.	Light to medium ribs spaced 1.5 m where required.
V – Very poor rock *RMR*: < 20	Multiple drifts 0.5-1.5 m advance in top heading. Install support concurrently with excavation. Shotcrete as soon as possible after blasting.	Systematic bolts 5-6 m long, spaced 1-1.5 m in crown and walls with wire mesh. Bolt invert.	150-200 mm in crown, 150 mm in sides, and 50 mm on face.	Medium to heavy ribs spaced 0.75 m with steel lagging and forepoling if required. Close invert.

It should be noted that Table 5 has not had a major revision since 1973. In many mining and civil engineering applications, steel fibre reinforced shotcrete may be considered in place of wire mesh and shotcrete.

Modifications to *RMR* for mining

Bieniawski's Rock Mass Rating (*RMR*) system was originally based upon case histories drawn from civil engineering. Consequently, the mining industry tended to regard the classification as somewhat conservative and several modifications have been proposed in order to make the classification more relevant to mining applications. A comprehensive summary of these modifications was compiled by Bieniawski (1989).

Laubscher (1977, 1984), Laubscher and Taylor (1976) and Laubscher and Page (1990) have described a Modified Rock Mass Rating system for mining. This MRMR system takes the basic *RMR* value, as defined by Bieniawski, and adjusts it to account for in situ and induced stresses, stress changes and the effects of blasting and weathering. A set of support recommendations is associated with the resulting *MRMR* value. In using Laubscher's *MRMR* system it should be borne in mind that many of the case histories upon which it is based are derived from caving operations. Originally, block caving in asbestos mines in Africa formed the basis for the modifications but, subsequently, other case histories from around the world have been added to the database.

Cummings et al (1982) and Kendorski et al (1983) have also modified Bieniawski's RMR classification to produce the *MBR* (modified basic *RMR*) system for mining. This system was developed for block caving operations in the USA. It involves the use of different ratings for the original parameters used to determine the value of *RMR* and the subsequent adjustment of the resulting *MBR* value to allow for blast damage, induced stresses, structural features, distance from the cave front and size of the caving block. Support recommendations are presented for isolated or development drifts as well as for the final support of intersections and drifts.

Rock Tunnelling Quality Index, *Q*

On the basis of an evaluation of a large number of case histories of underground excavations, Barton et al (1974) of the Norwegian Geotechnical Institute proposed a Tunnelling Quality Index (*Q*) for the determination of rock mass characteristics and tunnel support requirements. The numerical value of the index *Q* varies on a logarithmic scale from 0.001 to a maximum of 1,000 and is defined by:

$$Q = \frac{RQD}{J_n} \times \frac{J_r}{J_a} \times \frac{J_w}{SRF} \tag{2}$$

where *RQD* is the Rock Quality Designation
J_n is the joint set number
J_r is the joint roughness number
J_a is the joint alteration number
J_w is the joint water reduction factor
SRF is the stress reduction factor

In explaining the meaning of the parameters used to determine the value of *Q*, Barton et al (1974) offer the following comments:

> *The first quotient* (RQD/J_n), representing the structure of the rock mass, is a crude measure of the block or particle size, with the two extreme values (100/0.5 and 10/20) differing by a factor of 400. If the quotient is interpreted in units of centimetres, the extreme 'particle sizes' of 200 to 0.5 cm are seen to be crude but fairly realistic approximations. Probably the largest blocks should be several times this size and the smallest fragments less than half the size. (Clay particles are of course excluded).
>
> The second quotient (J_r/J_a) represents the roughness and frictional characteristics of the joint walls or filling materials. This quotient is weighted in favour of rough, unaltered joints in direct contact. It is to be expected that such surfaces will be close to peak strength, that they will dilate strongly when sheared, and they will therefore be especially favourable to tunnel stability.
>
> When rock joints have thin clay mineral coatings and fillings, the strength is reduced significantly. Nevertheless, rock wall contact after small shear displacements have occurred may be a very important factor for preserving the excavation from ultimate failure.

Where no rock wall contact exists, the conditions are extremely unfavourable to tunnel stability. The 'friction angles' (given in Table 6) are a little below the residual strength values for most clays, and are possibly down-graded by the fact that these clay bands or fillings may tend to consolidate during shear, at least if normal consolidation or if softening and swelling has occurred. The swelling pressure of montmorillonite may also be a factor here.

The third quotient (J_w/SRF) consists of two stress parameters. *SRF* is a measure of: 1) loosening load in the case of an excavation through shear zones and clay bearing rock, 2) rock stress in competent rock, and 3) squeezing loads in plastic incompetent rocks. It can be regarded as a total stress parameter. The parameter J_w is a measure of water pressure, which has an adverse effect on the shear strength of joints due to a reduction in effective normal stress. Water may, in addition, cause softening and possible out-wash in the case of clay-filled joints. It has proved impossible to combine these two parameters in terms of inter-block effective stress, because paradoxically a high value of effective normal stress may sometimes signify less stable conditions than a low value, despite the higher shear strength. The quotient (J_w/SRF) is a complicated empirical factor describing the 'active stress'.

It appears that the rock tunnelling quality *Q* can now be considered to be a function of only three parameters which are crude measures of:

1. Block size	(*RQD/Jn*)
2. Inter-block shear strength	(*Jr/ Ja*)
3. Active stress	(*Jw/SRF*)

Undoubtedly, there are several other parameters which could be added to improve the accuracy of the classification system. One of these would be the joint orientation. Although many case records include the necessary information on structural orientation in relation to excavation axis, it was not found to be the important general parameter that might be expected. Part of the reason for this may be that the orientations of many types of excavations can be, and normally are, adjusted to avoid the maximum effect of unfavourably oriented major joints. However, this choice is not available in the case of tunnels, and more than half the case records were in this category. The parameters *Jn*, *Jr* and *Ja* appear to play a more important role than orientation, because the number of joint sets determines the degree of freedom for block movement (if any), and the frictional and dilational characteristics can vary more than the down-dip gravitational component of unfavourably oriented joints. If joint orientations had been included the classification would have been less general, and its essential simplicity lost.

Table 6 (After Barton et al 1974) gives the classification of individual parameters used to obtain the Tunnelling Quality Index *Q* for a rock mass.

The use of Table 6 is illustrated in the following example. A 15 m span crusher chamber for an underground mine is to be excavated in a norite at a depth of 2,100 m below surface. The rock mass contains two sets of joints controlling stability. These joints are undulating, rough and unweathered with very minor surface staining. *RQD* values range from 85% to 95% and laboratory tests on core samples of intact rock give an average uniaxial compressive strength of 170 MPa. The principal stress directions are approximately vertical and horizontal and the magnitude of the horizontal principal stress is approximately 1.5 times that of the vertical principal stress. The rock mass is locally damp but there is no evidence of flowing water.

The numerical value of *RQD* is used directly in the calculation of *Q* and, for this rock mass, an average value of 90 will be used. Table 6.2 shows that, for two joint sets, the joint set number, *Jn* = 4. For rough or irregular joints which are undulating, Table 6.3 gives a joint roughness number of *Jr* = 3. Table 6.4 gives the joint alteration number, *Ja* = 1.0, for unaltered joint walls with surface staining only. Table 6.5 shows that, for an excavation with minor inflow, the joint water reduction factor, *Jw* = 1.0. For a depth below surface of 2,100 m the overburden stress will be approximately 57 MPa and, in this case, the major principal stress σ_1 = 85 MPa. Since the uniaxial compressive strength of the norite is approximately 170 MPa, this gives a ratio of $\sigma_c / \sigma_1 = 2$. Table 6.6 shows that, for competent rock with rock stress problems, this value of σ_c / σ_1 can be expected to produce heavy rock burst conditions and that the value of *SRF* should lie between 10 and 20. A value of *SRF* = 15 will be assumed for this calculation. Using these values gives:

$$Q = \frac{90}{4} \times \frac{3}{1} \times \frac{1}{15} = 4.5$$

In relating the value of the index *Q* to the stability and support requirements of underground excavations, Barton et al (1974) defined an additional parameter which they called the Equivalent Dimension, *De*, of the excavation. This dimension is obtained by dividing the span, diameter or wall height of the excavation by a quantity called the Excavation Support Ratio, *ESR*. Hence:

$$D_e = \frac{\text{Excavation span, diameter or height (m)}}{\text{Excavation Support Ratio } ESR}$$

The value of *ESR* is related to the intended use of the excavation and to the degree of security which is demanded of the support system installed to maintain the stability of the excavation. Barton et al (1974) suggest the following values:

Excavation category		*ESR*
A	Temporary mine openings.	3-5
B	Permanent mine openings, water tunnels for hydro power (excluding high pressure penstocks), pilot tunnels, drifts and headings for large excavations.	1.6
C	Storage rooms, water treatment plants, minor road and railway tunnels, surge chambers, access tunnels.	1.3
D	Power stations, major road and railway tunnels, civil defence chambers, portal intersections.	1.0
E	Underground nuclear power stations, railway stations, sports and public facilities, factories.	0.8

Table 6: Classification of individual parameters used in the Tunnelling Quality Index *Q*

DESCRIPTION	VALUE		NOTES
1. ROCK QUALITY DESIGNATION	***RQD***		
A. Very poor	0 - 25		1. Where *RQD* is reported or measured as ≤ 10 (including 0),
B. Poor	25 - 50		a nominal value of 10 is used to evaluate *Q*.
C. Fair	50 - 75		
D. Good	75 - 90		2. *RQD* intervals of 5, i.e. 100, 95, 90 etc. are sufficiently
E. Excellent	90 - 100		accurate.
2. JOINT SET NUMBER	J_n		
A. Massive, no or few joints	0.5 - 1.0		
B. One joint set	2		
C. One joint set plus random	3		
D. Two joint sets	4		
E. Two joint sets plus random	6		
F. Three joint sets	9		1. For intersections use ($3.0 \times J_n$)
G. Three joint sets plus random	12		
H. Four or more joint sets, random, heavily jointed, 'sugar cube', etc.	15		2. For portals use ($2.0 \times J_n$)
J. Crushed rock, earthlike	20		
3. JOINT ROUGHNESS NUMBER	J_r		
a. Rock wall contact			
b. Rock wall contact before 10 cm shear			
A. Discontinuous joints	4		
B. Rough and irregular, undulating	3		
C. Smooth undulating	2		
D. Slickensided undulating	1.5		1. Add 1.0 if the mean spacing of the relevant joint set is
E. Rough or irregular, planar	1.5		greater than 3 m.
F. Smooth, planar	1.0		
G. Slickensided, planar	0.5		2. J_r = 0.5 can be used for planar, slickensided joints having
c. No rock wall contact when sheared			lineations, provided that the lineations are oriented for
H. Zones containing clay minerals thick enough to prevent rock wall contact	1.0 (nominal)		minimum strength.
J. Sandy, gravely or crushed zone thick enough to prevent rock wall contact	1.0 (nominal)		
4. JOINT ALTERATION NUMBER	J_a	ϕr degrees (approx.)	
a. Rock wall contact			
A. Tightly healed, hard, non-softening, impermeable filling	0.75		1. Values of ϕr, the residual friction angle,
			are intended as an approximate guide
B. Unaltered joint walls, surface staining only	1.0	25 - 35	to the mineralogical properties of the
C. Slightly altered joint walls, non-softening mineral coatings, sandy particles, clay-free disintegrated rock, etc.	2.0	25 - 30	alteration products, if present.
D. Silty-, or sandy-clay coatings, small clay-fraction (non-softening)	3.0	20 - 25	
E. Softening or low-friction clay mineral coatings, i.e. kaolinite, mica. Also chlorite, talc, gypsum and graphite etc., and small quantities of swelling clays. (Discontinuous coatings, 1 - 2 mm or less)	4.0	8 - 16	

Table 6: (cont'd.) Classification of individual parameters used in the Tunnelling Quality Index Q (After Barton et al 1974).

4, JOINT ALTERATION NUMBER	J_a	ϕr degrees (approx.)	
b. Rock wall contact before 10 cm shear			
F. Sandy particles, clay-free, disintegrating rock etc.	4.0	25 - 30	
G. Strongly over-consolidated, non-softening clay mineral fillings (continuous < 5 mm thick)	6.0	16 - 24	
H. Medium or low over-consolidation, softening clay mineral fillings (continuous < 5 mm thick)	8.0	12 - 16	
J. Swelling clay fillings, i.e. montmorillonite, (continuous < 5 mm thick). Values of J_a depend on percent of swelling clay-size particles, and access to water.	8.0 - 12.0	6 - 12	
c. No rock wall contact when sheared			
K. Zones or bands of disintegrated or crushed	6.0		
L. rock and clay (see G, H and J for clay	8.0		
M. conditions)	8.0 - 12.0	6 - 24	
N. Zones or bands of silty- or sandy-clay, small clay fraction, non-softening	5.0		
O. Thick continuous zones or bands of clay	10.0 - 13.0		
P. & R. (see G.H and J for clay conditions)	6.0 - 24.0		
5. JOINT WATER REDUCTION	J_w	approx. water pressure (kgf/cm^2)	
A. Dry excavation or minor inflow i.e. < 5 l/m locally	1.0	< 1.0	
B. Medium inflow or pressure, occasional outwash of joint fillings	0.66	1.0 - 2.5	
C. Large inflow or high pressure in competent rock with unfilled joints	0.5	2.5 - 10.0	1. Factors C to F are crude estimates; increase J_w if drainage installed.
D. Large inflow or high pressure	0.33	2.5 - 10.0	
E. Exceptionally high inflow or pressure at blasting, decaying with time	0.2 - 0.1	> 10	2. Special problems caused by ice formation are not considered.
F. Exceptionally high inflow or pressure	0.1 - 0.05	> 10	
6. STRESS REDUCTION FACTOR		***SRF***	
a. Weakness zones intersecting excavation, which may cause loosening of rock mass when tunnel is excavated			
A. Multiple occurrences of weakness zones containing clay or chemically disintegrated rock, very loose surrounding rock any depth)		10.0	1. Reduce these values of *SRF* by 25 - 50% but only if the relevant shear zones influence do not intersect the excavation
B. Single weakness zones containing clay, or chemically dis- tegrated rock (excavation depth < 50 m)		5.0	
C. Single weakness zones containing clay, or chemically dis- tegrated rock (excavation depth > 50 m)		2.5	
D. Multiple shear zones in competent rock (clay free), loose surrounding rock (any depth)		7.5	
E. Single shear zone in competent rock (clay free). (depth of excavation < 50 m)		5.0	
F. Single shear zone in competent rock (clay free). (depth of excavation > 50 m)		2.5	
G. Loose open joints, heavily jointed or 'sugar cube', (any depth)		5.0	

Table 6: (cont'd.) Classification of individual parameters in the Tunnelling Quality Index Q (After Barton et al 1974).

DESCRIPTION	VALUE			NOTES
6. STRESS REDUCTION FACTOR			***SRF***	
b. Competent rock, rock stress problems				
	σ_c/σ_1	$\sigma_t\sigma_1$		2. For strongly anisotropic virgin stress field (if measured): when $5\leq\sigma_1/\sigma_3\leq10$, reduce σ_c to $0.8\sigma_c$ and σ_t to $0.8\sigma_t$. When $\sigma_1/\sigma_3 > 10$, reduce σ_c and σ_t to $0.6\sigma_c$ and $0.6\sigma_t$, where σ_c = unconfined compressive strength, and σ_t = tensile strength (point load) and σ_1 and σ_3 are the major and minor principal stresses.
H. Low stress, near surface	> 200	> 13	2.5	
J. Medium stress	200 - 10	13 - 0.66	1.0	
K. High stress, very tight structure (usually favourable to stability, may be unfavourable to wall stability)	10 - 5	0.66 - 0.33	0.5 - 2	
L. Mild rockburst (massive rock)	5 - 2.5	0.33 - 0.16	5 - 10	
M. Heavy rockburst (massive rock)	< 2.5	< 0.16	10 - 20	3. Few case records available where depth of crown below surface is less than span width. Suggest *SRF* increase from 2.5 to 5 for such cases (see H).
c. Squeezing rock, plastic flow of incompetent rock under influence of high rock pressure				
N. Mild squeezing rock pressure			5 - 10	
O. Heavy squeezing rock pressure			10 - 20	
d. Swelling rock, chemical swelling activity depending on presence of water				
P. Mild swelling rock pressure			5 - 10	
R. Heavy swelling rock pressure			10 - 15	

ADDITIONAL NOTES ON THE USE OF THESE TABLES

When making estimates of the rock mass Quality (Q), the following guidelines should be followed in addition to the notes listed in the tables:

1. When borehole core is unavailable, *RQD* can be estimated from the number of joints per unit volume, in which the number of joints per metre for each joint set are added. A simple relationship can be used to convert this number to *RQD* for the case of clay free rock masses: $RQD = 115 - 3.3\, J_v$ (approx.), where J_v = total number of joints per m^3 ($0 < RQD < 100$ for $35 > J_v > 4.5$).
2. The parameter J_n representing the number of joint sets will often be affected by foliation, schistosity, slaty cleavage or bedding etc. If strongly developed, these parallel 'joints' should obviously be counted as a complete joint set. However, if there are few 'joints' visible, or if only occasional breaks in the core are due to these features, then it will be more appropriate to count them as 'random' joints when evaluating J_n.
3. The parameters J_r and J_a (representing shear strength) should be relevant to the weakest significant joint set or clay filled discontinuity in the given zone. However, if the joint set or discontinuity with the minimum value of J_r/J_a is favourably oriented for stability, then a second, less favourably oriented joint set or discontinuity may sometimes be more significant, and its higher value of J_r/J_a should be used when evaluating Q. The value of J_r/J_a should in fact relate to the surface most likely to allow failure to initiate.
4. When a rock mass contains clay, the factor *SRF* appropriate to loosening loads should be evaluated. In such cases the strength of the intact rock is of little interest. However, when jointing is minimal and clay is completely absent, the strength of the intact rock may become the weakest link, and the stability will then depend on the ratio rock-stress/rock-strength. A strongly anisotropic stress field is unfavourable for stability and is roughly accounted for as in note 2 in the table for stress reduction factor evaluation.
5. The compressive and tensile strengths (σ_c and σ_t) of the intact rock should be evaluated in the saturated condition if this is appropriate to the present and future in situ conditions. A very conservative estimate of the strength should be made for those rocks that deteriorate when exposed to moist or saturated conditions.

The crusher station discussed earlier falls into the category of permanent mine openings and is assigned an excavation support ratio *ESR* = 1.6. Hence, for an excavation span of 15 m, the equivalent dimension, *De* = 15/1.6 = 9.4.

The equivalent dimension, *De*, plotted against the value of *Q*, is used to define a number of support categories in a chart published in the original paper by Barton et al (1974). This chart has recently been updated by Grimstad and Barton (1993) to reflect the increasing use of steel fibre reinforced shotcrete in underground excavation support. Figure 3 is reproduced from this updated chart.

From Figure 3, a value of *De* of 9.4 and a value of *Q* of 4.5 places this crusher excavation in category (4) which requires a pattern of rockbolts (spaced at 2.3 m) and 40 to 50 mm of unreinforced shotcrete.

Because of the mild to heavy rock burst conditions which are anticipated, it may be prudent to destress the rock in the walls of this crusher chamber. This is achieved by using relatively heavy production blasting to excavate the chamber and omitting the smooth blasting usually used to trim the final walls of an excavation such as an underground powerhouse at shallower depth. Caution is recommended in the use of destress blasting and, for critical applications, it may be advisable to seek the advice of a blasting specialist before embarking on this course of action.

Løset (1992) suggests that, for rocks with $4 < Q < 30$, blasting damage will result in the creation of new 'joints' with a consequent local reduction in the value of *Q* for the rock surrounding the excavation. He suggests that this can be accounted for by reducing the *RQD* value for the blast damaged zone.

Assuming that the *RQD* value for the destressed rock around the crusher chamber drops to 50 %, the resulting value of *Q* = 2.9. From Figure 3, this value of *Q*, for an equivalent dimension, *De* of 9.4, places the excavation just inside category (5) which requires rockbolts, at approximately 2 m spacing, and a 50 mm thick layer of steel fibre reinforced shotcrete.

Barton et al (1980) provide additional information on rockbolt length, maximum unsupported spans and roof support pressures to supplement the support recommendations published in the original 1974 paper.

The length L of rockbolts can be estimated from the excavation width B and the Excavation Support Ratio ESR:

$$L = 2 + \frac{0.15B}{ESR} \tag{3}$$

The maximum unsupported span can be estimated from:

$$\text{Maximum span (unsupported)} = 2\,ESR\;Q^{0.4} \tag{4}$$

Based upon analyses of case records, Grimstad and Barton (1993) suggest that the relationship between the value of Q and the permanent roof support pressure P_{roof} is estimated from:

$$P_{\text{roof}} = \frac{2\sqrt{Jn}\,Q^{-\frac{1}{3}}}{3Jr} \tag{5}$$

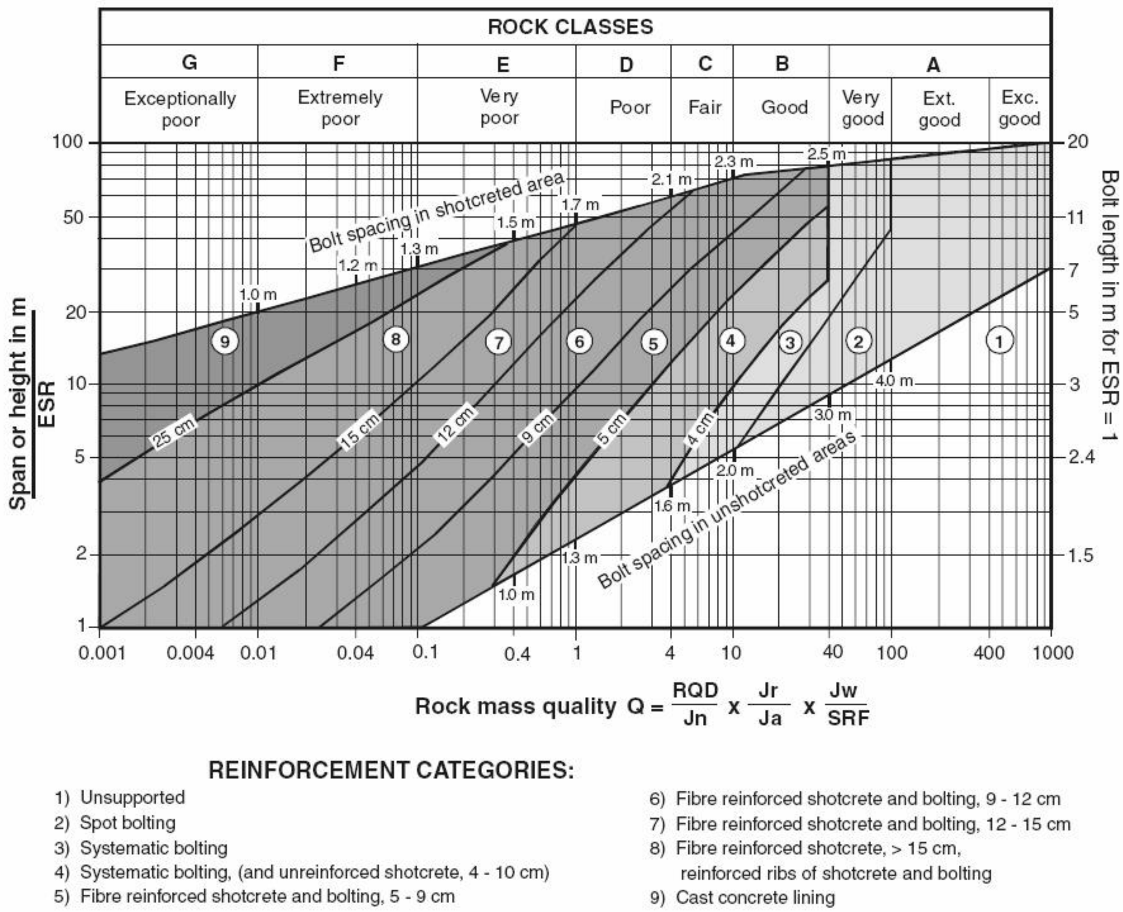

Figure 3: Estimated support categories based on the tunnelling quality index Q (After Grimstad and Barton, 1993, reproduced from Palmstrom and Broch, 2006).

Using rock mass classification systems

The two most widely used rock mass classifications are Bieniawski's *RMR* (1976, 1989) and Barton et al's *Q* (1974). Both methods incorporate geological, geometric and design/engineering parameters in arriving at a quantitative value of their rock mass quality. The similarities between *RMR* and *Q* stem from the use of identical, or very similar, parameters in calculating the final rock mass quality rating. The differences between the systems lie in the different weightings given to similar parameters and in the use of distinct parameters in one or the other scheme.

RMR uses compressive strength directly while *Q* only considers strength as it relates to in situ stress in competent rock. Both schemes deal with the geology and geometry of the rock mass, but in slightly different ways. Both consider groundwater, and both include some component of rock material strength. Some estimate of orientation can be incorporated into *Q* using a guideline presented by Barton et al (1974): ‘the parameters *Jr* and *Ja* should ... relate to the surface most likely to allow failure to initiate.’ The greatest difference between the two systems is the lack of a stress parameter in the *RMR* system.

When using either of these methods, two approaches can be taken. One is to evaluate the rock mass specifically for the parameters included in the classification methods; the other is to accurately characterise the rock mass and then attribute parameter ratings at a later time. The latter method is recommended since it gives a full and complete description of the rock mass which can easily be translated into either classification index. If rating values alone had been recorded during mapping, it would be almost impossible to carry out verification studies.

In many cases, it is appropriate to give a range of values to each parameter in a rock mass classification and to evaluate the significance of the final result. An example of this approach is given in Figure 4 which is reproduced from field notes prepared by Dr. N. Barton on a project. In this particular case, the rock mass is dry and is subjected to 'medium' stress conditions (Table 6.6.K) and hence $Jw = 1.0$ and SRF = 1.0. Histograms showing the variations in *RQD*, *Jn*, *Jr* and *Ja*, along the exploration adit mapped, are presented in this figure. The average value of $Q = 8.9$ and the approximate range of *Q* is $1.7 < Q < 20$. The average value of *Q* can be used in choosing a basic support system while the range gives an indication of the possible adjustments which will be required to meet different conditions encountered during construction.

A further example of this approach is given in a paper by Barton et al (1992) concerned with the design of a 62 m span underground sports hall in jointed gneiss. Histograms of all the input parameters for the *Q* system are presented and analysed in order to determine the weighted average value of *Q*.

Carter (1992) has adopted a similar approach, but extended his analysis to include the derivation of a probability distribution function and the calculation of a probability of failure in a discussion on the stability of surface crown pillars in abandoned metal mines.

Throughout this chapter it has been suggested that the user of a rock mass classification scheme should check that the latest version is being used. It is also worth repeating that the use of two rock mass classification schemes side by side is advisable.

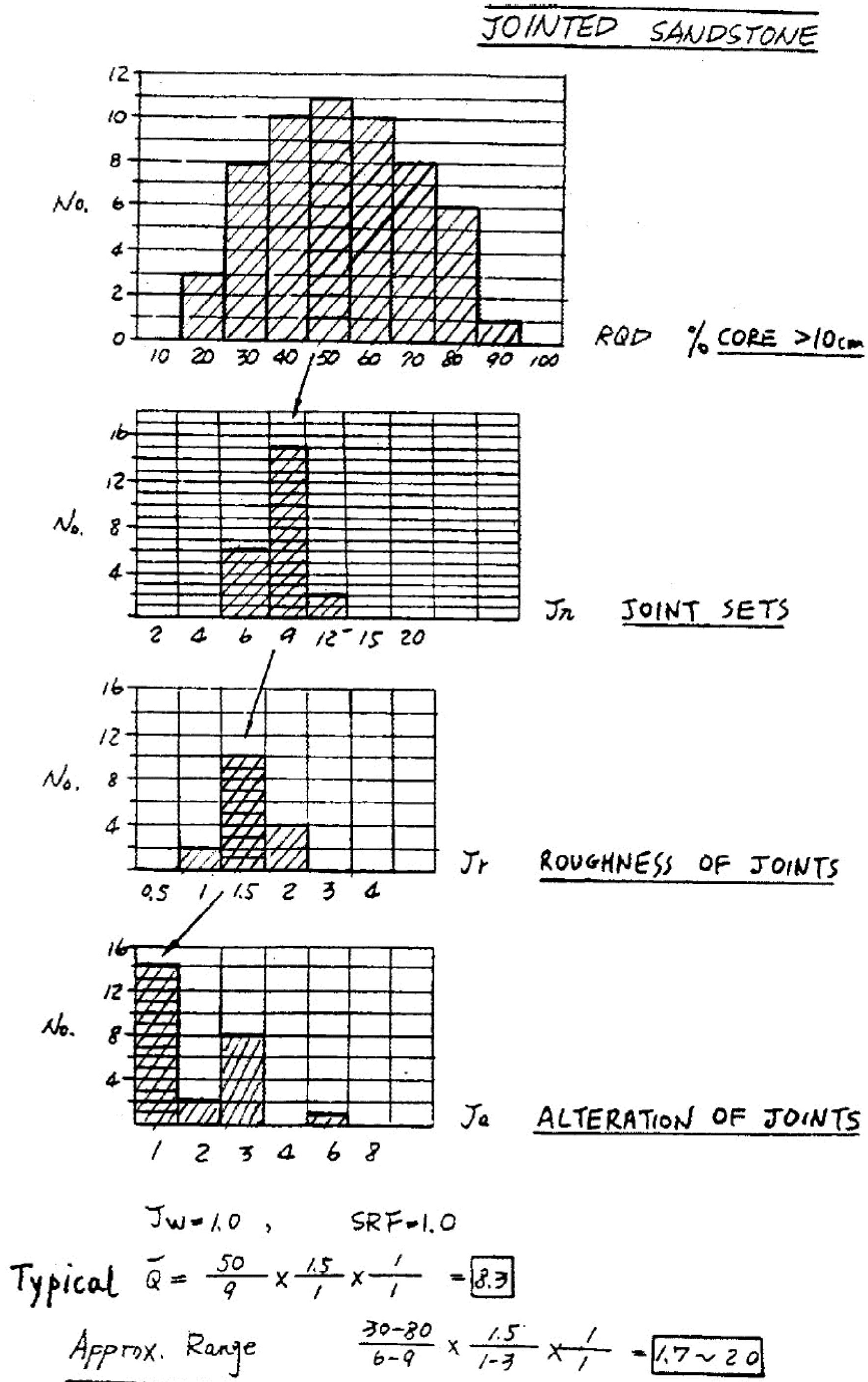

Figure 4: Histograms showing variations in *RQD*, *Jn*, *Jr* and *Ja* for a dry jointed sandstone under 'medium' stress conditions, reproduced from field notes prepared by Dr. N. Barton.

References

Barton, N., By, T.L., Chryssanthakis, L., Tunbridge, L., Kristiansen, J., Løset, F., Bhasin, R.K., Westerdahl, H. and Vik, G. 1992. Comparison of prediction and performance for a 62 m span sports hall in jointed gneiss. *Proc. 4th. int. rock mechanics and rock engineering conf.*, Torino. Paper 17.

Barton, N., Løset, F., Lien, R. and Lunde, J. 1980. Application of the Q-system in design decisions. In *Subsurface space*, (ed. M. Bergman) **2,** 553-561. New York: Pergamon.

Barton, N.R., Lien, R. and Lunde, J. 1974. Engineering classification of rock masses for the design of tunnel support. *Rock Mech.* **6**(4), 189-239.

Bieniawski, Z.T. 1973. Engineering classification of jointed rock masses. *Trans S. Afr. Inst. Civ. Engrs* **15**, 335-344.

Bieniawski, Z.T. 1976. Rock mass classification in rock engineering. In *Exploration for rock engineering, proc. of the symp.*, (ed. Z.T. Bieniawski) **1**, 97-106. Cape Town: Balkema.

Bieniawski, Z.T. 1989. *Engineering rock mass classifications.* New York: Wiley.

Carter, T.G. 1992. A new approach to surface crown pillar design. *Proc. 16th. Canadian Rock Mechanics Symposium, Sudbury*, 75-83.

Carter, T.G. 1992. Prediction and uncertainties in geological engineering and rock mass characterization assessments. *Proc. 4th. int. rock mechanics and rock engineering conf.*, Torino. Paper 1.

Cording, E.J. and Deere, D.U. 1972. Rock tunnel supports and field measurements. *Proc. North American rapid excav. tunneling conf.*, Chicago, (eds. K.S. Lane and L.A. Garfield) **1**, 601-622. New York: Soc. Min. Engrs, Am. Inst. Min. Metall. Petrolm Engrs.

Cummings, R.A., Kendorski, F.S. and Bieniawski, Z.T. 1982. *Caving rock mass classification and support estimation*. U.S. Bureau of Mines Contract Report #J0100103. Chicago: Engineers International Inc.

Deere, D.U. 1989. *Rock quality designation (RQD) after 20 years.* U.S. Army Corps Engrs Contract Report GL-89-1. Vicksburg, MS: Waterways Experimental Station.

Deere, D.U. and Deere, D.W. 1988. The rock quality designation (RQD) index in practice. In *Rock classification systems for engineering purposes*, (ed. L. Kirkaldie), ASTM Special Publication 984, 91-101. Philadelphia: Am. Soc. Test. Mat.

Deere, D.U., Hendron, A.J., Patton, F.D. and Cording, E.J. 1967. Design of surface and near surface construction in rock. In *Failure and breakage of rock, proc. 8th U.S. symp. rock mech.*, (ed. C. Fairhurst), 237-302. New York: Soc. Min. Engrs, Am. Inst. Min. Metall. Petrolm Engrs.

Grimstad, E. and Barton, N. 1993. Updating the Q-System for NMT. *Proc. int. symp. on sprayed concrete - modern use of wet mix sprayed concrete for underground support*, Fagernes. 46-66. Oslo: Norwegian Concrete Assn.

Kendorski, F., Cummings, R., Bieniawski, Z.T. and Skinner, E. 1983. Rock mass classification for block caving mine drift support. *Proc. 5th congr. Int. Soc. Rock Mech.*, Melbourne, B51-B63. Rotterdam: Balkema.

Laubscher, D.H. 1977. Geomechanics classification of jointed rock masses - mining applications. *Trans. Instn Min. Metall.* **86**, A1-8.

Laubscher, D.H. 1984. Design aspects and effectiveness of support systems in different mining conditions. *Trans Instn Min. Metall.* **93**, A70 - A82.

Laubscher, D.H. and Taylor, H.W. 1976. The importance of geomechanics classification of jointed rock masses in mining operations. In *Exploration for rock engineering*, (ed. Z.T. Bieniawski) **1**, 119-128. Cape Town: Balkema.

Laubscher, D.M. and Page, C.H. 1990. The design of rock support in high stress or weak rock environments. *Proc. 92nd Can. Inst. Min. Metall. AGM*, Ottawa, Paper # 91.

Lauffer, H. 1958. Gebirgsklassifizierung für den Stollenbau. *Geol. Bauwesen* **24**(1), 46-51.

Løset, F. 1992. Support needs compared at the Svartisen Road Tunnel. *Tunnels and Tunnelling,* June.

Merritt, A.H. 1972. Geologic prediction for underground excavations. *Proc. North American. rapid excav. tunneling conf.*, Chicago, (eds K.S. Lane and L.A. Garfield) **1,** 115-132. New York: Soc. Min. Engrs, Am. Inst. Min. Metall. Petrolm Engrs.

Pacher, F., Rabcewicz, L. and Golser, J. 1974. Zum der seitigen Stand der Gebirgsklassifizierung in Stollen-und Tunnelbau. *Proc. XXII Geomech. colloq.*, Salzburg, 51-58.

Palmström, A. 1982. The volumetric joint count - a useful and simple measure of the degree of rock jointing. *Proc. 4th congr. Int. Assn Engng Geol.*, Delhi **5**, 221-228.

Palmstrom, A. and Broch, E. 2006. Use and misuse of rock mass classification systems with particular reference to the Q-system. *Tunnels and Underground Space Technology*, **21**, 575-593.

Ritter, W. 1879. *Die Statik der Tunnelgewölbe.* Berlin: Springer.

Terzaghi, K. 1946. Rock defects and loads on tunnel supports. In *Rock tunneling with steel supports,* (eds R. V. Proctor and T. L. White) **1**, 17-99. Youngstown, OH: Commercial Shearing and Stamping Company.

Wickham, G.E., Tiedemann, H.R. and Skinner, E.H. 1972. Support determination based on geologic predictions. In *Proc. North American rapid excav. tunneling conf.*, Chicago, (eds K.S. Lane and L.A. Garfield), 43-64. New York: Soc. Min. Engrs, Am. Inst. Min. Metall. Petrolm Engrs.

Shear strength of discontinuities

Introduction

All rock masses contain discontinuities such as bedding planes, joints, shear zones and faults. At shallow depth, where stresses are low, failure of the intact rock material is minimal and the behaviour of the rock mass is controlled by sliding on the discontinuities. In order to analyse the stability of this system of individual rock blocks, it is necessary to understand the factors that control the shear strength of the discontinuities which separate the blocks. These questions are addressed in the discussion that follows.

Shear strength of planar surfaces

Suppose that a number of samples of a rock are obtained for shear testing. Each sample contains a through-going bedding plane that is cemented; in other words, a tensile force would have to be applied to the two halves of the specimen in order to separate them. The bedding plane is absolutely planar, having no surface irregularities or undulations. As illustrated in Figure 1, in a shear test each specimen is subjected to a stress σ_n normal to the bedding plane, and the shear stress τ, required to cause a displacement δ, is measured.

The shear stress will increase rapidly until the peak strength is reached. This corresponds to the sum of the strength of the cementing material bonding the two halves of the bedding plane together and the frictional resistance of the matching surfaces. As the displacement continues, the shear stress will fall to some residual value that will then remain constant, even for large shear displacements.

Plotting the peak and residual shear strengths for different normal stresses results in the two lines illustrated in Figure 1. For planar discontinuity surfaces the experimental points will generally fall along straight lines. The peak strength line has a slope of ϕ and an intercept of c on the shear strength axis. The residual strength line has a slope of ϕ_r.

The relationship between the peak shear strength τ_p and the normal stress σ_n can be represented by the Mohr-Coulomb equation:

$$\tau_p = c + \sigma_n \tan\phi \qquad (1)$$

where c is the cohesive strength of the cemented surface and
ϕ is the angle of friction.

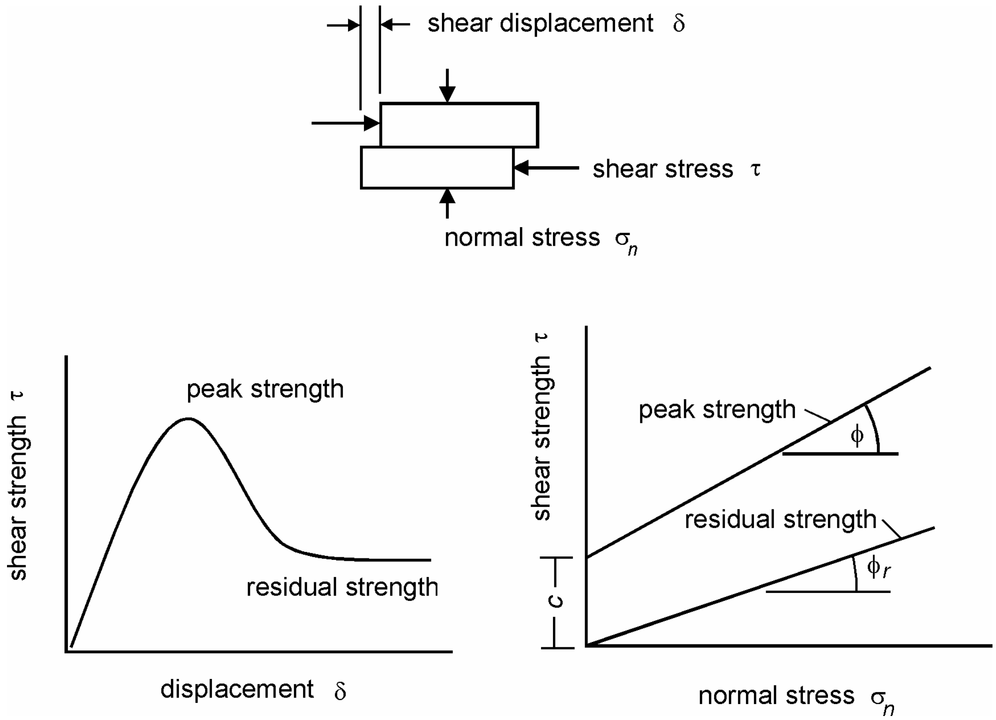

Figure 1: Shear testing of discontinuities

In the case of the residual strength, the cohesion c has dropped to zero and the relationship between ϕ_r and σ_n can be represented by:

$$\tau_r = \sigma_n \tan \phi_r \tag{2}$$

where ϕ_r is the residual angle of friction.

This example has been discussed in order to illustrate the physical meaning of the term cohesion, a soil mechanics term, which has been adopted by the rock mechanics community. In shear tests on soils, the stress levels are generally an order of magnitude lower than those involved in rock testing and the cohesive strength of a soil is a result of the adhesion of the soil particles. In rock mechanics, true cohesion occurs when cemented surfaces are sheared. However, in many practical applications, the term cohesion is used for convenience and it refers to a mathematical quantity related to surface roughness, as discussed in a later section. Cohesion is simply the intercept on the τ axis at zero normal stress.

The basic friction angle ϕ_b is a quantity that is fundamental to the understanding of the shear strength of discontinuity surfaces. This is approximately equal to the residual friction angle ϕ_r but it is generally measured by testing sawn or ground rock surfaces. These tests, which can be carried out on surfaces as small as 50 mm × 50 mm, will produce a straight line plot defined by the equation:

$$\tau_r = \sigma_n \tan \phi_b \tag{3}$$

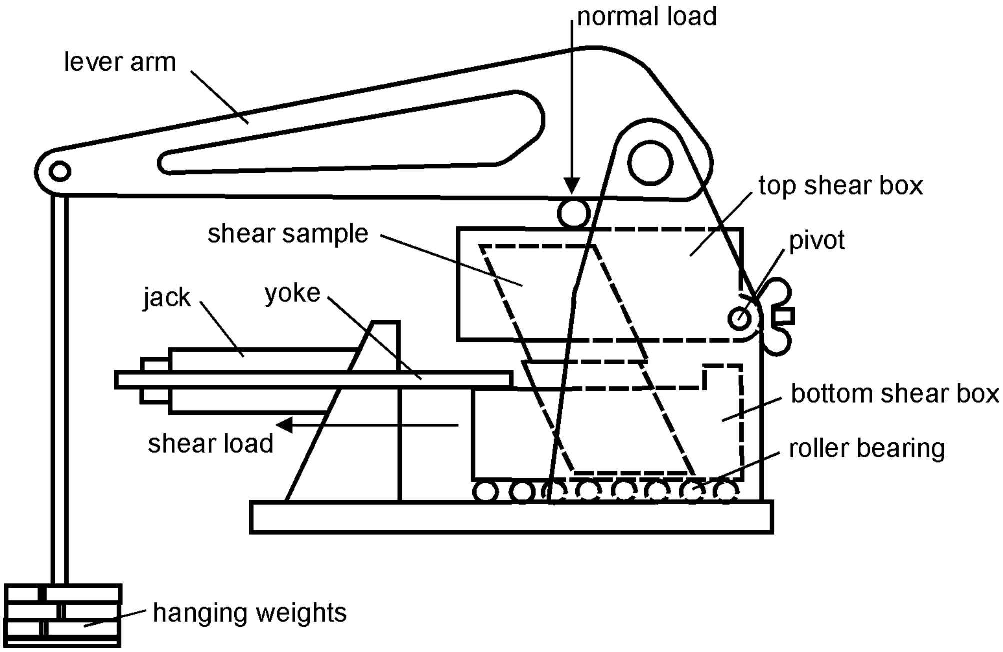

Figure 2: Diagrammatic section through shear machine used by Hencher and Richards (1982).

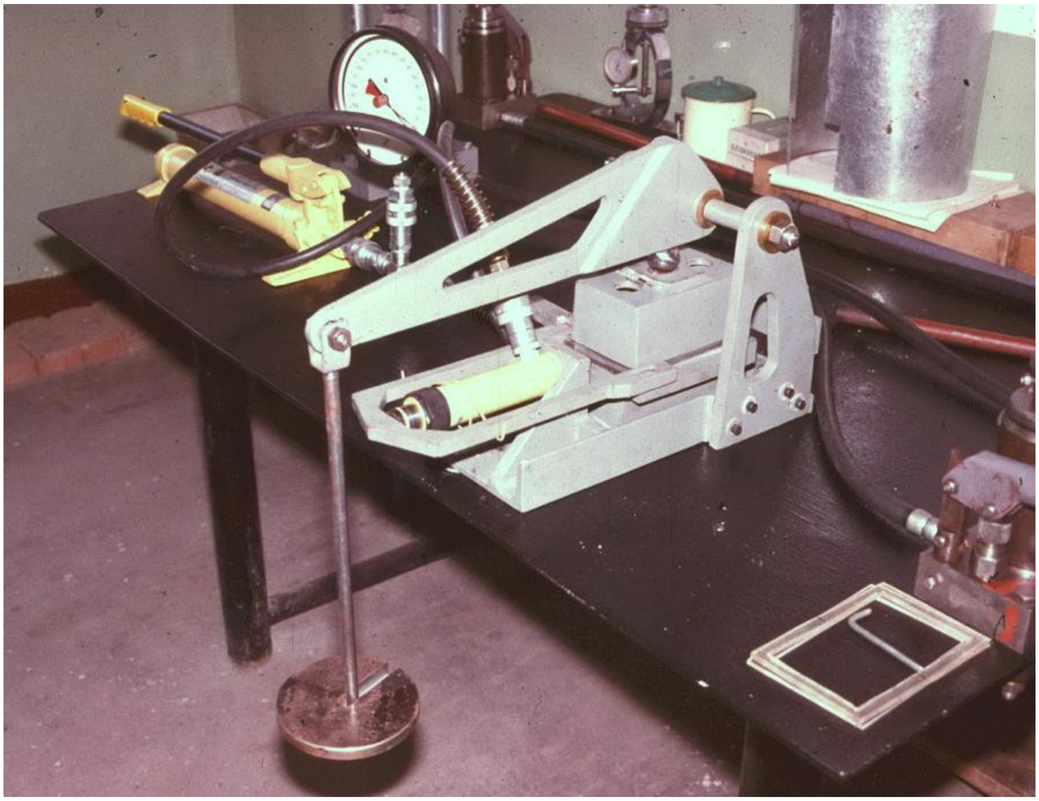

Figure 3: Shear machine of the type used by Hencher and Richards (1982) for measurement of the shear strength of sheet joints in Hong Kong granite.

A typical shear testing machine, which can be used to determine the basic friction angle ϕ_b is illustrated in Figures 2 and 3. This is a very simple machine and the use of a mechanical lever arm ensures that the normal load on the specimen remains constant throughout the test. This is an important practical consideration since it is difficult to maintain a constant normal load in hydraulically or pneumatically controlled systems and this makes it difficult to interpret test data. Note that it is important that, in setting up the specimen, great care has to be taken to ensure that the shear surface is aligned accurately in order to avoid the need for an additional angle correction.

Most shear strength determinations today are carried out by determining the basic friction angle, as described above, and then making corrections for surface roughness as discussed in the following sections of this chapter. In the past there was more emphasis on testing full scale discontinuity surfaces, either in the laboratory or in the field. There are a significant number of papers in the literature of the 1960s and 1970s describing large and elaborate in situ shear tests, many of which were carried out to determine the shear strength of weak layers in dam foundations. However, the high cost of these tests together with the difficulty of interpreting the results has resulted in a decline in the use of these large scale tests and they are seldom seen today.

The author’s opinion is that it makes both economical and practical sense to carry out a number of small scale laboratory shear tests, using equipment such as that illustrated in Figures 2 and 3, to determine the basic friction angle. The roughness component which is then added to this basic friction angle to give the effective friction angle is a number which is site specific and scale dependent and is best obtained by visual estimates in the field. Practical techniques for making these roughness angle estimates are described on the following pages.

Shear strength of rough surfaces

A natural discontinuity surface in hard rock is never as smooth as a sawn or ground surface of the type used for determining the basic friction angle. The undulations and asperities on a natural joint surface have a significant influence on its shear behaviour. Generally, this surface roughness increases the shear strength of the surface, and this strength increase is extremely important in terms of the stability of excavations in rock.

Patton (1966) demonstrated this influence by means of an experiment in which he carried out shear tests on 'saw-tooth' specimens such as the one illustrated in Figure 4. Shear displacement in these specimens occurs as a result of the surfaces moving up the inclined faces, causing dilation (an increase in volume) of the specimen.

The shear strength of Patton's saw-tooth specimens can be represented by:

$$\tau = \sigma_n \tan(\phi_b + i) \tag{4}$$

where ϕ_b is the basic friction angle of the surface and
i is the angle of the saw-tooth face.

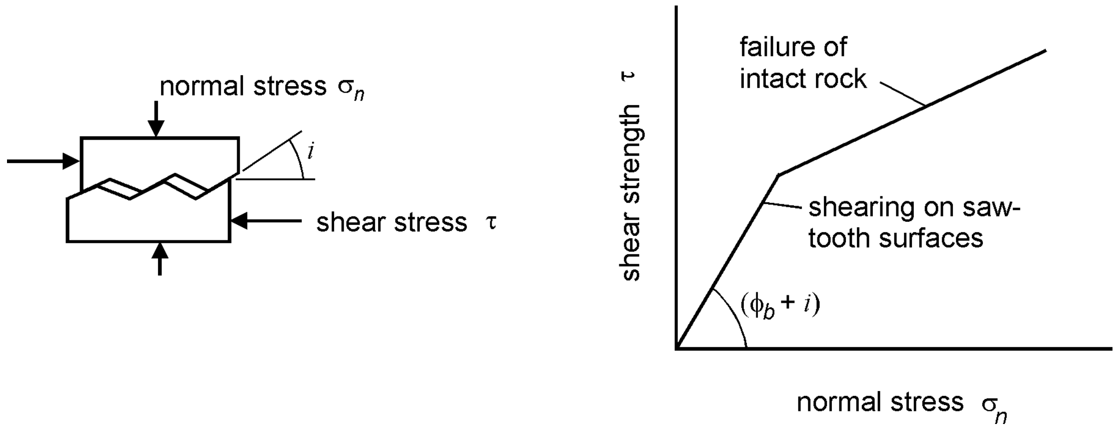

Figure 4: Patton's experiment on the shear strength of saw-tooth specimens.

Barton's estimate of shear strength

Equation (4) is valid at low normal stresses where shear displacement is due to sliding along the inclined surfaces. At higher normal stresses, the strength of the intact material will be exceeded and the teeth will tend to break off, resulting in a shear strength behaviour which is more closely related to the intact material strength than to the frictional characteristics of the surfaces.

While Patton's approach has the merit of being very simple, it does not reflect the reality that changes in shear strength with increasing normal stress are gradual rather than abrupt. Barton (1973, 1976) studied the behaviour of natural rock joints and proposed that equation (4) could be re-written as:

$$\tau = \sigma_n \tan\left(\phi_b + JRC \log_{10}\left(\frac{JCS}{\sigma_n}\right)\right) \tag{5}$$

where *JRC* is the joint roughness coefficient and
JCS is the joint wall compressive strength .

Barton developed his first non-linear strength criterion for rock joints (using the basic friction angle ϕ_b) from analysis of joint strength data reported in the literature. Barton and Choubey (1977), on the basis of their direct shear test results for 130 samples of variably weathered rock joints, revised this equation to

$$\tau = \sigma_n \tan\left(\phi_r + JRC \log_{10}\left(\frac{JCS}{\sigma_n}\right)\right) \tag{6}$$

Where ϕ_r is the residual friction angle
Barton and Choubey suggest that ϕ_r can be estimated from

$$\phi_r = (\phi_b - 20) + 20(r / R) \tag{7}$$

where r is the Schmidt rebound number wet and weathered fracture surfaces and *R* is the Schmidt rebound number on dry unweathered sawn surfaces.

Equations 6 and 7 have become part of the Barton-Bandis criterion for rock joint strength and deformability (Barton and Bandis, 1990).

Field estimates of *JRC*

The joint roughness coefficient *JRC* is a number that can be estimated by comparing the appearance of a discontinuity surface with standard profiles published by Barton and others. One of the most useful of these profile sets was published by Barton and Choubey (1977) and is reproduced in Figure 5.

The appearance of the discontinuity surface is compared visually with the profiles shown and the *JRC* value corresponding to the profile which most closely matches that of the discontinuity surface is chosen. In the case of small scale laboratory specimens, the scale of the surface roughness will be approximately the same as that of the profiles illustrated. However, in the field the length of the surface of interest may be several metres or even tens of metres and the *JRC* value must be estimated for the full scale surface.

An alternative method for estimating *JRC* is presented in Figure 6.

Field estimates of *JCS*

Suggested methods for estimating the joint wall compressive strength were published by the ISRM (1978). The use of the Schmidt rebound hammer for estimating joint wall compressive strength was proposed by Deere and Miller (1966), as illustrated in Figure 7.

Influence of scale on *JRC* and *JCS*

On the basis of extensive testing of joints, joint replicas, and a review of literature, Barton and Bandis (1982) proposed the scale corrections for *JRC* defined by the following relationship:

$$JRC_n = JRC_o \left(\frac{L_n}{L_o} \right)^{-0.02 JRC_o} \tag{8}$$

where JRC_o, and L_o (length) refer to 100 mm laboratory scale samples and JRC_n, and L_n refer to in situ block sizes.

Because of the greater possibility of weaknesses in a large surface, it is likely that the average joint wall compressive strength (*JCS*) decreases with increasing scale. Barton and Bandis (1982) proposed the scale corrections for *JCS* defined by the following relationship:

$$JCS_n = JCS_o \left(\frac{L_n}{L_o} \right)^{-0.03 JRC_o} \tag{9}$$

where JCS_o and L_o (length) refer to 100 mm laboratory scale samples and JCS_n and L_n refer to in situ block sizes.

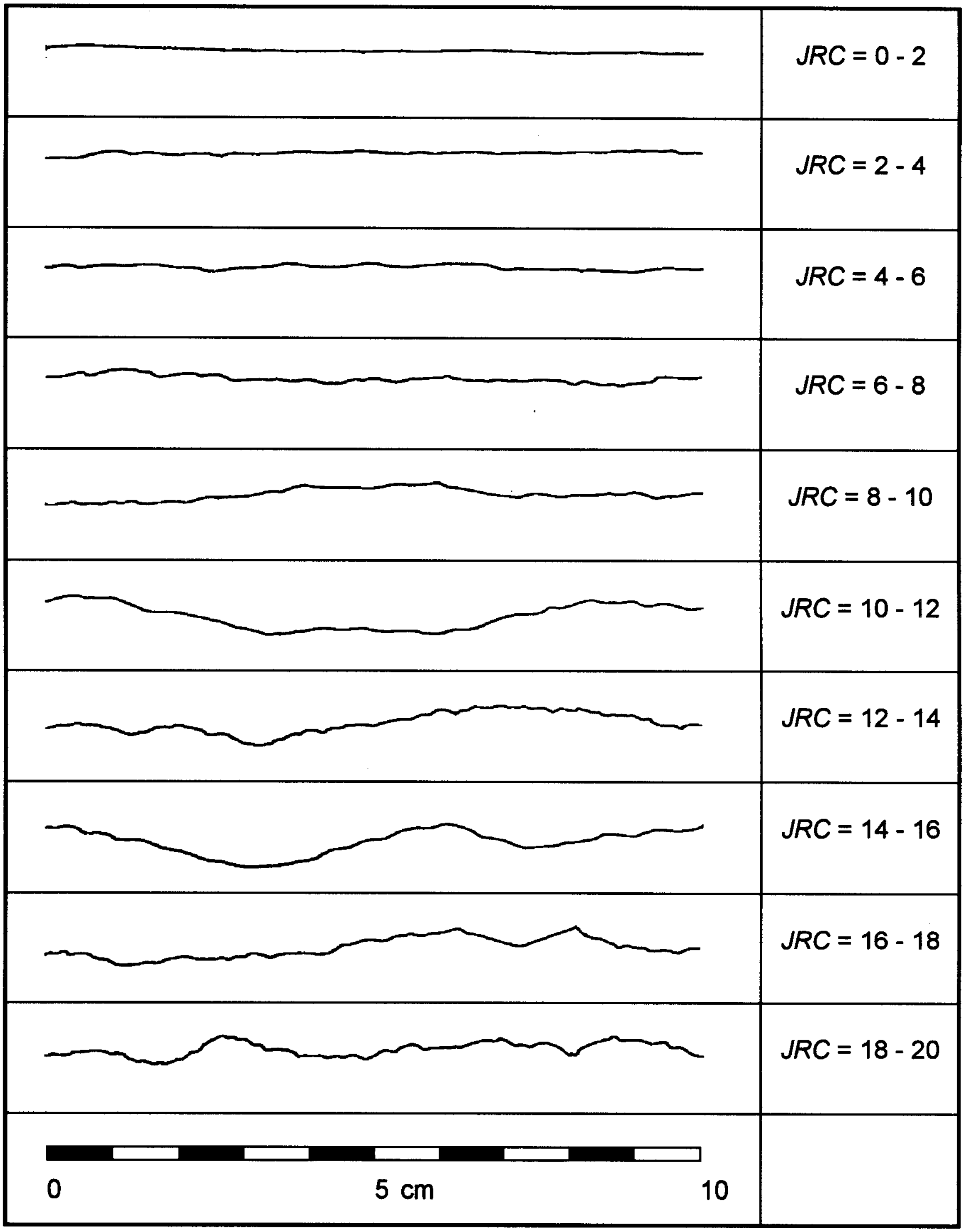

Figure 5: Roughness profiles and corresponding *JRC* values (After Barton and Choubey 1977).

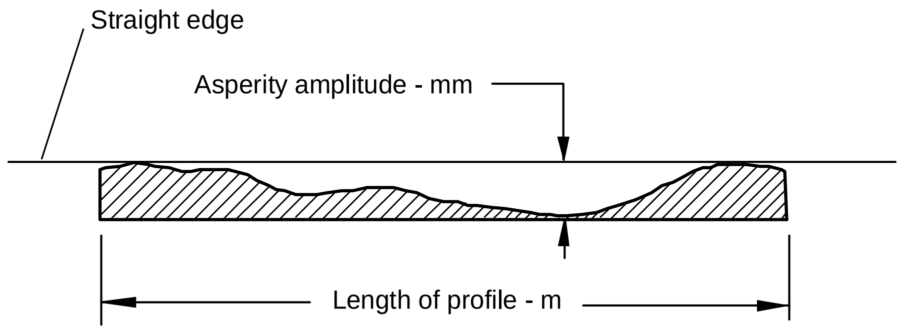

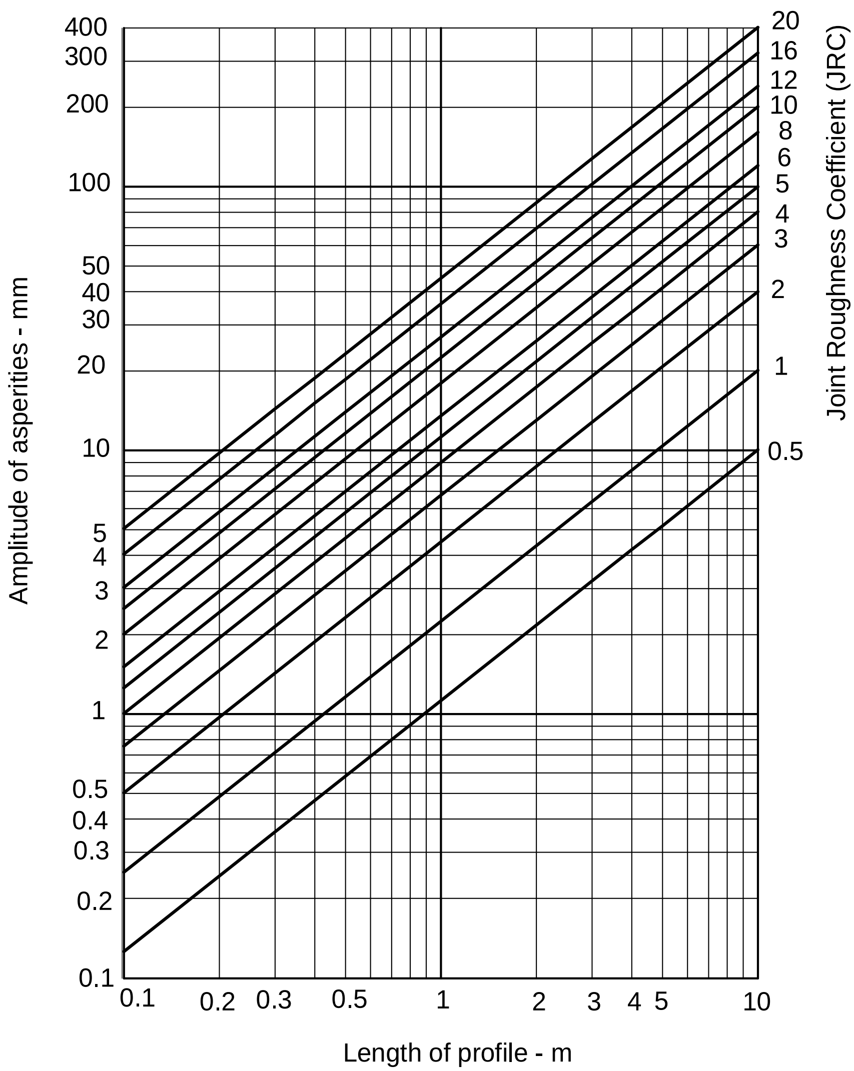

Figure 6: Alternative method for estimating *JRC* from measurements of surface roughness amplitude from a straight edge (Barton 1982).

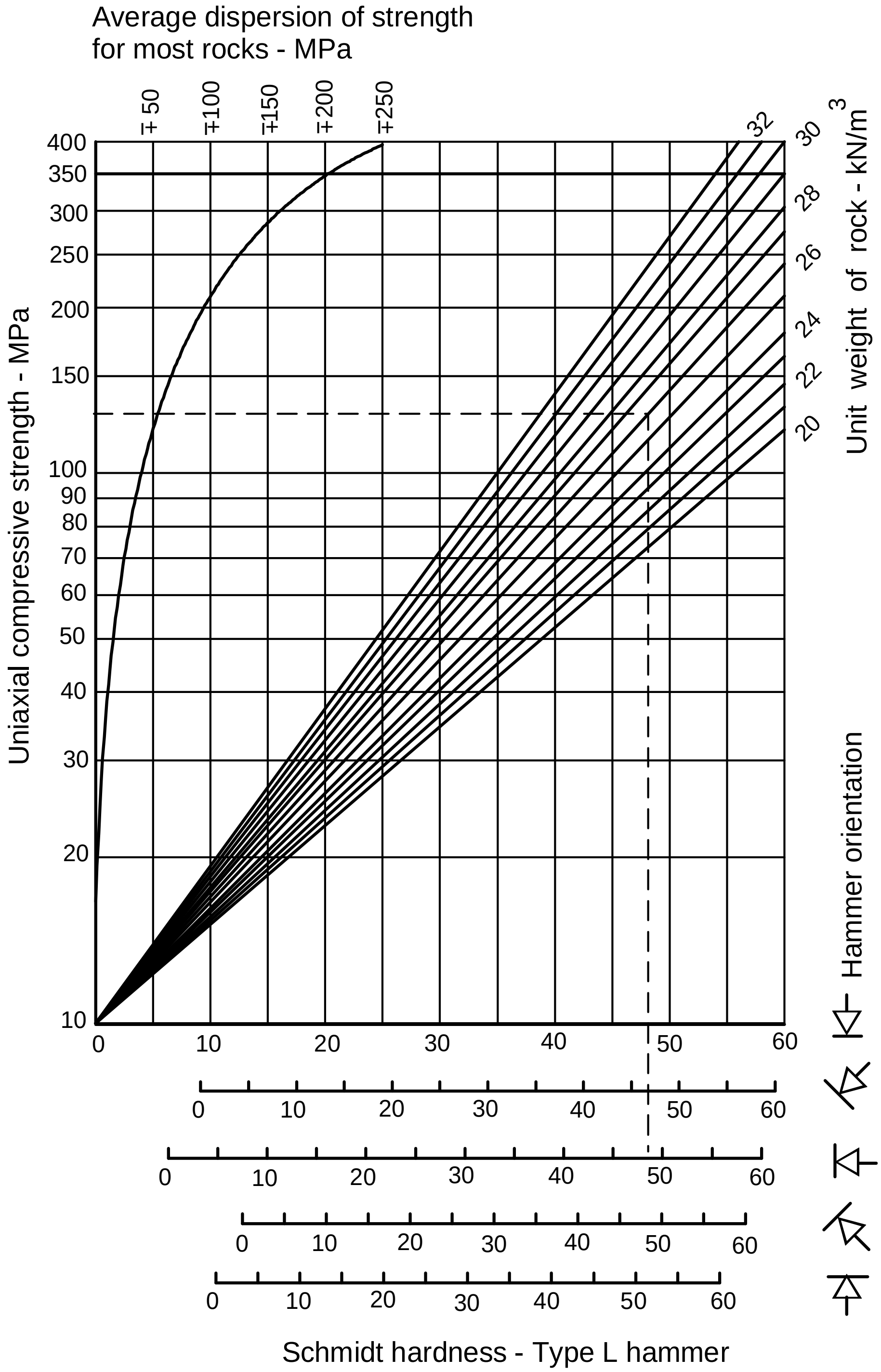

Figure 7: Estimate of joint wall compressive strength from Schmidt hardness.

Shear strength of filled discontinuities

The discussion presented in the previous sections has dealt with the shear strength of discontinuities in which rock wall contact occurs over the entire length of the surface under consideration. This shear strength can be reduced drastically when part or all of the surface is not in intimate contact, but covered by soft filling material such as clay gouge. For planar surfaces, such as bedding planes in sedimentary rock, a thin clay coating will result in a significant shear strength reduction. For a rough or undulating joint, the filling thickness has to be greater than the amplitude of the undulations before the shear strength is reduced to that of the filling material.

A comprehensive review of the shear strength of filled discontinuities was prepared by Barton (1974) and a summary of the shear strengths of typical discontinuity fillings, based on Barton's review, is given in Table 1.

Where a significant thickness of clay or gouge fillings occurs in rock masses and where the shear strength of the filled discontinuities is likely to play an important role in the stability of the rock mass, it is strongly recommended that samples of the filling be sent to a soil mechanics laboratory for testing.

Influence of water pressure

When water pressure is present in a rock mass, the surfaces of the discontinuities are forced apart and the normal stress σ_n is reduced. Under steady state conditions, where there is sufficient time for the water pressures in the rock mass to reach equilibrium, the reduced normal stress is defined by $\sigma_n' = (\sigma_n - u)$, where u is the water pressure. The reduced normal stress σ_n' is usually called the effective normal stress, and it can be used in place of the normal stress term σ_n in all of the equations presented above.

Instantaneous cohesion and friction

Due to the historical development of the subject of rock mechanics, many of the analyses, used to calculate factors of safety against sliding, are expressed in terms of the Mohr-Coulomb cohesion (c) and friction angle (ϕ), defined in Equation 1. Since the 1970s it has been recognised that the relationship between shear strength and normal stress is more accurately represented by a non-linear relationship such as that proposed by Barton and Bandis (1990). However, because this relationship (e.g. is not expressed in terms of c and ϕ, it is necessary to devise some means for estimating the equivalent cohesive strengths and angles of friction from relationships such as those proposed by Barton and Bandis.

Figure 8 gives definitions of the *instantaneous cohesion* c_i and the *instantaneous friction* angle ϕ_i for a normal stress of σ_n. These quantities are given by the intercept and the inclination, respectively, of the tangent to the non-linear relationship between shear strength and normal stress. These quantities may be used for stability analyses in which the Mohr-Coulomb failure criterion (Equation 1) is applied, provided that the normal stress σ_n is reasonably close to the value used to define the tangent point.

Table 1: Shear strength of filled discontinuities and filling materials (After Barton 1974)

Rock	Description	Peak c' (MPa)	Peak ϕ°	Residual c' (MPa)	Residual ϕ°
Basalt	Clayey basaltic breccia, wide variation from clay to basalt content	0.24	42		
Bentonite	Bentonite seam in chalk	0.015	7.5		
	Thin layers	0.09-0.12	12-17		
	Triaxial tests	0.06-0.1	9-13		
Bentonitic shale	Triaxial tests	0-0.27	8.5-29		
	Direct shear tests			0.03	8.5
Clays	Over-consolidated, slips, joints and minor shears	0-0.18	12-18.5	0-0.003	10.5-16
Clay shale	Triaxial tests	0.06	32		
	Stratification surfaces			0	19-25
Coal measure rocks	Clay mylonite seams, 10 to 25 mm	0.012	16	0	11-11.5
Dolomite	Altered shale bed, ± 150 mm thick	0.04	1(5)	0.02	17
Diorite, granodiorite and porphyry	Clay gouge (2% clay, PI = 17%)	0	26.5		
Granite	Clay filled faults	0-0.1	24-45		
	Sandy loam fault filling	0.05	40		
	Tectonic shear zone, schistose and broken granites, disintegrated rock and gouge	0.24	42		
Greywacke	1-2 mm clay in bedding planes			0	21
Limestone	6 mm clay layer			0	13
	10-20 mm clay fillings	0.1	13-14		
	<1 mm clay filling	0.05-0.2	17-21		
Limestone, marl and lignites	Interbedded lignite layers	0.08	38		
	Lignite/marl contact	0.1	10		
Limestone	Marlaceous joints, 20 mm thick	0	25	0	15-24
Lignite	Layer between lignite and clay	0.014-.03	15-17.5		
Montmorillonite	80 mm seams of bentonite (mont-	0.36	14	0.08	11
Bentonite clay	morillonite) clay in chalk	0.016-.02	7.5-11.5		
Schists, quartzites and siliceous schists	100-15- mm thick clay filling	0.03-0.08	32		
	Stratification with thin clay	0.61-0.74	41		
	Stratification with thick clay	0.38	31		
Slates	Finely laminated and altered	0.05	33		
Quartz / kaolin / pyrolusite	Remoulded triaxial tests	0.042-.09	36-38		

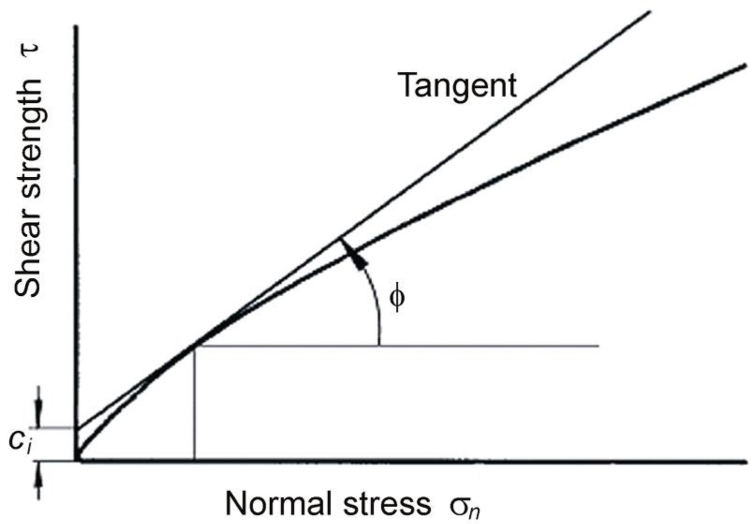

Figure 8: Definition of instantaneous cohesion c_i and instantaneous friction angle ϕ_i for a non-linear failure criterion.

Note that equation 6 is not valid for σ_n = 0 and it ceases to have any practical meaning for $\phi_r + JRC\log_{10}(JCS/\sigma_n) > 70°$. This limit can be used to determine a minimum value for σ_n. An upper limit for σ_n is given by σ_n = JCS.

In a typical practical application, a spreadsheet program can be used to solve Equation 6 and to calculate the instantaneous cohesion and friction values for a range of normal stress values. A portion of such a spreadsheet is illustrated in Figure 9. In this spreadsheet the instantaneous friction angle ϕ_i, for a normal stress of σ_n, has been calculated from the relationship

$$\phi_i = \arctan\left(\frac{\partial\tau}{\partial\sigma_n}\right) \tag{10}$$

$$\frac{\partial\tau}{\partial\sigma_n} = \tan\left(JRC\log_{10}\frac{JCS}{\sigma_n} + \phi_r\right) - \frac{\pi JRC}{180\ln 10}\left[\tan^2\left(JRC\log_{10}\frac{JCS}{\sigma_n} + \phi_r\right) + 1\right] \tag{11}$$

The instantaneous cohesion c_i is calculated from:

$$c_i = \tau - \sigma_n \tan\phi_i \tag{12}$$

In choosing the values of c_i and ϕ_i for use in a particular application, the average normal stress σ_n acting on the discontinuity planes should be estimated and used to determine the appropriate row in the spreadsheet. For many practical problems in the field, a single average value of σ_n will suffice but, where critical stability problems are being considered, this selection should be made for each important discontinuity surface.

Barton shear failure criterion

Input parameters:

Residual friction angle (PHIR) - degrees	29
Joint roughness coefficient (JRC)	16.9
Joint compressive strength (JCS)	96
Minimum normal stress (SIGNMIN)	0.360

Normal stress (SIGN) MPa	Shear strength (TAU) MPa	dTAU / dSIGN (DTDS)	Friction angle (PHI) degrees	Cohesive strength (COH) MPa
0.360	0.989	1.652	58.82	0.394
0.720	1.538	1.423	54.91	0.513
1.440	2.476	1.213	50.49	0.730
2.880	4.073	1.030	45.85	1.107
5.759	6.779	0.872	41.07	1.760
11.518	11.344	0.733	36.22	2.907
23.036	18.973	0.609	31.33	4.953
46.073	31.533	0.496	26.40	8.666

Cell formulae:

```
SIGNMIN = 10^(LOG(JCS)-((70-PHIR)/JRC))
    TAU = SIGN*TAN((PHIR+JRC*LOG(JCS/SIGN))*PI()/180)

   DTDS = TAN((JRC*LOG(JCS/SIGN)+PHIR)*PI()/180)-(JRC/LN(10))
          *(TAN((JRC*LOG(JCS/SIGN)+PHIR)*PI()/180)^2+1)*PI()/180

    PHI = ATAN(DTDS)*180/PI()
    COH = TAU-SIGN*DTDS
```

Figure 9 Printout of spreadsheet cells and formulae used to calculate shear strength, instantaneous friction angle and instantaneous cohesion for a range of normal stresses.

References

Barton, N. 1976. The shear strength of rock and rock joints. *Int. J. Rock Mech. Min. Sci. & Geomech. Abstr.* **13,** 1-24.

Barton, N.R. 1973. Review of a new shear strength criterion for rock joints. *Eng. Geol.* **7**, 287-332.

Barton, N.R. 1974. *A review of the shear strength of filled discontinuities in rock.* Norwegian Geotech. Inst. Publ. No. 105. Oslo: Norwegian Geotech. Inst.

Barton, N.R. 1976. The shear strength of rock and rock joints. *Int. J. Mech. Min. Sci. & Geomech. Abstr.* **13**(10), 1-24.

Barton, N.R. and Bandis, S.C. 1982. Effects of block size on the the shear behaviour of jointed rock. *23rd U.S. symp. on rock mechanics*, Berkeley, 739-760.

Barton, N.R. and Bandis, S.C. 1990. Review of predictive capabilites of JRC-JCS model in engineering practice. In *Rock joints, proc. int. symp. on rock joints*, Loen, Norway, (eds N. Barton and O. Stephansson), 603-610. Rotterdam: Balkema.

Barton, N.R. and Choubey, V. 1977. The shear strength of rock joints in theory and practice. *Rock Mech.* **10**(1-2), 1-54.

Deere, D.U. and Miller, R.P. 1966. *Engineering classification and index properties of rock.* Technical Report No. AFNL-TR-65-116. Albuquerque, NM: Air Force Weapons Laboratory

Hencher, S.R. & Richards, L.R. (1982). The basic frictional resistance of sheeting joints in Hong Kong granite *Hong Kong Engineer*, Feb., 21-25.

International Society for Rock Mechanics Commission on Standardisation of Laboratory and Field Tests. 1978. Suggested methods for the quantitative description of discontinuities in rock masses. *Int. J. Rock Mech. Min. Sci. & Geomech. Abstr.* **15**, 319-368.

Patton, F.D. 1966. Multiple modes of shear failure in rock. *Proc. 1st congr. Int. Soc. Rock Mech.*, Lisbon **1**, 509-513.

Structurally controlled instability in tunnels

Introduction

In tunnels excavated in jointed rock masses at relatively shallow depth, the most common types of failure are those involving wedges falling from the roof or sliding out of the sidewalls of the openings. These wedges are formed by intersecting structural features, such as bedding planes and joints, which separate the rock mass into discrete but interlocked pieces. When a free face is created by the excavation of the opening, the restraint from the surrounding rock is removed. One or more of these wedges can fall or slide from the surface if the bounding planes are continuous or rock bridges along the discontinuities are broken.

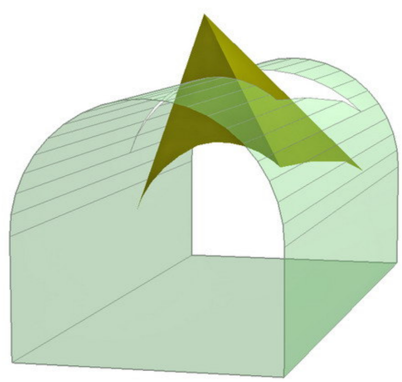

Roof fall

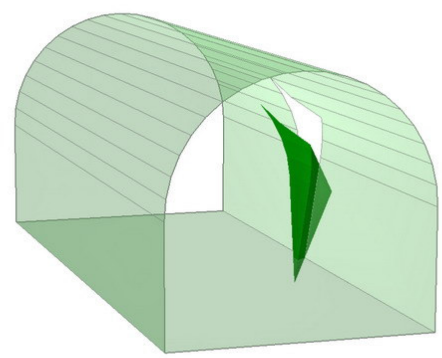

Sidewall wedge

Unless steps are taken to support these loose wedges, the stability of the back and walls of the opening may deteriorate rapidly. Each wedge, which is allowed to fall or slide, will cause a reduction in the restraint and the interlocking of the rock mass and this, in turn, will allow other wedges to fall. This failure process will continue until natural arching in the rock mass prevents further unravelling or until the opening is full of fallen material.

The steps which are required to deal with this problem are:

1. Determination of average dip and dip direction of significant discontinuity sets.
2. Identification of potential wedges which can slide or fall from the back or walls.
3. Calculation of the factor of safety of these wedges, depending upon the mode of failure.
4. Calculation of the amount of reinforcement required to bring the factor of safety of individual wedges up to an acceptable level.

Identification of potential wedges

The size and shape of potential wedges in the rock mass surrounding an opening depends upon the size, shape and orientation of the opening and also upon the orientation of the significant discontinuity sets. The three-dimensional geometry of the problem necessitates a set of relatively tedious calculations. While these can be performed by hand, it is far more efficient to utilise one of the computer programs which are available. One such program, called UNWEDGE[1], was developed specifically for use in underground hard rock mining and is utilised in the following discussion.

Consider a rock mass in which three strongly developed joint sets occur. The average dips and dip directions of these sets, shown as great circles in Figure 1, are as follows:

Joint set	*dip°*	*dip direction°*
J1	70 ± 5	036 ± 12
J2	85 ±8	144 ± 10
J3	55 ± 6	262 ± 15

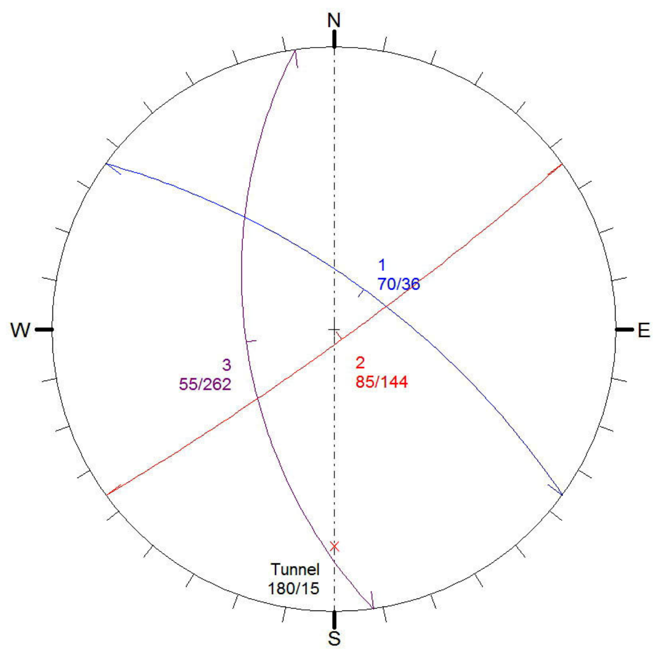

Figure 1: An equal area lower hemisphere plot of great circles representing the average dip and dip directions of three discontinuity sets in a rock mass. Also shown, as a chain dotted line, is the trend of the axis of a tunnel excavated in this rock mass. The tunnel plunge is marked with a red cross.

[1] Available from www.rocscience.com.

It is assumed that all of these discontinuities are planar and continuous and that the shear strength of the surfaces can be represented by a friction angle $\phi = 30°$ and a cohesive strength of zero. These shear strength properties are very conservative estimates, but they provide a reasonable starting point for most analyses of this type.

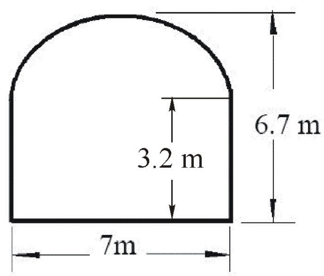

Tunnel section

A tunnel is to be excavated in this rock mass and the cross-section of the ramp is given in the sketch. The axis of the tunnel is inclined at 15° to the horizontal or, to use the terminology associated with structural geology analysis, the tunnel axis plunges at 15°. In the portion of the tunnel under consideration in this example, the axis runs due north-south or the trend of the axis is 180°.

The tunnel axis is shown as a chain dotted line in the stereonet in Figure 1. The trend of the axis is shown as 0°, measured clockwise from north. The plunge of the axis is 15° and this is shown as a cross on the chain dotted line representing the axis. The angle is measured inwards from the perimeter of the stereonet since this perimeter represents a horizontal reference plane.

The three structural discontinuity sets, represented by the great circles plotted in Figure 1, are entered into the program UNWEDGE, together with the cross-section of the tunnel and the plunge and trend of the tunnel axis. The program then determines the location and dimensions of the largest wedges which can be formed in the roof, floor and sidewalls of the excavation as shown in Figure 2.

The maximum number of simple tetrahedral wedges which can be formed by three discontinuities in the rock mass surrounding a circular tunnel is 6. In the case of a square or rectangular tunnel this number is reduced to 4. For the tunnel under consideration in this example, four wedges are formed.

Note that these wedges are the largest wedges which can be formed for the given geometrical conditions. The calculation used to determine these wedges assumes that the discontinuities are ubiquitous, in other words, they can occur anywhere in the rock mass. The joints, bedding planes and other structural features included in the analysis are also assumed to be planar and continuous. These conditions mean that the analysis will always find the largest possible wedges which can form. This result can generally be considered conservative since the size of wedges, formed in actual rock masses, will be limited by the persistence and the spacing of the structural features. The program UNWEDGE allows wedges to be scaled down to more realistic sizes if it is considered that maximum wedges are unlikely to form.

Details of the four wedges illustrated in Figure 2 are given in the following table:

Wedge	Weight - tonnes	Failure mode	Factor of Safety
Roof wedge	44.2	Falls	0
Right side wedge	5.2	Slides on J1/J2	0.36
Left side wedge	3.6	Slides on J3	0.40
Floor wedge	182	Stable	∞

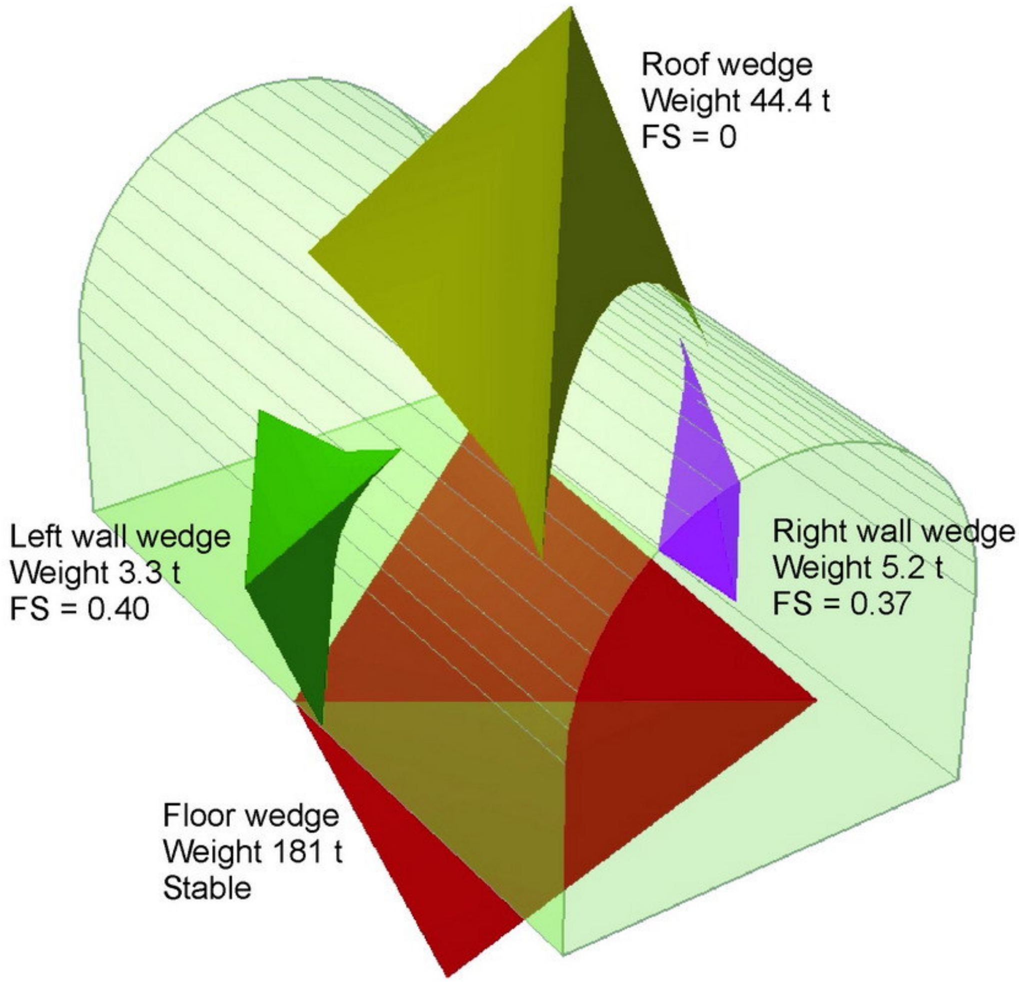

Figure 2: Wedges formed in the roof, floor and sidewalls of a ramp excavated in a jointed rock mass, in which the average dip and dip direction of three dominant structural features are defined by the great circles plotted in Figure 1.

The roof wedge will fall as a result of gravity loading and, because of its shape, there is no restraint from the three bounding discontinuities. This means that the factor of safety of the wedge, once it is released by excavation of the ramp opening, is zero. In some cases, sliding on one plane or along the line of intersection of two planes may occur in a roof wedge and this will result in a finite value for the factor of safety.

The two sidewall wedges are 'cousin' images of one another in that they are approximately the same shape but disposed differently in space. The factors of safety are different since, as shown in the table, sliding occurs on different surfaces in the two cases.

The floor wedge is completely stable and requires no further consideration.

Influence of in situ stress

The program UNWEDGE can take into account in situ stresses in the rock mass surrounding the opening. For the example under consideration, the influence of in situ stresses can be illustrated by the following example:

Stress	Magnitude	Plunge	Trend
Vertical stress σ_1	30 t/m^2	90º	030º
Intermediate stress σ_2	21 t/m^2	0º	030º
Minor stress σ_3	15 t/m^2	0º	120º

Wedge	Factor of Safety with no in situ stress	Factor of Safety with applied in situ stress
Roof wedge	0	1.23
Right side wedge	0.36	0.70
Side wedge 2	0.40	0.68
Floor wedge	∞	∞

The difference in the calculated factors of safety with and without in situ stresses show that the clamping forces acting on the wedges can have a significant influence on their stability. In particular the roof wedge is stable with the in situ stresses applied but completely unstable when released. This large difference suggests a tendency for sudden failure when the in situ stresses are diminished for any reason and is a warning sign that care has to be taken in terms of the excavation and support installation sequence.

Since it is very difficult to predict the in situ stresses precisely and to determine how these stresses can change with excavation of the tunnel or of adjacent tunnels or openings, many tunnel designers consider that it is prudent to design the tunnel support on the basis that there are no in situ stresses. This ensures that, for almost all cases, the support design will be conservative.

In rare cases the in situ stresses can actually result in a reduction of the factor of safety of sidewall wedges which may be forced out of their sockets. These cases are rare enough that they can generally be ignored for support design purposes.

Support to control wedge failure

A characteristic feature of wedge failures in blocky rock is that very little movement occurs in the rock mass before failure of the wedge. In the case of a roof wedge that falls, failure can occur as soon as the base of the wedge is fully exposed by excavation of the opening. For sidewall wedges, sliding of a few millimetres along one plane or the line of intersection of two planes is generally sufficient to overcome the peak strength of these surfaces. This dictates that movement along the surfaces must be minimised. Consequently, the support system has to provide a 'stiff' response to movement. This means that mechanically anchored rockbolts need to be tensioned while fully grouted rockbolts or other continuously coupled devices can be left untensioned provided that they are installed before any movement has taken place i.e. before the wedge perimeter has been fully exposed.

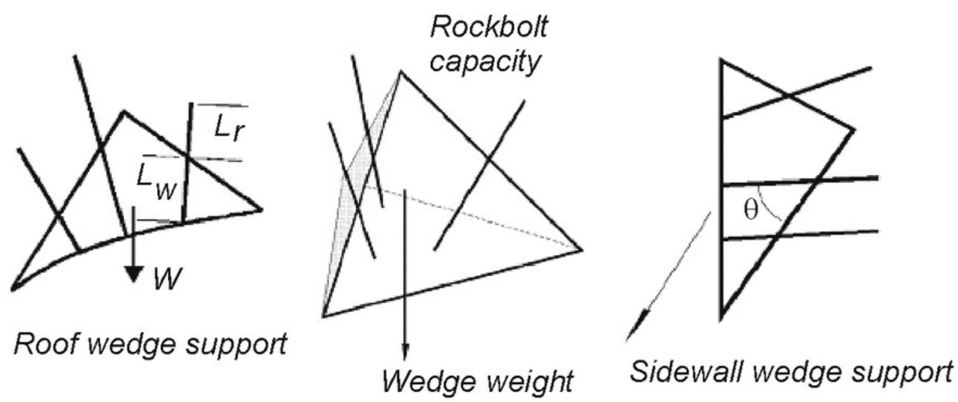

Figure 3: Rockbolt support mechanisms for wedges in the roof and sidewalls of tunnels

Rock bolting wedges

For roof wedges the total force, which should be applied by the reinforcement, should be sufficient to support the full dead weight of the wedge, plus an allowance for errors and poor quality installation. Hence, for the roof wedge illustrated in Figure 3; the total tension applied to the rock bolts or cables should be 1.3 to 1.5 × W, giving factors of safety of 1.3 to 1.5. The lower factor of safety would be acceptable in a temporary mine access opening, such as a drilling drive, while the higher factor of safety would be used in a more permanent access opening such as a highway tunnel.

When the wedge is clearly identifiable, some attempt should be made to distribute the support elements uniformly about the wedge centroid. This will prevent any rotations which can reduce the factor of safety.

In selecting the rock bolts or cable bolts to be used, attention must be paid to the length and location of these bolts. For grouted cable bolts, the length Lw through the wedge and the length Lr in the rock behind the wedge should both be sufficient to ensure that adequate anchorage is available, as shown in Figure 3. In the case of correctly grouted bolts or cables, these lengths should generally be a minimum of about one metre. Where there is uncertainty about the quality of the grout, longer anchorage lengths should be used. When mechanically anchored bolts with face plates are used, the lengths should be sufficient to ensure that enough rock is available to distribute the loads from these attachments. These conditions are automatically checked in the program UNWEDGE.

In the case of sidewall wedges, the bolts or cables can be placed in such a way that the shear strength of the sliding surfaces is increased. As illustrated in Figure 3; this means that more bolts or cables are placed to cross the sliding planes than across the separation planes. Where possible, these bolts or cables should be inclined so that the angle θ is between 15° and 30° since this inclination will induce the highest shear resistance along the sliding surfaces.

The program UNWEDGE includes a number of options for designing support for underground excavations. These include: pattern bolting, from a selected drilling position or placed normal to the excavation surface; and spot bolting, in which the location and length of the bolts are decided by the user for each installation. Mechanically anchored bolts with face plates or fully grouted bolts or cables can be selected to provide support. In addition, a layer of shotcrete can be applied to the excavation surface.

In most practical cases it is not practical to identify individual wedges in a tunnel perimeter and the general approach is to design a rockbolt pattern that will take care of all potential wedges. In the example under consideration the maximum wedge sizes have been identified, as shown in Figure 2, and it has been decided that in situ stresses will not be included in the stability analysis. Consequently, the wedges and their associated factors of safety shown in Figure 2 can be regarded as the most conservative estimate.

Figure 4 shows a typical pattern of 3 m long mechanically anchored 10 tonne capacity rockbolts on a 1.5 x 1.5 m grid. This pattern produces factors of safety of 1.40 for the roof wedge, 3.77 for the right sidewall wedge and 4.77 for the left sidewall wedge.

Shotcrete support for wedges

Shotcrete can be used for additional support of wedges in blocky ground, and can be very effective if applied correctly. This is because the base of a typical wedge has a large perimeter and hence, even for a relatively thin layer of shotcrete, a significant cross-sectional area of the material has to be punched through before the wedge can fail.

In the example under consideration, the application of a 10 cm thick shotcrete with a shear strength of 200 t/m^2 to the roof of the tunnel will increase the factor of safety from 1.40 (for the rockbolted case) to 8.5. Note that this only applies to fully cured (28 day) shotcrete and that the factor of safety increase given by the application of shotcrete cannot be relied on for short term stability. It is recommended that only the rockbolts be considered for immediate support after excavation and that the shotcrete only be taken into account for the long-term factor of safety.

It is important to ensure that the shotcrete is well bonded to the rock surface in order to prevent a reduction in support capacity by peeling-off of the shotcrete layer. Good adhesion to the rock is achieved by washing the rock surface, using water only as feed to the shotcrete machine, before the shotcrete is applied.

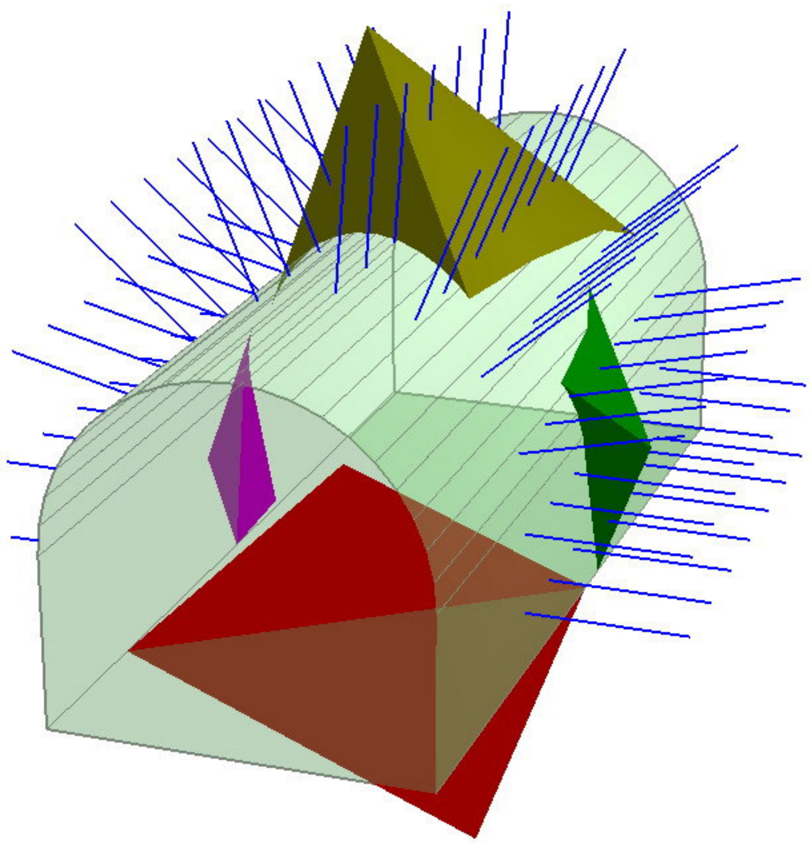

Figure 4: Rock bolting pattern to stabilize the roof and sidewall wedges in the tunnel example discussed earlier.

Figure 5: Ravelling of small wedges in a closely jointed rock mass. Shotcrete can provide effective support in such rock masses

The ideal application for shotcrete is in closely jointed rock masses such as that illustrated in Figure 5. In such cases wedge failure would occur as a progressive process, starting with smaller wedges exposed at the excavation surface and gradually working its way back into the rock mass. In these circumstances, shotcrete provides very effective support and deserves to be much more widely used than is currently the case.

Consideration of excavation sequence

As has been emphasised several times in this chapter, wedges tend to fall or slide as soon as they are fully exposed in an excavated face. Consequently, they require immediate support in order to ensure stability. Placing this support is an important practical question to be addressed when working in blocky ground, which is prone to wedge failure.

When the structural geology of the rock mass is reasonably well understood the program UNWEDGE can be used to investigate potential wedge sizes and locations. A support pattern, which will secure these wedges, can then be designed and rockbolts can be installed as excavation progresses.

When dealing with larger excavations such as caverns, underground crusher chambers or shaft stations, the problem of sequential support installation is a little simpler, since these excavations are usually excavated in stages. Typically, in an underground crusher chamber, the excavation is started with a top heading which is then slashed out before the remainder of the cavern is excavated by benching.

The margin sketch shows a large opening excavated in four stages with rock bolts or cables installed at each stage to support wedges, which are progressively exposed in the roof and sidewalls of the excavation. The length, orientation and spacing of the bolts or cables are chosen to ensure that each wedge is adequately supported before it is fully exposed in the excavation surface.

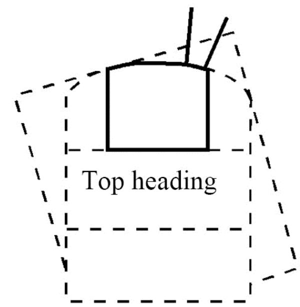

When dealing with large excavations of this type, the structural geology of the surrounding rock mass will have been defined from core drilling or access adits and a reasonable projection of potential wedges will be available. These projections can be confirmed by additional mapping as each stage of the excavation is completed. The program UNWEDGE provides an effective tool for exploring the size and shape of potential wedges and the support required to stabilise them.

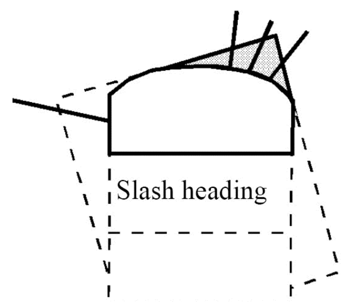

The margin sketch shows a support design which is based upon the largest possible wedges which can occur in the roof and walls of the excavation. These wedges can sometimes form in rock masses with very persistent discontinuity surfaces such as bedding planes in layered sedimentary rocks. In many metamorphic or igneous rocks, the discontinuity surfaces are not continuous and the size of the wedges that can form is limited by the persistence of these surfaces

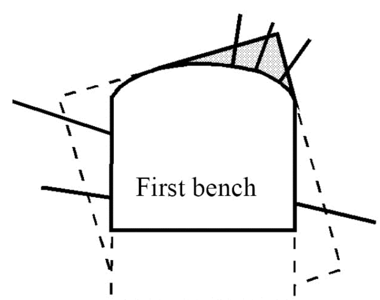

The program UNWEDGE provides several options for sizing wedges. One of the most commonly measured lengths in structural mapping is the length of a joint trace on an excavation surface and one of the sizing options is based upon this trace length. The surface area of the base of the wedge, the volume of the wedge and the apex height of the wedge are all calculated by the program and all of these values can be edited by the user to set a scale for the wedge. This scaling option is very important when using the program interactively for designing support for large openings, where the maximum wedge sizes become obvious as the excavation progresses.

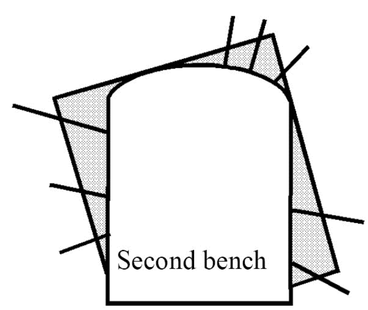

Application of probability theory

The program UNWEDGE has been designed for the analysis of a single wedge defined by three intersecting discontinuities. The "Combination Analyzer" in the program UNWEDGE can be used to sort through all possible joint combinations in a large discontinuity population in order to select the three joints which define most critical wedges.

Early attempts have been made by a number of authors, including Tyler et al (1991) and Hatzor and Goodman (1992), to apply probability theory to these problems and some promising results have been obtained. The analyses developed thus far are not easy to use and cannot be considered as design tools. However, these studies have shown the way for future development of such tools and it is anticipated that powerful and user-friendly methods of probabilistic analysis will be available within a few years.

References

Hatzor, Y. and Goodman, R.E. 1992. Application of block theory and the critical key block concept in tunneling; two case histories. *In Proc. Int. Soc. Rock Mech. conf. on fractured and jointed rock masses*, Lake Tahoe, California, 632-639.

Tyler, D.B., Trueman, R.T. and Pine, R.J. 1991. Rockbolt support design using a probabilistic method of key block analysis. In *Rock mechanics as a multidisciplinary science*, (ed. J.C. Roegiers), 1037-1047. Rotterdam: Balkema.

Tyler, D.B., Trueman, R. and Pine, R.J. 1991. Rockbolt support design using a probabilistic method of key block analysis. *Proc. 32nd U.S. Symp. Rock Mechanics*, Norman, Oklahoma, 1037-47.

The Rio Grande project - Argentina

Introduction

The Rio Grande pumped storage project is located on the Rio Grande river near the town of Santa Rosa de Calamucita in the Province of Cordoba in Argentina. It has an installed capacity of 1000 MW and provides electrical storage facilities for the power grid and, in particular, for a nuclear power plant about 50 km away from Rio Grande.

The project is owned by Agua y Energia Electrica, one of the principal Argentinean electrical utility organisations. Preliminary feasibility studies were carried out by the owner and these were followed by detailed design studies by Studio G. Pietrangeli of Rome. The scheme was partly financed by Italy and some of the construction was done by Condote de Agua, an Italian contractor. Golder Associates were involved in the design and supervision of support installed to control the stability of most of the major underground excavations.

The main underground facilities are located in massive gneiss of very good quality. The upper reservoir is impounded behind a rockfill dam and water is fed directly from the intakes down twin penstocks which then bifurcate to feed into the four pump-turbines. These turbines, together with valves and the control equipment, are housed in a large underground cavern with a span of 25 m and a height of 44 m.

Draft tubes from the turbines feed into twin tunnels which, with a down-stream surge shaft, form the surge control system for this project. The twin tunnels join just downstream of the surge tank and discharge into a single tailrace tunnel with a span of 12 m and height of 18 m. This tailrace tunnel is about 6 km long and was constructed by a full-face drill-and-blast top heading, with a span of 12 m and height of 8 m, followed by a 10 m benching operation. A view of the top heading is given in Figure 1.

Tailrace tunnel support

Because of the excellent quality of the gneiss, most of the underground excavations did not require support and minimal provision for support was made in the contract documents. Assessment of underground stability and installation of support, where required, was done on a 'design-as-you-go' basis which proved to be very effective and economical. Recent reports from site, many years after the start of construction and commissioning of the plant, show that there have been no problems with rockfalls or underground instability.

Figure 1: The 12 m span 8 m high top heading for the tailrace tunnel was constructed by full-face drill-and-blast and, because of the excellent quality of the massive gneiss, was largely unsupported.

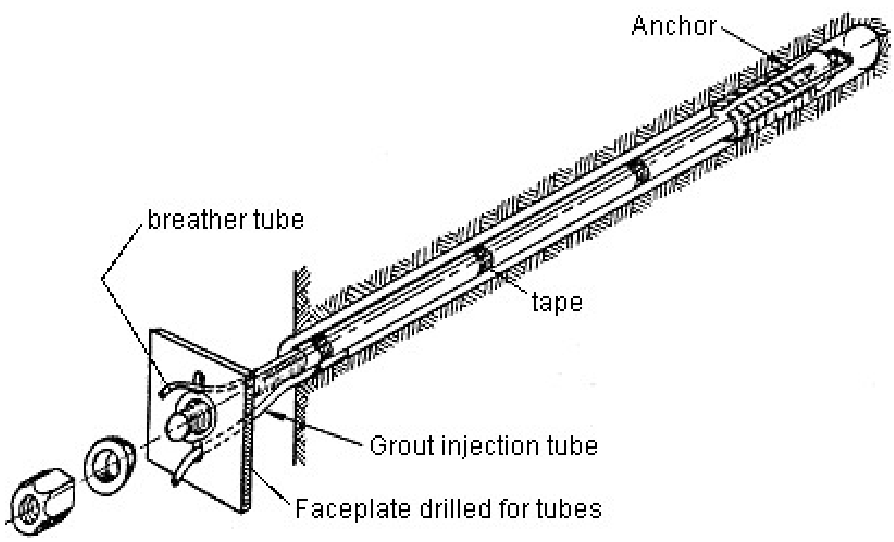

Figure 2: Mechanically anchored rockbolts of the type used on the Rio Grande project. These bolts were tensioned to 70% of their yield load upon installation and then, at a later stage, were re-tensioned and fully grouted.

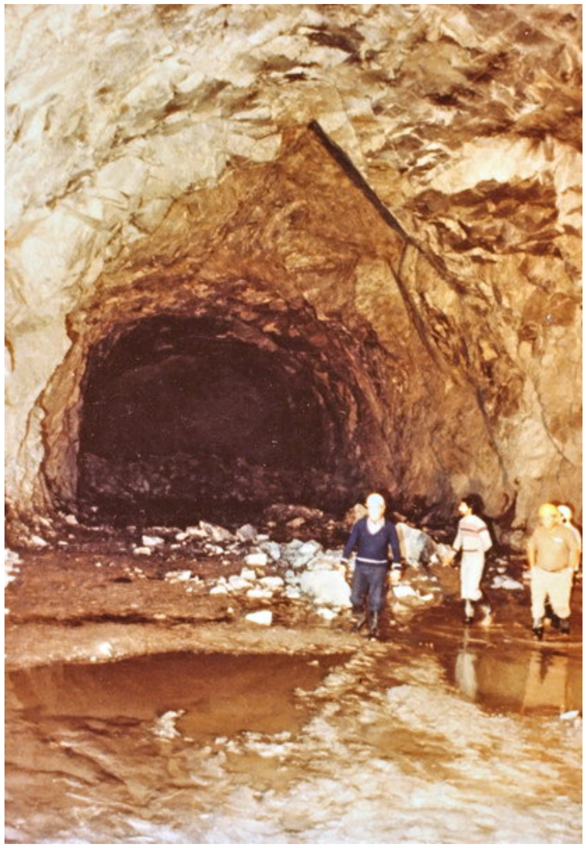

Figure 3: A wedge failure in the roof of the top heading of the Rio Grande tailrace tunnel.

Decisions on support were made on the basis of inspection of the excavated faces by a resident team of geotechnical engineers. Where the appearance of the face indicated that a zone of heavily jointed rock, usually associated with faulting, was being entered, the top heading was reduced to a 6 m span by 8 m high pilot tunnel to limit the volume of unstable rock which could be released from the roof. This pilot tunnel was large enough to accommodate the seven-boom jumbo, as illustrated in Figure 4, but small enough to limit the size of roof falls to manageable proportions. Bolting from inside the pilot heading was used to pre-support the potentially unstable wedges and blocks in the roof.

In the case of the tailrace tunnel, which is itself a large excavation, the support comprised mechanically anchored and cement grouted rockbolts as illustrated in Figure 2, with mesh reinforced shotcrete where required. These bolts were generally installed to control the type of wedge failure illustrated in Figure 3. In the case of particularly large wedges, calculations of the factor of safety and support requirements were carried out on a programmable calculator, using an early version of the program UNWEDGE.

Figure 4: A 6 m wide heading driven ahead of the tunnel face to permit pre-reinforcement of potentially unstable wedges in the roof. The seven-boom jumbo is seen working in the heading.

Support for power cavern

A cross-section of the power cavern is given in Figure 5 and this figure includes the five main excavation stages for the cavern. Careful mapping of significant structural features in the roof and walls of the central access drive at the top of the cavern provided information for estimating potentially unstable blocks and wedges which could form in the roof of the cavern. Figure 6 illustrates a number of such wedges in one section of the cavern roof. At each stage of the cavern excavation, long rockbolts (up to 10 m length) were installed to stabilise wedges or blocks which had been determined as being potentially unstable.

Because gneiss has usually undergone some tectonic deformation during its geological history, projection of structural features from visible exposures tends to be an imprecise process. Consequently, the potentially unstable blocks and wedges had to be reassessed after each excavation step revealed new information. The structural plan illustrated in Figure 6 had to be modified many times during excavation and that shown is the final plan prepared after the full cavern roof had been exposed.

A general view of the cavern excavation is given in Figure 7. This photograph was taken when the bulk of the cavern had been completed and only a few benches in the bottom of the cavern remained to be excavated. The enlarged top of the cavern is to accommodate the overhanging crane that is supported on columns from the cavern floor. An alternative design for this cavern would have been to support the crane on concrete beams anchored to the walls as is commonly done in good quality rock.

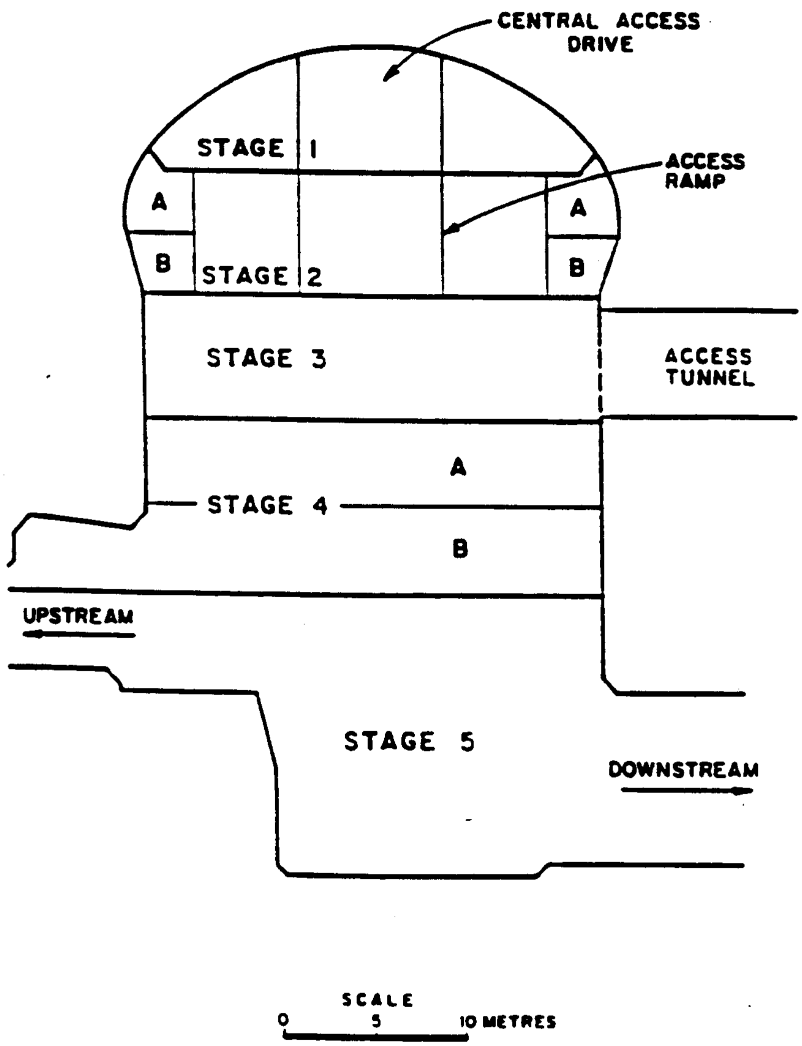

Figure 5: Cavern profile and excavation stages.

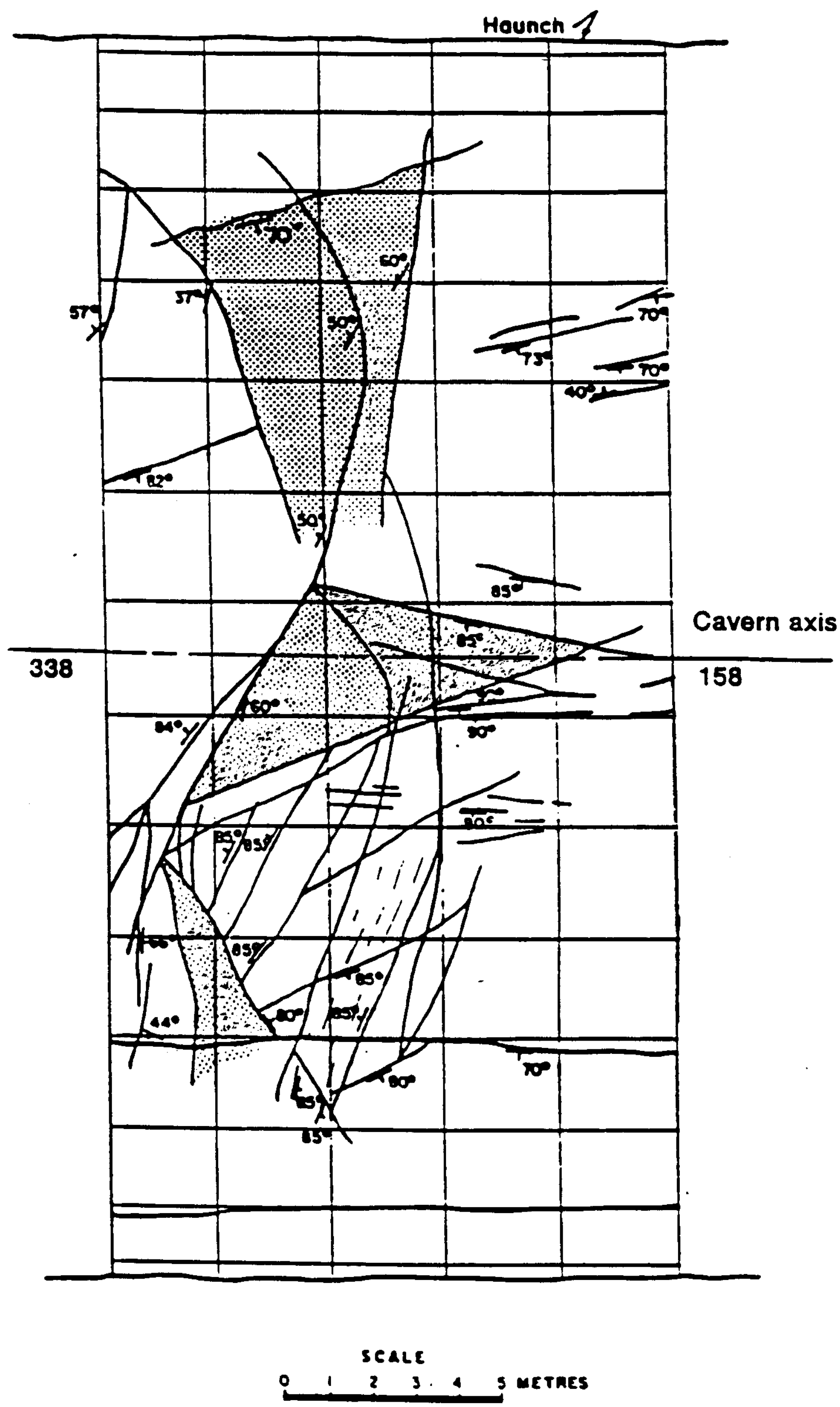

Figure 6: A plan of the traces of geological features mapped in part of the cavern roof. The shaded areas represent potentially unstable wedges requiring reinforcement.

Rio Grande project - Argentina

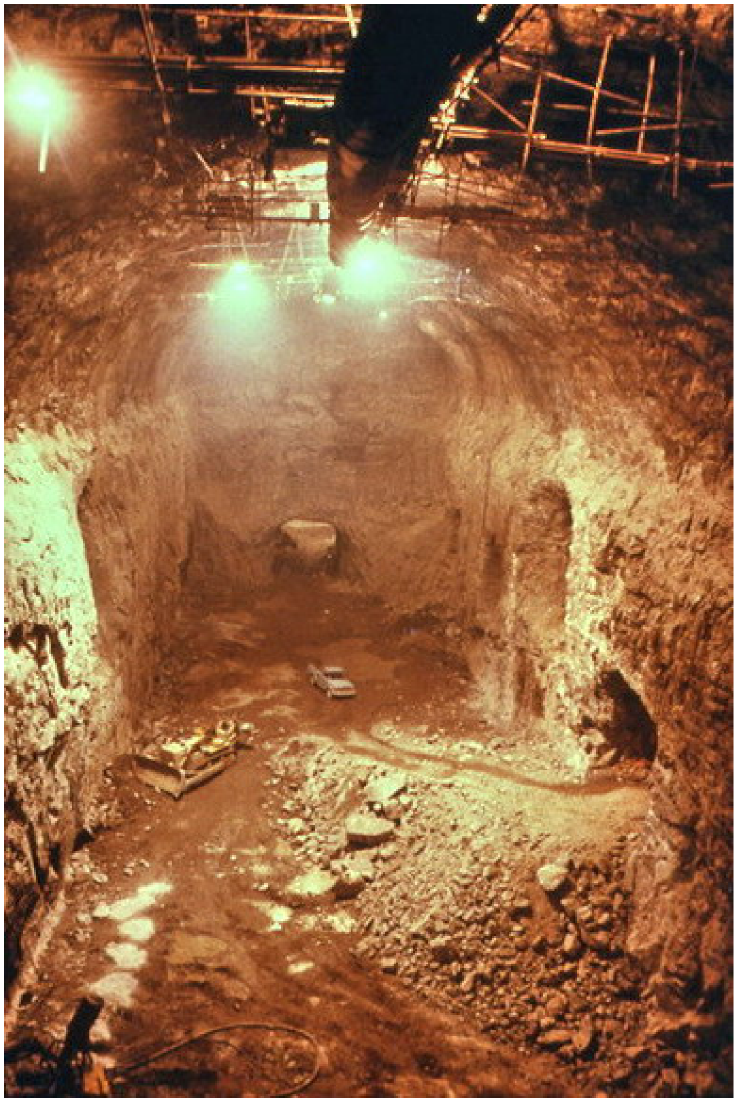

Figure 7: A view of the 25 m span Rio Grande power cavern during excavation of the lower benches.

Discussion of support design and costs

Apart from rockbolts installed to control isolated structurally controlled blocks and wedges in the roof and sidewalls and some areas of closely jointed rock which were shotcreted, the cavern was unsupported. While this was successful for this particular project, it is not the approach which should generally be used for a critical excavation such as an underground powerhouse.

The damage resulting from even a small rockfall in such a cavern is out of all proportion to the savings achieved by eliminating pattern rockbolting and full shotcrete lining. Hence, in addition to the rockbolts installed to control structural instability, as described earlier, I would recommend a normal pattern of 25 mm diameter, 5 m long bolts (20% of the excavation span) on a 2.5 m grid. In addition, I would recommend the placement of 50 mm of fibre-reinforced micro-silica shotcrete over the entire roof and upper sidewalls of the cavern. Based on current north American costs, this additional support, involving approximately 600 rockbolts and about 300 m^3 of shotcrete, would have cost approximately US $200,000. In terms of the overall project cost and the increased long-term security in the cavern, this would normally be regarded as a good investment.

In contrast, consider the 6 km long tailrace tunnel in which the consequences of a small rockfall are minimal. Assume that a pattern of 4 m long bolts on a 2 m grid (say 10 bolts per section) and a 50 mm shotcrete thickness had been specified for the roof and upper sidewalls of the tailrace tunnel. This would involve 30,000 bolts and 5,400 m^3 of shotcrete at a total cost approaching US $5 million. This example illustrates the need to give careful consideration to the function and risks associated with each underground excavation before deciding upon the support system to be used.

Analysis using UNWEDGE program

UNWEDGE[1] is a user-friendly micro-computer program which can be used to analyse the geometry and the stability of wedges defined by intersecting structural discontinuities in the rock mass surrounding an underground excavation. The analysis is based upon the assumption that the wedges, defined by three intersecting discontinuities, are subjected to gravitational loading only. In other words, the stress field in the rock mass surrounding the excavation is not taken into account. While this assumption leads to some inaccuracy in the analysis, it generally leads to a lower factor of safety than that which would occur if the in situ stresses were taken into account.

The application of the program UNWEDGE to the analysis of a potentially unstable wedge in the Rio Grande cavern is illustrated in the following discussion.

Input Data

The dips and dip directions of a number of planes can be entered directly into the table which appears when the ‘Input data’ option is chosen or this information can be entered in the form of a DIPS file. Once the data has been read into the program, the great circles representing the discontinuities are displayed on the screen as illustrated in Figure 8 and the user is prompted to select the three joint planes to be included in the analysis. Alternatively, the program can be instructed to compute the three most critical planes – those giving the largest wedges with the lowest factors of safety. Once the information on these planes has been entered, the unit weight of the rock

[1] Available from www.rocscience.com

and the shear strengths of the joints are entered. Finally, the water pressure acting on the joint surface is entered. In most cases, the default water pressure of 0 will be chosen but the user may check the sensitivity of the wedge to pore water pressure by entering appropriate values.

In the case of the rock mass surrounding the Rio Grande Cavern, the dips and dip directions of the following three sets of joints are included in Figure 8:

1 88/225 shear joint set
2 85/264 shear joint set
3 50/345 tension joint set
Cavern axis: trend 158, plunge 0

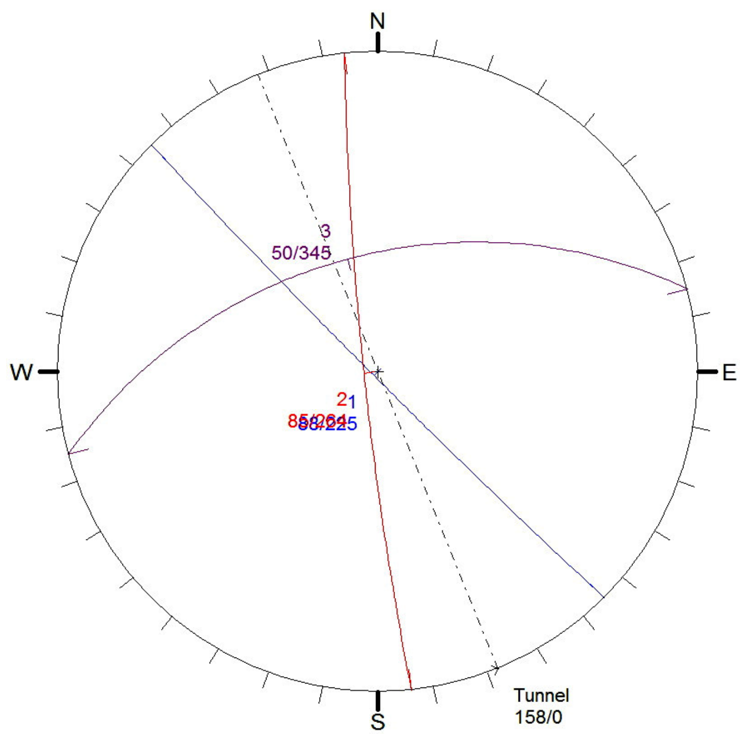

Figure 8: Great circles representing four joint sets which occur in the rock mass surrounding the Rio Grande cavern - imported as a DIPS file.

Input of excavation cross-section

In setting up this analysis, the co-ordinates shown in Figure 9 were used to define the cavern profile. These co-ordinates must be entered sequentially and must form a closed figure. The profile is formed from straight line and arc segments and a sufficient number of co-ordinates should be entered to ensure that a smooth profile is generated.

Determination of wedge geometry

Depending upon the shape of the cross-section, a maximum of six wedges can be formed with three intersecting joint planes. Selecting the '3D wedge view" option gives a number of views showing the shape and size of these wedges. The two wedges formed on the cavern end walls can be viewed by activating the 'End wedges' option.

Figure 10 shows the wedges formed in the case of the Rio Grande power cavern for the three joint planes defined in Figure 8. The weight of each of these wedges, the failure mode and the calculated factor of safety are shown in the figure. Obviously, the most dangerous wedge in this situation is the wedge formed in the roof while the wedge formed in the floor is stable and need not be considered further in this analysis.

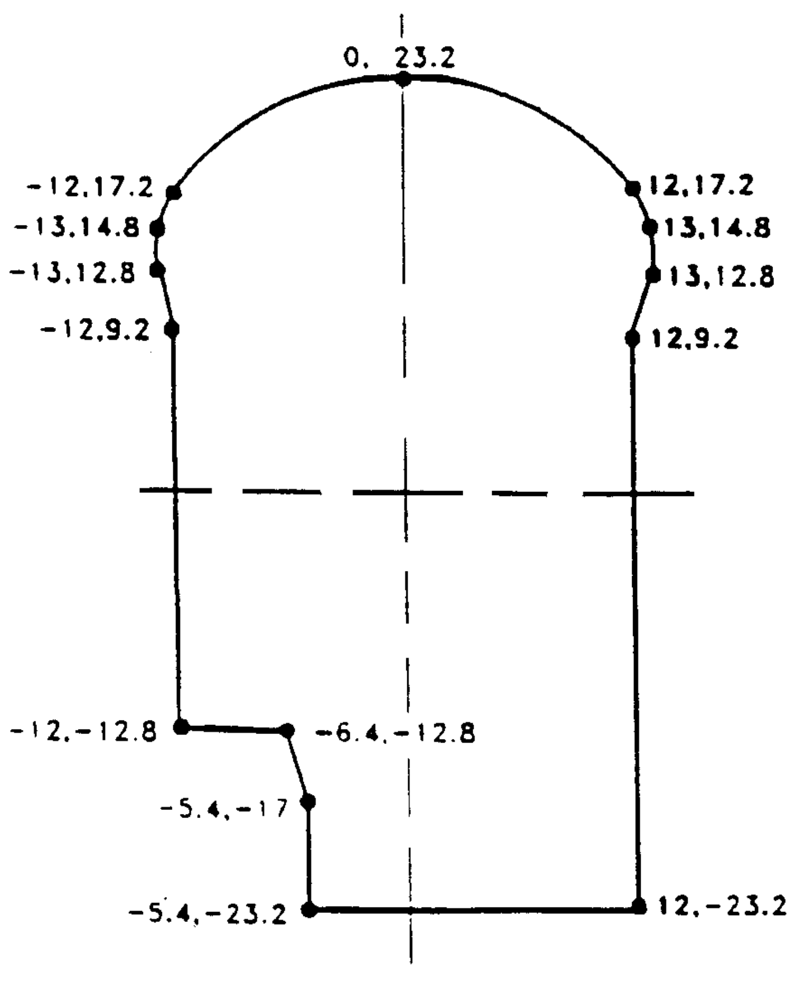

Figure 9: Co-ordinates used to define the profile of the cavern.

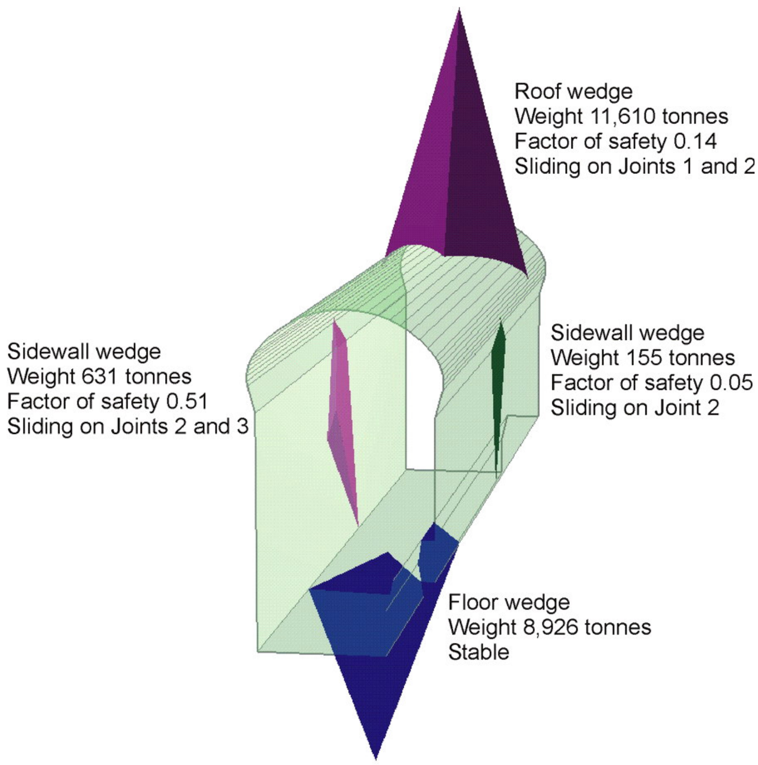

Figure 10: Perspective view of the wedges formed in the rock mass surrounding the Rio Grande power cavern.

Sizing or wedges

The program UNWEDGE automatically determined the largest wedge that can occur in the rock mass adjacent to the excavation profile. In the case of the roof wedge, shown in Figure 10, the wedge extends over the full 25 m span of the cavern and weighs 11,610 tonnes. While, in exceptional circumstances, such wedges may occur, the limited extent of joints in many rock masses will restrict the size of the wedges to much smaller dimensions than those determined by UNWEDGE for the large excavations.

As illustrated in Figure 6, the trace length of joint number 3 (50/345) in the upper roof wedge is approximately 6 m. When the 'Scale wedges' is chosen, the user can define the size of the wedge in terms of the area of the face on the excavation surface, the volume of the wedge, the height of the apex of the wedge, the length of one of the joint traces or the persistence of one of the joints. In this case a trace length of 6 m is entered for joint number 3, defined by 50/345, and the resulting wedge is illustrated in Figure 11. This wedge weighs 220 tonnes and will require about seven 50 tonne capacity fully grouted cables to give a factor of safety of about 1.5 which is considered appropriate for a cavern of this type.

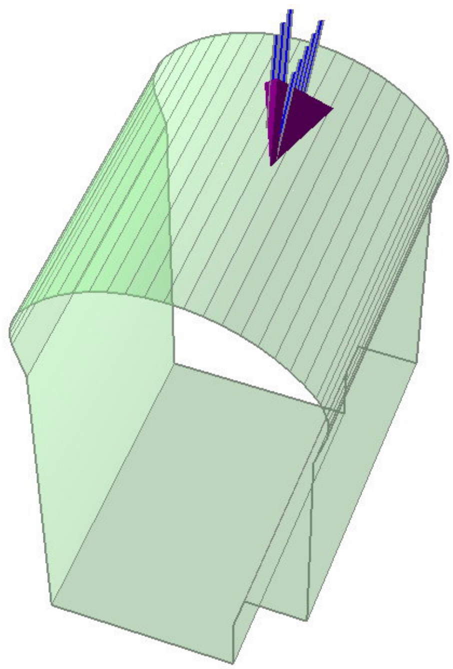

Figure 11: Perspective view of roof wedge in the Rig Grande cavern roof. The size of this wedge has been defined by setting the trace length of the 50/345 joint to 6 m. Eight 10 m long 50 tonne capacity grouted anchors give a factor of safety of 1.6 .

UNWEDGE allows the user to add a layer of shotcrete and calculates the factor of safety increase as a result of such an addition. Since the shotcrete can only be added once the surface of the wedge is fully exposed it is not taken into account in calculating the support required to stabilise the wedge. The increase in safety factor which occurs after the shotcrete has set can be regarded as a long term bonus and it does allow the user to choose a slightly lower factor of safety for the immediate support of the wedge.

A slope stability problem in Hong Kong

Introduction

In the early 1970s a series of landslides occurred in Hong Kong as a result of exceptionally heavy rains. These slides caused some loss of life and a significant amount of property damage. Consequently, an extensive review was carried out on the stability of soil and rock slopes in the Territory.

During this review, a rock slope on Sau Mau Ping Road in Kowloon was identified as being potentially unstable. The stability of this particular slope was critical because it was located immediately across the road from two blocks of apartments, each housing approximately 5,000 people.

Figure 1 gives a general view down Sau Mau Ping Road, showing the steep rock slopes on the left and the apartment blocks on the right.

The concern was that a major rock slide could cross the road and damage the apartment blocks. In order to decide upon whether or not the residents of the two apartment blocks should be evacuated, the two questions which required an immediate response were:

What was the factor of safety of the slope under normal conditions and under conditions which could occur during an earthquake or during exceptionally heavy rains associated with a typhoon?

What factor of safety could be considered acceptable for long term conditions and what steps would be required in order to achieve this factor of safety?

Description of problem

The rock mass in which the slope adjacent to the Sau Mau Ping Road was cut is unweathered granite with exfoliation or sheet joints similar to those illustrated in Figure 2. These joints are parallel to the surface of the granite and the spacing between successive joints increases with increasing distance into the rock mass. Undercutting of these sheet joints can cause a rock slide such as that illustrated in Figure 3.

During excavation of the original slopes for the Sau Mau Ping Road, a small rock slide was induced by blasting. The surface on which this failure occurred is illustrated in Figure 4. Blasting, such as that used in civil construction in an urban environment, does not impose very large loads on rock slopes and it can be assumed that the factor of safety of the slope was close to unity.

Figure 1: A view down Sau Mau Ping Road in Kowloon showing apartment blocks across the road from the steep rock slopes.

Figure 2: Sheet jointing in granite. These features, sometimes referred to as 'onion skin' joints, are the result of exfoliation processes during cooling of the granite.

Figure 3: A rock slide on a road caused by the undercutting of sheet joints in a granite slope. In hard rocks such as granite, failure can occur very suddenly if the factor of safety of the slope is close to 1. A rise in groundwater levels during a heavy storm or ice jacking in winter may be sufficient to induce failure.

Figure 4: The failure surface defined by a sheet joint surface on which a small slide occurred during blasting of the original cut slope for the Sau Mau Ping Road. The potentially unstable slope under consideration is visible in the background.

The potentially unstable slope under consideration is visible in the background of this photograph. It is obvious from this photograph that the sheet joint surface continues under the potentially unstable slope. Hence, from the evidence of the small scale failure, it can be deduced that the factor of safety of the slope in question is not very high.

The geometry of the slope is illustrated in Figure 5 which shows a 60 m high slope with three 20 m high benches. The overall slope angle is 50° and the individual bench faces are inclined at 70° to the horizontal. An exfoliation joint surface dips at 35° and undercuts the slope as shown in the figure. The slope face strikes parallel to the underlying exfoliation surface and hence the slope can be analysed by means of a two-dimensional model.

Tension cracks are frequently observed behind the crest of slopes which have a factor of safety of less than about 1.2. These cracks are dangerous in that they allow water to enter the slope at a particularly critical location. Unfortunately, in the case of the Sau Mau Ping slope, recently cultivated market gardens located on the top of the slope made it impossible to determine whether or not such tension cracks were present and hence it was decided to carry out two sets of analyses - one with and one without tension cracks. These analyses were carried out for both the overall slope and for individual benches.

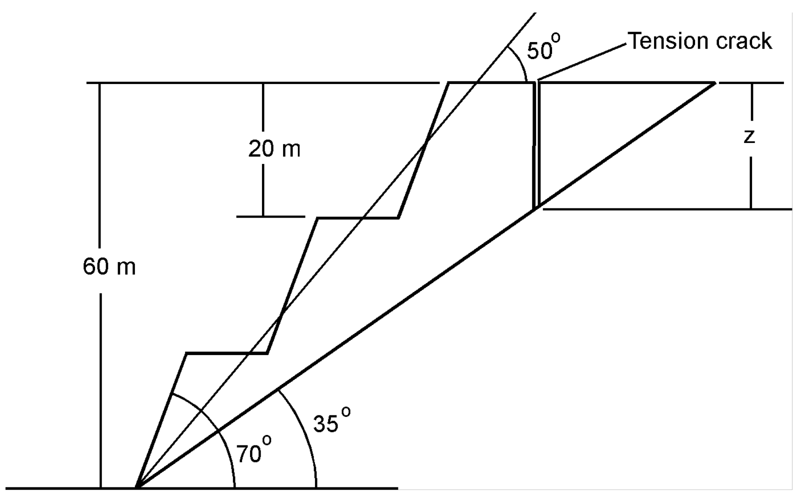

Figure 5: Geometry assumed for the two-dimensional analysis of the Sau Mau Ping Road slope.

Limit equilibrium models

At the time of this investigation, no rock mechanics facilities existed in Hong Kong and no diamond drilling or laboratory testing had ever been carried out on the granitic rocks in which this slope had been excavated. Consequently, the problem was tackled on the basis of a crude form of risk analysis, using simple analytical models to predict the response of the slope to a range of possible conditions. The two models are defined in Figure 6 and Figure 7.

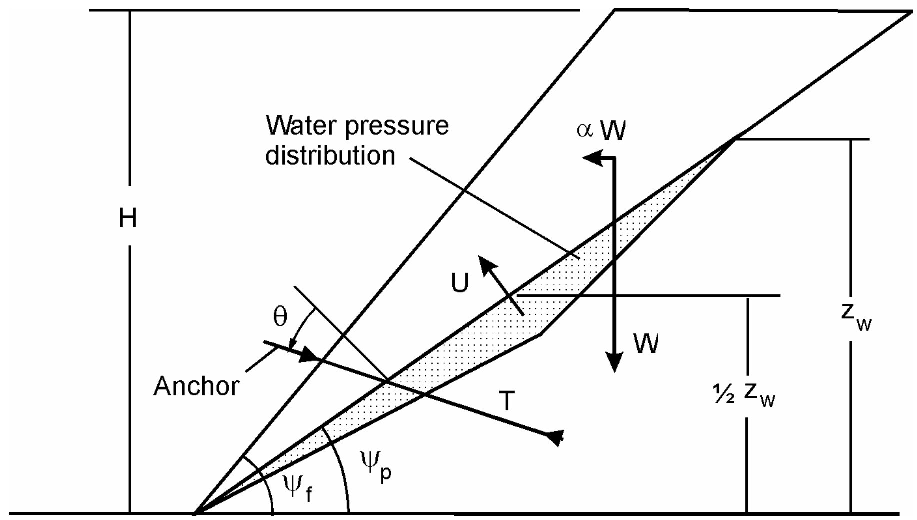

$$F = \frac{cA + \left(W(\cos\psi_p - \alpha\sin\psi_p) - U + T\cos\theta\right)\tan\phi}{W(\sin\psi_p + \alpha\cos\psi_p) - T\sin\theta} \tag{1}$$

where

$$A = \frac{H}{\sin\psi_p} \tag{2}$$

$$W = \frac{\gamma_r H^2}{2}(\cot\psi_p - \cot\psi_f) \tag{3}$$

$$U = \frac{\gamma_w H_w^2}{4\sin\psi_p} \tag{4}$$

Figure 6: Factor of Safety calculation for a slope with no tension crack.

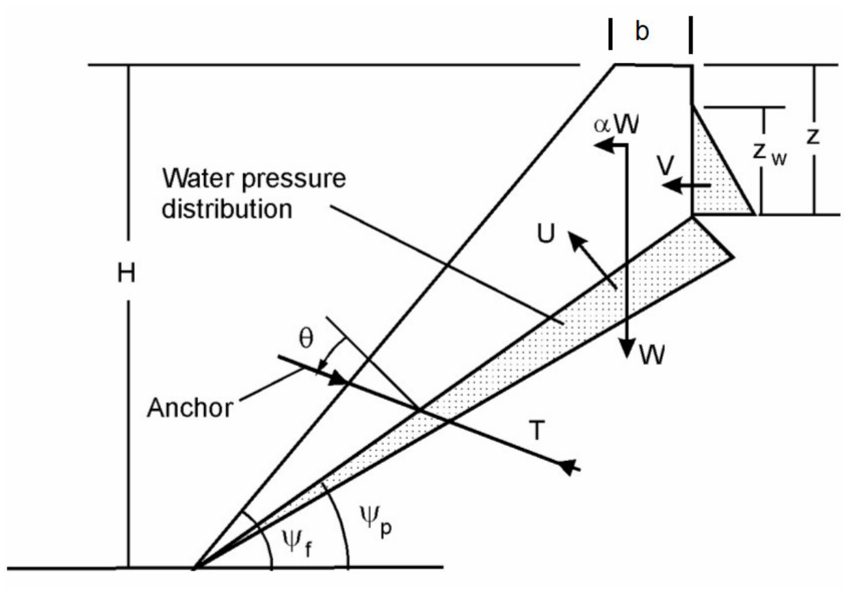

$$F = \frac{cA + \left(W(\cos\psi_p - \alpha\sin\psi_p) - U - V\sin\psi_p + T\cos\theta\right)\tan\phi}{W(\sin\psi_p + \alpha\, con\,\psi_p) + V\cos\psi_p - T\sin\theta} \tag{5}$$

where

$$z = H\left(1 - \sqrt{\cot\psi_f\,\tan\psi_p}\right) \tag{6}$$

$$b = H\left(\sqrt{\cot\psi_f \cdot \cot\psi_p} - \cot\psi_f\right) \tag{7}$$

$$A = \frac{H - z}{\sin\psi_p} \tag{8}$$

$$W = \frac{\gamma_r H^2}{2}\left(\left(1 - \left(\frac{z}{H}\right)^2\right)\cot\psi_p - \cot\psi_f\right) \tag{9}$$

$$U = \frac{\gamma_w z_w A}{2} \tag{10}$$

$$V = \frac{\gamma_w z_w^2}{2} \tag{11}$$

Figure 7: Factor of Safety calculation for a slope with a water-filled tension crack.

The Symbols and dimensions used in these models are as follows:

Symbol	Parameter	Dimensions
F	Factor of safety against sliding along sheet joint	Calculated
H	Height of the overall slope or of each bench	60 m or 20 m respectively
ψf	Angle of slope face, measured from horizontal	50°
ψp	Angle of failure surface, measured from horizontal	35°
b	Distance of tension crack behind crest	Calculated (m)
z	Depth of tension crack	Calculated (m)
zw	Depth of water in tension crack or on failure surface	Variable (m)
α	Horizontal earthquake acceleration	0.08 g (proportion of g)
γr	Unit weight of rock	0.027 MN/m3
γw	Unit weight of water	0.01 MN/m3
W	Weight of rock wedge resting on failure surface	Calculated (MN)
A	Base area of wedge	Calculated (m2)
U	Uplift force due to water pressure on failure surface	Calculated (MN)
V	Horizontal force due to water in tension crack	Calculated (MN)
c	Cohesive strength along sliding surface	Variable (MN/m2)
ϕ	Friction angle of sliding surface	Variable (degrees)
T	Force applied by anchor system (if present)	Specified (MN)
θ	Inclination of anchor, anti-clockwise from normal	Specified (degrees)

Note that this is a two-dimensional analysis and these dimensions refer to a 1 metre thick slice through the slope. It is also important to recognise that this analysis considers only force equilibrium and assumes that all forces pass through the centroid of the wedge. In other words, moment equilibrium is not considered in this analysis. While this is a simplification of the actual situation depicted in Figure 6 and Figure 7, the errors introduced are not considered to be significant, given the uncertainty of the other input data used in these analyses.

In Figure 7 the depth z of the tension crack is calculated by equation 6. This equation is obtained by minimising equation 5 with respect to the tension crack depth z (Hoek and Bray, 1974). This minimisation is carried out for a dry slope and the accuracy of equation 6 decreases as the water depth in the tension crack increases. However, for the purposes of this analysis, the estimate given by equation 6 is considered acceptable.

Estimates of shear strength

One of the most critical steps in any limit equilibrium analysis is the determination or the estimation of the shear strength parameters (c and ϕ) for the surface along which it is anticipated that sliding will take place. In the case of this slope on Sau Mau Ping Road, no information on shear strength was available at the time of the initial studies and so estimates had to be made on the basis of published information for similar rocks.

Hoek and Bray (1974) published a plot, reproduced in Figure 8, of cohesive strengths and friction angles for rocks and soils, based upon the results of published back analysis of slope failures. Superimposed on this plot is an elliptical zone which encompasses the estimated range of shear strength for sheet joints in unweathered granite. In choosing this range it was considered that the friction angle ϕ probably ranges from 30° for very smooth planar surfaces to 45° for rough or partly cemented surfaces. The cohesive strength c is more difficult to estimate and the range of 0.05 to 0.2 MPa was chosen on the basis of the results of back-analyses of slope failures, plotted in Figure 8.

Some readers may be surprised that a cohesive strength has been assumed for joint surfaces which obviously have no tensile strength or 'stickiness' as would be found in a clayey soil. In fact, this assumed cohesive strength is defined by the intercept, on the shear strength axis, of a tangent to a curvilinear Mohr envelope. This curvature is the result of the interlocking of asperities on the matching surfaces of the joints and the increase in shear strength given by this interlocking plays a crucial role in the stability of slopes such as that under consideration in this chapter.

Estimate of earthquake acceleration

Hong Kong is not considered a highly seismic region but relatively minor earthquakes are not unknown in the region. Consequently, it was felt that some allowance should be made for the possible influence of earthquake loading on the stability of the Sau Mau Ping slope.

The traditional method of incorporating the acceleration induced by earthquakes or large blasts in slope stability analyses is to add an outward force αW to the forces acting on the slope (see Figure 6 and Figure 7), where α is the acceleration as a proportion of g, the acceleration due to gravity. This 'pseudo-static' form of analysis is known to be very conservative but, in the case of the Sau Mau Ping slope, this conservatism was not considered to be out of place.

In discussion with local engineers and geologists, the consensus opinion was that the horizontal acceleration which could be induced by a 10 year return period earthquake in the region would be approximately 0.08 g. This value was used in all of the sensitivity analyses discussed in the following sections.

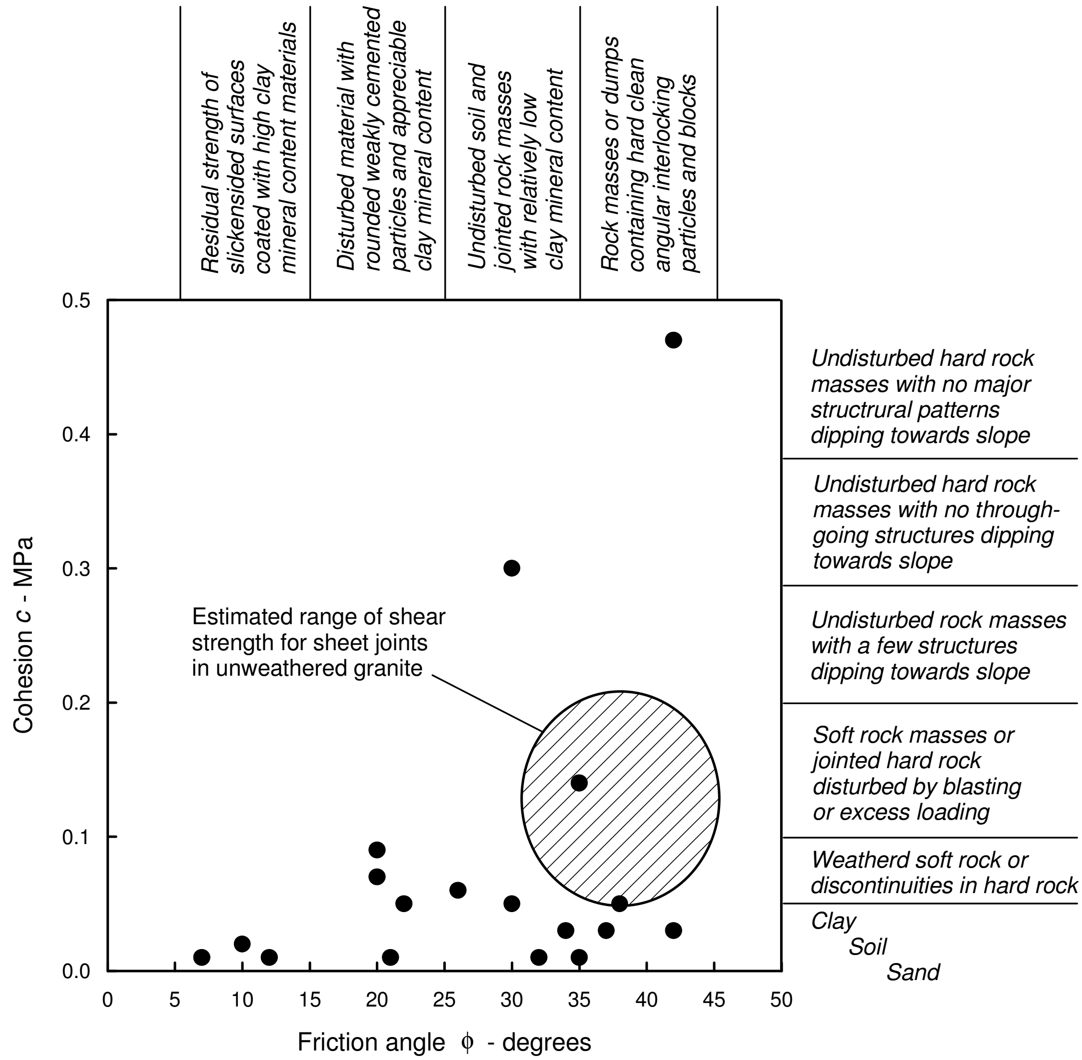

Figure 8: Relationship between friction angles and cohesive strengths mobilised at failure of slopes in various materials. The plotted points were obtained from published information from the back analysis of slope failures. (After Hoek and Bray 1974).

Analysis of mobilised shear strength

One method for assessing the stability of slopes is to calculate the shear strength that would be mobilised at failure and to compare this strength with the shear strength which is available along the failure surface. In the case of the Sau Mau Ping slope, this was done by substituting F = 1 in equations 1 and 5 and solving for the cohesive strength c and the friction angle ϕ. The results of this analysis are plotted in Figure 9. The estimated range of available shear strength (from Figure 8) is also shown on this plot.

Figure 9 shows that only two of the cases analysed result in conditions where the shear strength mobilised at failure falls within the estimated range of available shear strength. These two cases are designated 2 and 4 and they are for fully saturated slopes, with and without tension cracks.

Decision on short-term stability of the Sau Mau Ping slope

From the results of the sensitivity study described above it was concluded that instability of this particular slope could occur if the slope was fully saturated and subjected to earthquake loading. Typhoons occur several times every year in Hong Kong and the intensity of precipitation during these events is certainly sufficient to saturate the slopes. As discussed earlier, minor earthquakes do occur in the region but they are not very frequent. Consequently, the chance of simultaneous saturation and earthquake loading was considered to be small and in was concluded that there was no serious short-term threat of instability of the Sau Mau Ping slope.

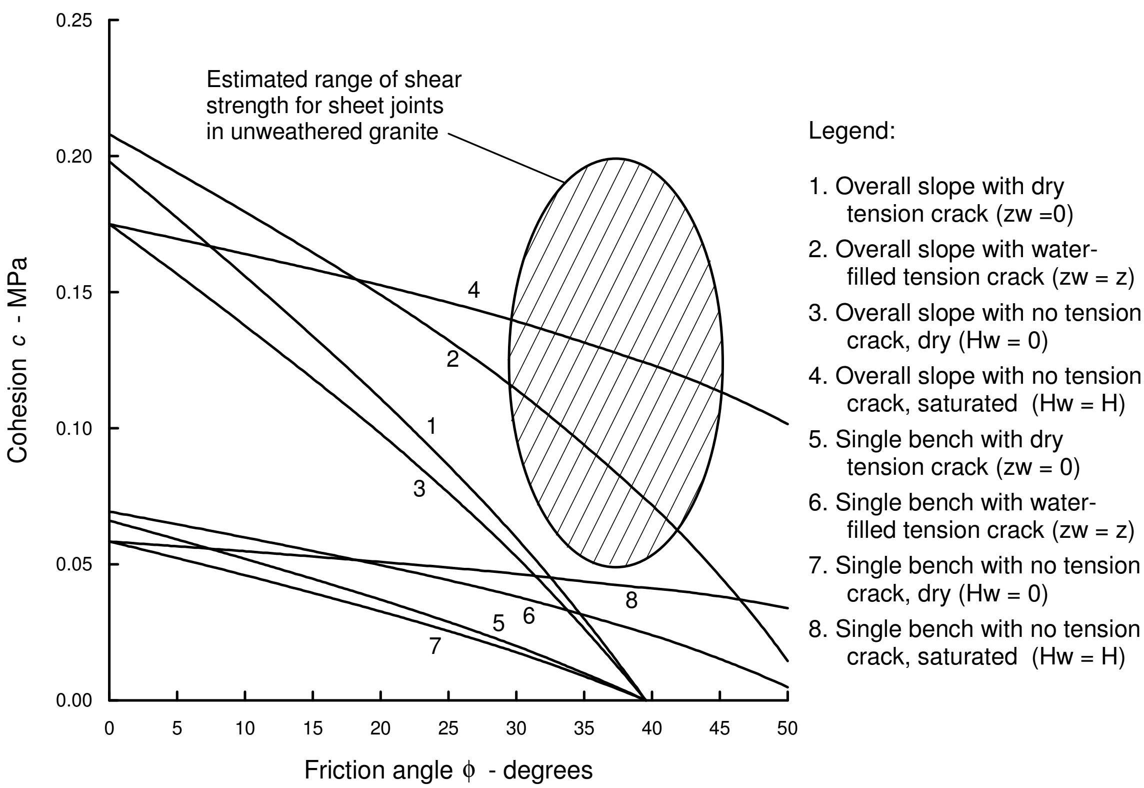

Figure 9: Comparison of the shear strength mobilised by failure under various conditions with the estimated shear strength available on sheet joints in unweathered granite.

In discussion with the highway authorities in Hong Kong, the following decisions were made:

No evacuation of the residents of the two apartment blocks, located across the street from the slope in question, would be carried out.
Horizontal drainage holes would be drilled into the slope face to penetrate the potential failure surface in an attempt to reduce uplift pressures in the slope.
Piezometers would be installed in holes drilled from the top of the slope. These piezometers would be measured regularly during periods of significant rainfall and the road would be closed to traffic if water levels rose to levels decided by the engineers responsible for the project.

An investigation would be carried out into the most effective remedial measures to stabilise the slope for the long-term.

Figure 10 shows the drilling of the horizontal drain holes into the slope face and Figure 11 shows the drilling of the vertical holes into which the piezometers were installed. These piezometers were monitored for the next few years, while preparations for the final stabilisation of the slope were made, and the road was closed to traffic on two occasions when water levels were considered to be dangerously high.

Figure 10: Drilling horizontal drain holes into the face of one of the benches of the Sau Mau Ping slope.

Figure 11: Drilling vertical diamond core holes into the Sau Mau Ping slope. These holes were used for geotechnical investigation purposes and also for the installation of piezometers in the rock mass.

Evaluation of long-term remedial measures

While the short-term threat of instability was considered to be small, the longer-term stability of the slope was considered to be unacceptable and a study was carried out to evaluate various options for stabilising the slope. It was agreed that a factor of safety of 1.5 was required to meet long term requirements. The following alternatives were considered:

1. Reducing the height of the slope.
2. Reducing the angle of the slope face.
3. Drainage of the slope.
4. Reinforcement of the slope.

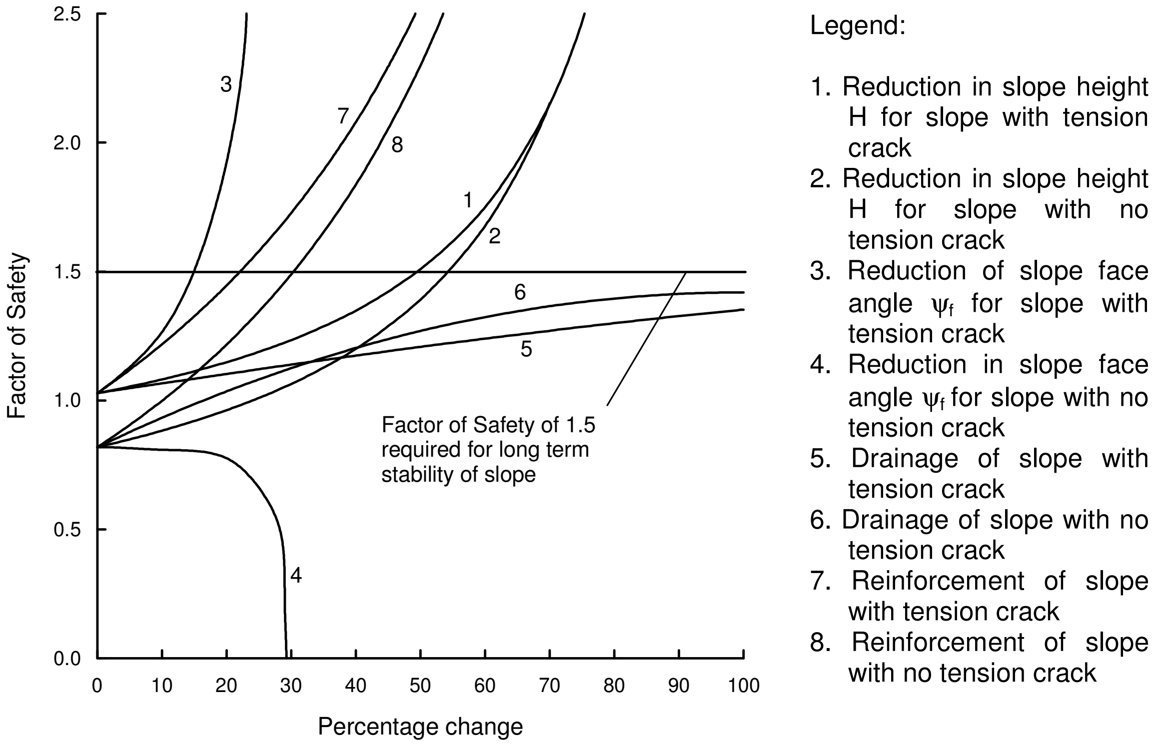

Figure 12: Evaluation of remedial options to increase the stability of the slope

The limit equilibrium models defined in Figure 6 and Figure 7 were used for this evaluation and the results are plotted in Figure 12.

In calculating the factors of safety shown in this figure, the shear strength was maintained constant and was defined by c = 0.10 MPa and ϕ = 35°. Similarly, an earthquake acceleration of α = 0.08 g was used for all the analyses. The percentage change refers to the ratios of slope height, slope angle and water depth to the original dimensions defined in Figure 5.

In the case of the reinforcement options, the percentage change refers to the ratio of anchor force T to the weight of the wedges (24.8 MN for the slope with the tension crack and 28.6 MN for the slope with no tension crack). The anchor inclination was kept constant at $\theta = \phi = 35°$. This anchor inclination gives the minimum anchor load for a dry slope and it can be determined by minimising equations 1 or 5 with respect to θ.

The curves presented in Figure 12 show clearly that some remedial measures are much more effective than others and it is worth examining each of the options in turn.

Curves 1 (slope with tension crack) and 2 (slope without tension crack) show that reduction of the slope height is not an effective solution to the problem. In order to achieve the required factor of safety of 1.5, the slope height would have to be reduced by 50%. If this solution were to be adopted, it would be more practical to excavate the entire slope since most of the volume of the rock to be excavated is contained in the upper half of the slope.

Curve 3 (slope with tension crack) shows that reduction of the slope angle is a very effective remedial measure. The required factor of safety of 1.5 is achieved for a reduction of less than 25% of the slope angle. In other words, a reduction of the overall slope face angle from 50° to 37.5° would achieve the desired result. This finding is generally true and a reduction in the face angle of a slope is usually an effective remedial step. In the case of slopes under construction, using a flatter slope is always one of the prime choices for achieving greater stability.

Curve 4 (slope without tension crack) is an anomaly and demonstrates that calculations can sometimes produce nonsense. The reduction in factor of safety shown by this curve is a result of the reduction in the weight of the sliding block as the face angle is reduced. Since the water pressure on the sliding surface remains constant, the effective stress acting on the sliding surface decreases and hence the frictional component of the resisting forces decreases. When a very thin sliver of rock remains, the water pressure will float it off the slope. The problem with this analysis lies in the assumption that the block is completely impermeable and that the water remains trapped beneath the failure surface. In fact, the block would break up long before it floated and hence the water pressure acting on the failure plane would be dissipated.

Curves 5 and 6 show that drainage is not a very effective option for either of the slope models considered. In neither case is a factor of safety of 1.5 achieved. This is something of a surprise since drainage is usually one of the most effective and economical remedial measures. The reasons for the poor performance of drainage in this case is due to the combination of the geometry of the slope and the shear strength of the failure surface.

Curves 7 and 8 show that, for both slope models considered, slope reinforcement by means of rockbolts or cables can be an effective remedial measure. The anchor force required for a factor of safety of 1.5 would be about 100 tonnes per metre of slope length for the slope with no tension crack.

Final decision on long term remedial works

The two most attractive options for long term remedial works on this slope are reinforcement by means of cables or bolts or reduction of the slope face angle. The first option was finally rejected because of the high cost and because of the uncertainty about the long term corrosion resistance of reinforcement which could be placed in the slope.

This latter concern may not have been justified but, considering the very poor quality of some of the construction in Hong Kong at the time of this study, it was decided that the risk was not worth taking.

The option finally chosen was to reduce the slope face angle down to 35° by excavating the entire block resting on the failure surface and hence removing the problem entirely. Since good quality aggregate is always required in Hong Kong it was decided to work this slope face as a quarry. It took several years to organise this activity and, during this time, the water levels in the slope were monitored by means of piezometers. Although the road was closed twice during this period, no major problems occurred and the slope was finally excavated back to the failure plane.

References

Hoek E. and Bray, J.W. 1974. *Rock Slope Engineering.* London: Instn Min. Metall.

Factor of safety and probability of failure

Introduction

How does one assess the acceptability of an engineering design? Relying on judgement alone can lead to one of the two extremes illustrated in Figure 1. The first case is economically unacceptable while the example illustrated in the drawing on the right violates all normal safety standards.

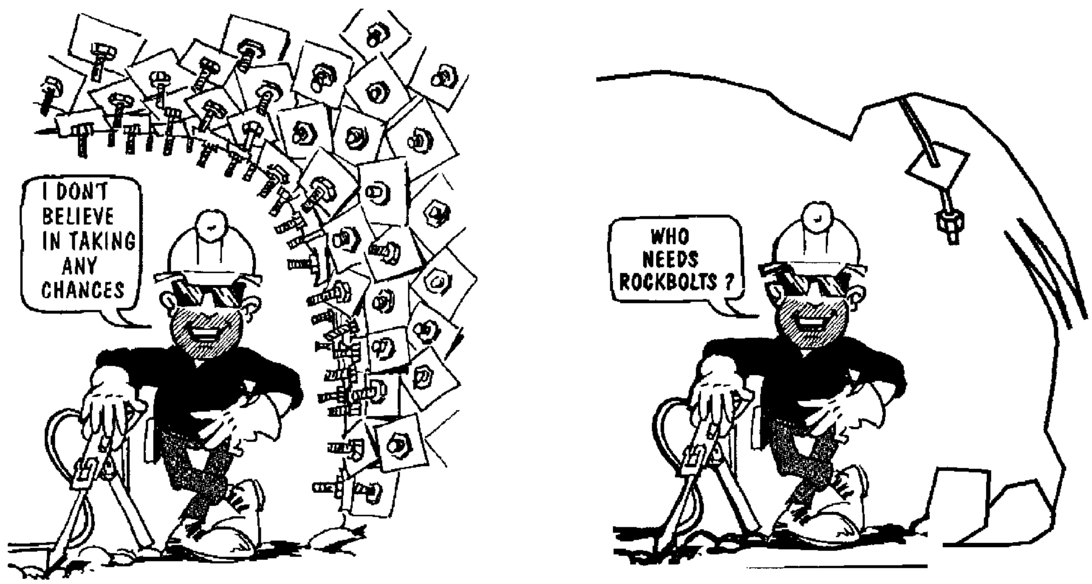

Figure 1: Rockbolting alternatives involving individual judgement. (Drawings based on a cartoon in a brochure on rockfalls published by the Department of Mines of Western Australia.)

Sensitivity studies

The classical approach used in designing engineering structures is to consider the relationship between the capacity C (strength or resisting force) of the element and the demand D (stress or disturbing force). The Factor of Safety of the structure is defined as $F = C/D$ and failure is assumed to occur when F is less than unity.

Rather than base an engineering design decision on a single calculated factor of safety, an approach which is frequently used to give a more rational assessment of the risks associated with a particular design is to carry out a sensitivity study. This involves a series of calculations in which each significant parameter is varied systematically over its maximum credible range in order to determine its influence upon the factor of safety.

This approach was used in the analysis of the Sau Mau Ping slope in Hong Kong, described in detail in another chapter of these notes. It provided a useful means of exploring a range of possibilities and reaching practical decisions on some difficult problems. On the following pages this idea of sensitivity studies will be extended to the use of probability theory and it will be shown that, even with very limited field data, practical, useful information can be obtained from an analysis of probability of failure.

An introduction to probability theory

A complete discussion on probability theory exceeds the scope of these notes and the techniques discussed on the following pages are intended to introduce the reader to the subject and to give an indication of the power of these techniques in engineering decision making. A more detailed treatment of this subject will be found in a book by Harr (1987) entitled 'Reliability-based design in civil engineering'. A paper on geotechnical applications of probability theory entitled 'Evaluating calculated risk in geotechnical engineering' was published by Whitman (1984) and is recommended reading for anyone with a serious interest in this subject. Pine (1992), Tyler et al (1991), Hatzor and Goodman (1993) and Carter (1992) have published papers on the application of probability theory to the analysis of problems encountered in underground mining and civil engineering.

Most geotechnical engineers regard the subject of probability theory with doubt and suspicion. At least part of the reason for this mistrust is associated with the language which has been adopted by those who specialise in the field of probability theory and risk assessment. The following definitions are given in an attempt to dispel some of the mystery which tends to surround this subject.

Random variables: Parameters such as the angle of friction of rock joints, the uniaxial compressive strength of rock specimens, the inclination and orientation of discontinuities in a rock mass and the measured in situ stresses in the rock surrounding an opening do not have a single fixed value but may assume any number of values. There is no way of predicting exactly what the value of one of these parameters will be at any given location. Hence, these parameters are described as random variables.

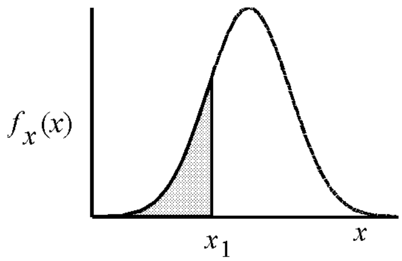

Probability density function (PDF)

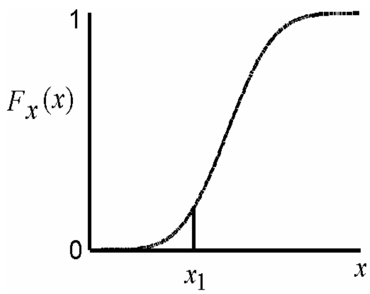

Cumulative distribution function (CDF)

Probability distribution: A probability density function (PDF) describes the relative likelihood that a random variable will assume a particular value. A typical probability density function is illustrated opposite. In this case the random variable is continuously distributed (i.e., it can take on all possible values). The area under the PDF is always unity.

An alternative way of presenting the same information is in the form of a cumulative distribution function (CDF), which gives the probability that the variable will have a value less than or equal to the selected value. The CDF is the integral of the corresponding probability density function, i.e., the ordinate at x_1 on the cumulative distribution is the area under the probability density function to the left of x_1. Note the fx(x) is used for the ordinate of a PDF while Fx(x) is used for a CDF.

One of the most common graphical representations of a probability distribution is a histogram in which the fraction of all observations falling within a specified interval is plotted as a bar above that interval.

Data analysis: For many applications it is not necessary to use all of the information contained in a distribution function and quantities summarised only by the dominant features of the distribution may be adequate.

The sample mean or expected value or first moment indicates the centre of gravity of a probability distribution. A typical application would be the analysis of a set of results $x_1, x_2, ..., x_n$ from uniaxial strength tests carried out in the laboratory. Assuming that there are *n* individual test values x_i, the mean $\bar{x}$ is given by:

$$\bar{x} = \frac{1}{n} \sum_{i=1}^{n} x_i \tag{1}$$

The sample variance s^2 *or the second moment* about the mean of a distribution is defined as the mean of the square of the difference between the value of xi and the mean value $\bar{x}$.

Hence:

$$s^2 = \frac{1}{n-1}\sum_{i=1}^{n}(x_i - \bar{x})^2 \qquad (2)$$

Note that, theoretically, the denominator for calculation of variance of samples should be *n*, not (*n* - 1). However, for a finite number of samples, it can be shown that the correction factor *n*/(*n*-1), known as Bessel's correction, gives a better estimate. For practical purposes the correction is only necessary when the sample size is less than 30.

The *standard deviation s* is given by the positive square root of the variance s^2. In the case of the commonly used normal distribution, about 68% of the test values will fall within an interval defined by the *mean ± one standard deviation* while approximately 95% of all the test results will fall within the range defined by the *mean ± two standard deviations*. A small standard deviation will indicate a tightly clustered data set while a large standard deviation will be found for a data set in which there is a large scatter about the mean.

The *coefficient of variation* (COV) is the ratio of the standard deviation to the mean, i.e. COV = $s/\bar{x}$. COV is dimensionless and it is a particularly useful measure of uncertainty. A small uncertainty would typically be represented by a COV = 0.05 while considerable uncertainty would be indicated by a COV = 0.25.

Normal distribution: The *normal* or *Gaussian* distribution is the most common type of probability distribution function and the distributions of many random variables conform to this distribution. It is generally used for probabilistic studies in geotechnical engineering unless there are good reasons for selecting a different distribution. Typically, variables which arise as a sum of a number of random effects, none of which dominate the total, are normally distributed.

The problem of defining a normal distribution is to estimate the values of the governing parameters which are the true mean (μ) and true standard deviation (σ). Generally, the best estimates for these values are given by the sample mean and standard deviation, determined from a number of tests or observations. Hence, from equations 1 and 2:

$$\mu = \bar{x} \qquad (3)$$

$$\sigma = s \qquad (4)$$

It is important to recognise that equations 3 and 4 give the most probable values of μ and σ and not necessarily the true values.

Obviously, it is desirable to include as many samples as possible in any set of observations but, in geotechnical engineering, there are serious practical and financial limitations to the amount of data which can be collected. Consequently, it is often necessary to make estimates on the basis of judgement, experience or from comparisons with results published by others. These difficulties are often used as an excuse for not using probabilistic tools in geotechnical engineering but, as will be shown later in this chapter, useful results can still be obtained from very limited data.

Having estimated the mean μ and standard deviation σ, the probability density function for a normal distribution is defined by:

$$f_X(x) = \frac{\exp\left[-\frac{1}{2}\left(\frac{x-\mu}{\sigma}\right)^2\right]}{\sigma\sqrt{2\pi}} \tag{5}$$

for $-\infty \le x \le \infty$.

As will be seen later, this range of $-\infty \le x \le \infty$ can cause problems when a normal distribution is used as a basis for a Monte Carlo analysis in which the entire range of values is randomly sampled. This can give rise to a few very small numbers (sometimes negative) and very large numbers which, in certain analyses, can cause numerical instability. In order to overcome this problem the normal distribution is sometimes truncated so that only values falling within a specified range are considered valid.

There is no closed form solution for the cumulative distribution function (CDF) which must by found by numerical integration.

Other distributions: In addition to the commonly used normal distribution there are a number of alternative distributions which are used in probability analyses. Some of the most useful are:

Beta distributions (Harr, 1987) are very versatile distributions which can be used to replace almost any of the common distributions and which do not suffer from the extreme value problems discussed above because the domain (range) is bounded by specified values.

Exponential distributions are sometimes used to define events such as the occurrence of earthquakes or rockbursts or quantities such as the length of joints in a rock mass.

Lognormal distributions are useful when considering processes such as the crushing of aggregates in which the final particle size results from a number of collisions of particles of many sizes moving in different directions with different velocities. Such multiplicative mechanisms tend to result in variables which are lognormally distributed as opposed to the normally distributed variables resulting from additive mechanisms.

Weibul distributions are used to represent the lifetime of devices in reliability studies or the outcome of tests such as point load tests on rock core in which a few very high values may occur.

It is no longer necessary for the person starting out in the field of probability theory to know and understand the mathematics involved in all of these probability distributions since commercially available software programs can be used to carry out many of the computations automatically. Note that the author is not advocating the blind use of 'black-box' software and the reader should exercise extreme caution is using such software without trying to understand exactly what the software is doing. However there is no point in writing reports by hand if one is prepared to spend the time learning how to use a good word-processor correctly and the same applies to mathematical software.

One of the most useful software packages for probability analysis is a Microsoft Excel add-in program called @RISK[1] which can be used for risk evaluations using the techniques described below.

Sampling techniques: Consider a problem in which the factor of safety depends upon a number of random variables such as the cohesive strength c, the angle of friction ϕ and the acceleration α due to earthquakes or large blasts. Assuming that the values of these variables are distributed about their means in a manner which can be described by one of the continuous distribution functions such as the normal distribution described earlier, the problem is how to use this information to determine the distribution of factor of safety values and the probability of failure.

The Monte Carlo method uses random or pseudo-random numbers to sample from probability distributions and, if sufficiently large numbers of samples are generated and used in a calculation such as that for a factor of safety, a distribution of values for the end product will be generated. The term 'Monte Carlo' is believed to have been introduced as a code word to describe this hit-and-miss technique used during secret work on the development of the atomic bomb during World War II (Harr 1987). Today, Monte Carlo techniques can be applied to a wide variety of problems involving random behaviour and a number of algorithms are available for generating random Monte Carlo samples from different types of input probability distributions. With highly optimised software programs such as @RISK, problems involving relatively large samples can be run efficiently on most desktop or portable computers.

---

[1] @RISK is available from www.palisade.com.

The *Latin Hypercube* sampling technique (Imam et al, 1980, Startzman and Watterbarger, 1985) is a relatively recent development which gives comparable results to the Monte Carlo technique but with fewer samples. The method is based upon stratified sampling with random selection within each stratum. Typically an analysis using 1000 samples obtained by the Latin Hypercube technique will produce comparable results to an analysis using 5000 samples obtained using the Monte Carlo method. Both techniques are incorporated in the program @RISK.

Note that both the Monte Carlo and the Latin Hypercube techniques require that the distribution of all the input variables should either be known or that they be assumed. When no information on the distribution is available it is usual to assume a normal or a truncated normal distribution.

The *Generalised Point Estimate Method*, developed by Rosenbleuth (1981) and discussed in detail by Harr (1987), can be used for rapid calculation of the mean and standard deviation of a quantity such as a factor of safety which depends upon random behaviour of input variables. Hoek (1989) discussed the application of this technique to the analysis of surface crown pillar stability while Pine (1992) has applied this technique to the analysis of slope stability and other mining problems.

To calculate a quantity such as a factor of safety, two point estimates are made at one standard deviation on either side of the mean ($\mu \pm \sigma$) from each distribution representing a random variable. The factor of safety is calculated for every possible combination of point estimates, producing 2^n solutions where n is the number of random variables involved. The mean and the standard deviation of the factor of safety are then calculated from these 2^n solutions.

While this technique does not provide a full distribution of the output variable, as do the Monte Carlo and Latin Hypercube methods, it is very simple to use for problems with relatively few random variables and is useful when general trends are being investigated. When the probability distribution function for the output variable is known, for example, from previous Monte Carlo analyses, the mean and standard deviation values can be used to calculate the complete output distribution.

Some of the techniques described above have been incorporated into specialized commercial software packages and one of these called RocPlane[2] will be used to analyse the Sau Mau Ping slope.

[2] Available from www.rocscience.com

Probability of failure

In the case of the Sau Mau Ping slope problem the input parameters and assumed distributions for the calculation of the factor of safety of the overall slope with a tension crack are as follows:

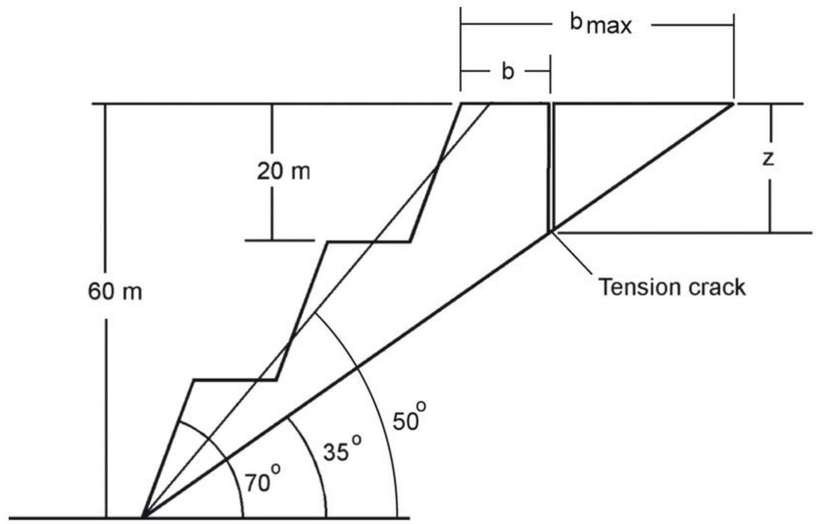

1. Fixed dimensions:

Overall slope height	$H = 60$ m
Overall slope angle	$\psi_f = 50°$
Failure plane angle	$\psi_p = 35°$
Upper slope inclination	horizontal
Bench width $b_{max} = H(\cot \psi_p - \text{Cot } \psi_f)$	$b_{max} = 35.34$ m
Unit weight of rock	$\gamma_r = 2.6$ tonnes/m^3
Unit weight of water	$\gamma_w = 1.0$ tonnes/m^3

2. Random variables	*Mean values*	*Standard deviation*	*Distribution*
Friction angle on joint surface	$\phi = 35°$	± 5	Normal
Cohesive strength of joint surface	$c = 10$ tonnes/m^2	± 2	Normal
Depth of tension crack	$z = 14$ m	± 3	Normal
Distance from crest to tension crack	$b = 15.3$ m	± 4	Normal
Depth of water in tension crack	$z_w = z/2$	min = 0, max = z	Exponential
Ratio of horizontal earthquake to gravitational acceleration	$\alpha = 0.08$	min = 0, max = 2α	Exponential

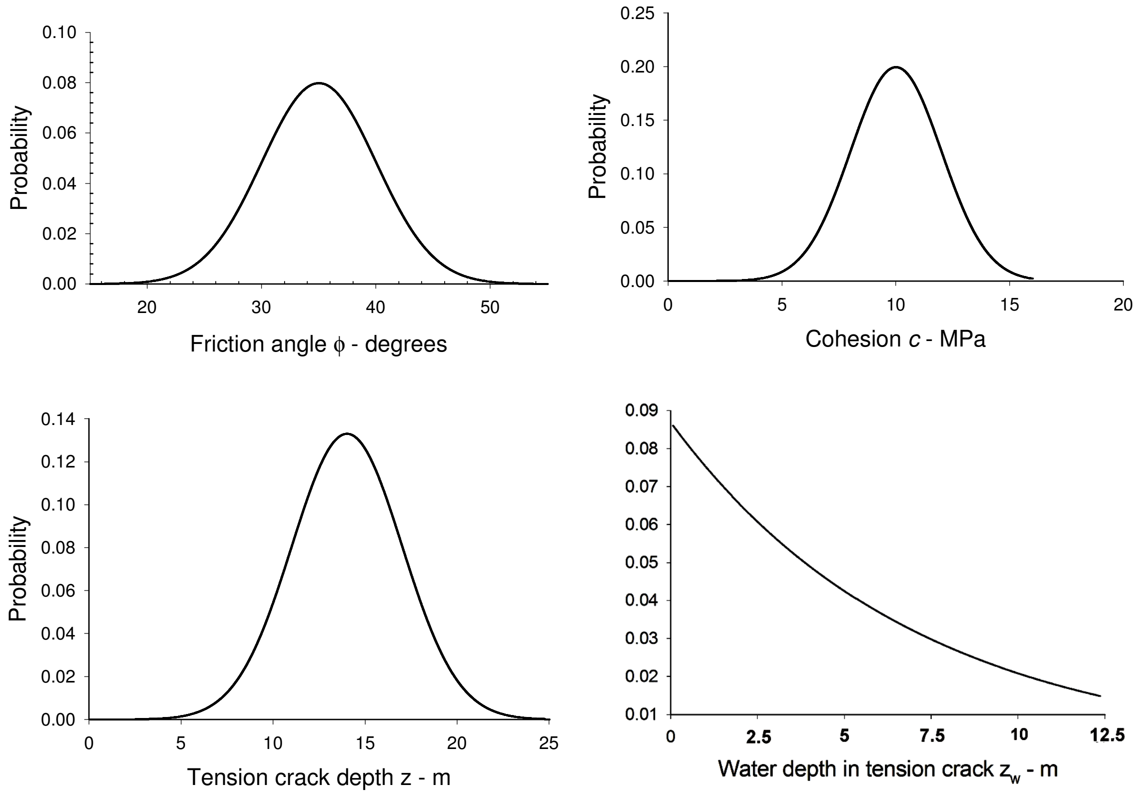

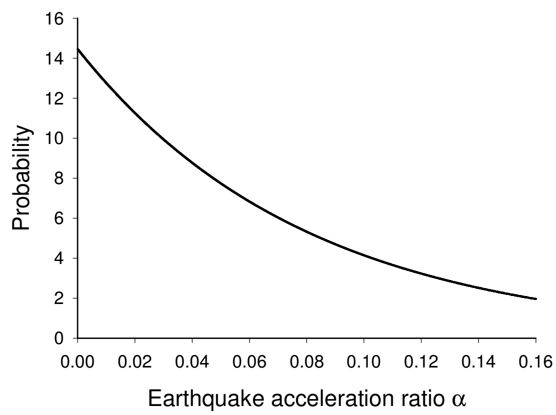

Figure 2: Distributions of random input variables for the Sau Mau Ping slope.

Figure 2 illustrates the plots of the probability distribution functions of the random input variables. It is worth discussing each of the plots in detail to demonstrate the reasoning behind the choice of the probability distribution functions.

Friction angle ϕ - A truncated normal distribution has been assumed for this variable. The mean is assumed to be 35° which is the approximate centre of the assumed shear strength range illustrated in Figure 8 of "A slope stability problem in Hong Kong". The standard deviation of 5° implies that about 68% of the friction angle values defined by the distribution will lie between 30° and 40°. The normal distribution is truncated by a minimum value of 15° and a maximum value of 70° which have been arbitrarily chosen as the extreme values represented by a smooth slickensided surface and a fresh, rough tension fracture.

Cohesive strength c - Again using the assumed range of shear strength values illustrated in Figure 8 of "A slope stability problem in Hong Kong", a value of 10 tonnes/m^2 has been chosen as the mean cohesive strength and the standard deviation has been set at 2 tonnes/m^2 on the basis of this diagram. In order to allow for the wide range of possible cohesive strengths the minimum and maximum values used to truncate the normal distribution are 0 and 25 tonnes/m^2 respectively. Those with experience in the interpretation of laboratory shear strength test results may argue that the friction angle ϕ and the cohesive strength c are not independent variables as has been assumed in this analysis. This is because the cohesive strength generally drops as the friction angle rises and vice versa. The program @RISK allows the user to define variables as dependent but, for the sake of simplicity, the friction angle ϕ and the cohesive strength c have been kept independent for this analysis.

Distance of tension crack behind face b – The program RocPlane uses the horizontal distance b of the tension crack behind the slope crest as input in place of the tension crack depth z because b can be measured in the field and also because it is not influenced by the inclination of the upper slope. Hoek and Bray (1974) give the value of b as $b = H\left(\sqrt{\cot\psi_f \tan\psi_p} - \cot\psi_f\right)$ with the limits as $0 < b < H(\cot\psi_p - \cot\psi_f)$.

Tension crack depth z - Equation 6 in "A slope stability problem in Hong Kong", defining the tension crack depth, has been derived by minimisation of equation 5 in that chapter. For the purposes of this analysis it has been assumed that this value of z (14 m for the assumed conditions) represents the mean tension crack depth. A truncated normal distribution is assumed to define the possible range of tension crack depths and the standard deviation has been arbitrarily chosen at 3 m. The minimum tension crack depth is zero but a value of 0.1 m has been chosen to avoid possible numerical problems. The maximum tension crack depth is given by $z = H(1 - \tan\psi_p / \tan\psi_f)$ = 24.75 m which occurs when the vertical tension crack is located at the crest of the slope.

Water depth z_w in tension crack - The water which would fill the tension crack in this slope would come from direct surface run-off during heavy rains. In Hong Kong the heaviest rains occur during typhoons and it is likely that the tension crack would be completely filled during such events. The probability of occurrence of typhoons has been defined by a truncated exponential distribution where the mean water depth is assumed to be one half the tension crack depth. The maximum water depth cannot exceed the tension crack depth z and, as defined by the exponential distribution, this value would occur very rarely. The minimum water depth is zero during dry conditions and this is assumed to be a frequent occurrence.

Ratio of horizontal earthquake acceleration to gravitational acceleration α - The frequent occurrence of earthquakes of different magnitudes can be estimated by means of an exponential distribution which suggests that large earthquakes are very rare while small ones are very common. In the case of Hong Kong local wisdom suggested a 'design' horizontal acceleration of 0.08g. In other words, this level of acceleration could be anticipated at least once during the operating life of a civil engineering structure. A rough rule of thumb suggests that the 'maximum credible' acceleration is approximately twice the 'design' value. Based upon these very crude guidelines, the distribution of values of α used in these calculations was defined by a truncated exponential distribution with a mean value of $\alpha = 0.08$, a maximum of 0.16 and a minimum of 0.

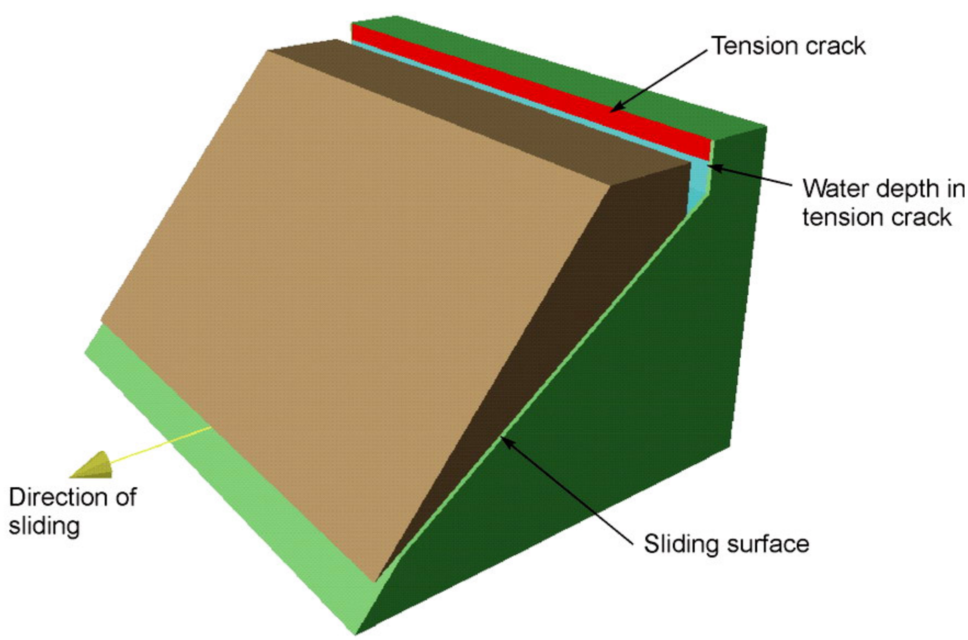

Figure 3: RocPlane model of Sau Mau Ping slope.

Using the distributions shown in Figure 2, the RocPlane model shown in Figure 3 was used, with Latin Hypercube sampling, to carry out 5,000 iterations on the factor of safety. The resulting probability distribution is plotted in Figure 4. This histogram gives a mean factor of safety of 1.34 with a standard deviation of 0.23, a minimum of 0.61 and a maximum of 2.33. The best fit distribution is a beta distribution with the same mean, standard deviation, minimum and maximum.

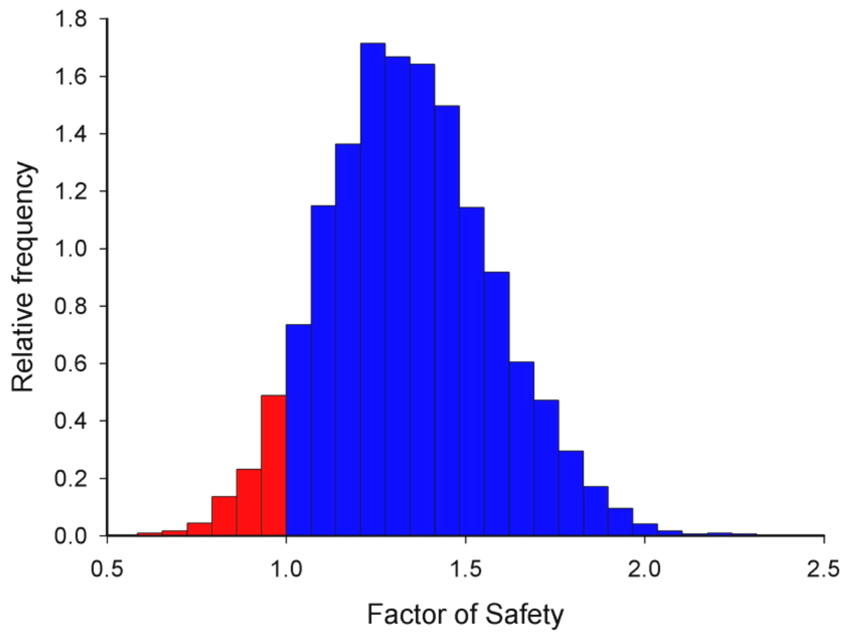

Figure 4: Distribution of the factor of safety for the Sau Mau Ping slope computed by means of the program RocPlane.

The calculated *probability of failure* is found to be 6.4% and is given by the ratio of the area under the distribution curve for F<1 (shown in red in Figure 4) divided by the total area under the distribution curve. This means that, for the combination of slope geometry, shear strength, water pressure and earthquake acceleration parameters assumed, 64 out of 1000 similar slopes could be expected to fail at some time during the life of the slope. Alternatively, a length of 64 m could be expected to fail in every 1000 m of slope.

This is a reasonable risk of failure for short term conditions and a risk of this magnitude may be acceptable in an open pit mine, with limited access of trained miners, and even on a rural road. However, in the long term, this probability of failure is not acceptable for a densely populated region such as Kowloon. As described in the chapter “A slope stability problem in Hong Kong”, remedial measures were taken to improve the long term stability of the slope and the effectiveness of these remedial measures could be evaluated using the same probabilistic techniques as described above.

Acknowledgements

The author wishes to express his thanks to Dr Eugenio Casteli, Mr Damiano Giordano and Dr Bak Kong Low for bringing to his attention a number of errors in the original Monte Carlo analysis. These errors have been corrected in this revision on the notes.

References

Carter, T.G. 1992. A new approach to surface crown pillar design. *Proc. 16th. Canadian Rock Mechanics Symp., Sudbury,* 75-83.

Carter, T.G. 1992. Prediction and uncertainties in geological engineering and rock mass characterization assessments. *Proc. 4th. int. rock mechanics and rock engineering conf.,* Torino. Paper 1.

Harr, M.E. 1987. *Reliability-based design in civil engineering*. New York: McGraw-Hill.

Hatzor. Y. and Goodman. R.E. 1993. Determination of the ‘design block’ for tunnel supports in highly jointed rock. In *Comprehensive Rock Engineering, Principles, Practice and Projects.* (ed. J.A. Houson) **2,** 263-292. Oxford: Pergamon.

Hoek E. and Bray, J.W. 1974. *Rock Slope Engineering* . London: Instn Min. Metall.

Hoek, E. 1989. A limit equilibrium analysis of surface crown pillar stability. In *Surface crown pillar evaluation for active and abandoned metal mines,* (ed. M.C. Betourney), 3-13. Ottawa: Dept. Energy, Mines & Resources Canada.

Iman, R.L., Davenport, J.M. and Zeigler, D.K. 1980. *Latin Hypercube sampling (A progam user’s guide).* Technical Report SAND79-1473. Albuquerque, New Mexico: Sandia Laboratories.

Pine. R.J. 1992. Risk analysis design applications in mining geomechanics. *Trans. Instn Min. Metall.* (Sect.A) **101,** 149-158.

Rosenbleuth, E. 1981. Two-point estimates in probabilities. *J. Appl. Math. Modelling* **5**, October, 329-335.

Startzman, R.A. and Wattenbarger, R.A. 1985. An improved computation procedure for risk analysis problems with unusual probability functions. *Proc. symp. Soc. Petrolm Engrs hydrocarbon economics and evaluation,* Dallas.

Tyler, D.B., Trueman, R.T. and Pine, R.J. 1991. Rockbolt support design using a probabilistic method of key block analysis. In *Rock mechanics as a multidisciplinary science*, (ed. J.C. Roegiers), 1037-1047. Rotterdam: Balkema.

Whitman. R.V. 1984. Evaluating calculated risk in geotechnical engineering*. J. Geotech. Engng, ASCE* **110(**2), 145-186.

Analysis of rockfall hazards

Introduction

Rockfalls are a major hazard in rock cuts for highways and railways in mountainous terrain. While rockfalls do not pose the same level of economic risk as large scale failures which can and do close major transportation routes for days at a time, the number of people killed by rockfalls tends to be of the same order as people killed by all other forms of rock slope instability. Badger and Lowell (1992) summarised the experience of the Washington State Department of Highways. They stated that 'A significant number of accidents and nearly a half dozen fatalities have occurred because of rockfalls in the last 30 years … [and] … 45 percent of all unstable slope problems are rock fall related'. Hungr and Evans (1989) note that, in Canada, there have been 13 rockfall deaths in the past 87 years. Almost all of these deaths have been on the mountain highways of British Columbia.

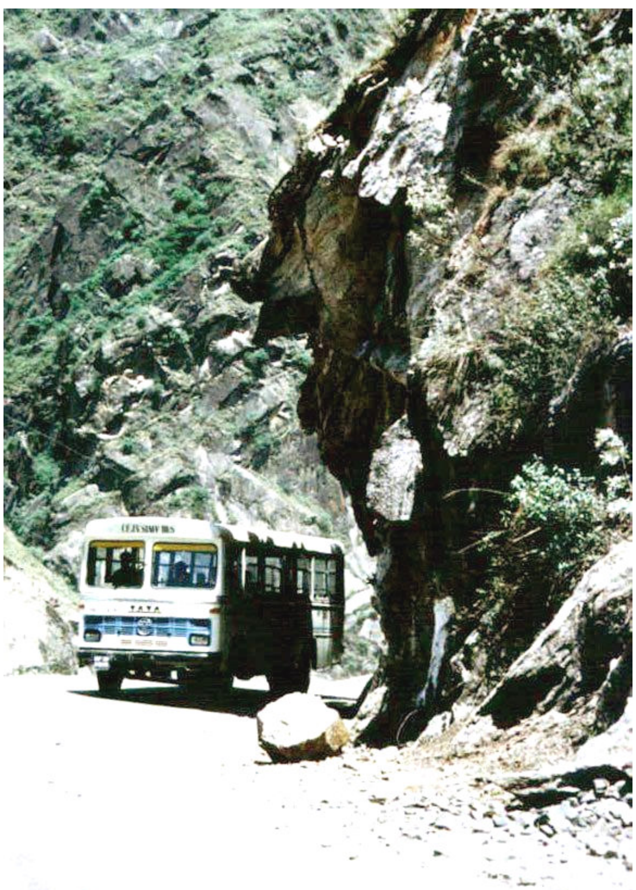

Figure 1: A rock slope on a mountain highway. Rockfalls are a major hazard on such highways

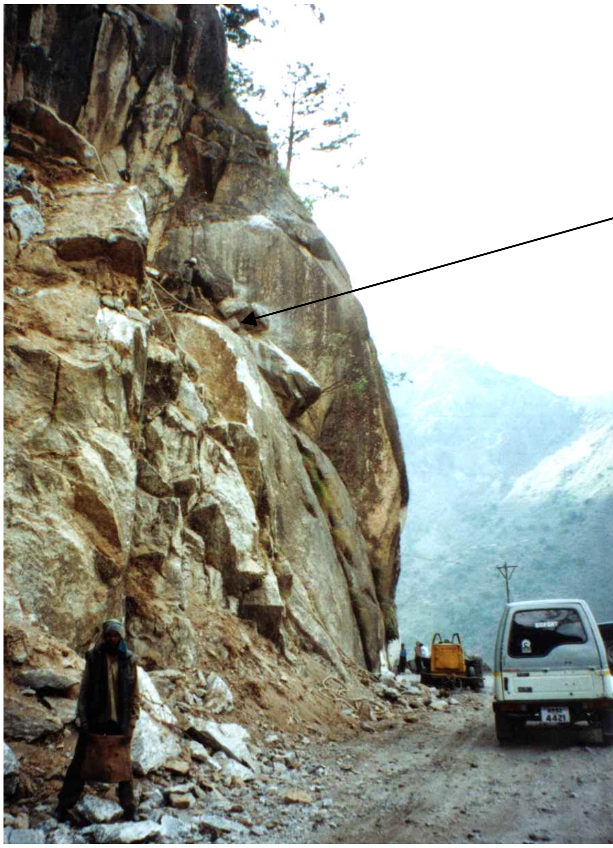

Figure 2: Construction on an active roadway, which is sometimes necessary when there is absolutely no alternative access, increases the rockfall hazard many times over that for slopes without construction or for situations in which the road can be closed during construction.

Mechanics of rockfalls

Rockfalls are generally initiated by some climatic or biological event that causes a change in the forces acting on a rock. These events may include pore pressure increases due to rainfall infiltration, erosion of surrounding material during heavy rain storms, freeze-thaw processes in cold climates, chemical degradation or weathering of the rock, root growth or leverage by roots moving in high winds. In an active construction environment, the potential for mechanical initiation of a rockfall will probably be one or two orders of magnitude higher than the climatic and biological initiating events described above.

Once movement of a rock perched on the top of a slope has been initiated, the most important factor controlling its fall trajectory is the geometry of the slope. In particular, dip slope faces, such as those created by the sheet joints in granites, are important because they impart a horizontal component to the path taken by a rock after it bounces on the slope or rolls off the slope. The most dangerous of these surfaces act as 'ski-jumps' and impart a high horizontal velocity to the falling rock, causing it to bounce a long way out from the toe of the slope.

Clean faces of hard unweathered rock are the most dangerous because they do not retard the movement of the falling or rolling rock to any significant degree. On the other hand, surfaces covered in talus material, scree or gravel absorb a considerable amount of the energy of the falling rock and, in many cases, will stop it completely.

This retarding capacity of the surface material is expressed mathematically by a term called the *coefficient of restitution*. The value of this coefficient depends upon the nature of the materials that form the impact surface. Clean surfaces of hard rock have high coefficients of restitution while soil, gravel and completely decomposed granite have low coefficients of restitution. This is why gravel layers are placed on catch benches in order to prevent further bouncing of falling rocks.

Other factors such as the size and shape of the rock boulders, the coefficients of friction of the rock surfaces and whether or not the rock breaks into smaller pieces on impact are all of lesser significance than the slope geometry and the coefficients of restitution described above. Consequently, relative crude rockfall simulation models are capable of producing reasonably accurate predictions of rockfall trajectories. Obviously more refined models will produce better results, provided that realistic input information is available. Some of the more recent rockfall models are those of Bozzolo et al (1988), Hungr and Evans (1989), Spang and Rautenstrauch (1988) and Azzoni et al (1995).

Most of these rockfall models include a Monte Carlo simulation technique to vary the parameters included in the analysis. This technique is similar to the random process of throwing dice - one for each parameter being considered. The program Rocfall[1] is a program that can be used for rockfall analyses using a number of probabilistic options. Figure 3 shows a single rockfall trajectory while Figure 4 shows the trajectories for 100 rockfalls using the Monte Carlo simulation process.

Possible measures which could be taken to reduce rockfall hazards

Identification of potential rockfall problems

It is neither possible nor practical to detect all potential rockfall hazards by any techniques currently in use in rock engineering. In some cases, for example, when dealing with boulders on the top of slopes, the rockfall hazards are obvious. However, the most dangerous types of rock failure occur when a block is suddenly released from an apparently sound face by relatively small deformations in the surrounding rock mass. This can occur when the forces acting across discontinuity planes, which isolate a block from its neighbours, change as a result of water pressures in the discontinuities or a reduction of the shear strength of these planes because of long term deterioration due to weathering. This release of 'keyblocks' can sometimes precipitate rockfalls of significant size or, in extreme cases, large scale slope failures.

[1] Available from www.rocscience.com

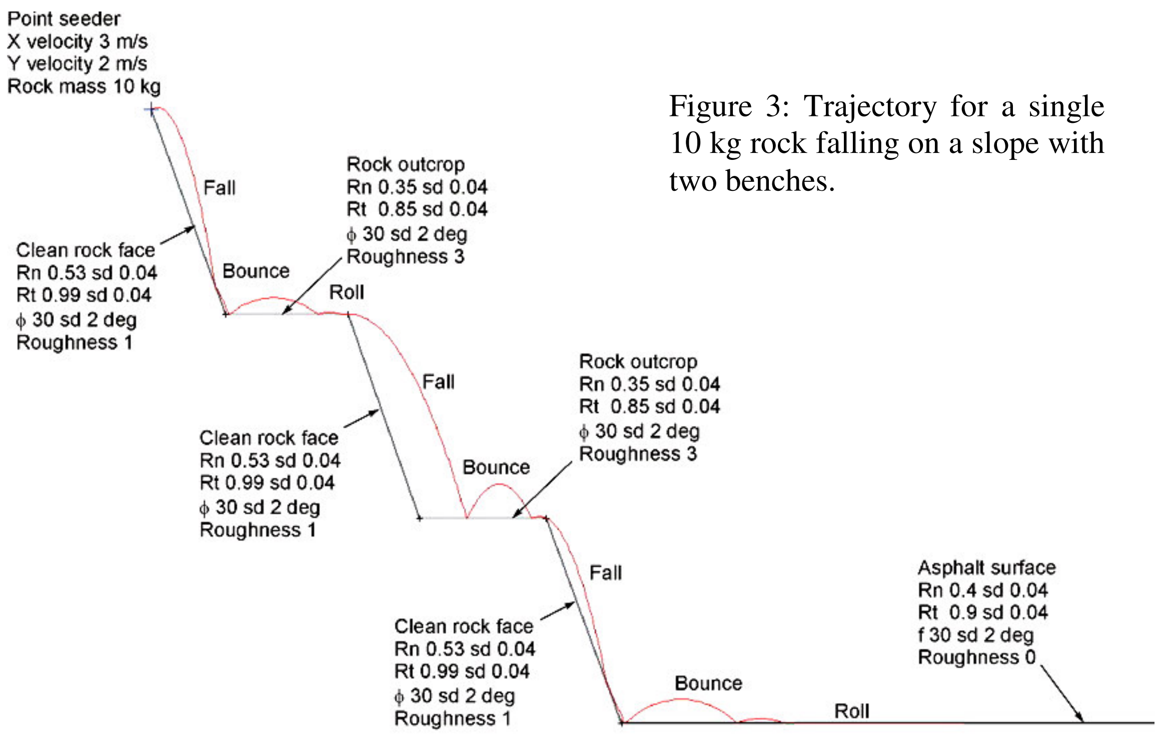

Figure 3: Trajectory for a single 10 kg rock falling on a slope with two benches.

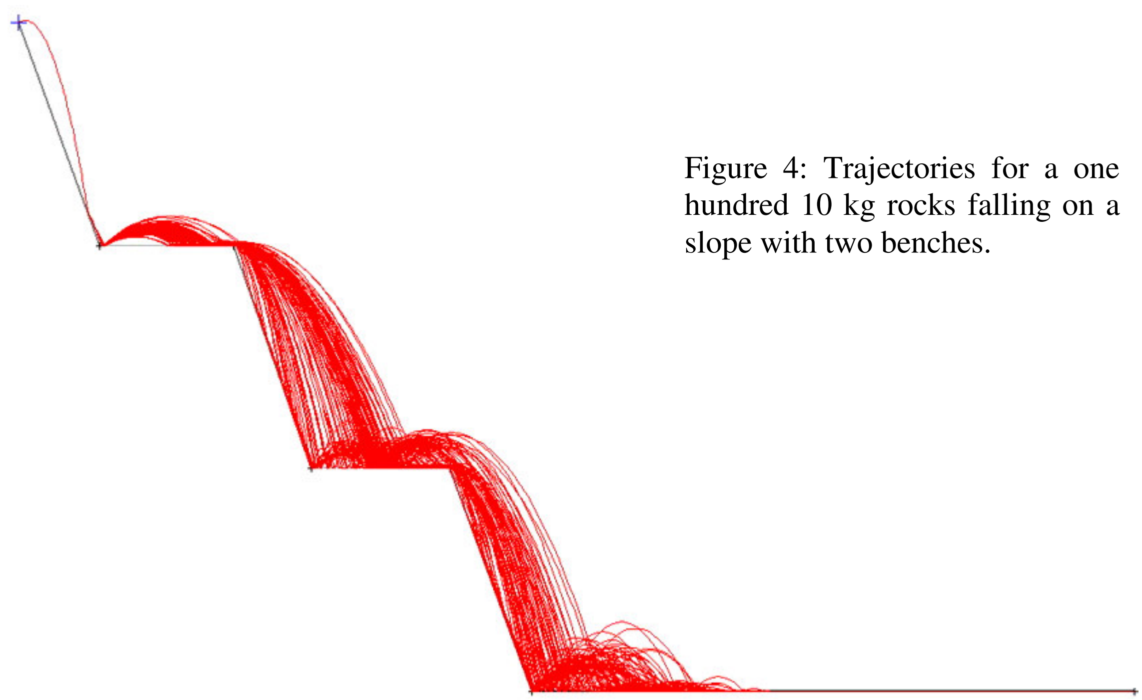

Figure 4: Trajectories for a one hundred 10 kg rocks falling on a slope with two benches.

While it is not suggested that rock faces should not be carefully inspected for potential rockfall problems, it should not be assumed that all rockfall hazards will be detected by such inspections.

Reduction of energy levels associated with excavation

Traditional excavation methods for hard rock slopes involve the use of explosives. Even when very carefully planned controlled blasts are carried out, high intensity short duration forces act on the rock mass. Blocks and wedges which are at risk can be dislodged by these forces. Hence, an obvious method for reducing rockfall hazards is to eliminate excavation by blasting or by any other method, such as ripping, which imposes concentrated, short duration forces or vibrations on the rock mass. Mechanical and hand excavation methods can be used and, where massive rock has to be broken, chemical expanding rock breaking agents may be appropriate.

Physical restraint of rockfalls

If it is accepted that it is not possible to detect or to prevent all rockfalls, then methods for restraining those rockfalls, which do occur, must be considered. These methods are illustrated in Figure 5.

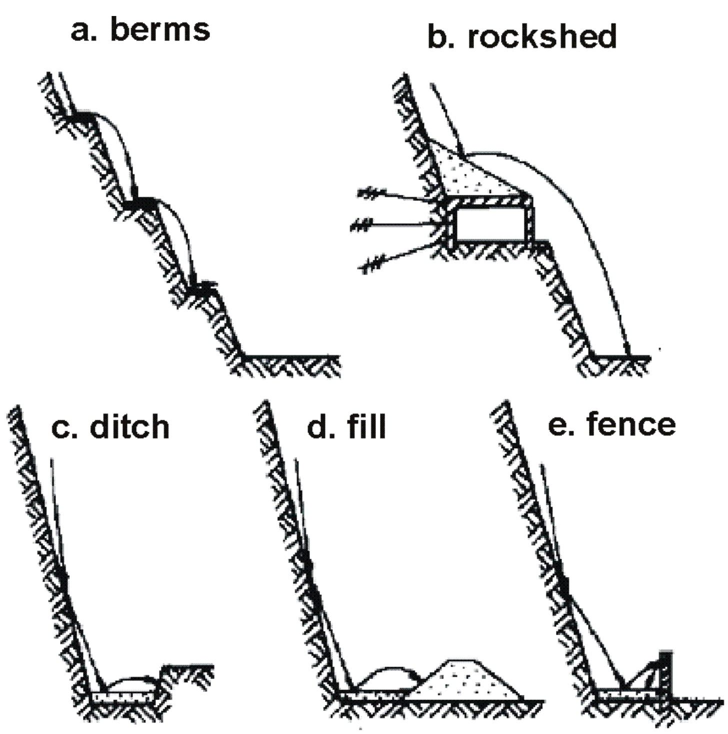

Figure 5: Possible measures to reduce the damage due to rockfalls. After Spang (1987).

Berms are a very effective means of catching rockfalls and are frequently used on permanent slopes. However, berms can only be excavated from the top downwards and they are of limited use in minimising the risk of rockfalls during construction.

Rocksheds or avalanche shelters are widely used on steep slopes above narrow railways or roadways. An effective shelter requires a steeply sloping roof covering a relatively narrow span. In the case of a wide multi-lane highway, it may not be possible to design a rockshed structure with sufficient strength to withstand large rockfalls. It is generally advisable to place a fill of gravel or soil on top of the rockshed in order to act as both a retarder and a deflector for rockfalls.

Rock traps work well in catching rockfalls provided that there is sufficient room at the toe of the slope to accommodate these rock traps. In the case of very narrow roadways at the toe of steep slopes, there may not be sufficient room to accommodate rock traps. This restriction also applies to earth or rock fills and to gabion walls or massive concrete walls.

Catch fences or barrier fences in common use are estimated to have an energy absorption capacity[2] of 100 kNm. This is equivalent to a 250 kg rock moving at about 20 metres per second. More robust barrier fences, such as those used in the European Alps[3], have an energy absorbing capacity of up to 2500 kNm which means that they could stop a 6250 kg boulder moving at approximately 20 metres per second. Details of a typical high capacity net are illustrated in Figure 6.

Another restraint system which merits further consideration is the use of *mesh draped* over the face. This type of restraint is commonly used for permanent slopes and is illustrated in Figure 7. The mesh is draped over the rock face and attached at several locations along the slope. The purpose of the mesh is not to stop rockfalls but to trap the falling rock between the mesh and the rock face and so to reduce the horizontal velocity component which causes the rock to bounce out onto the roadway below.

Probably the most effective permanent rockfall protective system for most highways is the construction of a catch ditch at the toe of the slope. The base of this ditch should be covered by a layer of gravel to absorb the energy of falling rocks and a sturdy barrier fence should be placed between the ditch and the roadway. The location of the barrier fence can be estimated by means of a rockfall analysis such as that used to calculate the trajectories presented in Figure 3. The criterion for the minimum distance between the toe of the slope and the rock fence is that no rocks can be allowed to strike the fence before their kinetic energy has been diminished by the first impact on the gravel layer in the rock trap.

---

[2] The kinetic energy of a falling body is given by 0.5 x mass x velocity^2.

[3] Wire mesh fence which incorporates cables and energy absorbing slipping joints is manufactured by Geobrugg Protective Systems, CH-8590 Romanshorn, Switzerland, Fax +41 71466 81 50.

a: Anchor grouted into rock with cables attached.

b: Geobrugg ring net shown restraining a boulder. These nets can be designed with energy absorbing capacities of up to 2500 kNm which is equivalent to a 6 tonne boulder moving at 20 m per second.

c: Geobrugg energy absorbing ring. When subjected to impact loading the ring deforms plastically and absorbs the energy of the boulder

Figure 6: Details of a rockfall net system manufactured by Geobrugg of Switzerland.

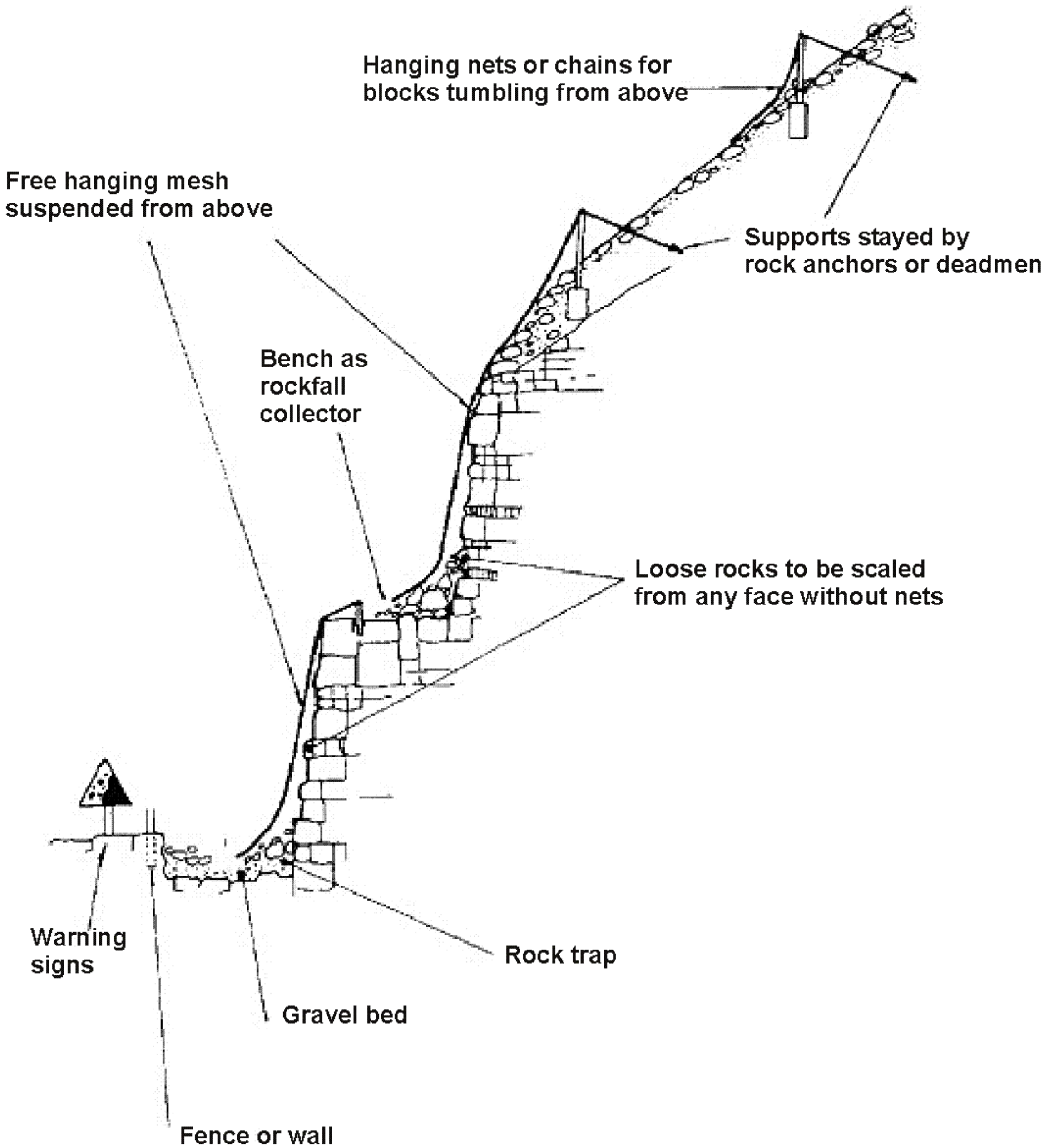

Figure 7: Rockfall control measures. After Fookes and Sweeney (1976).

A simple design chart for ditch design, based upon work by Ritchie (1963), is reproduced in Figure 8.

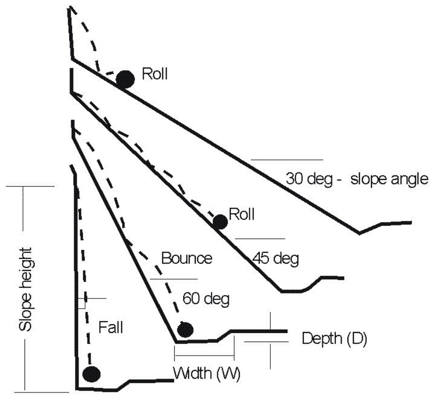

Rock falls on slopes

Figures taken from FHWA Manual 'Rock Slopes'
November 1991. USDOT Chapter 12 Page 19.

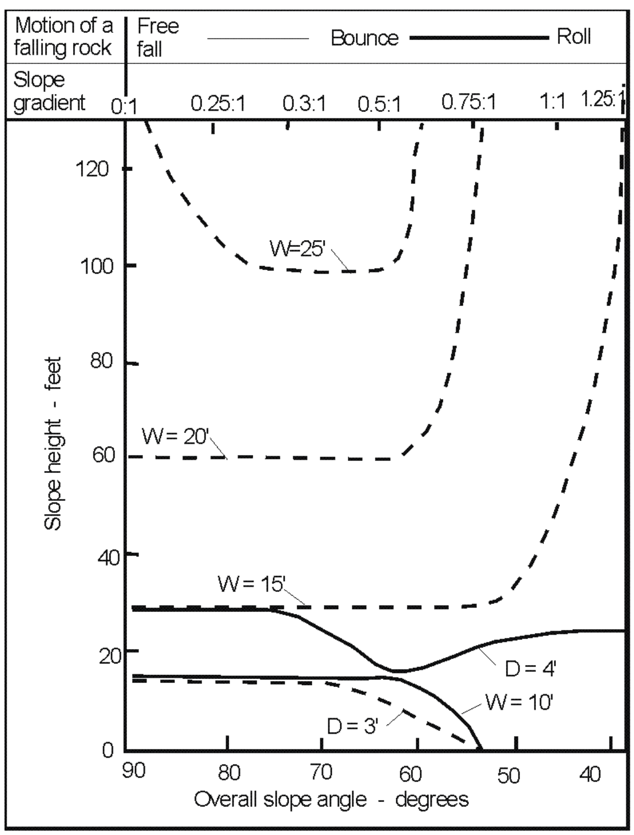

Ditch Design Chart

Figure 8: Rockfall ditch design chart based upon work by Ritchie (1963).

Rockfall Hazard Rating System

Highway and railway construction in mountainous regions presents a special challenge to geologists and geotechnical engineers. This is because the extended length of these projects makes it difficult to obtain sufficient information to permit stability assessments to be carried out for each of the slopes along the route. This means that, except for sections which are identified as particularly critical, most highway slopes tend to be designed on the basis of rather rudimentary geotechnical analyses. Those analyses which are carried out are almost always concerned with the overall stability of the slopes against major sliding or toppling failures which could jeopardise the operation of the highway or railway. It is very rare to find a detailed analysis of rockfall hazards except in heavily populated regions in highly developed countries such as Switzerland.

In recognition of the seriousness of this problem and of the difficulty of carrying out detailed investigations and analyses on the hundreds of kilometres of mountain highway in the western United States and Canada, highway and railway departments have worked on classification schemes which can be carried out by visual inspection and simple calculations. The purpose of these classifications is to identify slopes which are particularly hazardous and which require urgent remedial work or further detailed study.

In terms of rockfall hazard assessment, one of the most widely accepted[4] is the Rockfall Hazard Rating System (RHRS) developed by the Oregon State Highway Division (Pierson et al. 1990). Table 1 gives a summary of the scores for different categories included in the classification while Figure 9 shows a graph which can be used for more refined estimates of category scores.

The curve shown in Figure 9 is calculated from the equation $y = 3^x$ where, in this case, x = (Slope height- feet)/25. Similar curves for other category scores can be calculated from the following values of the exponent x.

Slope height	x = slope height (feet) / 25
Average vehicle risk	x = % time / 25
Sight distance	x = (120 - % Decision sight distance) / 20
Roadway width	x = (52 - Roadway width (feet)) / 8
Block size	x = Block size (feet)
Volume	x = Volume (cu.ft.) / 3

[4] This system has been adopted by the States of Oregon, Washington, New Mexico and Idaho and, in slightly modified form, by California, Colorado and British Columbia.

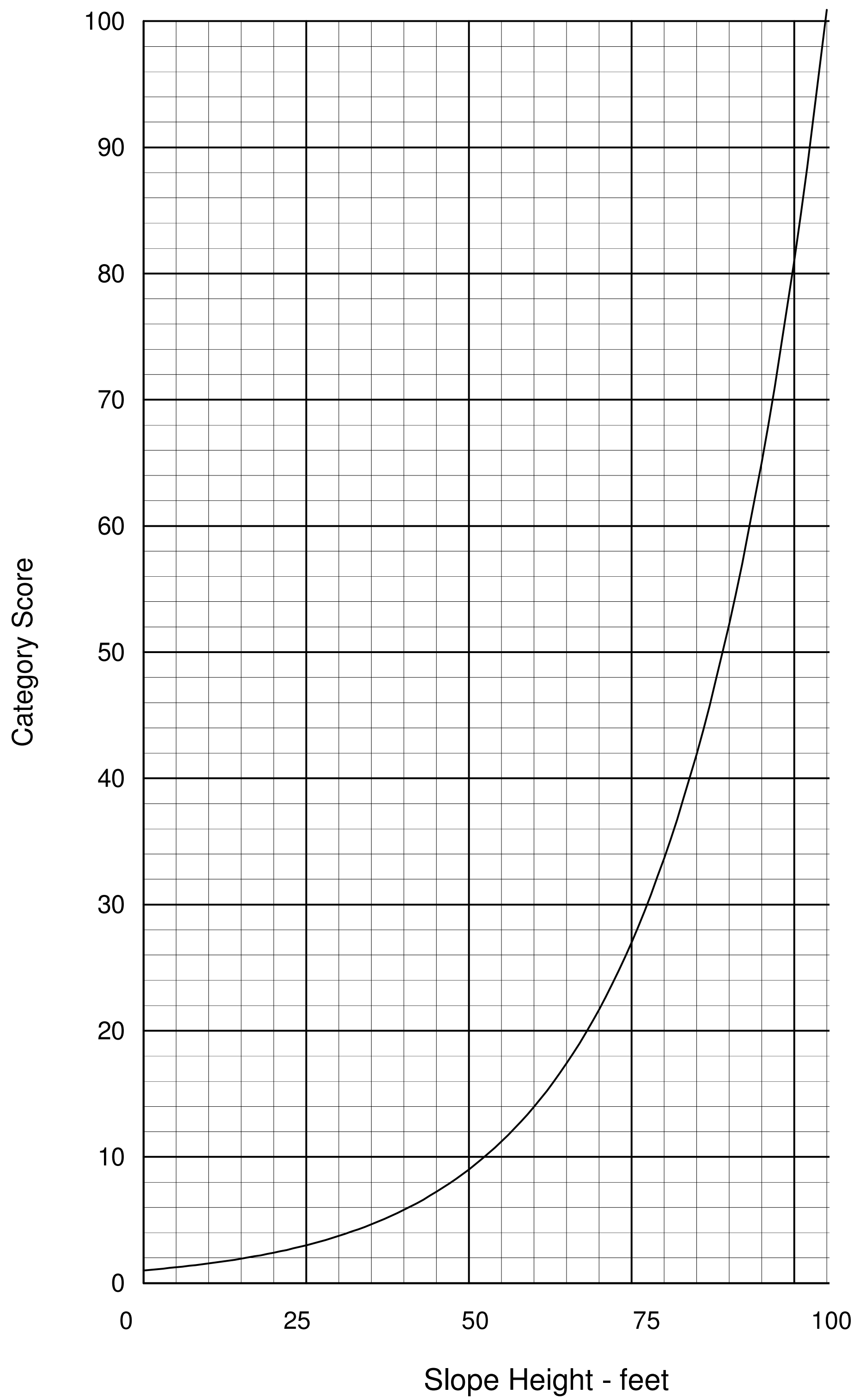

Figure 9: Category score graph for slope height.

Table 1: Rockfall Hazard Rating System.

CATEGORY			RATING CRITERIA AND SCORE			
			POINTS 3	POINTS 9	POINTS 27	POINTS 81
SLOPE HEIGHT			25 FT	50 FT	75 FT	100 FT
DITCH EFFECTIVENESS			Good catchment	Moderate catchment	Limited catchment	No catchment
AVERAGE VEHICLE RISK			25% of the time	50% of the time	75% of the time	100% of the time
PERCENT OF DECISION SIGHT DISTANCE			Adequate site distance, 100% of low design value	Moderate sight distance, 80% of low design value	Limited site distance, 60% of low design value	Very limited sight distance, 40% of low design value
ROADWAY WIDTH INCLUDING PAVED SHOULDERS			44 feet	36 feet	28 feet	20 feet
GEOLOGIC CHARACTER	CASE 1	STRUCTURAL CONDITION	Discontinuous joints, favorable orientation	Discontinuous joints, random orientation	Discontinuous joints, adverse orientation	Continuous joints, adverse orientation
		ROCK FRICTION	Rough, irregular	Undulating	Planar	Clay infilling or slickensided
	CASE 2	STRUCTURAL CONDITION	Few differential erosion features	Occasional erosion features	Many erosion features	Major erosion features
		DIFFERENCE IN EROSION RATES	Small difference	Moderate difference	Large difference	Extreme difference
BLOCK SIZE ——— QUANTITY OF ROCKFALL/EVENT			1 FT ——— 3 cubic yards	2 FT ——— 6 cubic yards	3 FT ——— 9 cubic yards	4 FT ——— 12 cubic yards
CLIMATE AND PRESENCE OF WATER ON SLOPE			Low to moderate precipitation; no freezing periods, no water on slope	Moderate precipitation or short freezing periods or intermittent water on slope	High precipitation or long freezing periods or continual water on slope	High precipitation and long freezing periods or continual water on slope and long freezing periods
ROCKFALL HISTORY			Few falls	Occasional falls	Many falls	Constant falls

Slope Height

This item represents the vertical height of the slope not the slope distance. Rocks on high slopes have more potential energy than rocks on lower slopes, thus they present a greater hazard and receive a higher rating. Measurement is to the highest point from which rockfall is expected. If rocks are coming from the natural slope above the cut, use the cut height plus the additional slope height (vertical distance). A good approximation of vertical slope height can be obtained using the relationships shown below.

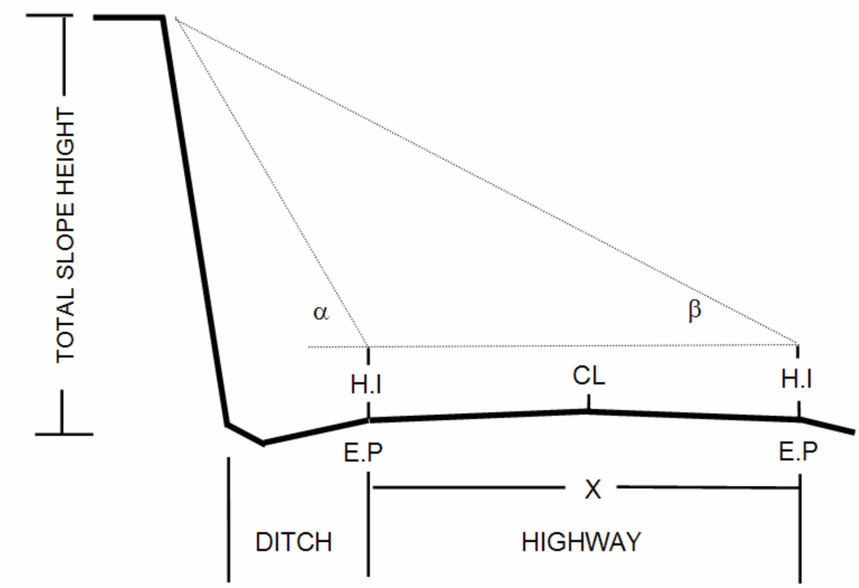

$$\text{TOTAL SLOPE HEIGHT} = \frac{(X)\sin\alpha \sin\beta}{\sin(\alpha - \beta)} + \text{H.I}$$

where X = distance between angle measurements
H.I = height of the instrument.

Figure 10: Measurement of slope height.

Ditch Effectiveness

The effectiveness of a ditch is measured by its ability to prevent falling rock from reaching the roadway. In estimating the ditch effectiveness, the rater should consider several factors, such as: 1) slope height and angle; 2) ditch width, depth and shape; 3) anticipated block size and quantity of rockfall; 4) impact of slope irregularities (launching features) on falling rocks. It's especially important for the rater to evaluate the impact of slope irregularities because a launching feature can negate the benefits expected from a fallout area. The rater should first evaluate whether any of the irregularities, natural or man-made, on a slope will launch falling rocks onto the paved roadway. Then based on the number and size of the launching features estimate what portion of the falling rocks will be affected. Valuable information on ditch performance can be obtained from maintenance personnel. Rating points should be assigned as follows:

3 points	*Good Catchment*. All or nearly all of falling rocks are retained in the catch ditch.
9 points	*Moderate Catchment*. Falling rocks occasionally reach the roadway.
27 points	*Limited Catchment*. Falling rocks frequently reach the roadway.
81 points	*No Catchment*. No ditch or ditch is totally ineffective. All or nearly all falling rocks reach the roadway.

Reference should also be made to Figure 8 in evaluating ditch effectiveness.

Average Vehicle Risk (AVR)

This category measures the percentage of time that a vehicle will be present in the rockfall hazard zone. The percentage is obtained by using a formula (shown below) based on slope length, average daily traffic (ADT), and the posted speed limit at the site. A rating of 100% means that on average a car can be expected to be within the hazard section 100% of the time. Care should be taken to measure only the length of a slope where rockfall is a problem. Over estimated lengths will strongly skew the formula results. Where high ADT's or longer slope lengths exist values greater than 100% will result. When this occurs it means that at any particular time more than one car is present within the measured section. The formula used is:

$$\frac{\text{ADT (cars/hour)} \times \text{Slope Length (miles)} \times 100\%}{\text{Posted Speed Limit (miles per hour)}} = \text{AVR}$$

Percent of Decision Sight Distance

The decision sight distance (DSD) is used to determine the length of roadway in feet a driver must have to make a complex or instantaneous decision. The DSD is critical when obstacles on the road are difficult to perceive, or when unexpected or unusual manoeuvres are required. Sight distance is the shortest distance along a roadway that an object of specified height is continuously visible to the driver.

Throughout a rockfall section the sight distance can change appreciably. Horizontal and vertical highway curves along with obstructions such as rock outcrops and roadside vegetation can severely limit a driver's ability to notice a rock in the road. To determine where these impacts are most severe, first drive through the rockfall section from both directions. Decide which direction has the shortest line of sight. Both horizontal and vertical sight distances should be evaluated. Normally an object will be most obscured when it is located just beyond the sharpest part of a curve. Place a six-inch object in that position on the fogline or on the edge of pavement if there is no fogline. The rater then walks along the fogline (edge of pavement) in the opposite direction of traffic flow, measuring the distance it takes for the object to disappear when your eye height is 3.5 ft above the road surface. This is the measured sight distance. The decision sight distance can be determined by the table below. The distances listed represent the low design value. The posted speed limit through the rockfall section should be used.

Posted Speed Limit (mph)	Decision Sight Distance (ft)
30	450
40	600
50	750
60	1,000
70	1.100

These two values can be substituted into the formula below to calculate the 'Percent of Decision Sight Distance.'

$$\frac{\text{Actual Site Distance} \quad (\qquad) \quad x \quad 100\%}{\text{Decision Site Distance} \quad (} = \underline{\qquad\qquad\qquad}\%$$

Roadway Width

This dimension is measured perpendicular to the highway centreline from edge of pavement to edge of pavement. This measurement represents the available manoeuvring room to avoid a rockfall. This measurement should be the minimum width when the roadway width is not consistent.

Geologic Character

The geologic conditions of the slope are evaluated with this category. Case 1 is for slopes where joints, bedding planes, or other discontinuities, are the dominant structural feature of a rock slope. Case 2 is for slopes where differential erosion or oversteepened slopes is the dominant condition that controls rockfall. The rater should use whichever case best fits the slope when doing the evaluation. If both situations are present, both are scored but only the worst case (highest score) is used in the rating.

Case 1

Structural Condition Adverse joint orientation, as it is used here, involves considering such things as rock friction angle, joint filling, and hydrostatic head if water is present. Adverse joints are those that cause block, wedge or toppling failures. 'Continuous' refers to joints greater than 10 feet in length.

3 points *Discontinuous Joints, Favourable Orientation* Jointed rock with no adversely oriented joints, bedding planes, etc.

9 points *Discontinuous Joints, Random Orientation* Rock slopes with randomly oriented joints creating a three-dimensional pattern. This type of pattern is likely to have some scattered blocks with adversely oriented joints but no dominant adverse joint pattern is present.

27 points *Discontinuous Joints, Adverse Orientation* Rock slope exhibits a prominent joint pattern, bedding plane, or other discontinuity, with an adverse orientation. These features have less than 10 feet of continuous length.

81 points *Continuous Joints, Adverse Orientation* Rock slope exhibits a dominant joint pattern, bedding plane, or other discontinuity, with an adverse orientation and a length of greater than 10 feet.

Rock Friction This parameter directly affects the potential for a block to move relative to another. Friction along a joint, bedding plane or other discontinuity is governed by the macro and micro roughness of a surface. Macro roughness is the degree of undulation of the joint. Micro roughness is the texture of the surface of the joint. In areas where joints contain highly weathered or hydrothermally altered products, where movement has occurred causing slickensides or fault gouge to form, where open joints dominate the slope, or where joints are water filled, the rockfall potential is greater. Noting the failure angles from previous rockfalls on a slope can aid in estimating general rock friction along discontinuities.

3 points *Rough, Irregular* The surfaces of the joints are rough and the joint planes are irregular enough to cause interlocking. This macro and micro roughness provides an optimal friction situation.

9 points *Undulating* Also macro and micro rough but without the interlocking ability.

27 points *Planar* Macro smooth and micro rough joint surfaces. Surface contains no undulations. Friction is derived strictly from the roughness of the rock surface.

81 points *Clay Infilling or Slickensided* Low friction materials, such as clay and weathered rock, separate the rock surfaces negating any micro or macro roughness of the joint planes. These infilling materials have much lower friction angles than a rock on rock contact. Slickensided joints also have a very low friction angle and belong in this category.

Case 2

Structural Condition This case is used for slopes where differential erosion or oversteepening is the dominant condition that leads to rockfall. Erosion features include oversteepened slopes, unsupported rock units or exposed resistant rocks on a slope that may eventually lead to a rockfall event. Rockfall is caused by a loss of support either locally or throughout the slope. Common slopes that are susceptible to this condition are: layered units containing easily weathered rock that erodes undermining more durable rock; talus slopes; highly variable units such as conglomerates, mudflows, etc. that weather causing resistant rocks and blocks to fall, and rock/soil slopes that weather allowing rocks to fall as the soil matrix material is eroded.

3 points	*Few Differential Erosion Features* Minor differential erosion features that are not distributed throughout the slope.
9 points	*Occasional Erosion Features* Minor differential erosion features that are widely distributed throughout the slope.
27 points	*Many Erosion Features* Differential erosion features are large and numerous throughout the slope.
81 points	*Major Erosion Features* Severe cases such as dangerous erosion-created overhangs; or significantly oversteepened soil/rock slopes or talus slopes.

Difference in Erosion Rates The Rate of Erosion on a Case 2 slope directly relates to the potential for a future rockfall event. As erosion progresses, unsupported or oversteepened slope conditions develop. The impact of the common physical and chemical erosion processes as well as the effects of man's actions should be considered. The degree of hazard caused by erosion and thus the score given this category should reflect how quickly erosion is occurring; the size of rocks, blocks, or units being exposed; the frequency of rockfall events; and the amount of material released during an event.

3 points	*Small Difference* The difference in erosion rates is such that erosion features develop over many years. Slopes that are near equilibrium with their environment are covered by this category.
9 points	*Moderate Difference* The difference in erosion rates is such that erosion features develop over a few years.
27 points	*Large Difference* The difference in erosion rates is such that erosion features develop annually.
81 points	*Extreme Difference* The difference in erosion rates is such that erosion features develop rapidly

Block Size or Quantity of Rockfall Per Event

This measurement should be representative of whichever type of rockfall event is most likely to occur. If individual blocks are typical of the rockfall, the block size should be used for scoring. If a mass of blocks tends to be the dominant type of rockfall, the quantity per event should be used. This can be determined from the maintenance history or estimated from observed conditions when no history is available. This measurement will also be beneficial in determining remedial measures.

Climate and Presence of Water on Slope

Water and freeze/thaw cycles both contribute to the weathering and movement of rock materials. If water is known to flow continually or intermittently from the slope it is rated accordingly. Areas receiving less than 20 inches per year are ‘low precipitation areas.’ Areas receiving more than 50 inches per year are considered ‘high precipitation areas.’ The impact of freeze/thaw cycles can be interpreted from knowledge of the freezing conditions and its effects at the site.

The rater should note that the 27-point category is for sites with long freezing periods or water problems such as high precipitation or continually flowing water. The 81-point category is reserved for sites that have both long freezing periods and one of the two extreme water conditions.

Rockfall History

This information is best obtained from the maintenance person responsible for the slope in question. It directly represents the known rockfall activity at the site. There may be no history available at newly constructed sites or where poor documentation practices have been followed and a turnover of personnel has occurred. In these cases, the maintenance cost at a particular site may be the only information that reflects the rockfall activity at that site. This information is an important check on the potential for future rockfalls. If the score you give a section does not compare with the rockfall history, a review should be performed. As a better database of rockfall occurrences is developed, more accurate conclusions for the rockfall potential can be made.

3 points	*Few Falls* - Rockfalls have occurred several times according to historical information but it is not a persistent problem. If rockfall only occurs a few times a year or less, or only during severe storms this category should be used. This category is also used if no rockfall history data is available.
9 points	*Occasional Falls* - Rockfall occurs regularly. Rockfall can be expected several times per year and during most storms.

27 points	*Many Falls* - Typically rockfall occurs frequently during a certain season, such as the winter or spring wet period, or the winter freeze-thaw, etc. This category is for sites where frequent rockfalls occur during a certain season and is not a significant problem during the rest of the year. This category may also be used where severe rockfall events have occurred.
81 points	*Constant Falls* - Rockfalls occur frequently throughout the year. This category is also for sites where severe rockfall events are common.

In addition to scoring the above categories, the rating team should gather enough field information to recommend which rockfall remedial measure is best suited to the rockfall problem. Both total fixes and hazard reduction approaches should be considered. A preliminary cost estimate should be prepared.

Risk analysis of rockfalls on highways

The analysis of the risk of damage to vehicles or the death of vehicle occupants as a result of rockfalls on highways has not received very extensive coverage in the geotechnical literature. Papers which deal directly with the probability of a slope failure event and the resulting death, injury or damage have been published by Hunt (1984), Fell (1994), Morgan (1991), Morgan et al (1992) and Varnes (1984). Most of these papers deal with landslides rather than with rockfalls. An excellent study of risk analysis applied to rockfalls on highways is contained in an MSc thesis by Christopher M. Bunce (1994), submitted to the Department of Civil Engineering at the University of Alberta. This thesis reviews risk assessment methodology and then applies this methodology to a specific case in which a rockfall killed a passenger and injured the driver of a vehicle.

RHRS rating for Argillite Cut

Bunce carried out a study using the Rockfall Hazard Rating System for the Argillite Cut in which the rockfall occurred. A summary of his ratings for the section in which the rockfall happened and for the entire cut is presented in Table 2. The ratings which he obtained were 394 for the rockfall section and 493 for the entire cut. Note that this highway has been upgraded and the Argillite Cut no longer exists. However, Bunce's work still provides a good case history for the application of the Rockfall Hazard Rating System.

The RHRS system does not include recommendations on actions to be taken for different ratings. This is because decisions on remedial action for a specific slope depend upon many factors such as the budget allocation for highway work which cannot be taken into account in the ratings. However, in personal discussions with Mr Lawrence Pierson, the principal author of the RHRS, I was informed that in the State of Oregon, slopes with a rating of less than 300 are assigned a very low priority while slopes with a rating in excess of 500 are identified for urgent remedial action.

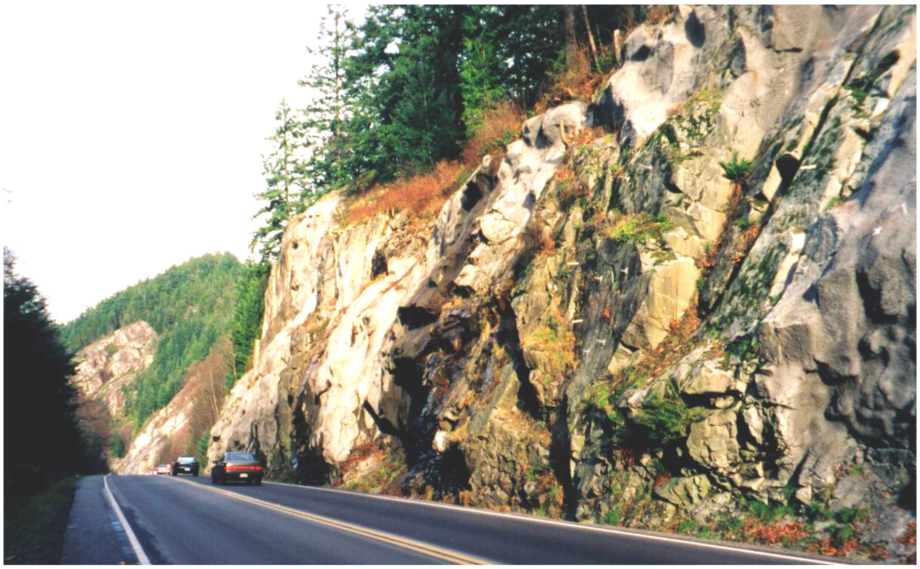

Figure 11: The Argillite Cut on Highway 99 in British Columbia, Canada.

Risk analysis for Argillite Cut

Bunce (1994) presented a number of approaches for the estimation of the annual probability of a fatality occurring as a result of a rockfall in the Argillite Cut. Some of these approaches are relatively sophisticated and I have to question whether this level of sophistication is consistent with the quality of the input information which is available on highway projects.

Table 2: RHRS ratings for Argillite Cut on Highway 99 in British Columbia (after Bunce, 1994).

	Section where rockfall occurred		Rating for entire cut	
Parameter	Value	Rating	Value	Rating
Slope height	36	100	35	100
Ditch effectiveness	Limited	27	Limited	27
Average vehicle risk	7	1	225	100
Sight distance	42	73	42	73
Roadway width	9.5	17	9.5	17
Geological structure	Very adverse	81	Adverse	60
Rock friction	Planar	27	Planar	27
Block size	0.3 m	3	1 m	35
Climate and water	High precip.	27	High precip.	27
Rockfall history	Many falls	40	Many falls	27
Total score		394		493

One approach which I consider to be compatible with the rockfall problem and with quality of input information available is the event tree analysis. This technique is best explained by means of the practical example of the analysis for the Argillite Cut, shown in Figure 12. I have modified the event tree presented by Bunce (1994) to make it simpler to follow.

In the event tree analysis, a probability of occurrence is assigned to each event in a sequence which could lead to a rockfall fatality. For example, in Figure 12; it is assumed that it rains 33% of the time, that rockfalls occur on 5% of rainy days, that vehicles are impacted by 2% of these rockfalls, that 50% of these impacts are significant, i.e. they would result in at least one fatality. Hence, the annual probability of fatality resulting from a vehicle being hit by a rockfall triggered by rain is given by (0.333 * 0.05 * 0.02 * 0.5) = $1.67*10^{-4}$.

The event tree has been extended to consider the annual probability of occurrence of one, two and three or more fatalities in a single accident. These probabilities are shown in the final column of Figure 12. Since there would be at least one fatality in any of these accidents, the total probability of occurrence of a single fatality is $(8.33 + 5.56 + 2.78)*10^{-5} = 1.7 * 10^{-4}$, as calculated above. The total probability of at least two fatalities is $(5.56 + 2.78) * 10^{-5} = 8.34 * 10^{-5}$ while the probability of three or more fatalities remains at $2.78 * 10^{-5}$ as shown in Figure 12.

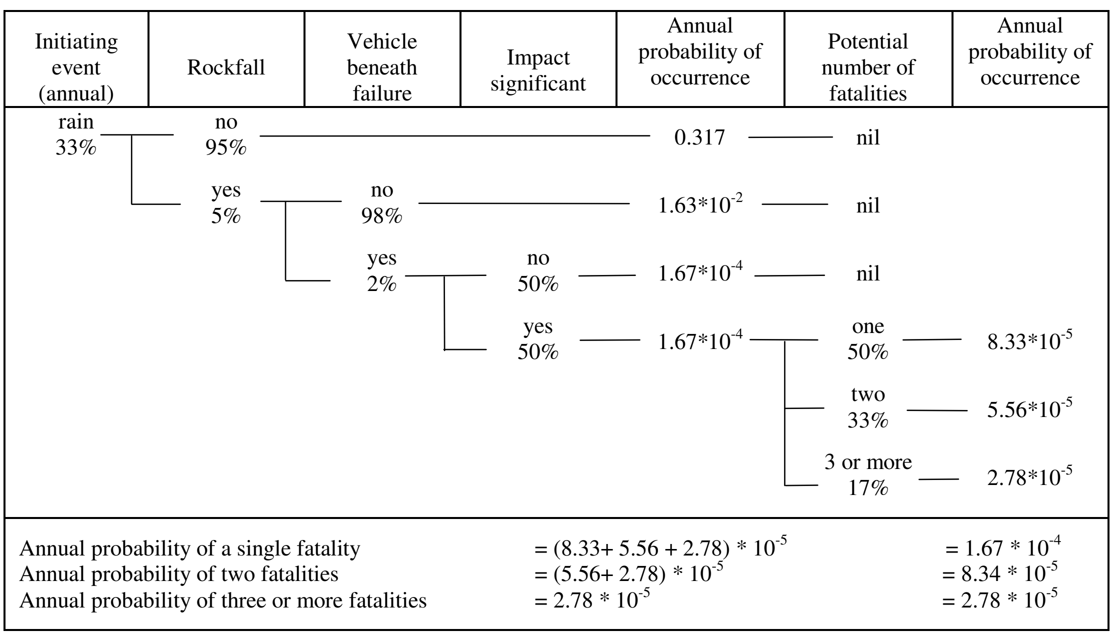

Figure 12: Event tree analysis of rockfalls in the Argillite Cut in British Columbia.

Suppose that it is required to carry out construction work on the slopes of a cut and that it is required to maintain traffic flow during this construction. It is assumed that the construction work lasts for 6 months (50% of a year) and that rockfalls are initiated 20% of the working time, i.e. on 36 days. Using the Argillite cut as an example, all other factors in the event tree remain the same as those assumed in Figure 12. The results of this analysis are presented in Figure 13 which shows that there is an almost ten fold increase in the risk of fatalities from rockfalls as a result of the ongoing construction activities.

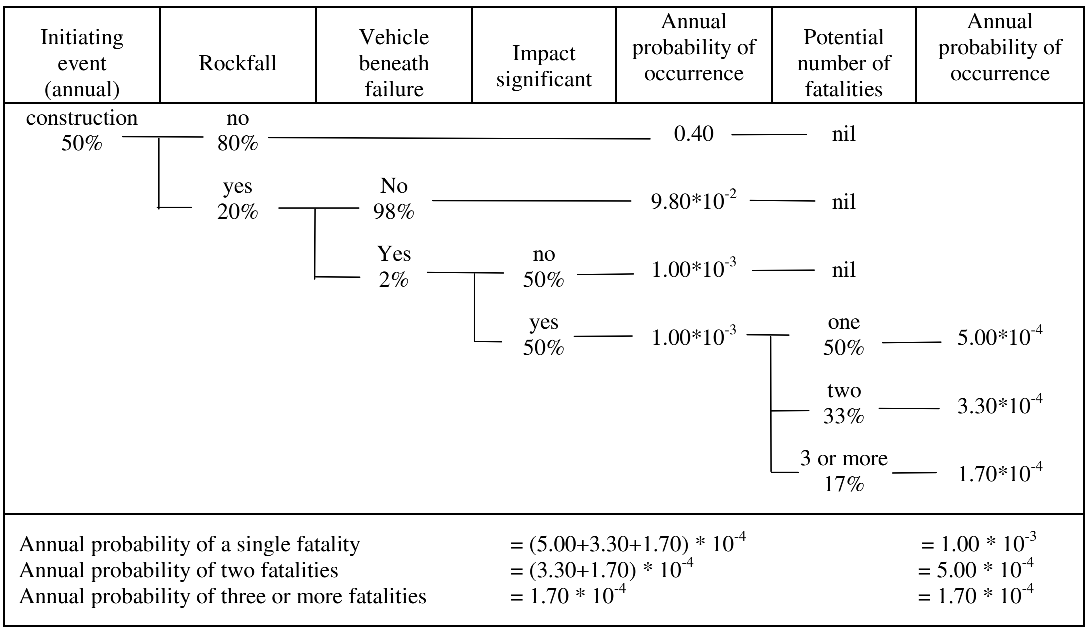

Figure 13: Event tree for a hypothetical example in which construction activities on the Argillite Cut are carried out for a period of six months while the highway is kept open.

Comparison between assessed risk and acceptable risk

The estimated annual probabilities of fatalities from rockfalls, discussed in the previous sections, have little meaning unless they are compared with acceptable risk guidelines used on other major civil engineering construction projects.

One of the earliest attempts to develop an acceptable risk criterion was published by Whitman (1984). This paper was very speculative and was published in order to provide a basis for discussion on this important topic. In the time since this paper was published a great deal of work has been done to refine the concepts of acceptable risk and there are now more reliable acceptability criteria than those suggested by Whitman.

Figure 14, based on a graph published by Nielsen, Hartford and MacDonald (1994), summarises published and proposed guidelines for tolerable risk. The line marked 'Proposed BC Hydro Societal Risk' is particularly interesting since this defines an annual probability of occurrence of fatalities due to dam failures as 0.001 lives per year or 1 fatality per 1000 years. A great deal of effort has gone into defining this line and I consider it to be directly applicable to rock slopes on highways which, like dams, must be classed as major civil engineering structures for which the risks to the public must be reduced to acceptable levels.

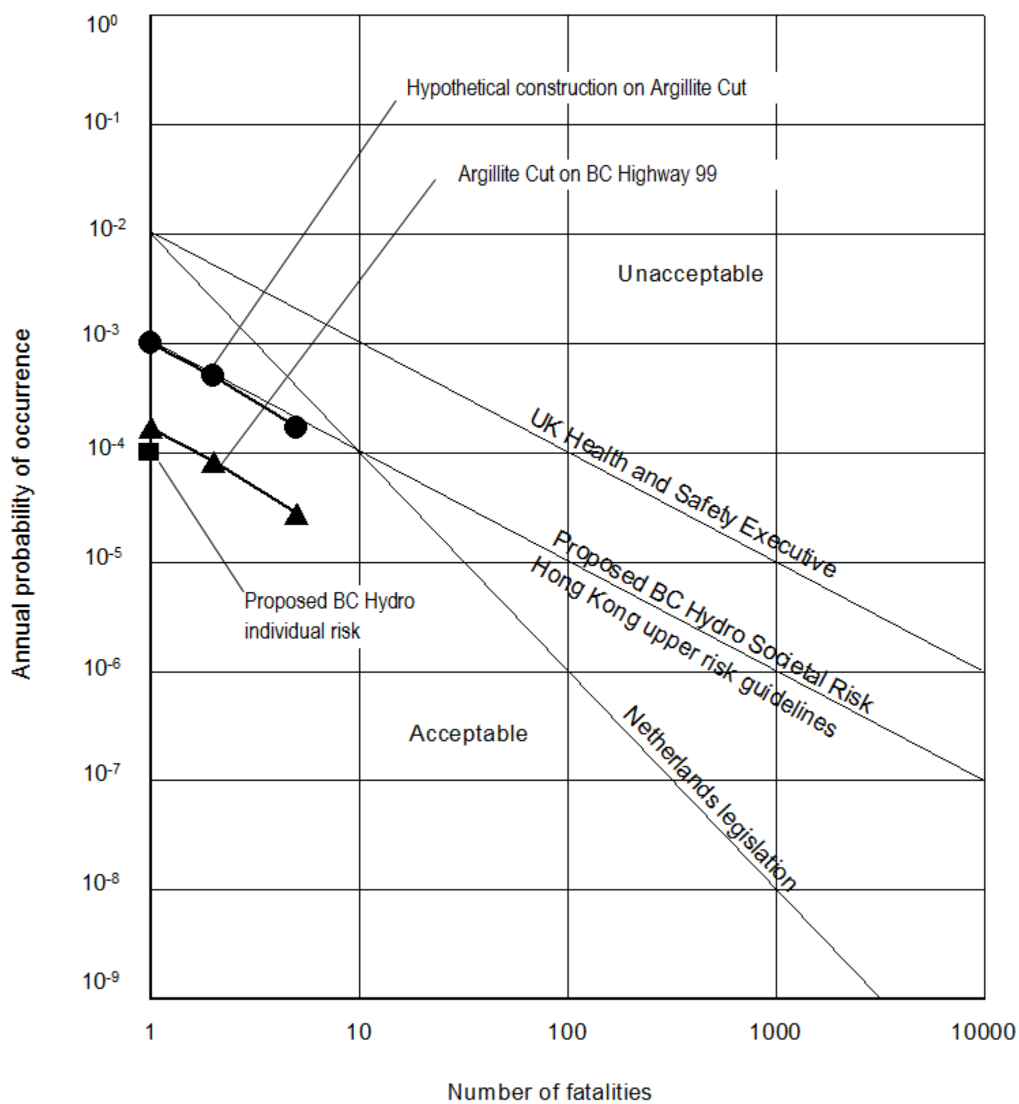

Figure 14: Comparison between risks of fatalities due to rockfalls with published and proposed acceptable risk criteria.

Another point to be noted in Figure 14 is that marked 'Proposed BC Hydro Individual risk'. This annual probability of fatalities of 10^{-4} (1 in 10,000) is based upon the concept that the risk to an individual from a dam failure should not exceed the individual 'natural death' risk run by the safest population group (10 to 14 year old children). Consensus is also developing that the annual probability of fatality of 10^{-4} defines the boundary between voluntary (restricted access to site personnel) and involuntary (general public access) risk (Nielsen, Hartford and MacDonald, 1994).

On Figure 14, I have plotted the estimated annual probabilities of fatalities from rockfalls on the Argillite Cut on BC Highway 99, with and without construction. These plots show that the estimated risk for these slopes, without construction, is significantly lower than the 0.001 lives per year line. The estimated risk for the Argillite Cut slopes during active construction is approximately ten times higher and is marginally higher than the 0.001 lives per year criterion. Given the fact that courts tend to be unsympathetic to engineers who knowingly put the public at risk, it would be unwise to proceed with construction while attempting to keep the traffic flowing. A more prudent course of action would be to close the highway during periods of active construction on the slopes, even if this meant having to deal with the anger of frustrated motorists.

Conclusions

The Rockfall Hazard Rating System and the Event Tree risk assessments, discussed on the previous pages, are very crude tools which can only be regarded as semi-quantitative. However, the trends indicated by these tools together with common sense engineering judgement, give a reasonable assessment of the relative hazards due to rockfalls from cut slopes adjacent to highways and railways.

References

Azzoni, A., La Barbera, G. and Zaninetti, A. 1995. Analysis and prediction of rockfalls using a mathematical model. *Int. J. Rock Mech. Min. Sci. and Geomech. Abstracts.* . **32,** (7) 709-724.

Badger, T.C. and Lowell, S. 1992. Rockfall Control Washington State. In *Rockfall Prediction and Control and Landslide Case Histories, Transportation Research Record,* National Research Council, Washington, No 1342, 14-19.

Bozzolo, D., Pamini, R. and Hutter, K. 1988. Rockfall analysis - a mathematical model and its test with field data. *Proc. 5th Intl symposium on Landslides, Lusanne.* July 1988, **1**, 555-560.

Bunce, C.M. 1994. Risk Analysis for Rock Fall on Highways. *MSc thesis submitted to the Department of Civil Engineering, University of Alberta, Canada.* 129 pages.

Fell, R. 1994. Landslide risk assessment and acceptable risk. *Can. Geotech. J.* **31**, 261-272.

Fookes, P.G. and Sweeney, M. 1976. Stabilisation and control of local rockfalls and degrading of slopes. *Quart. J. Engng Geol.* **9**,37-55.

Hoek, E. 1986. Rockfall: a computer program for predicting rockfall trajectories. Unpublished internal notes, Golder Associates, Vancouver.

Hungr, O. and Evans, S.G. 1989. Engineering aspects of rockfall hazard in Canada. Geological Survey of Canada, Open File 2061, 102 pages.

Hunt, R.E. 1984. Slope failure risk mapping for highways: Methodology and case history. In *Rockfall prediction and Control and Landslide Case Histories.* Transportation Research Record, National Research Council, Washington, No. 1343. 42-51.

Morgan, G.C. 1991. Qualification of risks from slope hazards. In *Landslide Hazards in the Canadian Cordillera.* Geological Association of Canada, Special Publication.

Morgan, G.C., Rawlings, G.E. and Sobkowicz, J.C. 1992. Evaluation of total risk to communities from large debris flows. *Geotechnical and Natural Hazards,* Vancouver Geotechnical Society and Canadian Geotechnical Society, Vancouver, BC, Canada, May 6-9, 1992, 225—236.

Nielsen, N.M., Hartford, D.N.D. and MacDonald. 1994. Selection of tolerable risk criteria for dam safety decision making. *Proc. 1994 Canadian Dam Safety Conference, Winnipeg, Manitoba.* Vancouver: BiTech Publishers, 355-369.

Pierson, L.A., Davis, S.A. and Van Vickle, R. 1990. Rockfall Hazard Rating System Implementation Manual. Federal Highway Administration (FHWA) Report FHWA-OR—EG-90-01. FHWA, U.S. Department of Transportation.

Ritchie, A.M., 1963. The evaluation of rockfall and its control. *Highway Record.* **17**.

Spang, R.M. and Rautenstrauch, R.W. 1988. Empirical and mathematical approaches to rockfall prediction and their practical applications. *Proc. 5th Int. Symp. on Landslides, Lusanne*. **2**,1237-1243.

Varnes, D.J. 1984. Landslide hazard zonation: a review of principles and practice. *Natural Hazards 3.* UNESCO, Paris, 63 pages.

Whitman. R.V. 1984. Evaluating calculated risk in geotechnical engineering. *J. Geotech. Eng, ASCE* **110(**2), 145-186.

In situ and induced stresses

Introduction

Rock at depth is subjected to stresses resulting from the weight of the overlying strata and from locked in stresses of tectonic origin. When an opening is excavated in this rock, the stress field is locally disrupted and a new set of stresses are induced in the rock surrounding the opening. Knowledge of the magnitudes and directions of these in situ and induced stresses is an essential component of underground excavation design since, in many cases, the strength of the rock is exceeded and the resulting instability can have serious consequences on the behaviour of the excavations.

This chapter deals with the question of in situ stresses and also with the stress changes that are induced when tunnels or caverns are excavated in stressed rock. Problems, associated with failure of the rock around underground openings and with the design of support for these openings, will be dealt with in later chapters.

The presentation, which follows, is intended to cover only those topics which are essential for the reader to know about when dealing with the analysis of stress induced instability and the design of support to stabilise the rock under these conditions.

In situ stresses

Consider an element of rock at a depth of 1,000 m below the surface. The weight of the vertical column of rock resting on this element is the product of the depth and the unit weight of the overlying rock mass (typically about 2.7 tonnes/m^3 or 0.027 MN/m^3). Hence the vertical stress on the element is 2,700 tonnes/m^2 or 27 MPa. This stress is estimated from the simple relationship:

$$\sigma_v = \gamma z \tag{1}$$

where σ_v is the vertical stress
γ is the unit weight of the overlying rock and
z is the depth below surface.

Measurements of vertical stress at various mining and civil engineering sites around the world confirm that this relationship is valid although, as illustrated in Figure 1, there is a significant amount of scatter in the measurements.

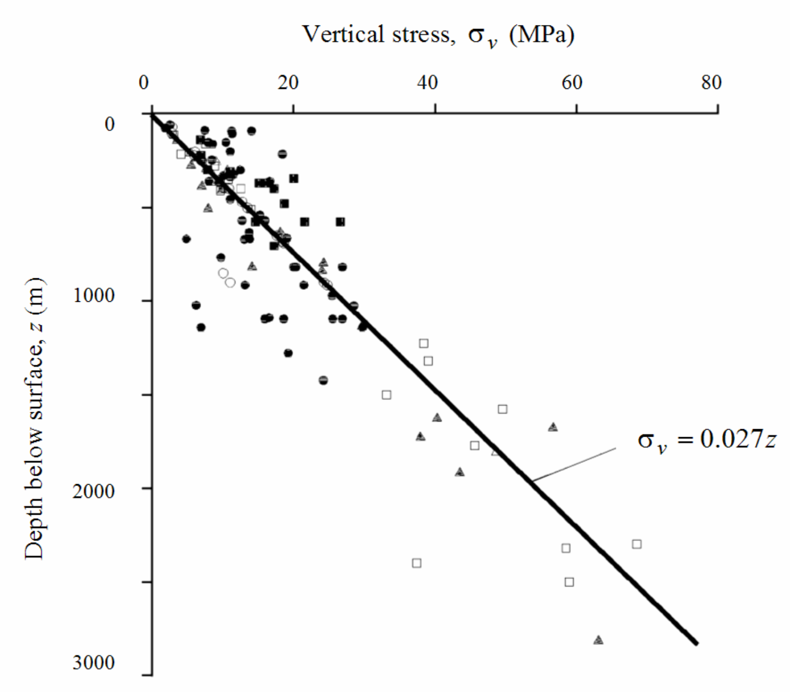

Figure 1: Vertical stress measurements from mining and civil engineering projects around the world. (After Brown and Hoek 1978).

The horizontal stresses acting on an element of rock at a depth z below the surface are much more difficult to estimate than the vertical stresses. Normally, the ratio of the average horizontal stress to the vertical stress is denoted by the letter k such that:

$$\sigma_h = k\sigma_v = k\,\gamma\,z \tag{2}$$

Terzaghi and Richart (1952) suggested that, for a gravitationally loaded rock mass in which no lateral strain was permitted during formation of the overlying strata, the value of k is independent of depth and is given by $k = \nu/(1-\nu)$, where ν is the Poisson's ratio of the rock mass. This relationship was widely used in the early days of rock mechanics but, as discussed below, it proved to be inaccurate and is seldom used today.

Measurements of horizontal stresses at civil and mining sites around the world show that the ratio k tends to be high at shallow depth and that it decreases at depth (Brown and Hoek, 1978, Herget, 1988). In order to understand the reason for these horizontal stress variations it is necessary to consider the problem on a much larger scale than that of a single site.

Sheorey (1994) developed an elasto-static thermal stress model of the earth. This model considers curvature of the crust and variation of elastic constants, density and thermal expansion coefficients through the crust and mantle. A detailed discussion on Sheorey's model is beyond the scope of this chapter, but he did provide a simplified equation which can be used for estimating the horizontal to vertical stress ratio *k*. This equation is:

$$k = 0.25 + 7E_h\left(0.001 + \frac{1}{z}\right) \qquad (3)$$

where z (m) is the depth below surface and E_h (GPa) is the average deformation modulus of the upper part of the earth's crust measured in a horizontal direction. This direction of measurement is important particularly in layered sedimentary rocks, in which the deformation modulus may be significantly different in different directions.

A plot of this equation is given in Figure 2 for a range of deformation moduli. The curves relating *k* with depth below surface *z* are similar to those published by Brown and Hoek (1978), Herget (1988) and others for measured in situ stresses. Hence equation 3 is considered to provide a reasonable basis for estimating the value of *k*.

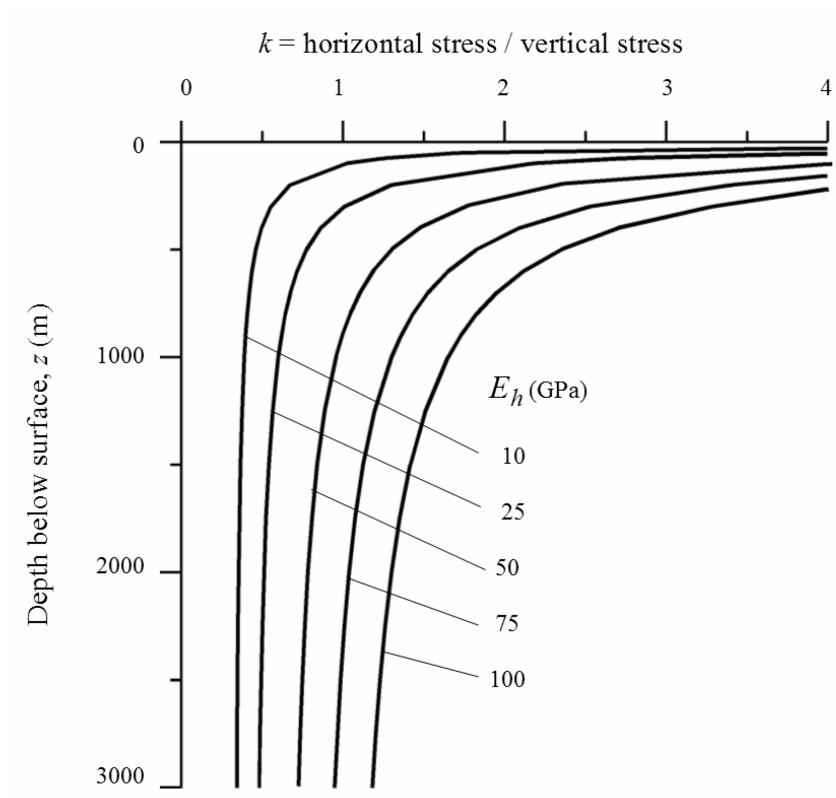

Figure 2: Ratio of horizontal to vertical stress for different deformation moduli based upon Sheorey's equation. (After Sheorey 1994).

As pointed out by Sheorey, his work does not explain the occurrence of measured vertical stresses that are higher than the calculated overburden pressure, the presence of very high horizontal stresses at some locations or why the two horizontal stresses are seldom equal. These differences are probably due to local topographic and geological features that cannot be taken into account in a large scale model such as that proposed by Sheorey.

Where sensitivity studies have shown that the in situ stresses are likely to have a significant influence on the behaviour of underground openings, it is recommended that the in situ stresses should be measured. Suggestions for setting up a stress measuring programme are discussed later in this chapter.

The World stress map

The World Stress Map project, completed in July 1992, involved over 30 scientists from 18 countries and was carried out under the auspices of the International Lithosphere Project (Zoback, 1992). The aim of the project was to compile a global database of contemporary tectonic stress data.

The World Stress Map (WSM) is now maintained and it has been extended by the Geophysical Institute of Karlsruhe University as a research project of the Heidelberg Academy of Sciences and Humanities. The 2005 version of the map contains approximately 16,000 data sets and various versions of the map for the World, Europe, America, Africa, Asia and Australia can be downloaded from the Internet. The WSM is an open-access database that can be accessed at www.world-stress-map.org (Reinecker et al, 2005)

The 2005 World Stress Map is reproduced in Figure 3 while a stress map for the Mediterranean is reproduced in Figure 4.

The stress maps display the orientations of the maximum horizontal compressive stress. The length of the stress symbols represents the data quality, with A being the best quality. Quality A data are assumed to record the orientation of the maximum horizontal compressive stress to within 10°-15°, quality B data to within 15°-20°, and quality C data to within 25°. Quality D data are considered to give questionable tectonic stress orientations.

The 1992 version of the World Stress Map was derived mainly from geological observations on earthquake focal mechanisms, volcanic alignments and fault slip interpretations. Less than 5% of the data was based upon hydraulic fracturing or overcoring measurements of the type commonly used in mining and civil engineering projects. In contrast, the 2005 version of the map includes a significantly greater number of observations from borehole break-outs, hydraulic fracturing, overcoring and borehole slotting. It is therefore worth considering the relative accuracy of these measurements as compared with the geological observations upon which the original map was based.

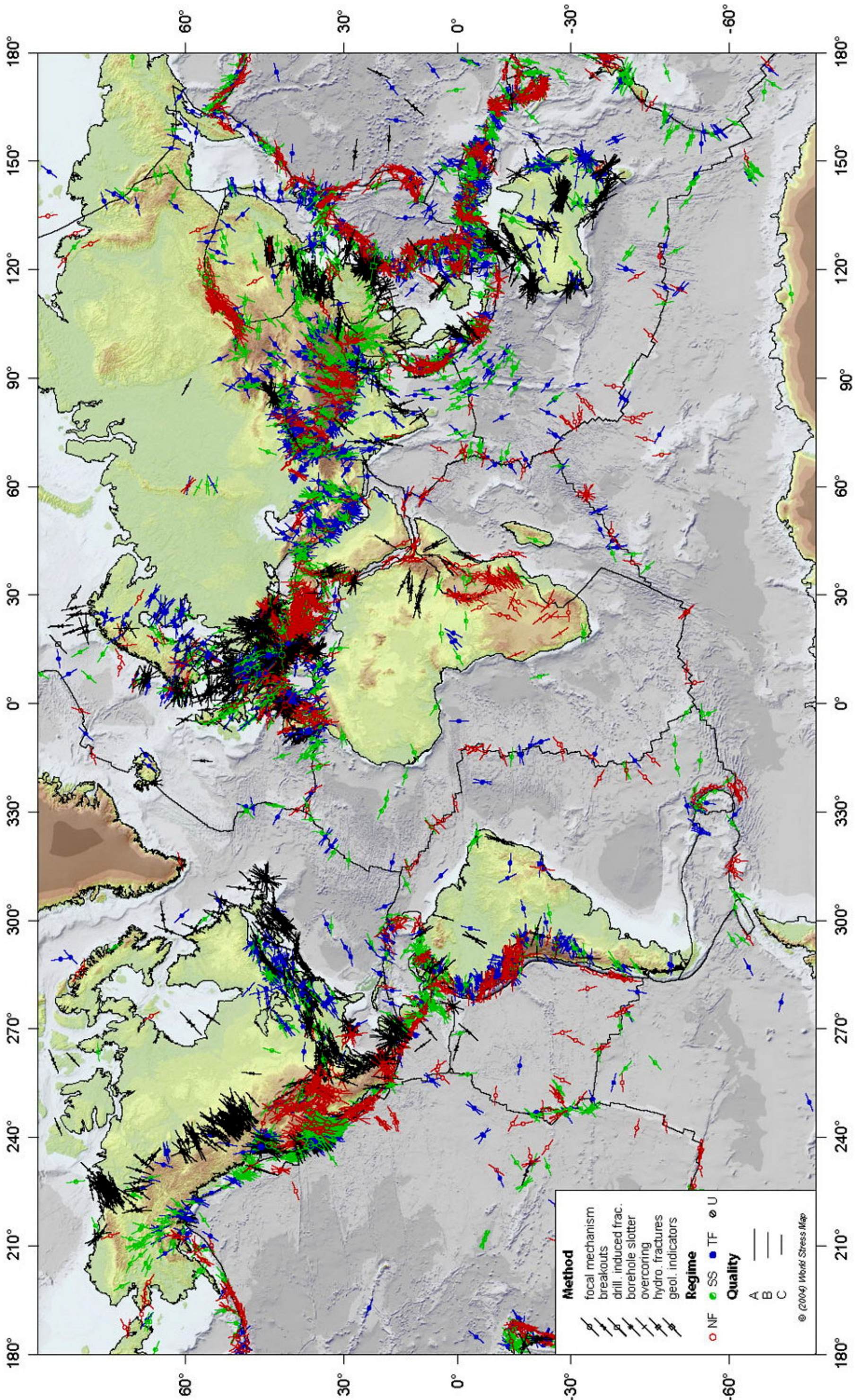

Figure 3: World stress map giving orientations of the maximum horizontal compressive stress. From www.world-stress-map.org.

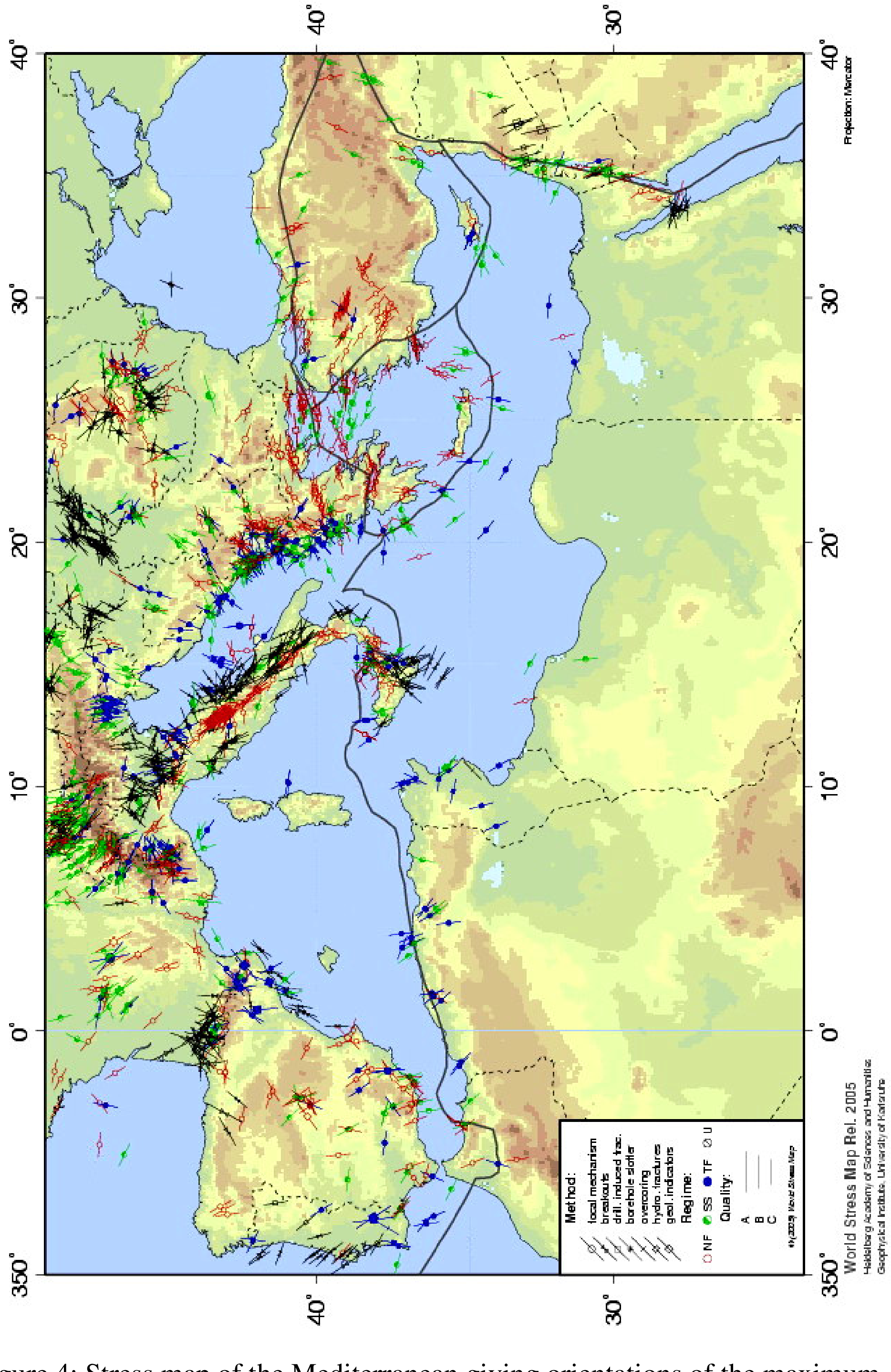

Figure 4: Stress map of the Mediterranean giving orientations of the maximum horizontal compressive stress. From www.world-stress-map.org.

In discussing hydraulic fracturing and overcoring stress measurements, Zoback (1992) has the following comments:

> 'Detailed hydraulic fracturing testing in a number of boreholes beginning very close to surface (10-20 m depth) has revealed marked changes in stress orientations and relative magnitudes with depth in the upper few hundred metres, possibly related to effects of nearby topography or a high degree of near surface fracturing.
>
> Included in the category of 'overcoring' stress measurements are a variety of stress or strain relief measurement techniques. These techniques involve a three-dimensional measurement of the strain relief in a body of rock when isolated from the surrounding rock volume; the three-dimensional stress tensor can subsequently be calculated with a knowledge of the complete compliance tensor of the rock. There are two primary drawbacks with this technique which restricts its usefulness as a tectonic stress indicator: measurements must be made near a free surface, and strain relief is determined over very small areas (a few square millimetres to square centimetres). Furthermore, near surface measurements (by far the most common) have been shown to be subject to effects of local topography, rock anisotropy, and natural fracturing (Engelder and Sbar, 1984). In addition, many of these measurements have been made for specific engineering applications (e.g. dam site evaluation, mining work), places where topography, fracturing or nearby excavations could strongly perturb the regional stress field.'

Obviously, from a global or even a regional scale, the type of engineering stress measurements carried out in a mine or on a civil engineering site are not regarded as very reliable. Conversely, the World Stress Map versions presented in Figures 3 and 4 can only be used to give first order estimates of the stress directions which are likely to be encountered on a specific site. Since both stress directions and stress magnitudes are critically important in the design of underground excavations, it follows that a stress measuring programme may be required in any major underground mining or civil engineering project.

Developing a stress measuring programme

Consider the example of a tunnel to be driven a depth of 1,000 m below surface in a hard rock environment. The depth of the tunnel is such that it is probable that in situ and induced stresses will be an important consideration in the design of the excavation. Typical steps that could be followed in the analysis of this problem are:

The World Stress Map for the area under consideration will give a good first indication of the possible complexity of the regional stress field and possible directions for the maximum horizontal compressive stress.

1. During preliminary design, the information presented in equations 1 and 3 can be used to obtain a first rough estimate of the vertical and average horizontal stress in the vicinity of the tunnel. For a depth of 1,000 m, these equations give the vertical stress σ_v = 27 MPa, the ratio k = 1.3 (for E_h = 75 GPa) and hence the average horizontal stress σ_h= 35.1 MPa. A preliminary analysis of the stresses induced around the proposed tunnel shows that these induced stresses are likely to exceed the strength of the rock and that the question of stress measurement must be considered in more detail. Note that for many openings in strong rock at shallow depth, stress problems may not be significant and the analysis need not proceed any further.

For this particular case, stress problems are considered to be important. A typical next step would be to search the literature in an effort to determine whether the results of in situ stress measurement programmes are available for mines or civil engineering projects within a radius of say 50 km of the site. With luck, a few stress measurement results will be available for the region in which the tunnel is located and these results can be used to refine the analysis discussed above.

Assuming that the results of the analysis of induced stresses in the rock surrounding the proposed tunnel indicate that significant zones of rock failure are likely to develop, and that support costs are likely to be high, it is probably justifiable to set up a stress measurement project on the site. These measurements can be carried out in deep boreholes from the surface, using hydraulic fracturing techniques, or from underground access using overcoring methods. The choice of the method and the number of measurements to be carried out depends upon the urgency of the problem, the availability of underground access and the costs involved in the project. Note that very few project organisations have access to the equipment required to carry out a stress measurement project and, rather than purchase this equipment, it may be worth bringing in an organisation which has the equipment and which specialises in such measurements.

2. Where regional tectonic features such as major faults are likely to be encountered the in situ stresses in the vicinity of the feature may be rotated with respect to the regional stress field. The stresses may be significantly different in magnitude from the values estimated from the general trends described above. These differences can be very important in the design of the openings and in the selection of support and, where it is suspected that this is likely to be the case, in situ stress measurements become an essential component of the overall design process.

Analysis of induced stresses

When an underground opening is excavated into a stressed rock mass, the stresses in the vicinity of the new opening are re-distributed. Consider the example of the stresses induced in the rock surrounding a horizontal circular tunnel as illustrated in Figure 5, showing a vertical slice normal to the tunnel axis.

Before the tunnel is excavated, the in situ stresses σ_v, σ_{h1} and σ_{h2} are uniformly distributed in the slice of rock under consideration. After removal of the rock from within the tunnel, the stresses in the immediate vicinity of the tunnel are changed and new stresses are induced. Three principal stresses σ_1, σ_2 and σ_3 acting on a typical element of rock are shown in Figure 5.

The convention used in rock engineering is that *compressive* stresses are always *positive* and the three principal stresses are numbered such that σ_1 is the largest compressive stress and σ_3 is the smallest compressive stress or the largest tensile stress of the three.

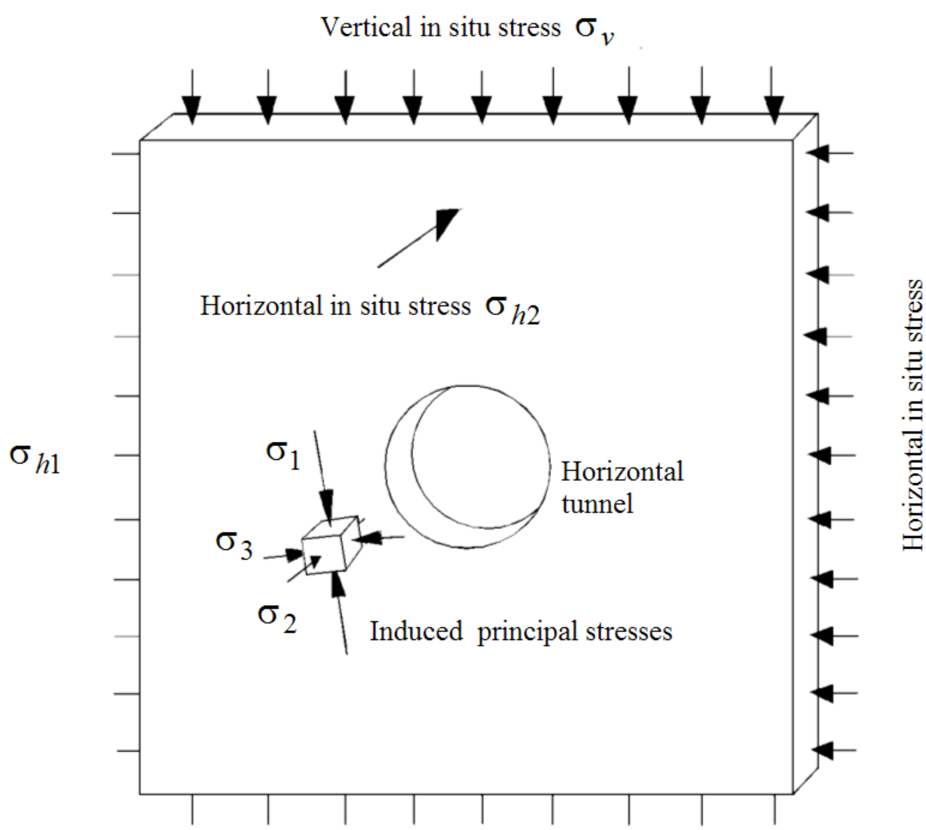

Figure 5: Illustration of principal stresses induced in an element of rock close to a horizontal tunnel subjected to a vertical in situ stress σ_v, a horizontal in situ stress σ_{h1} in a plane normal to the tunnel axis and a horizontal in situ stress σ_{h2} parallel to the tunnel axis.

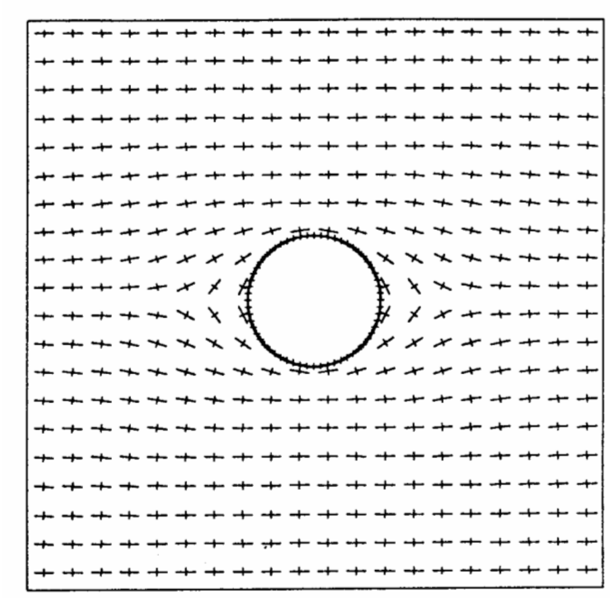

Figure 6: Principal stress directions in the rock surrounding a horizontal tunnel subjected to a horizontal in situ stress σ_{h1} equal to $3\sigma_v$, where σ_v is the vertical in situ stress.

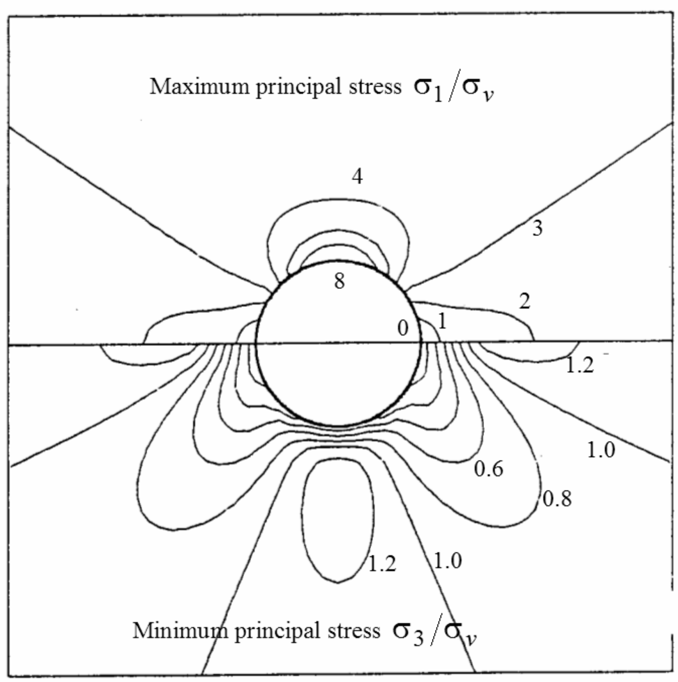

Figure 7: Contours of maximum and minimum principal stress magnitudes in the rock surrounding a horizontal tunnel, subjected to a vertical in situ stress of σ_v and a horizontal in situ stress of $3\sigma_v$.

The three principal stresses are mutually perpendicular but they may be inclined to the direction of the applied in situ stress. This is evident in Figure 6 which shows the directions of the stresses in the rock surrounding a horizontal tunnel subjected to a horizontal in situ stress σ_{h1} equal to three times the vertical in situ stress σ_v. The longer bars in this figure represent the directions of the maximum principal stress σ_1, while the shorter bars give the directions of the minimum principal stress σ_3 at each element considered. In this particular case, σ_2 is coaxial with the in situ stress σ_{h2}, but the other principal stresses σ_1 and σ_3 are inclined to σ_{h1} and σ_v in the immediate vicinity of the tunnel.

Contours of the magnitudes of the maximum principal stress σ_1 and the minimum principal stress σ_3 are given in Figure 7. This figure shows that the redistribution of stresses is concentrated in the rock close to the tunnel and that, at a distance of say three times the radius from the centre of the hole, the disturbance to the in situ stress field is negligible.

An analytical solution for the stress distribution in a stressed elastic plate containing a circular hole was published by Kirsch (1898) and this formed the basis for many early studies of rock behaviour around tunnels and shafts. Following along the path pioneered by Kirsch, researchers such as Love (1927), Muskhelishvili (1953) and Savin (1961) published solutions for excavations of various shapes in elastic plates. A useful summary of these solutions and their application in rock mechanics was published by Brown in an introduction to a volume entitled *Analytical and Computational Methods in Engineering Rock Mechanics* (1987).

Closed form solutions still possess great value for conceptual understanding of behaviour and for the testing and calibration of numerical models. For design purposes, however, these models are restricted to very simple geometries and material models. They are of limited practical value. Fortunately, with the development of computers, many powerful programs that provide numerical solutions to these problems are now readily available. A brief review of some of these numerical solutions is given below.

Numerical methods of stress analysis

Most underground excavations are irregular in shape and are frequently grouped close to other excavations. These groups of excavations can form a set of complex three-dimensional shapes. In addition, because of the presence of geological features such as faults and dykes, the rock properties are seldom uniform within the rock volume of interest. Consequently, closed form solutions are of limited value in calculating the stresses, displacements and failure of the rock mass surrounding underground excavations. A number of computer-based numerical methods have been developed over the past few decades and these methods provide the means for obtaining approximate solutions to these problems.

Numerical methods for the analysis of stress driven problems in rock mechanics can be divided into two classes:

- *Boundary discretization methods*, in which only the boundary of the excavation is divided into elements and the interior of the rock mass is represented mathematically as an infinite continuum. These methods are normally restricted to elastic analyses.
- *Domain discretization methods*, in which the interior of the rock mass is divided into geometrically simple elements each with assumed properties. The collective behaviour and interaction of these simplified elements model the more complex overall behaviour of the rock mass. In other words domain methods allow consideration of more complex material models than boundary methods. *Finite element* and *finite difference* methods are domain techniques which treat the rock mass as a continuum. The *distinct element* method is also a domain method which models each individual block of rock as a unique element.

These two classes of analysis can be combined in the form of *hybrid models* in order to maximise the advantages and minimise the disadvantages of each method.

It is possible to make some general observations about the two types of approaches discussed above. In domain methods, a significant amount of effort is required to create the mesh that is used to divide the rock mass into elements. In the case of complex models, such as those containing multiple openings, meshing can become extremely difficult. In contrast, boundary methods require only that the excavation boundary be discretized and the surrounding rock mass is treated as an infinite continuum. Since fewer elements are required in the boundary method, the demand on computer memory and on the skill and experience of the user is reduced. The availability of highly optimised mesh-generators in many domain models has narrowed this difference to the point where most users of domain programs would be unaware of the mesh generation problems discussed above and hence the choice of models can be based on other considerations.

In the case of domain methods, the outer boundaries of the model must be placed sufficiently far away from the excavations in order that errors, arising from the interaction between these outer boundaries and the excavations, are reduced to an acceptable minimum. On the other hand, since boundary methods treat the rock mass as an infinite continuum, the far field conditions need only be specified as stresses acting on the entire rock mass and no outer boundaries are required. The main strength of boundary methods lies in the simplicity achieved by representing the rock mass as a continuum of infinite extent. It is this representation, however, that makes it difficult to incorporate variable material properties and discontinuities such as joints and faults. While techniques have been developed to allow some boundary element modelling of variable rock properties, these types of problems are more conveniently modelled by domain methods.

Before selecting the appropriate modelling technique for particular types of problems, it is necessary to understand the basic components of each technique.

Boundary Element Method

The boundary element method derives its name from the fact that only the boundaries of the problem geometry are divided into elements. In other words, only the excavation surfaces, the free surface for shallow problems, joint surfaces where joints are considered explicitly and material interfaces for multi-material problems are divided into elements. In fact, several types of boundary element models are collectively referred to as 'the boundary element method' (Crouch and Starfield, 1983). These models may be grouped as follows:

Indirect (Fictitious Stress) method, so named because the first step in the solution is to find a set of fictitious stresses that satisfy prescribed boundary conditions. These stresses are then used in the calculation of actual stresses and displacements in the rock mass.

Direct method, so named because the displacements are solved directly for the specified boundary conditions.

Displacement Discontinuity method, so named because the solution is based on the superposition of the fundamental solution of an elongated slit in an elastic continuum and shearing and normal displacements in the direction of the slit.

The differences between the first two methods are not apparent to the program user. The direct method has certain advantages in terms of program development, as will be discussed later in the section on Hybrid approaches.

The fact that a boundary element model extends 'to infinity' can also be a disadvantage. For example, a heterogeneous rock mass consists of regions of finite, not infinite, extent. Special techniques must be used to handle these situations. Joints are modelled explicitly in the boundary element method using the displacement discontinuity approach, but this can result in a considerable increase in computational effort. Numerical convergence is often found to be a problem for models incorporating many joints. For these reasons, problems, requiring explicit consideration of several joints and/or sophisticated modelling of joint constitutive behaviour, are often better handled by one of the domain methods such as finite elements.

A widely-used application of displacement discontinuity boundary elements is in the modelling of tabular ore bodies. Here, the entire ore seam is represented as a 'discontinuity' which is initially filled with ore. Mining is simulated by reduction of the ore stiffness to zero in those areas where mining has occurred, and the resulting stress redistribution to the surrounding pillars may be examined (Salamon, 1974, von Kimmelmann et al., 1984).

Finite element and finite difference methods

In practice, the finite element method is usually indistinguishable from the finite difference method; thus, they will be treated here as one and the same. For the boundary element method, it was seen that conditions on a domain boundary could be related to the state at *all* points throughout the remaining rock, even to infinity. In comparison, the finite element method relates the conditions at a few points within the rock (nodal points) to the state within a finite closed region formed by these points (the element). In the finite element method the physical problem is modelled numerically by dividing the entire problem region into elements.

The finite element method is well suited to solving problems involving heterogeneous or non-linear material properties, since each element explicitly models the response of its contained material. However, finite elements are not well suited to modelling infinite boundaries, such as occur in underground excavation problems. One technique for handling infinite boundaries is to discretize beyond the zone of influence of the excavation and to apply appropriate boundary conditions to the outer edges. Another approach has been to develop elements for which one edge extends to infinity i.e. so-called 'infinity' finite elements. In practice, efficient pre- and post-processors allow the user to perform parametric analyses and assess the influence of approximated far-field boundary conditions. The time required for this process is negligible compared to the total analysis time.

Joints can be represented explicitly using specific 'joint elements'. Different techniques have been proposed for handling such elements, but no single technique has found universal favour. Joint interfaces may be modelled, using quite general constitutive relations, though possibly at increased computational expense depending on the solution technique.

Once the model has been divided into elements, material properties have been assigned and loads have been prescribed, some technique must be used to redistribute any unbalanced loads and thus determine the solution to the new equilibrium state. Available solution techniques can be broadly divided into two classes - implicit and explicit. Implicit techniques assemble systems of linear equations that are then solved using standard matrix reduction techniques. Any material non-linearity is accounted for by modifying stiffness coefficients (secant approach) and/or by adjusting prescribed variables (initial stress or initial strain approach). These changes are made in an iterative manner such that all constitutive and equilibrium equations are satisfied for the given load state.

The response of a non-linear system generally depends upon the sequence of loading. Thus it is necessary that the load path modelled be representative of the actual load path experienced by the body. This is achieved by breaking the total applied load into load increments, each increment being sufficiently small, so that solution convergence for the increment is achieved after only a few iterations. However, as the system being modelled becomes increasingly non-linear and the load increment represents an ever smaller portion of the total load, the incremental solution technique becomes similar to modelling the quasi-dynamic behaviour of the body, as it responds to gradual application of the total load.

In order to overcome this, a 'dynamic relaxation' solution technique was proposed (Otter et al., 1966) and first applied to geomechanics modelling by Cundall (1971). In this technique no matrices are formed. Rather, the solution proceeds explicitly - unbalanced forces, acting at a material integration point, result in acceleration of the mass associated with the point; applying Newton's law of motion expressed as a difference equation yields incremental displacements, applying the appropriate constitutive relation produces the new set of forces, and so on marching in time, for each material integration point in the model. This solution technique has the advantage that both geometric and material non-linearities are accommodated, with relatively little additional computational effort as compared to a corresponding linear analysis, and computational expense increases only linearly with the number of elements used. A further practical advantage lies in the fact that numerical divergence usually results in the model predicting obviously anomalous physical behaviour. Thus, even relatively inexperienced users may recognise numerical divergence.

Most commercially available finite element packages use implicit (i.e. matrix) solution techniques. For linear problems and problems of moderate non-linearity, implicit techniques tend to perform faster than explicit solution techniques. However, as the degree of non-linearity of the system increases, imposed loads must be applied in smaller increments which implies a greater number of matrix re-formations and reductions, and hence increased computational expense. Therefore, highly non-linear problems are best handled by packages using an explicit solution technique.

Distinct Element Method

In ground conditions conventionally described as blocky (i.e. where the spacing of the joints is of the same order of magnitude as the excavation dimensions), intersecting joints form wedges of rock that may be regarded as rigid bodies. That is, these individual pieces of rock may be free to rotate and translate, and the deformation that takes place at block contacts may be significantly greater than the deformation of the intact rock. Hence, individual wedges may be considered rigid. For such conditions it is usually necessary to model many joints explicitly. However, the behaviour of such systems is so highly non-linear, that even a jointed finite element code, employing an explicit solution technique, may perform relatively inefficiently.

An alternative modelling approach is to develop data structures that represent the blocky nature of the system being analysed. Each block is considered a unique free body that may interact at contact locations with surrounding blocks. Contacts may be represented by the overlaps of adjacent blocks, thereby avoiding the necessity of unique joint elements. This has the added advantage that arbitrarily large relative displacements at the contact may occur, a situation not generally tractable in finite element codes.

Due to the high degree of non-linearity of the systems being modelled, explicit solution techniques are favoured for distinct element codes. As is the case for finite element codes employing explicit solution techniques, this permits very general constitutive modelling of joint behaviour with little increase in computational effort and results in computation time being only linearly dependent on the number of elements used. The use of explicit solution techniques places fewer demands on the skills and experience than the use of codes employing implicit solution techniques.

Although the distinct element method has been used most extensively in academic environments to date, it is finding its way into the offices of consultants, planners and designers. Further experience in the application of this powerful modelling tool to practical design situations and subsequent documentation of these case histories is required, so that an understanding may be developed of where, when and how the distinct element method is best applied.

Hybrid approaches

The objective of a hybrid method is to combine the above methods in order to eliminate undesirable characteristics while retaining as many advantages as possible. For example, in modelling an underground excavation, most non-linearity will occur close to the excavation boundary, while the rock mass at some distance will behave in an elastic fashion. Thus, the near-field rock mass might be modelled, using a distinct element or finite element method, which is then linked at its outer limits to a boundary element model, so that the far-field boundary conditions are modelled exactly. In such an approach, the direct boundary element technique is favoured as it results in increased programming and solution efficiency.

Lorig and Brady (1984) used a hybrid model consisting of a discrete element model for the near field and a boundary element model for the far field in a rock mass surrounding a circular tunnel.

Two-dimensional and three-dimensional models

A two-dimensional model, such as that illustrated in Figure 5, can be used for the analysis of stresses and displacements in the rock surrounding a tunnel, shaft or borehole, where the length of the opening is much larger than its cross-sectional dimensions. The stresses and displacements in a plane, normal to the axis of the opening, are not influenced by the ends of the opening, provided that these ends are far enough away.

On the other hand, an underground powerhouse or crusher chamber has a much more equi-dimensional shape and the effect of the end walls cannot be neglected. In this case, it is much more appropriate to carry out a three-dimensional analysis of the stresses and displacements in the surrounding rock mass. Unfortunately, this switch from two to three dimensions is not as simple as it sounds and there are relatively few good three-dimensional numerical models, which are suitable for routine stress analysis work in a typical engineering design office.

EXAMINE3D (www.rocscience.com) is a three-dimensional boundary element program that provides a starting point for an analysis of a problem in which the three-dimensional geometry of the openings is important. Such three-dimensional analyses provide clear indications of stress concentrations and of the influence of three-dimensional geometry. In many cases, it is possible to simplify the problem to two-dimensions by considering the stresses on critical sections identified in the three-dimensional model.

More sophisticated three-dimensional finite element models such as FLAC3D (www.itascacg.com) are available, but the definition of the input parameters and interpretation of the results of these models would stretch the capabilities of all but the most experienced modellers. It is probably best to leave this type of modelling in the hands of these specialists.

It is recommended that, where the problem being considered is obviously three-dimensional, a preliminary elastic analysis be carried out by means of one of the three-dimensional boundary element programs. The results can then be used to decide whether further three-dimensional analyses are required or whether appropriate two-dimensional sections can be modelled using a program such as PHASE2 (www.rocscience.com), a powerful but user-friendly finite element program that generally meets the needs of most underground excavation design projects.

Examples of two-dimensional stress analysis

A boundary element program called EXAMINE2D is available as a free download from www.rocscience.com. While this program is limited to elastic analyses it can provide a very useful introduction for those who are not familiar with the numerical stress analysis methods described above. The following examples demonstrate the use of this program to explore some common problems in tunnelling.

Tunnel shape

Most contractors like a simple horseshoe shape for tunnels since this gives a wide flat floor for the equipment used during construction. For relatively shallow tunnels in good quality rock this is an appropriate tunnel shape and there are many hundreds of kilometres of horseshoe shaped tunnels all over the world.

In poor quality rock masses or in tunnels at great depth, the simple horseshoe shape is not a good choice because of the high stress concentrations at the corners where the sidewalls meet the floor or invert. In some cases failures initiating at these corners can lead to severe floor heave and even to failure of the entire tunnel perimeter as shown in Figure 8.

Figure 8: Failure of the lining in a horseshoe shaped tunnel in a highly stressed poor quality rock mass. This failure initiated at the corners where the invert meets the sidewalls.

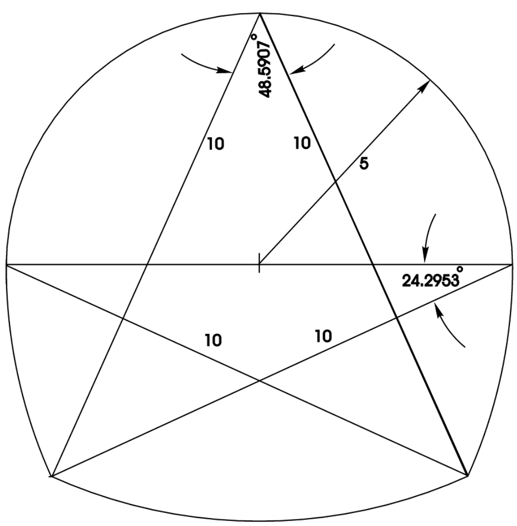

Figure 9: Dimensions of a 10 m span modified horseshoe tunnel shape designed to overcome some of the problems illustrated in Figure 8.

The stress distribution in the rock mass surrounding the tunnel can be improved by modifying the horseshoe shape as shown in Figure 9. In some cases this can eliminate or minimise the types of failure shown in Figure 8 while, in other cases, it may be necessary to use a circular tunnel profile.

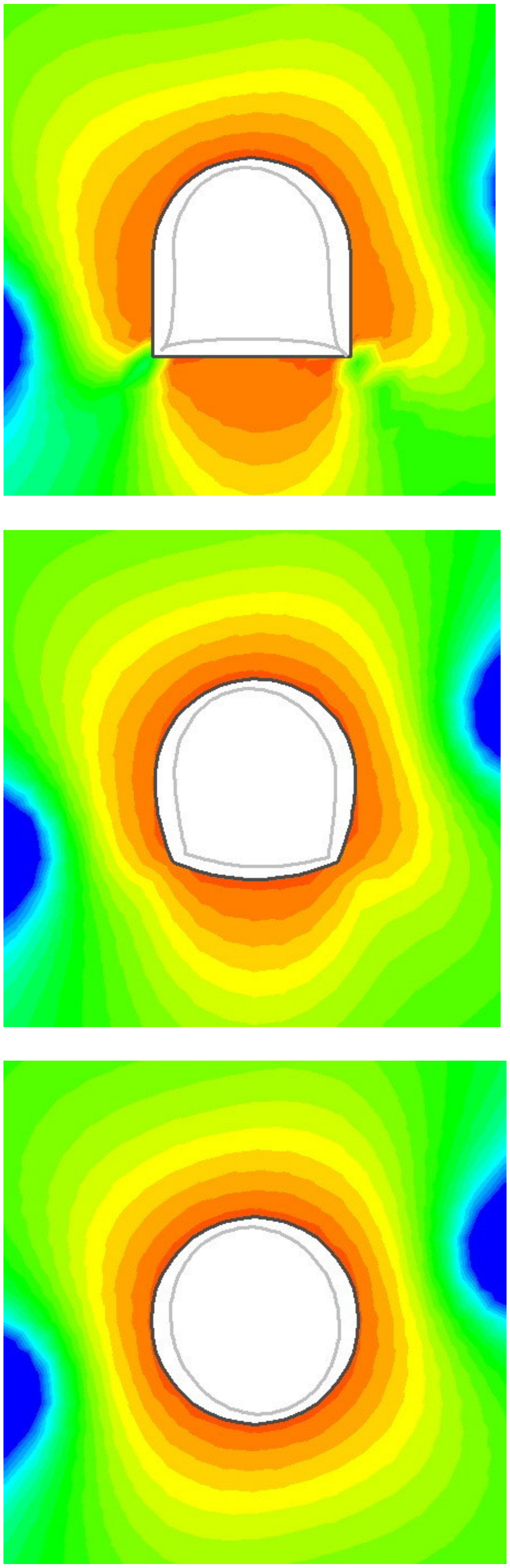

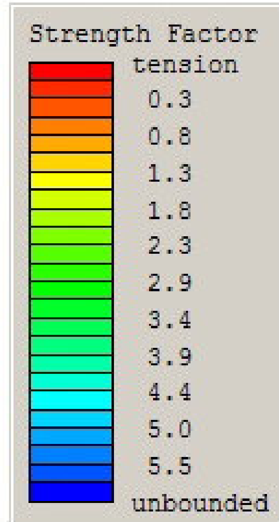

In situ stresses:

Major principal stress σ_1 = 10 MPa
Minor principal stress σ_3 = 7 MPa
Intermediate principal stress σ_2 = 9 MPa
Inclination of major principal stress to the horizontal axis = 15°

Rock mass properties:

Friction angle ϕ = 35°
Cohesion c = 1 MPa
Tensile strength = zero
Deformation modulus E = 4600 MPa

Figure 10: Comparison of three tunnel excavation profiles using EXAMINE2D. The contours are for the Strength Factor defined by the ratio of rock mass strength to the induced stress at each point. The deformed boundary profile (exaggerated) is shown inside each excavation.

The application of the program EXAMINE2D to compare three tunnel shapes is illustrated in Figure 10. Typical "average" in situ stresses and rock mass properties were used in this analysis and the three figures compare Strength Factor contours and deformed excavation profiles (exaggerated) for the three tunnel shapes.

It is clear that the flat floor of the horseshoe tunnel (top figure) allows upward displacement or heaving of the floor. The sharp corners at the junction between the floor and the tunnel sidewalls create high stress concentrations and also generate large bending moments in any lining installed in the tunnel. Failure of the floor generally initiates at these corners as illustrated in Figure 8.

Floor heave is reduced significantly by the concave curvature of the floor of the modified horseshoe shape (middle figure). In marginal cases these modifications to the horseshoe shape may be sufficient to prevent or at least minimise the type of damage illustrated in Figure 8. However, in severe cases, a circular tunnel profile is invariably the best choice, as shown by the smooth Strength Factor contours and the deformed tunnel boundary shape in the bottom figure in Figure 10.

Large underground caverns

A typical underground complex in a hydroelectric project has a powerhouse with a span of 20 to 25 m and a height of 40 to 50 m. Four to six turbine-generator sets are housed in this cavern and a cutaway sketch through one of these sets is shown in Figure 11. Transformers are frequently housed in a chamber or gallery parallel to the powerhouse. Ideally these two caverns should be as close as possible in order to minimise the length of the bus-bars connecting the generators and transformers. This has to be balanced against the size and hence the stability of the pillar between the caverns. The relative location and distance between the caverns is explored in the series of EXAMINE2D models shown in Figure 12, using the same in situ stresses and rock mass properties as listed in Figure 10.

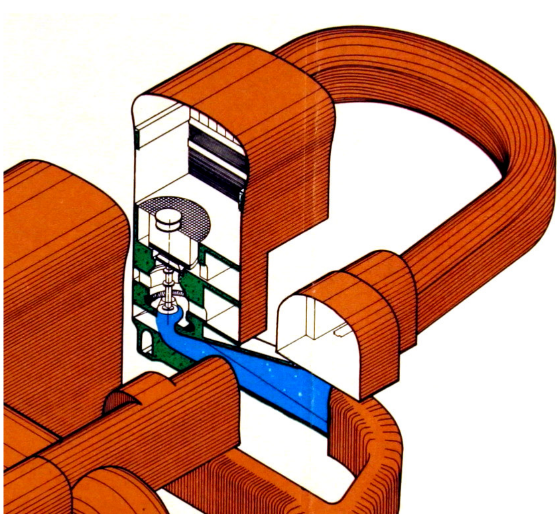

Figure 11: Cutaway sketch of the layout of an underground powerhouse cavern and a parallel transformer gallery.

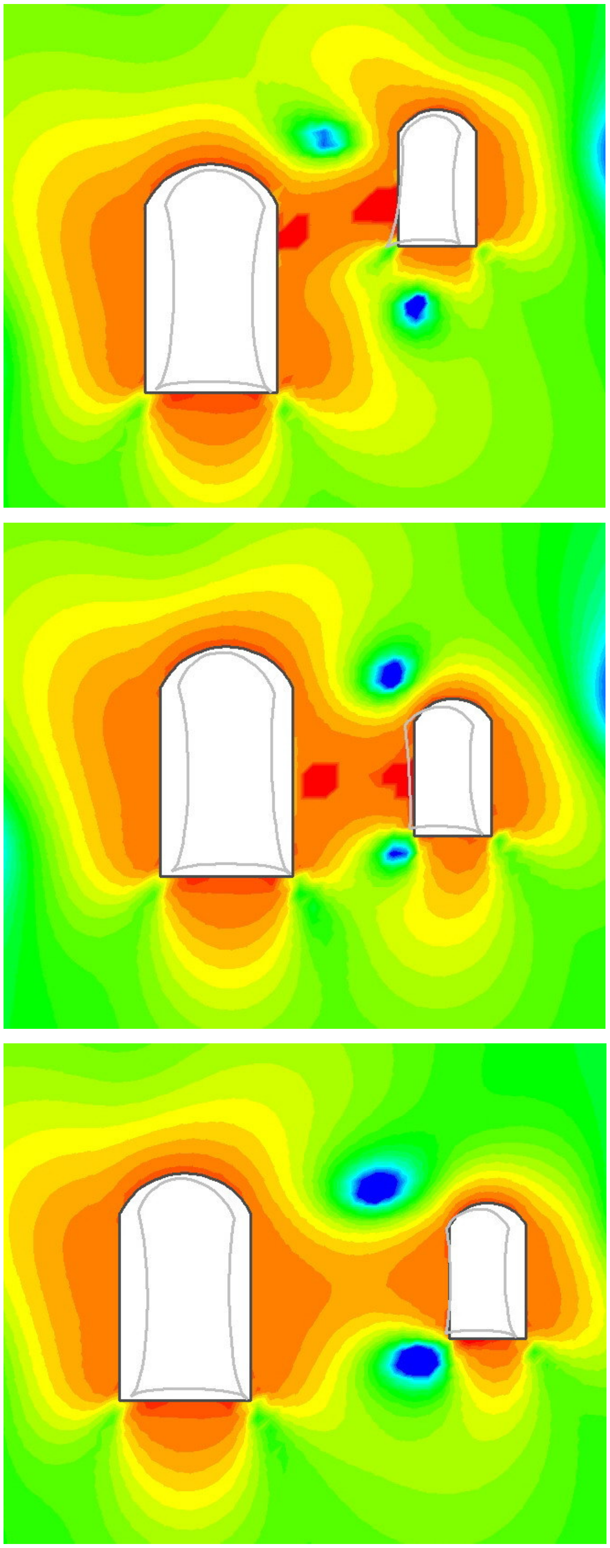

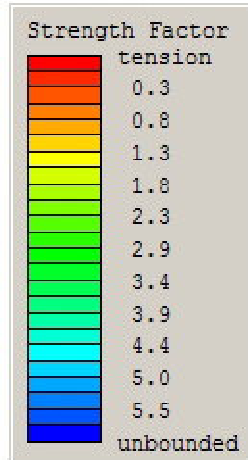

In situ stresses:

Major principal stress σ_1 = 10 MPa
Minor principal stress σ_3 = 7 MPa
Intermediate stress σ_2 = 9 MPa
Inclination of major principal stress to the horizontal axis = 15º

Rock mass properties:

Friction angle ϕ = 35º
Cohesion c = 1 MPa
Tensile strength = zero
Deformation modulus E = 4600 MPa

Figure 12: Comparison of three underground powerhouse and transformer gallery layouts, using EXAMINE2D. The contours are for the Strength Factor defined by the ratio of rock mass strength to the induced stress at each point. The deformed boundary profile (exaggerated) is shown inside each excavation.

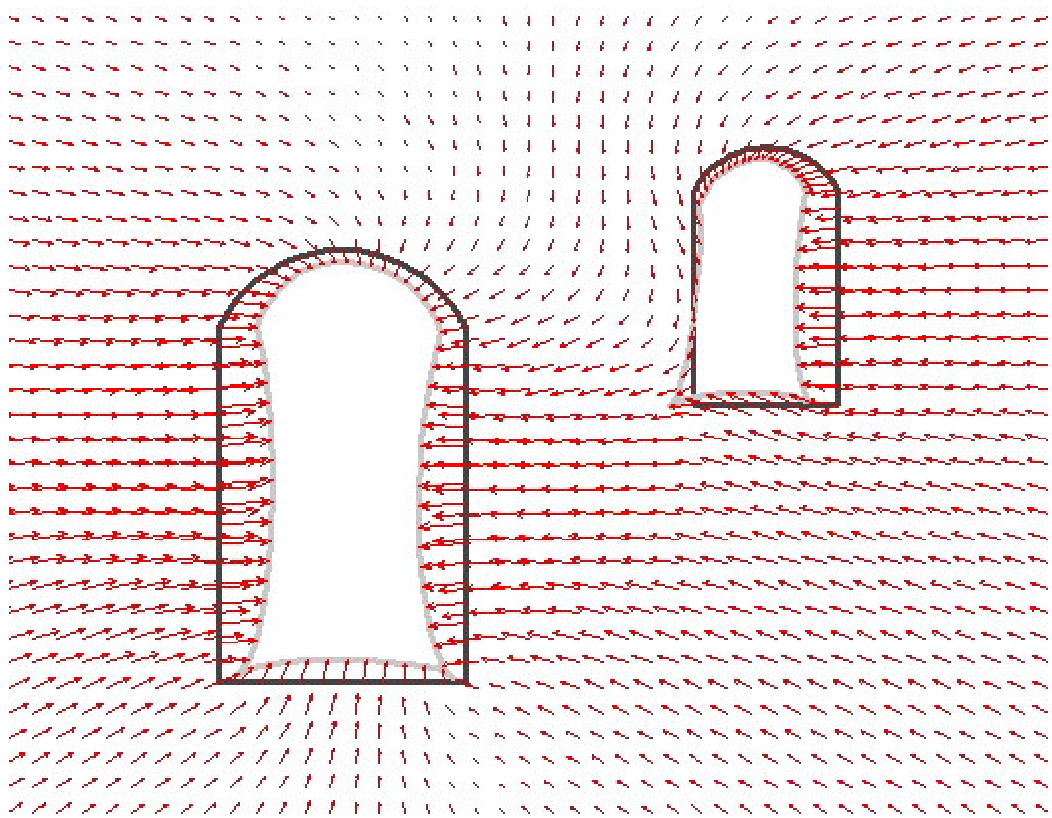

Figure 13: Displacement vectors and deformed excavation shapes for the underground powerhouse and transformer gallery.

A closer examination of the deformations induced in the rock mass by the excavation of the underground powerhouse and transformer gallery, in Figure 13, shows that the smaller of the two excavations is drawn towards the larger cavern and its profile is distorted in this process. This distortion can be reduced by relocating the transformer gallery and by increasing the spacing between the galleries as has been done in Figure 12.

Where the combination of rock mass strength and in situ stresses is likely to cause overstressing around the caverns and in the pillar, a good rule of thumb is that the distance between the two caverns should be approximately equal to the height of the larger cavern.

The interested reader is encouraged to download the program EXAMINE2D (free from www.rocscience.com) and to use it to explore the problem, such as those illustrated in Figures 10 and 12, for themselves.

References

Brown, E.T. 1987. Introduction. *Analytical and computational methods in engineering rock mechanics*, (ed. E.T. Brown), 1-31. London: Allen and Unwin.

Brown, E.T. and Hoek, E. 1978. Trends in relationships between measured rock in situ stresses and depth. *Int. J. Rock Mech. Min. Sci. & Geomech. Abstr.* **15**, pp.211-215.

Crouch, S.L. and Starfield, A.M. 1983. *Boundary element methods in solid mechanics* . London: Allen and Unwin.

Cundall, P.A. 1971. A computer model for simulating progressive large scale movements in blocky rock systems. In.*Rock Fracture , Proc. symp. ISRM, Nancy* **1,** Paper 2-8.

Engelder, T. and Sbar, M.L. 1984. Near-surface in situ stress: introduction. *J. Geophys. Res*. **89**, pp.9321-9322. Princeton, NJ: Princeton University Press.

Herget, G. 1988. *Stresses in rock.* Rotterdam: Balkema.

Hoek, E., Carranza – Torres, C. and Corkum, B., 2002. Hoek - Brown failure criterion – *2002 edition*. In *Proceedings of NARMS-TAC 2002,* Toronto (eds. Bawden,R.W., Curran, J., Telesnicki, M) pp. 267-273. Download from www.rocscience.com

Kirsch, G., 1898. Die theorie der elastizitat und die bedurfnisse der festigkeitslehre. *Veit. Deit. Ing.* **42** (28), 797-807.

Lorig, L.J. and Brady, B.H.G. 1984. A hybrid computational scheme for excavation and support design in jointed rock media. In *Design and performance of underground excavations*, (eds E.T. Brown and J.A. Hudson), 105-112. London: Brit. Geotech. Soc.

Love, A.E.H. 1927. A treatise on the mathematical theory of elasticity. New York: Dover.

Muskhelishvili, N.I. 1953. *Some basic problems of the mathematical theory of elasticity*. 4th edn, translated by J.R.M. Radok. Gronigen: Noordhoff.

Otter, J.R.H., Cassell, A.C. and Hobbs, R.E. 1966. Dynamic relaxation. *Proc. Instn Civ. Engrs* **35**, 633-665.

Reinecker, J., Heidbach, O., Tingay, M., Sperner, B., & Müller, B. 2005: The release 2005 of the World Stress Map (available online at www.world-stress-map.org).

Salamon, M.D.G. 1974. Rock mechanics of underground excavations. In *Advances in rock mechanics , Proc. 3rd Cong.ISRM., Denver* **1B,** 951-1009. Washington, DC: National Academy of Sciences

Savin, G.N. 1961. *Stress concentrations around holes.* London: Pergamon.

Sheory, P.R. 1994. A theory for in situ stresses in isotropic and transversely isotropic rock. *Int. J. Rock Mech. Min. Sci. & Geomech. Abstr*. **31**(1), 23-34.

Terzaghi, K. and Richart, F.E. 1952. Stresses in rock about cavities. *Geotechnique* **3**, 57-90.

von Kimmelmann, M.R., Hyde, B. and Madgwick, R.J. 1984. The use of computer applications at BCL Limited in planning pillar extraction and the design of mine layouts. In *Design and performance of underground excavations*, (eds E.T. Brown and J.A. Hudson), 53-64. London: Brit. Geotech. Soc.

Zoback, M. L. 1992. First- and second-order patterns of stress in the lithosphere: the World Stress Map Project. *J. Geophys. Res.* **97**(B8), 11761-11782.

Rock mass properties

Introduction

Reliable estimates of the strength and deformation characteristics of rock masses are required for almost any form of analysis used for the design of slopes, foundations and underground excavations. Hoek and Brown (1980a, 1980b) proposed a method for obtaining estimates of the strength of jointed rock masses, based upon an assessment of the interlocking of rock blocks and the condition of the surfaces between these blocks. This method was modified over the years in order to meet the needs of users who were applying it to problems that were not considered when the original criterion was developed (Hoek 1983, Hoek and Brown 1988). The application of the method to very poor quality rock masses required further changes (Hoek, Wood and Shah 1992) and, eventually, the development of a new classification called the Geological Strength Index (Hoek, Kaiser and Bawden 1995, Hoek 1994, Hoek and Brown 1997, Hoek, Marinos and Benissi, 1998, Marinos and Hoek, 2001). A major revision was carried out in 2002 in order to smooth out the curves, necessary for the application of the criterion in numerical models, and to update the methods for estimating Mohr Coulomb parameters (Hoek, Carranza-Torres and Corkum, 2002). A related modification for estimating the deformation modulus of rock masses was made by Hoek and Diederichs (2006).

This chapter presents the most recent version of the Hoek-Brown criterion in a form that has been found practical in the field and that appears to provide the most reliable set of results for use as input for methods of analysis in current use in rock engineering.

Generalised Hoek-Brown criterion

The Generalised Hoek-Brown failure criterion for jointed rock masses is defined by:

$$\sigma_1' = \sigma_3' + \sigma_{ci}\left(m_b \frac{\sigma_3'}{\sigma_{ci}} + s \right)^a \tag{1}$$

where σ_1' and σ_3' are the maximum and minimum effective principal stresses at failure,

m_b is the value of the Hoek-Brown constant m for the rock mass,

s and a are constants which depend upon the rock mass characteristics, and

σ_{ci} is the uniaxial compressive strength of the intact rock pieces.

Normal and shear stresses are related to principal stresses by the equations published by Balmer[1] (1952).

$$\sigma_n^{'} = \frac{\sigma_1^{'} + \sigma_3^{'}}{2} - \frac{\sigma_1^{'} - \sigma_3^{'}}{2} \cdot \frac{d\sigma_1^{'} / d\sigma_3^{'} - 1}{d\sigma_1^{'} / d\sigma_3^{'} + 1} \tag{2}$$

$$\tau = \left(\sigma_1^{'} - \sigma_3^{'}\right) \frac{\sqrt{d\sigma_1^{'} / d\sigma_3^{'}}}{d\sigma_1^{'} / d\sigma_3^{'} + 1} \tag{3}$$

where

$$d\sigma_1^{'} / d\sigma_3^{'} = 1 + a m_b \left(m_b \sigma_3^{'} / \sigma_{ci} + s\right)^{a-1} \tag{4}$$

In order to use the Hoek-Brown criterion for estimating the strength and deformability of jointed rock masses, three 'properties' of the rock mass have to be estimated. These are:

- uniaxial compressive strength σ_{ci} of the intact rock pieces,
- value of the Hoek-Brown constant m_i for these intact rock pieces, and
- value of the Geological Strength Index GSI for the rock mass.

Intact rock properties

For the intact rock pieces that make up the rock mass, equation (1) simplifies to:

$$\sigma_1^{'} = \sigma_3^{'} + \sigma_{ci}\left(m_i \frac{\sigma_3^{'}}{\sigma_{ci}} + 1\right)^{0.5} \tag{5}$$

The relationship between the principal stresses at failure for a given rock is defined by two constants, the uniaxial compressive strength σ_{ci} and a constant m_i. Wherever possible the values of these constants should be determined by statistical analysis of the results of a set of triaxial tests on carefully prepared core samples.

Note that the range of minor principal stress ($\sigma_3^{'}$) values over which these tests are carried out is critical in determining reliable values for the two constants. In deriving the original values of σ_{ci} and m_i, Hoek and Brown (1980a) used a range of $0 < \sigma_3^{'} < 0.5\,\sigma_{ci}$ and, in order to be consistent, it is essential that the same range be used in any laboratory triaxial tests on intact rock specimens. At least five well spaced data points should be included in the analysis.

[1] The original equations derived by Balmer contained errors that have been corrected in equations 2 and 3.

One type of triaxial cell that can be used for these tests is illustrated in Figure 1. This cell, described by Franklin and Hoek (1970), does not require draining between tests and is convenient for the rapid testing on a large number of specimens. More sophisticated cells are available for research purposes but the results obtained from the cell illustrated in Figure 1 are adequate for the rock strength estimates required for estimating σ_{ci} and m_i. This cell has the additional advantage that it can be used in the field when testing materials such as coals or mudstones that are extremely difficult to preserve during transportation and normal specimen preparation for laboratory testing.

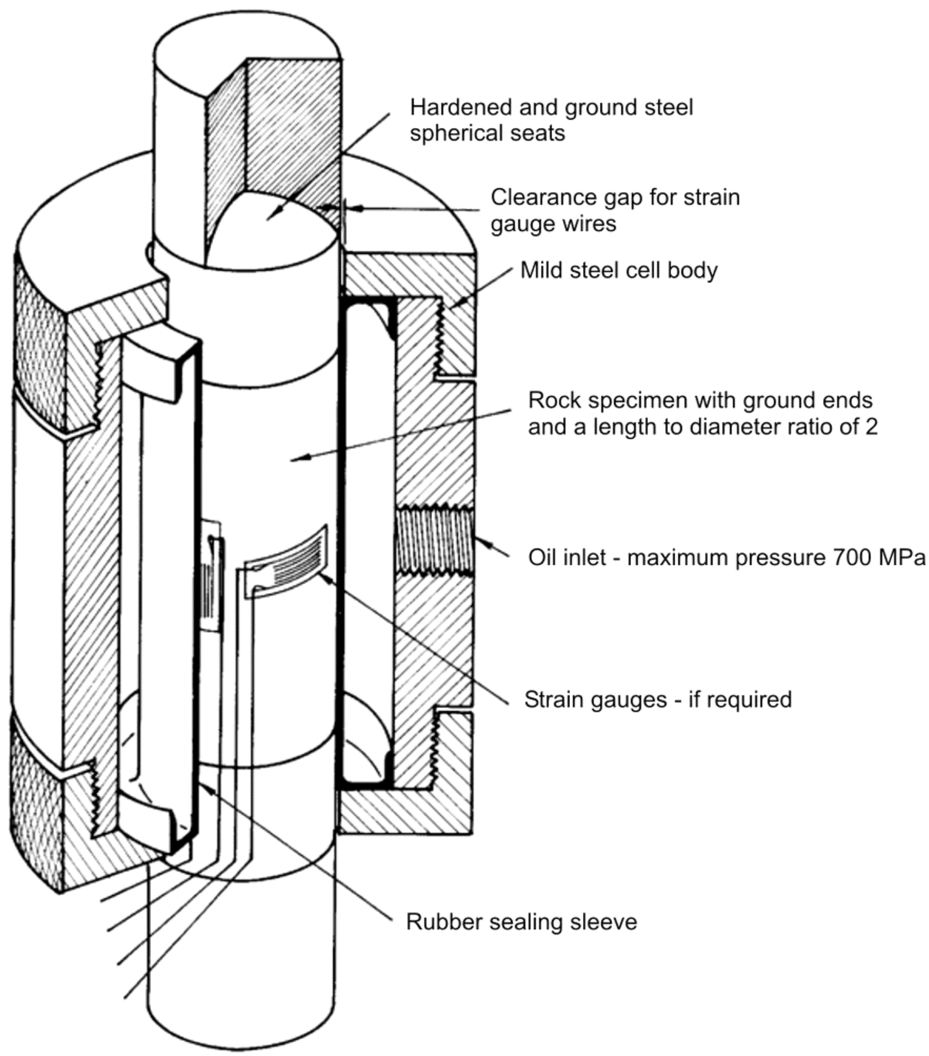

Figure 1: Cut-away view of a triaxial cell for testing rock specimens.

Laboratory tests should be carried out at moisture contents as close as possible to those which occur in the field. Many rocks show a significant strength decrease with increasing moisture content and tests on samples, which have been left to dry in a core shed for several months, can give a misleading impression of the intact rock strength.

Once the five or more triaxial test results have been obtained, they can be analysed to determine the uniaxial compressive strength σ_{ci} and the Hoek-Brown constant m_i as described by Hoek and Brown (1980a). In this analysis, equation (5) is re-written in the form:

$$y = m\sigma_{ci}x + s\sigma_{ci} \tag{6}$$

where $x = \sigma_3'$ and $y = (\sigma_1' - \sigma_3')^2$

For n specimens the uniaxial compressive strength σ_{ci}, the constant and m_i the coefficient of determination r^2 are calculated from:

$$\sigma_{ci}^2 = \frac{\sum y}{n} - \left[\frac{\sum xy - (\sum x \sum y/n)}{\sum x^2 - ((\sum x)^2/n)}\right]\frac{\sum x}{n} \tag{7}$$

$$m_i = \frac{1}{\sigma_{ci}}\left[\frac{\sum xy - (\sum x \sum y/n)}{\sum x^2 - ((\sum x)^2/n)}\right] \tag{8}$$

$$r^2 = \frac{[\sum xy - (\sum x \sum y/n]^2}{[\sum x^2 - (\sum x)^2/n][\sum y^2 - (\sum y)^2/n]} \tag{9}$$

A spreadsheet for the analysis of triaxial test data is given in Table 1. Note that high quality triaxial test data will usually give a coefficient of determination r^2 of greater than 0.9. These calculations, together with many more related to the Hoek-Brown criterion can also be performed by the program RocLab that can be downloaded (free) from www.rocscience.com.

When laboratory tests are not possible, Table 2 and Table 3 can be used to obtain estimates of σ_{ci} and m_i.

Table 1: Spreadsheet for the calculation of σ_{ci} and m_i from triaxial test data

Triaxial test data

x		y	xy	xsq	ysq
sig3	sig1				
0	38.3	1466.89	0.0	0.0	2151766
5	72.4	4542.76	22713.8	25.0	20636668
7.5	80.5	5329.00	39967.5	56.3	28398241
15	115.6	10120.36	151805.4	225.0	102421687
20	134.3	13064.49	261289.8	400.0	170680899
47.5	441.1	34523.50	475776.5	706.3	324289261
sumx		sumy	sumxy	sumxsq	sumysq

Calculation results

Number of tests	n =	5
Uniaxial strength	sigci =	37.4
Hoek-Brown constant	mi =	15.50
Hoek-Brown constant	s =	1.00
Coefficient of determination	r2 =	0.997

Cell formulae

y = (sig1-sig3)^2

sigci = SQRT(sumy/n - (sumxy-sumx*sumy/n)/(sumxsq-(sumx^2)/n)*sumx/n)

mi = (1/sigci)*((sumxy-sumx*sumy/n)/(sumxsq-(sumx^2)/n))

r2 = ((sumxy-(sumx*sumy/n))^2)/((sumxsq-(sumx^2)/n)*(sumysq-(sumy^2)/n))

Note: These calculations, together with many other calculations related to the Hoek-Brown criterion, can also be carried out using the program RocLab that can be downloaded (free) from www.rocscience.com.

Table 2: Field estimates of uniaxial compressive strength.

Grade*	Term	Uniaxial Comp. Strength (MPa)	Point Load Index (MPa)	Field estimate of strength	Examples
R6	Extremely Strong	> 250	>10	Specimen can only be chipped with a geological hammer	Fresh basalt, chert, diabase, gneiss, granite, quartzite
R5	Very strong	100 - 250	4 - 10	Specimen requires many blows of a geological hammer to fracture it	Amphibolite, sandstone, basalt, gabbro, gneiss, granodiorite, limestone, marble, rhyolite, tuff
R4	Strong	50 - 100	2 - 4	Specimen requires more than one blow of a geological hammer to fracture it	Limestone, marble, phyllite, sandstone, schist, shale
R3	Medium strong	25 - 50	1 - 2	Cannot be scraped or peeled with a pocket knife, specimen can be fractured with a single blow from a geological hammer	Claystone, coal, concrete, schist, shale, siltstone
R2	Weak	5 - 25	**	Can be peeled with a pocket knife with difficulty, shallow indentation made by firm blow with point of a geological hammer	Chalk, rocksalt, potash
R1	Very weak	1 - 5	**	Crumbles under firm blows with point of a geological hammer, can be peeled by a pocket knife	Highly weathered or altered rock
R0	Extremely weak	0.25 - 1	**	Indented by thumbnail	Stiff fault gouge

* Grade according to Brown (1981).
** Point load tests on rocks with a uniaxial compressive strength below 25 MPa are likely to yield highly ambiguous results.

Table 3: Values of the constant m_i for intact rock, by rock group. Note that values in parenthesis are estimates.

Rock type	Class	Group	Texture: Coarse	Medium	Fine	Very fine
SEDIMENTARY	Clastic		Conglomerates* (21 ± 3) Breccias (19 ± 5)	Sandstones 17 ± 4	Siltstones 7 ± 2 Greywackes (18 ± 3)	Claystones 4 ± 2 Shales (6 ± 2) Marls (7 ± 2)
	Non-Clastic	Carbonates	Crystalline Limestone (12 ± 3)	Sparitic Limestones (10 ± 2)	Micritic Limestones (9 ± 2)	Dolomites (9 ± 3)
		Evaporites		Gypsum 8 ± 2	Anhydrite 12 ± 2	
		Organic				Chalk 7 ± 2
METAMORPHIC	Non Foliated		Marble 9 ± 3	Hornfels (19 ± 4) Metasandstone (19 ± 3)	Quartzites 20 ± 3	
	Slightly foliated		Migmatite (29 ± 3)	Amphibolites 26 ± 6		
	Foliated**		Gneiss 28 ± 5	Schists 12 ± 3	Phyllites (7 ± 3)	Slates 7 ± 4
IGNEOUS	Plutonic	Light	Granite 32 ± 3 Diorite 25 ± 5 Granodiorite (29 ± 3)			
		Dark	Gabbro 27 ± 3 Norite 20 ± 5	Dolerite (16 ± 5)		
	Hypabyssal		Porphyries (20 ± 5)		Diabase (15 ± 5)	Peridotite (25 ± 5)
	Volcanic	Lava		Rhyolite (25 ± 5) Andesite 25 ± 5	Dacite (25 ± 3) Basalt (25 ± 5)	Obsidian (19 ± 3)
		Pyroclastic	Agglomerate (19 ± 3)	Breccia (19 ± 5)	Tuff (13 ± 5)	

* Conglomerates and breccias may present a wide range of m_i values depending on the nature of the cementing material and the degree of cementation, so they may range from values similar to sandstone to values used for fine grained sediments.

**These values are for intact rock specimens tested normal to bedding or foliation. The value of m_i will be significantly different if failure occurs along a weakness plane.

Anisotropic and foliated rocks such as slates, schists and phyllites, the behaviour of which is dominated by closely spaced planes of weakness, cleavage or schistosity, present particular difficulties in the determination of the uniaxial compressive strengths.

Salcedo (1983) has published the results of a set of directional uniaxial compressive tests on a graphitic phyllite from Venezuela. These results are summarised in Figure 2. It will be noted that the uniaxial compressive strength of this material varies by a factor of about 5, depending upon the direction of loading.

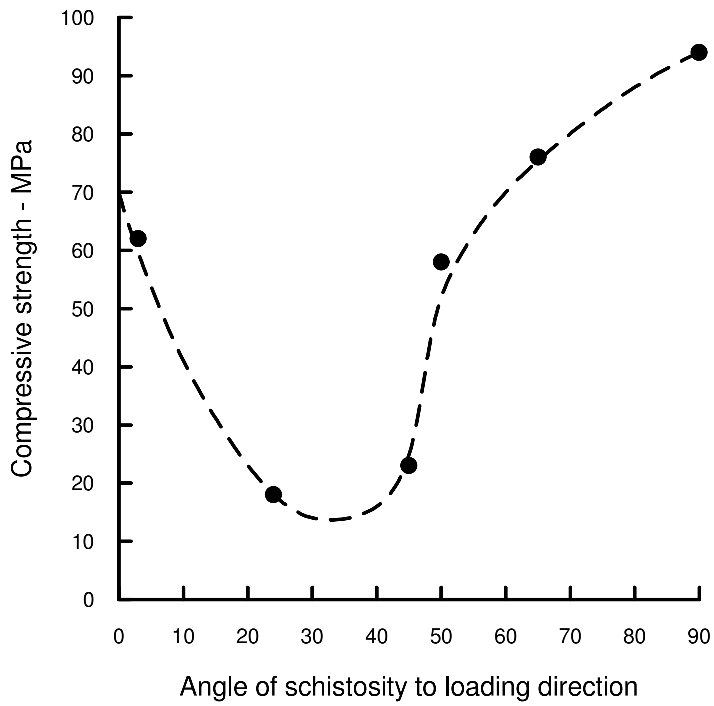

Figure 2: Influence of loading direction on the strength of graphitic phyllite tested by Salcedo (1983).

In deciding upon the value of σ_{ci} for foliated rocks, a decision has to be made on whether to use the highest or the lowest uniaxial compressive strength obtained from results such as those given in Figure 2. Mineral composition, grain size, grade of metamorphism and tectonic history all play a role in determining the characteristics of the rock mass. The author cannot offer any precise guidance on the choice of σ_{ci} but some insight into the role of schistosity in rock masses can be obtained by considering the case of the Yacambú-Quibor tunnel in Venezuela.

This tunnel has been excavated in graphitic phyllite, similar to that tested by Salcedo, at depths of up to 1200 m through the Andes mountains. The appearance of the rock mass at the tunnel face is shown in Figure 3 and a back analysis of the behaviour of this material suggests that an appropriate value for σ_{ci} is approximately 50 MPa. In other words, on the scale of the 5.5 m diameter tunnel, the rock mass properties are "averaged" and there is no sign of anisotropic behaviour in the deformations measured in the tunnel.

Figure 3: Tectonically deformed and sheared graphitic phyllite in the face of the Yacambú-Quibor tunnel at a depth of 1200 m below surface.

Influence of sample size

The influence of sample size upon rock strength has been widely discussed in geotechnical literature and it is generally assumed that there is a significant reduction in strength with increasing sample size. Based upon an analysis of published data, Hoek and Brown (1980a) have suggested that the uniaxial compressive strength σ_{cd} of a rock specimen with a diameter of *d* mm is related to the uniaxial compressive strength σ_{c50} of a 50 mm diameter sample by the following relationship:

$$\sigma_{cd} = \sigma_{c50}\left(\frac{50}{d}\right)^{0.18} \tag{10}$$

This relationship, together with the data upon which it was based, is shown in Figure 4.

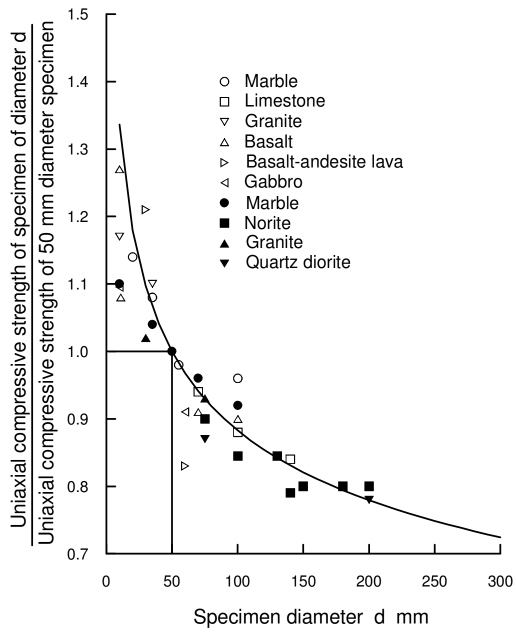

Figure 4: Influence of specimen size on the strength of intact rock. After Hoek and Brown (1980a).

It is suggested that the reduction in strength is due to the greater opportunity for failure through and around grains, the 'building blocks' of the intact rock, as more and more of these grains are included in the test sample. Eventually, when a sufficiently large number of grains are included in the sample, the strength reaches a constant value.

The Hoek-Brown failure criterion, which assumes isotropic rock and rock mass behaviour, should only be applied to those rock masses in which there are a sufficient number of closely spaced discontinuities, with similar surface characteristics, that isotropic behaviour involving failure on discontinuities can be assumed. When the structure being analysed is large and the block size small in comparison, the rock mass can be treated as a Hoek-Brown material.

Where the block size is of the same order as that of the structure being analysed or when one of the discontinuity sets is significantly weaker than the others, the Hoek-Brown criterion should not be used. In these cases, the stability of the structure should be analysed by considering failure mechanisms involving the sliding or rotation of blocks and wedges defined by intersecting structural features.

It is reasonable to extend this argument further and to suggest that, when dealing with large scale rock masses, the strength will reach a constant value when the size of individual rock pieces is sufficiently small in relation to the overall size of the structure being considered. This suggestion is embodied in Figure 5 which shows the transition from an isotropic intact rock specimen, through a highly anisotropic rock mass in which failure is controlled by one or two discontinuities, to an isotropic heavily jointed rock mass.

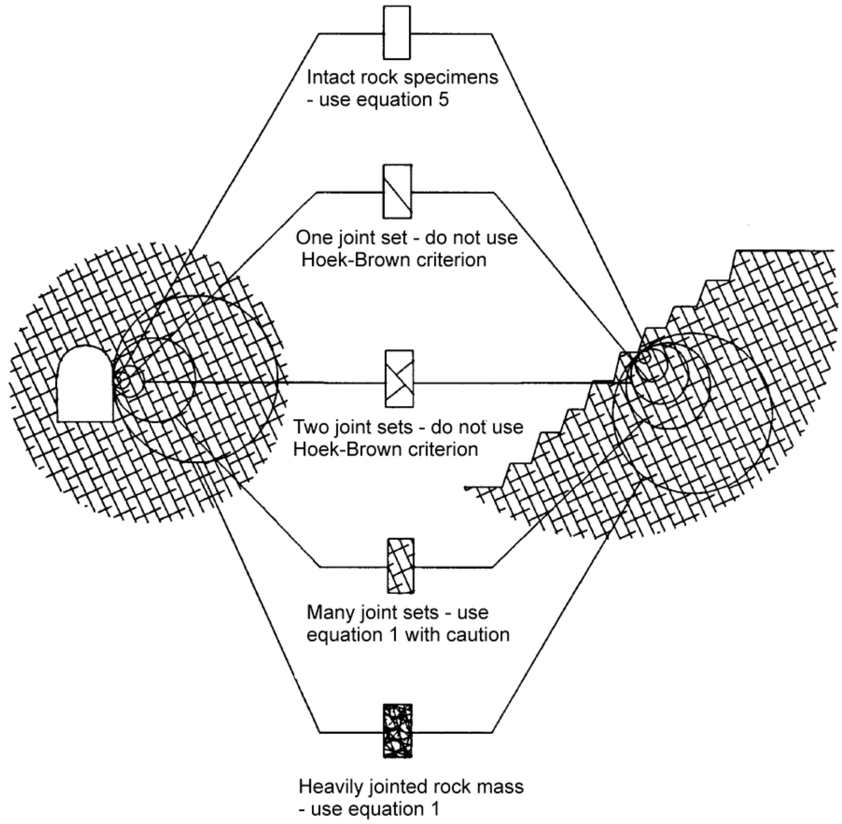

Figure 5: Idealised diagram showing the transition from intact to a heavily jointed rock mass with increasing sample size.

Geological strength Index

The strength of a jointed rock mass depends on the properties of the intact rock pieces and also upon the freedom of these pieces to slide and rotate under different stress conditions. This freedom is controlled by the geometrical shape of the intact rock pieces as well as the condition of the surfaces separating the pieces. Angular rock pieces with clean, rough discontinuity surfaces will result in a much stronger rock mass than one which contains rounded particles surrounded by weathered and altered material.

The Geological Strength Index (GSI), introduced by Hoek (1994) and Hoek, Kaiser and Bawden (1995) provides a number which, when combined with the intact rock properties, can be used for estimating the reduction in rock mass strength for different geological conditions. This system is presented in Table 5, for blocky rock masses, and Table 6 for heterogeneous rock masses such as flysch. Table 6 has also been extended to deal with molassic rocks (Hoek et al 2006) and ophiolites (Marinos et al, 2005).

Before the introduction of the GSI system in 1994, the application of the Hoek-Brown criterion in the field was based on a correlation with the 1976 version of Bieniawski's Rock Mass Rating, with the Groundwater rating set to 10 (dry) and the Adjustment for Joint Orientation set to 0 (very favourable) (Bieniawski, 1976). If the 1989 version of Bieniawski's RMR classification (Bieniawski, 1989) is used, then the Groundwater rating set to 15 and the Adjustment for Joint Orientation set to zero.

During the early years of the application of the GSI system the value of GSI was estimated directly from RMR. However, this correlation has proved to be unreliable, particularly for poor quality rock masses and for rocks with lithological peculiarities that cannot be accommodated in the RMR classification. Consequently, it is recommended that GSI should be estimated directly by means of the charts presented in Tables 5 and 6 and not from the RMR classification.

Experience shows that most geologists and engineering geologists are comfortable with the descriptive and largely qualitative nature of the GSI tables and generally have little difficulty in arriving at an estimated value. On the other hand, many engineers feel the need for a more quantitative system in which they can "measure" some physical dimension. Conversely, these engineers have little difficulty understanding the importance of the intact rock strength σ_{ci} and its incorporation in the assessment of the rock mass properties. Many geologists tend to confuse intact and rock mass strength and consistently underestimate the intact strength.

An additional practical question is whether borehole cores can be used to estimate the GSI value behind the visible faces? Borehole cores are the best source of data at depth but it has to be recognized that it is necessary to extrapolate the one dimensional information provided by core to the three-dimensional rock mass. However, this is a common problem in borehole investigation and most experienced engineering geologists are comfortable with this extrapolation process. Multiple boreholes and inclined boreholes are of great help the interpretation of rock mass characteristics at depth.

The most important decision to be made in using the GSI system is whether or not it should be used. If the discontinuity spacing is large compared with the dimensions of the tunnel or slope under consideration then, as shown in Figure 5, the GSI tables and the Hoek-Brown criterion should not be used and the discontinuities should be treated individually. Where the discontinuity spacing is small compared with the size of the structure (Figure 5) then the GSI tables can be used with confidence.

Table 5: Characterisation of blocky rock masses on the basis of interlocking and joint conditions.

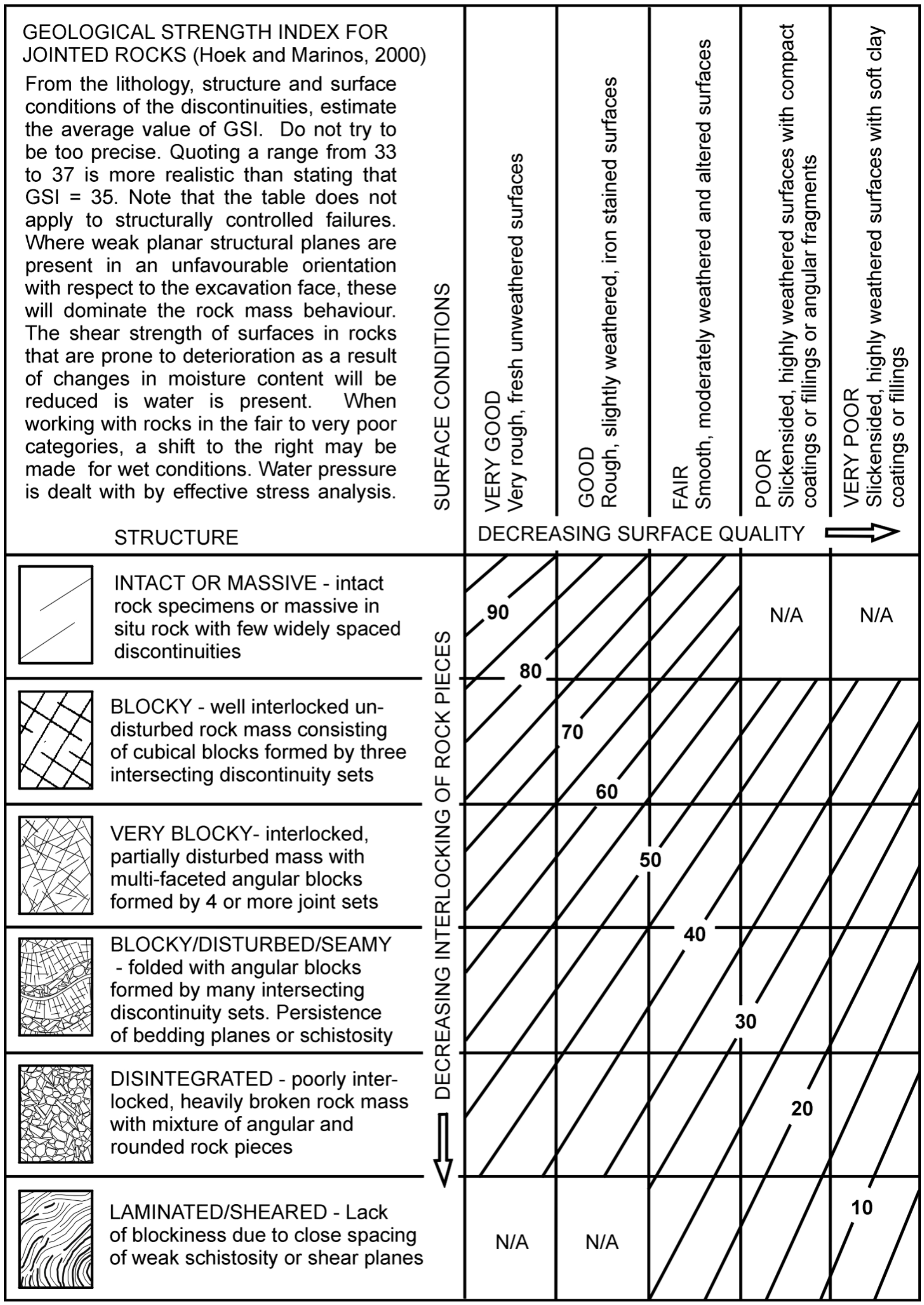

Table 6: Estimate of Geological Strength Index GSI for heterogeneous rock masses such as flysch. (After Marinos and Hoek, 2001)

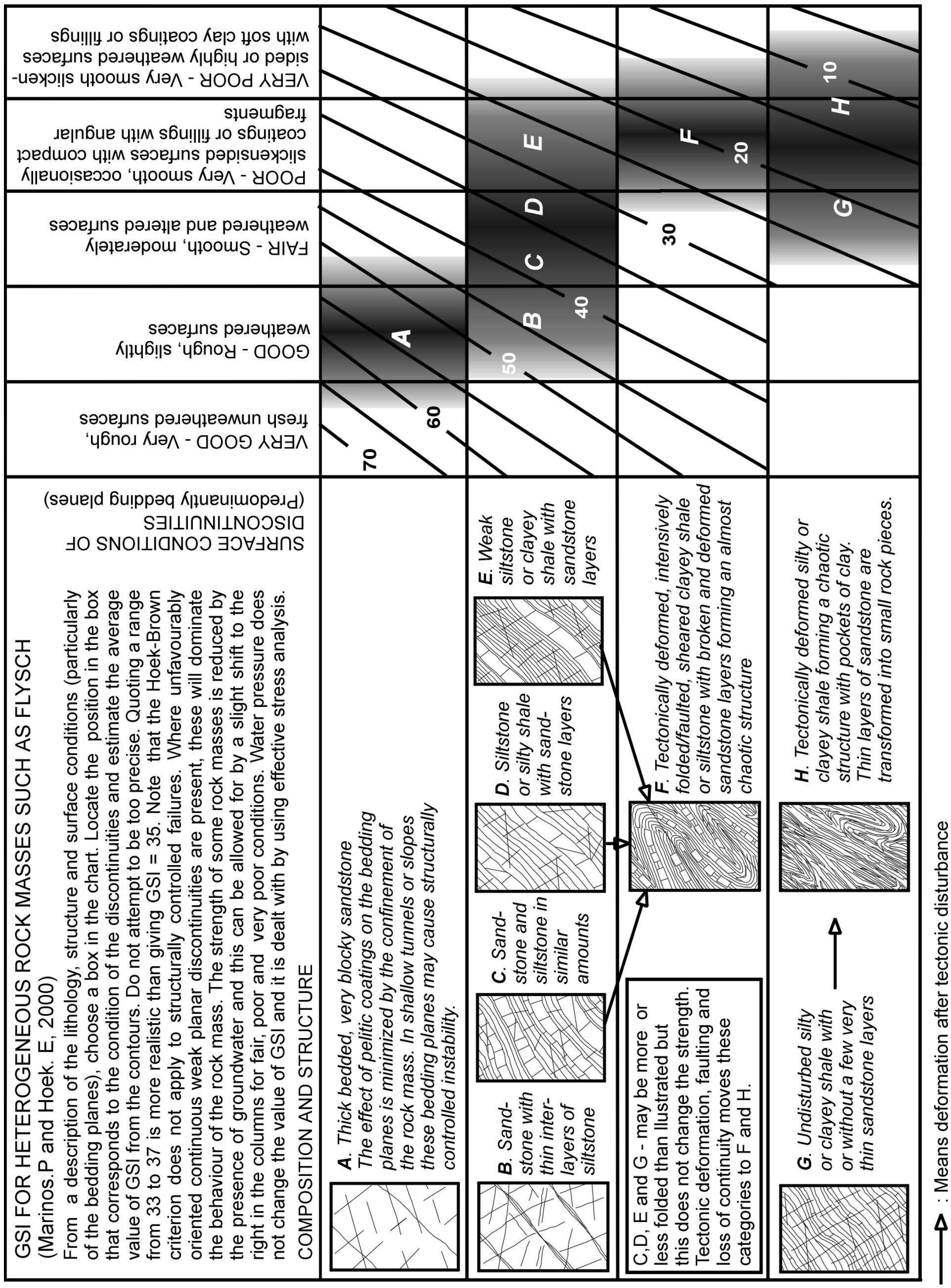

One of the practical problems that arises when assessing the value of GSI in the field is related to blast damage. As illustrated in Figure 6, there is a considerable difference in the appearance of a rock face which has been excavated by controlled blasting and a face which has been damaged by bulk blasting. Wherever possible, the undamaged face should be used to estimate the value of GSI since the overall aim is to determine the properties of the undisturbed rock mass.

Figure 6: Comparison between the results achieved using controlled blasting (on the left) and normal bulk blasting for a surface excavation in gneiss.

The influence of blast damage on the near surface rock mass properties has been taken into account in the 2002 version of the Hoek-Brown criterion (Hoek, Carranza-Torres and Corkum, 2002) as follows:

$$m_b = m_i \exp\left(\frac{GSI-100}{28-14D}\right) \tag{11}$$

$$s = \exp\left(\frac{GSI - 100}{9 - 3D}\right) \tag{12}$$

and

$$a = \frac{1}{2} + \frac{1}{6}\left(e^{-GSI/15} - e^{-20/3}\right) \tag{13}$$

D is a factor which depends upon the degree of disturbance due to blast damage and stress relaxation. It varies from 0 for undisturbed in situ rock masses to 1 for very disturbed rock masses. Guidelines for the selection of D are presented in Table 7.

Note that the factor D applies only to the blast damaged zone and it should not be applied to the entire rock mass. For example, in tunnels the blast damage is generally limited to a 1 to 2 m thick zone around the tunnel and this should be incorporated into numerical models as a different and weaker material than the surrounding rock mass. Applying the blast damage factor D to the entire rock mass is inappropriate and can result in misleading and unnecessarily pessimistic results.

The uniaxial compressive strength of the rock mass is obtained by setting $\sigma_3' = 0$ in equation 1, giving:

$$\sigma_c = \sigma_{ci} . s^a \tag{14}$$

and, the tensile strength of the rock mass is:

$$\sigma_t = -\frac{s\sigma_{ci}}{m_b} \tag{15}$$

Equation 15 is obtained by setting $\sigma_1' = \sigma_3' = \sigma_t$ in equation 1. This represents a condition of biaxial tension. Hoek (1983) showed that, for brittle materials, the uniaxial tensile strength is equal to the biaxial tensile strength.

Note that the "switch" at GSI = 25 for the coefficients *s* and *a* (Hoek and Brown, 1997) has been eliminated in equations 11 and 12 which give smooth continuous transitions for the entire range of GSI values. The numerical values of *s* and *a*, given by these equations, are very close to those given by the previous equations and it is not necessary for readers to revisit and make corrections to old calculations.

Table 7: Guidelines for estimating disturbance factor D

Appearance of rock mass	Description of rock mass	Suggested value of D
	Excellent quality controlled blasting or excavation by Tunnel Boring Machine results in minimal disturbance to the confined rock mass surrounding a tunnel.	D = 0
	Mechanical or hand excavation in poor quality rock masses (no blasting) results in minimal disturbance to the surrounding rock mass. Where squeezing problems result in significant floor heave, disturbance can be severe unless a temporary invert, as shown in the photograph, is placed.	D = 0 D = 0.5 No invert
	Very poor quality blasting in a hard rock tunnel results in severe local damage, extending 2 or 3 m, in the surrounding rock mass.	D = 0.8
	Small scale blasting in civil engineering slopes results in modest rock mass damage, particularly if controlled blasting is used as shown on the left hand side of the photograph. However, stress relief results in some disturbance.	D = 0.7 Good blasting D = 1.0 Poor blasting
	Very large open pit mine slopes suffer significant disturbance due to heavy production blasting and also due to stress relief from overburden removal. In some softer rocks excavation can be carried out by ripping and dozing and the degree of damage to the slopes is less.	D = 1.0 Production blasting D = 0.7 Mechanical excavation

Mohr-Coulomb parameters

Since many geotechnical software programs are written in terms of the Mohr-Coulomb failure criterion, it is sometimes necessary to determine equivalent angles of friction and cohesive strengths for each rock mass and stress range. This is done by fitting an average linear relationship to the curve generated by solving equation 1 for a range of minor principal stress values defined by $\sigma_t < \sigma_3 < \sigma_{3max}$, as illustrated in Figure 7. The fitting process involves balancing the areas above and below the Mohr-Coulomb plot. This results in the following equations for the angle of friction ϕ' and cohesive strength c':

$$\phi' = \sin^{-1}\left[\frac{6am_b(s+m_b\sigma'_{3n})^{a-1}}{2(1+a)(2+a)+6am_b(s+m_b\sigma'_{3n})^{a-1}}\right] \qquad (16)$$

$$c' = \frac{\sigma_{ci}\left[(1+2a)s+(1-a)m_b\sigma'_{3n}\right](s+m_b\sigma'_{3n})^{a-1}}{(1+a)(2+a)\sqrt{1+\left(6am_b(s+m_b\sigma'_{3n})^{a-1}\right)\Big/\left((1+a)(2+a)\right)}} \qquad (17)$$

where $\sigma_{3n} = \sigma'_{3\max} / \sigma_{ci}$

Note that the value of σ'_{3max}, the upper limit of confining stress over which the relationship between the Hoek-Brown and the Mohr-Coulomb criteria is considered, has to be determined for each individual case. Guidelines for selecting these values for slopes as well as shallow and deep tunnels are presented later.

The Mohr-Coulomb shear strength τ, for a given normal stress σ, is found by substitution of these values of c' and ϕ' in to the equation:

$$\tau = c' + \sigma \tan\phi' \qquad (18)$$

The equivalent plot, in terms of the major and minor principal stresses, is defined by:

$$\sigma'_1 = \frac{2c'\cos\phi'}{1-\sin\phi'} + \frac{1+\sin\phi'}{1-\sin\phi'}\sigma'_3 \qquad (19)$$

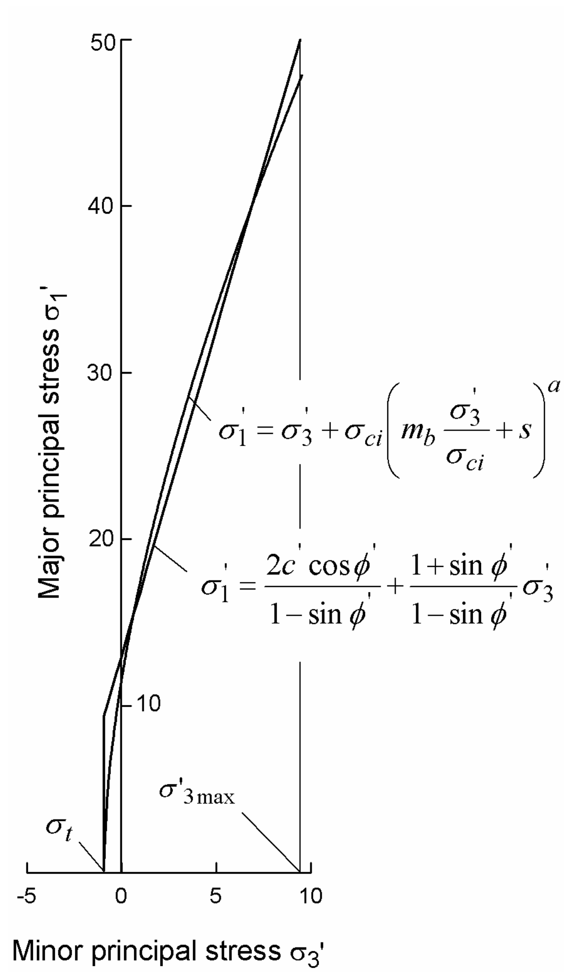

Figure 7: Relationships between major and minor principal stresses for Hoek-Brown and equivalent Mohr-Coulomb criteria.

Rock mass strength

The uniaxial compressive strength of the rock mass σ_c is given by equation 14. Failure initiates at the boundary of an excavation when σ_c is exceeded by the stress induced on that boundary. The failure propagates from this initiation point into a biaxial stress field and it eventually stabilizes when the local strength, defined by equation 1, is higher than the induced stresses σ_1' and σ_3'. Most numerical models can follow this process of fracture propagation and this level of detailed analysis is very important when considering the stability of excavations in rock and when designing support systems.

However, there are times when it is useful to consider the overall behaviour of a rock mass rather than the detailed failure propagation process described above. For example, when considering the strength of a pillar, it is useful to have an estimate of the overall strength of the pillar rather than a detailed knowledge of the extent of fracture propagation in the pillar. This leads to the concept of a global "rock mass strength" and Hoek and Brown (1997) proposed that this could be estimated from the Mohr-Coulomb relationship:

$$\sigma'_{cm} = \frac{2c' \cos\phi'}{1-\sin\phi'} \tag{20}$$

with c' and ϕ' determined for the stress range $\sigma_t < \sigma'_3 < \sigma_{ci}/4$ giving

$$\sigma'_{cm} = \sigma_{ci} \cdot \frac{(m_b + 4s - a(m_b - 8s))(m_b/4 + s)^{a-1}}{2(1+a)(2+a)} \tag{21}$$

Determination of $\sigma'_{3\max}$

The issue of determining the appropriate value of $\sigma'_{3\max}$ for use in equations 16 and 17 depends upon the specific application. Two cases will be investigated:

Tunnels – where the value of $\sigma'_{3\max}$ is that which gives equivalent characteristic curves for the two failure criteria for deep tunnels or equivalent subsidence profiles for shallow tunnels.

Slopes – here the calculated factor of safety and the shape and location of the failure surface have to be equivalent.

For the case of deep tunnels, closed form solutions for both the Generalized Hoek-Brown and the Mohr-Coulomb criteria have been used to generate hundreds of solutions and to find the value of $\sigma'_{3\max}$ that gives equivalent characteristic curves.

For shallow tunnels, where the depth below surface is less than 3 tunnel diameters, comparative numerical studies of the extent of failure and the magnitude of surface subsidence gave an identical relationship to that obtained for deep tunnels, provided that caving to surface is avoided.

The results of the studies for deep tunnels are plotted in Figure 8 and the fitted equation for both deep and shallow tunnels is:

$$\frac{\sigma'_{3\max}}{\sigma'_{cm}} = 0.47\left(\frac{\sigma'_{cm}}{\gamma H}\right)^{-0.94} \tag{22}$$

where σ'_{cm} is the rock mass strength, defined by equation 21, γ is the unit weight of the rock mass and H is the depth of the tunnel below surface. In cases where the horizontal stress is higher than the vertical stress, the horizontal stress value should be used in place of γH.

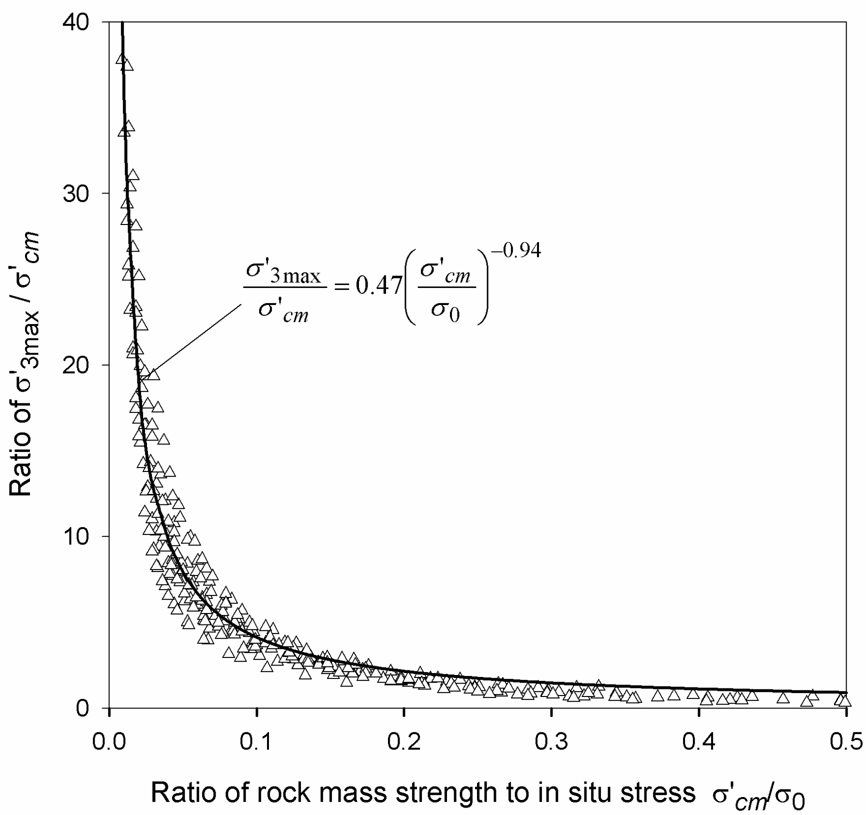

Figure 8: Relationship for the calculation of $\sigma'_{3\max}$ for equivalent Mohr-Coulomb and Hoek-Brown parameters for tunnels.

Equation 22 applies to all underground excavations, which are surrounded by a zone of failure that does not extend to surface. For studies of problems such as block caving in mines it is recommended that no attempt should be made to relate the Hoek-Brown and Mohr-Coulomb parameters and that the determination of material properties and subsequent analysis should be based on only one of these criteria.

Similar studies for slopes, using Bishop's circular failure analysis for a wide range of slope geometries and rock mass properties, gave:

$$\frac{\sigma'_{3\max}}{\sigma'_{cm}} = 0.72\left(\frac{\sigma'_{cm}}{\gamma H}\right)^{-0.91} \tag{23}$$

where H is the height of the slope.

Deformation modulus

Hoek and Diederichs (2005) re-examined existing empirical methods for estimating rock mass deformation modulus and concluded that none of these methods provided reliable estimates over the whole range of rock mass conditions encountered. In particular, large errors were found for very poor rock masses and, at the other end of the spectrum, for massive strong rock masses. Fortunately, a new set of reliable measured data from China and Taiwan was available for analyses and it was found that the equation which gave the best fit to this data is a sigmoid function having the form:

$$y = c + \frac{a}{1 + e^{-((x - x_0)/b)}} \tag{24}$$

Using commercial curve fitting software, Equation 24 was fitted to the Chinese and Taiwanese data and the constants *a* and *b* in the fitted equation were then replaced by expressions incorporating GSI and the disturbance factor D. These were adjusted to give the equivalent average curve and the upper and lower bounds into which > 90% of the data points fitted. Note that the constant *a* = 100 000 in Equation 25 is a scaling factor and it is not directly related to the physical properties of the rock mass.

The following best-fit equation was derived:

$$E_{rm}(MPa) = 100\,000\left(\frac{1 - D/2}{1 + e^{((75 + 25D - GSI)/11)}}\right) \tag{25}$$

The rock mass deformation modulus data from China and Taiwan includes information on the geology as well as the uniaxial compressive strength (σ_{ci}) of the intact rock This information permits a more detailed analysis in which the ratio of mass to intact modulus (E_{rm}/E_i) can be included. Using the modulus ratio *MR* proposed by Deere (1968) (modified by the authors based in part on this data set and also on additional correlations from Palmstrom and Singh (2001)) it is possible to estimate the intact modulus from:

$$E_i = MR \cdot \sigma_{ci} \tag{26}$$

This relationship is useful when no direct values of the intact modulus (E_i) are available or where completely undisturbed sampling for measurement of E_i is difficult. A detailed analysis of the Chinese and Taiwanese data, using Equation (26) to estimate E_i resulted in the following equation:

$$E_{rm} = E_i \left(0.02 + \frac{1 - D/2}{1 + e^{((60+15D-GSI)/11)}} \right) \tag{27}$$

This equation incorporates a finite value for the parameter *c* (Equation 24) to account for the modulus of broken rock (transported rock, aggregate or soil) described by GSI = 0. This equation is plotted against the average normalized field data from China and Taiwan in Figure 9.

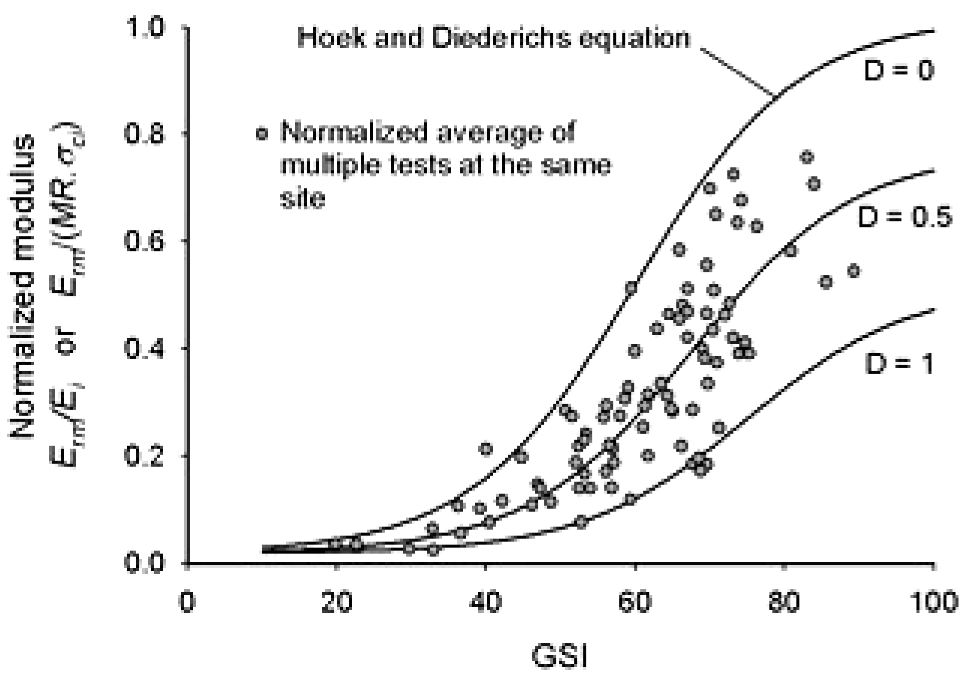

Figure 9: Plot of normalized in situ rock mass deformation modulus from China and Taiwan against Hoek and Diederichs Equation (27). Each data point represents the average of multiple tests at the same site in the same rock mass.

Table 8: Guidelines for the selection of modulus ratio (MR) values in Equation (26) - based on Deere (1968) and Palmstrom and Singh (2001)

	Class	Group	Texture: Coarse	Texture: Medium	Texture: Fine	Texture: Very fine
SEDIMENTARY	Clastic		Conglomerates 300-400 Breccias 230-350	Sandstones 200-350	Siltstones 350-400 Greywackes 350	Claystones 200-300 Shales 150-250 * Marls 150-200
	Non-Clastic	Carbonates	Crystalline Limestone 400-600	Sparitic Limestones 600-800	Micritic Limestones 800-1000	Dolomites 350-500
		Evaporites		Gypsum (350)**	Anhydrite (350)**	
		Organic				Chalk 1000+
METAMORPHIC	Non Foliated		Marble 700-1000	Hornfels 400-700 Metasandstone 200-300	Quartzites 300-450	
	Slightly foliated		Migmatite 350-400	Amphibolites 400-500	Gneiss 300-750*	
	Foliated*			Schists 250-1100*	Phyllites /Mica Schist 300-800*	Slates 400-600*
IGNEOUS	Plutonic	Light	Granite+ 300-550 Granodiorite+ 400-450	Diorite+ 300-350		
		Dark	Gabbro 400-500 Norite 350-400	Dolerite 300-400		
	Hypabyssal		Porphyries (400)**		Diabase 300-350	Peridotite 250-300
	Volcanic	Lava		Rhyolite 300-500 Andesite 300-500	Dacite 350-450 Basalt 250-450	
		Pyroclastic	Agglomerate 400-600	Volcanic breccia (500) **	Tuff 200-400	

* Highly anisotropic rocks: the value of MR will be significantly different if normal strain and/or loading occurs parallel (high MR) or perpendicular (low MR) to a weakness plane. Uniaxial test loading direction should be equivalent to field application.
+ Felsic Granitoids: Coarse Grained or Altered (high MR), fined grained (low MR).
** No data available, estimated on the basis of geological logic.

Table 8, based on the modulus ratio (*MR*) values proposed by Deere (1968) can be used for calculating the intact rock modulus E_i. In general, measured values of E_i are seldom available and, even when they are, their reliability is suspect because of specimen damage. This specimen damage has a greater impact on modulus than on strength and, hence, the intact rock strength, when available, can usually be considered more reliable.

Post-failure behaviour

When using numerical models to study the progressive failure of rock masses, estimates of the post-peak or post-failure characteristics of the rock mass are required. In some of these models, the Hoek-Brown failure criterion is treated as a yield criterion and the analysis is carried out using plasticity theory. No definite rules for dealing with this problem can be given but, based upon experience in numerical analysis of a variety of practical problems, the post-failure characteristics, illustrated in Figure 10, are suggested as a starting point.

Reliability of rock mass strength estimates

The techniques described in the preceding sections of this chapter can be used to estimate the strength and deformation characteristics of isotropic jointed rock masses. When applying this procedure to rock engineering design problems, most users consider only the 'average' or mean properties. In fact, all of these properties exhibit a distribution about the mean, even under the most ideal conditions, and these distributions can have a significant impact upon the design calculations.

In the text that follows, a slope stability calculation and a tunnel support design calculation are carried out in order to evaluate the influence of these distributions. In each case the strength and deformation characteristics of the rock mass are estimated by means of the Hoek-Brown procedure, assuming that the three input parameters are defined by normal distributions.

Input parameters

Figure 11 has been used to estimate the value of the value of GSI from field observations of blockiness and discontinuity surface conditions. Included in this figure is a crosshatched circle representing the 90% confidence limits of a GSI value of 25 ± 5 (equivalent to a standard deviation of approximately 2.5). This represents the range of values that an experienced geologist would assign to a rock mass described as BLOCKY/DISTURBED or DISINTEGRATED and POOR. Typically, rocks such as flysch, schist and some phyllites may fall within this range of rock mass descriptions.

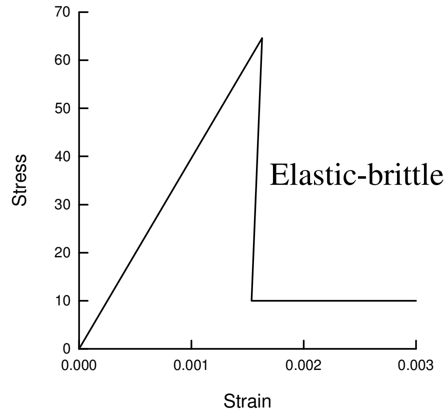

(a) Very good quality hard rock mass

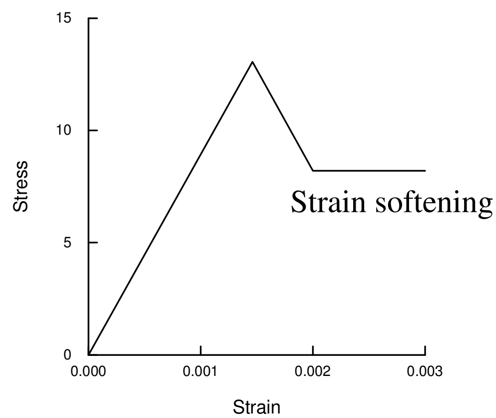

(b) Average quality rock mass

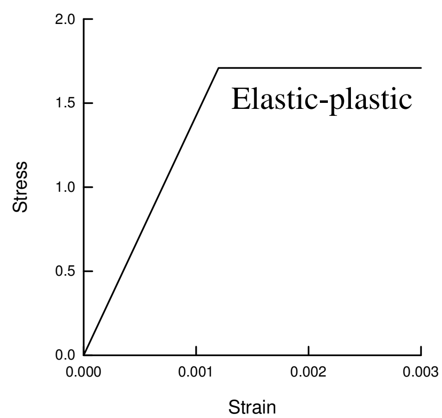

(c) Very poor quality soft rock mass

Figure 10: Suggested post failure characteristics for different quality rock masses.

Figure 11: Estimate of Geological Strength Index GSI based on geological descriptions.

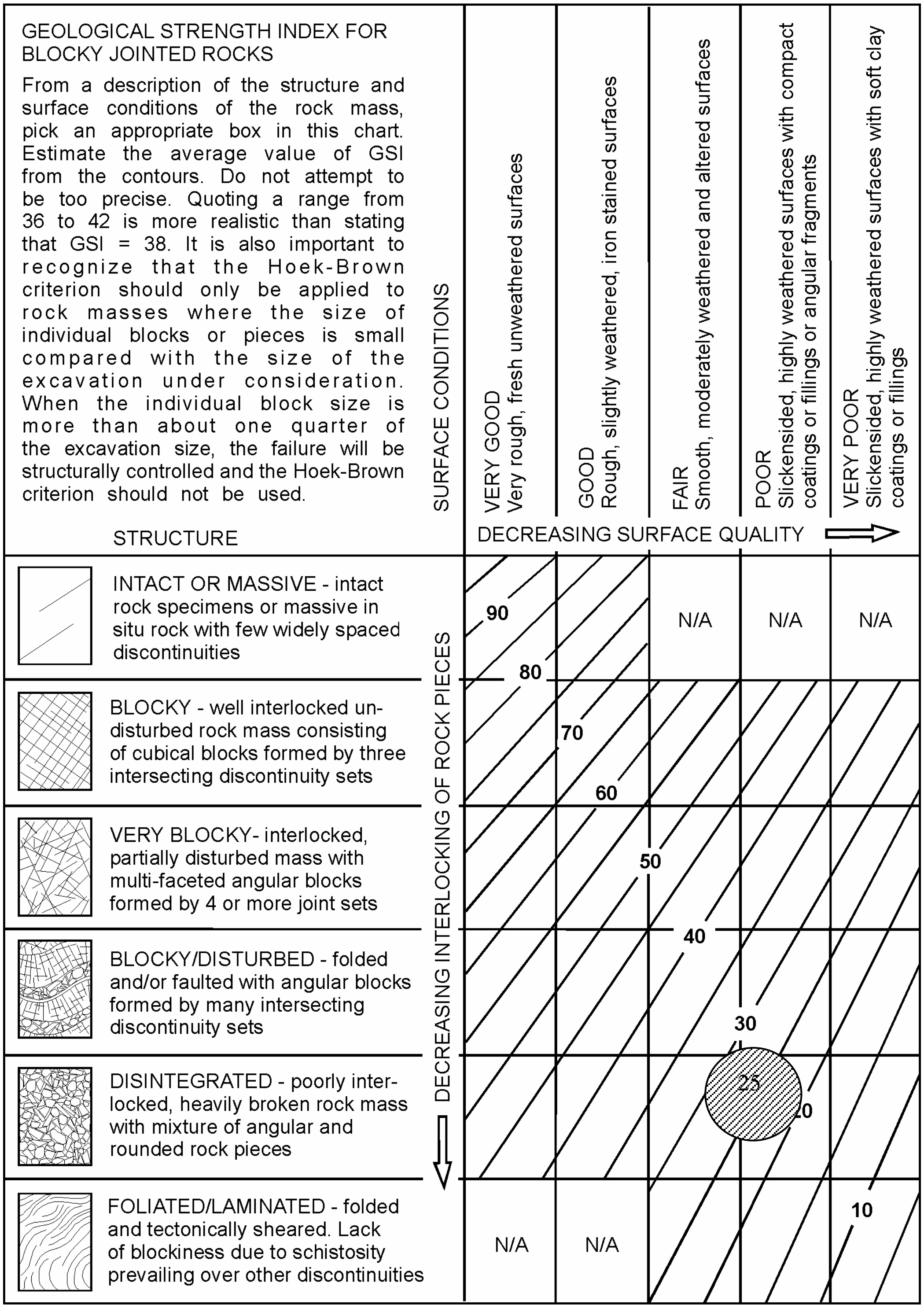

In the author's experience, some geologists go to extraordinary lengths to try to determine an 'exact' value of GSI. Geology does not lend itself to such precision and it is simply not realistic to assign a single value. A range of values, such as that illustrated in Figure 11 is more appropriate. In fact, in some complex geological environments, the range indicated by the crosshatched circle may be too optimistic.

The two laboratory properties required for the application of the Hoek-Brown criterion are the uniaxial compressive strength of the intact rock (σ_{ci}) and the intact rock material constant m_i. Ideally these two parameters should be determined by triaxial tests on carefully prepared specimens as described by Hoek and Brown (1997).

It is assumed that all three input parameters (GSI, σ_{ci} and m_i) can be represented by normal distributions as illustrated in Figure 12. The standard deviations assigned to these three distributions are based upon the author's experience of geotechnical programs for major civil and mining projects where adequate funds are available for high quality investigations. For preliminary field investigations or 'low budget' projects, it is prudent to assume larger standard deviations for the input parameters.

Note that where software programs will accept input in terms of the Hoek-Brown criterion directly, it is preferable to use this input rather than estimates of Mohr Coulomb parameters c and ϕ given by equations 16 and 17. This eliminates the uncertainty associated with estimating equivalent Mohr-Coulomb parameters, as described above and allows the program to compute the conditions for failure at each point directly from the curvilinear Hoek-Brown relationship. In addition, the input parameters for the Hoek-Brown criterion (m_i, s and a) are independent variables and can be treated as such in any probabilistic analysis. On the other hand the Mohr Coulomb c and ϕ parameters are correlated and this results in an additional complication in probabilistic analyses.

Based on the three normal distributions for GSI, σ_{ci} and m_i given in Figure 12, distributions for the rock mass parameters m_b, s and a can be determined by a variety of methods. One of the simplest is to use a Monte Carlo simulation in which the distributions given in Figure 12 are used as input for equations 11, 12 and 13 to determine distributions for mi, s and a. The results of such an analysis, using the Excel add-in @RISK[2], are given in Figure 13.

Slope stability calculation

In order to assess the impact of the variation in rock mass parameters, illustrated in Figure 12 and 13, a calculation of the factor of safety for a homogeneous slope was

[2] Available from www.palisade.com

carried out using Bishop's circular failure analysis in the program SLIDE[3]. The geometry of the slope and the phreatic surface are shown in Figure 14. The probabilistic option offered by the program was used and the rock mass properties were input as follows:

Property	Distribution	Mean	Std. dev.	Min*	Max*
m_b	Normal	0.6894	0.1832	0.0086	1.44
s	Lognormal	0.0002498	0.0000707	0.0000886	0.000704
a	Normal	0.5317	0.00535	0.5171	0.5579
σ_{ci}	Normal	10000 kPa	2500 kPa	1000 kPa	20000 kPa
Unit weight γ		23 kN/m3			

* Note that, in SLIDE, these values are input as values relative to the mean value and not as the absolute values shown here.

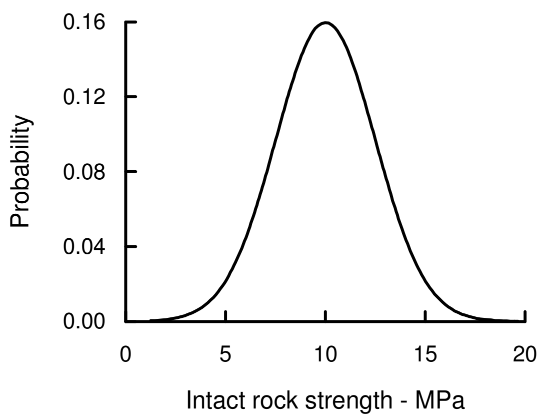

σ_{ci} - Mean 10 MPa, Stdev 2.5 MPa

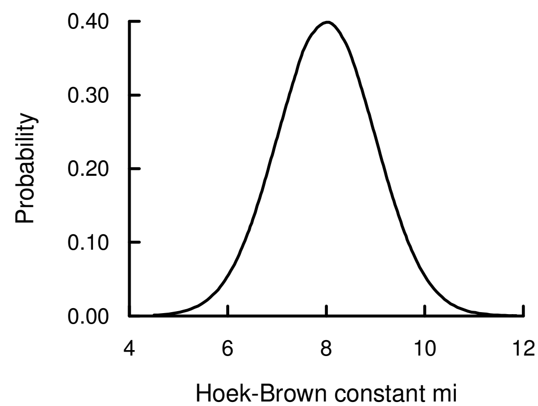

m_i – Mean 8, Stdev 1

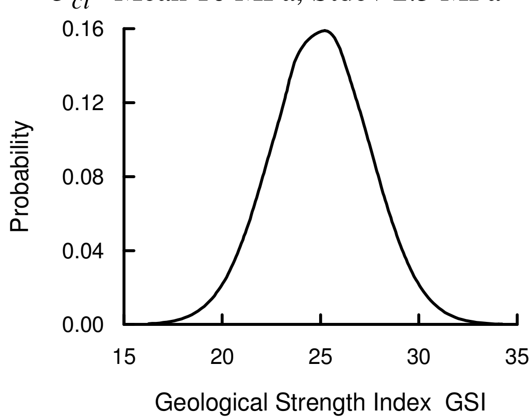

GSI – Mean 25, Stdev 2.5

Figure 12: Assumed normal distributions for input parameters.

[3] available from www.rocscience.com

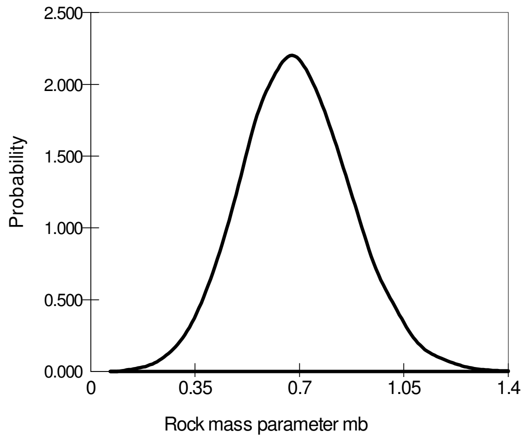

m_b - Mean 0.689, Stdev 0.183

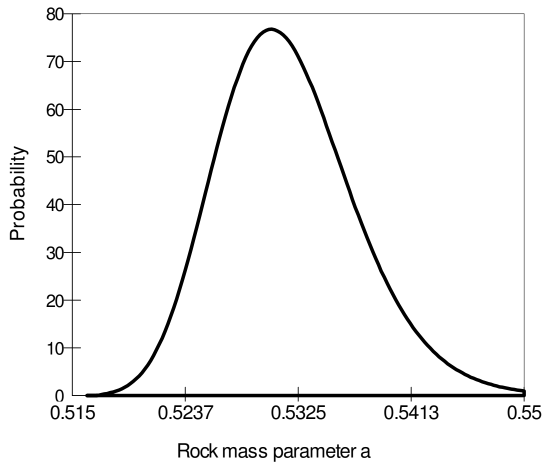

a – Mean 0.532, Stdev 0.00535

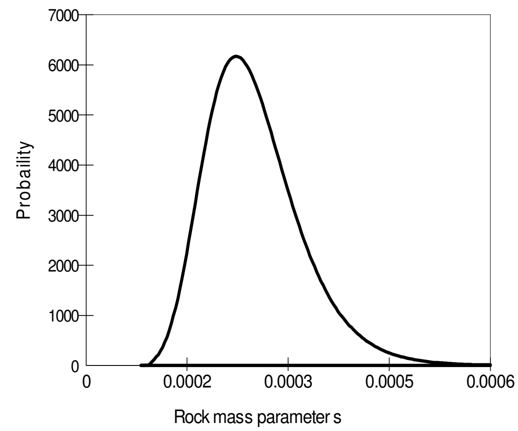

s – Mean 0.00025, Stdev 0.00007

Figure 13: Calculated distributions for rock mass parameters.

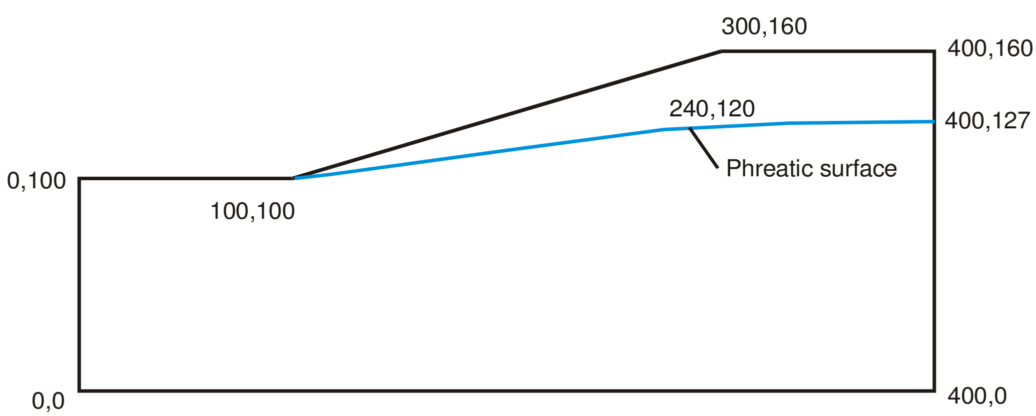

Figure 14: Slope and phreatic surface geometry for a homogeneous slope.

The distribution of the factor of safety is shown in Figure 15 and it was found that this is best represented by a beta distribution with a mean value of 2.998, a standard deviation of 0.385, a minimum value of 1.207 and a maximum value of 4.107. There is zero probability of failure for this slope as indicated by the minimum factor of safety of 1.207. All critical failure surface exit at the toe of the slope.

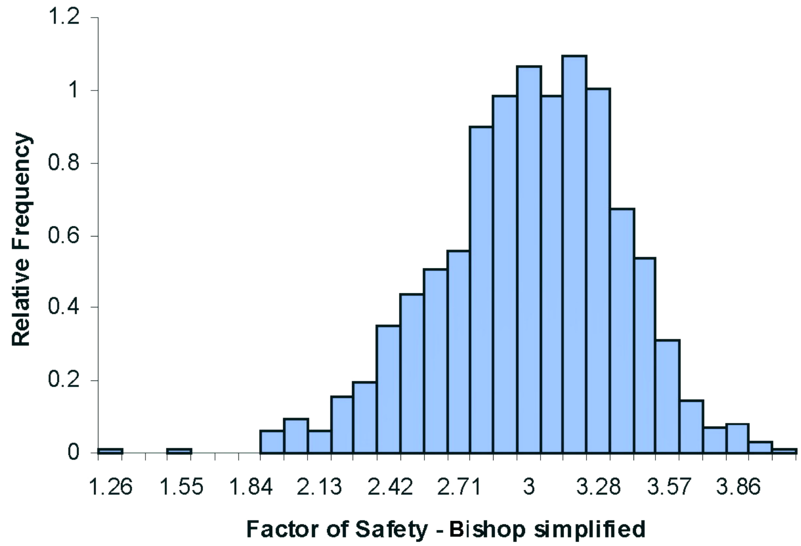

Figure 15: Distribution of factors of safety for the slope shown in Figure 14 from a probabilistic analysis using the program SLIDE.

Tunnel stability calculations

Consider a circular tunnel, illustrated in Figure 16, with a radius r_o in a stress field in which the horizontal and vertical stresses are both p_o. If the stresses are high enough, a 'plastic' zone of damaged rock of radius r_p surrounds the tunnel. A uniform support pressure p_i is provided around the perimeter of the tunnel.

A probabilistic analysis of the behaviour of this tunnel was carried out using the program RocSupport (available from www.rocscience.com) with the following input parameters:

Property	Distribution	Mean	Std. dev.	Min*	Max*
Tunnel radius r_o		5 m			
In situ stress p_o		2.5 MPa			
m_b	Normal	0.6894	0.1832	0.0086	1.44
s	Lognormal	0.0002498	0.0000707	0.0000886	0.000704
a	Normal	0.5317	0.00535	0.5171	0.5579
σ_{ci}	Normal	10 MPa	2.5 MPa	1 MPa	20 MPa
E		1050 MPa			

* Note that, in RocSupport, these values are input as values relative to the mean value and not as the absolute values shown here.

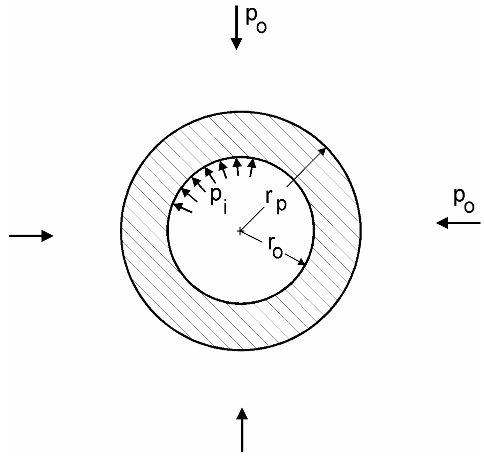

Figure 16: Development of a plastic zone around a circular tunnel in a hydrostatic stress field.

The resulting characteristic curve or support interaction diagram is presented in Figure 17. This diagram shown the tunnel wall displacements induced by progressive failure of the rock mass surrounding the tunnel as the face advances. The support is provided by a 5 cm shotcrete layer with 15 cm wide flange steel ribs spaced 1 m apart. The support is assumed to be installed 2 m behind the face after a wall displacement of 25 mm or a tunnel convergence of 50 mm has occurred. At this stage the shotcrete is assigned a 3 day compressive strength of 11 MPa.

The Factor of Safety of the support system is defined by the ratio of support capacity to demand as defined in Figure 17. The capacity of the shotcrete and steel set support is 0.4 MPa and it can accommodate a tunnel convergence of approximately 30 mm. As can be seen from Figure 17, the mobilised support pressure at equilibrium (where the characteristic curve and the support reaction curves cross) is approximately 0.15 MPa. This gives a first deterministic estimate of the Factor of Safety as 2.7.

The probabilistic analysis of the factor of safety yields the histogram shown in Figure 18. A Beta distribution is found to give the best fit to this histogram and the mean Factor of Safety is 2.73, the standard deviation is 0.46, the minimum is 2.23 and the maximum is 9.57.

This analysis is based on the assumption that the tunnel is circular, the rock mass is homogeneous and isotropic, the in situ stresses are equal in all directions and the support is placed as a closed circular ring. These assumptions are seldom valid for actual tunnelling conditions and hence the analysis described above should only be used as a first rough approximation in design. Where the analysis indicates that tunnel stability is likely to be a problem, it is essential that a more detailed numerical analysis, taking into account actual tunnel geometry and rock mass conditions, should be carried out.

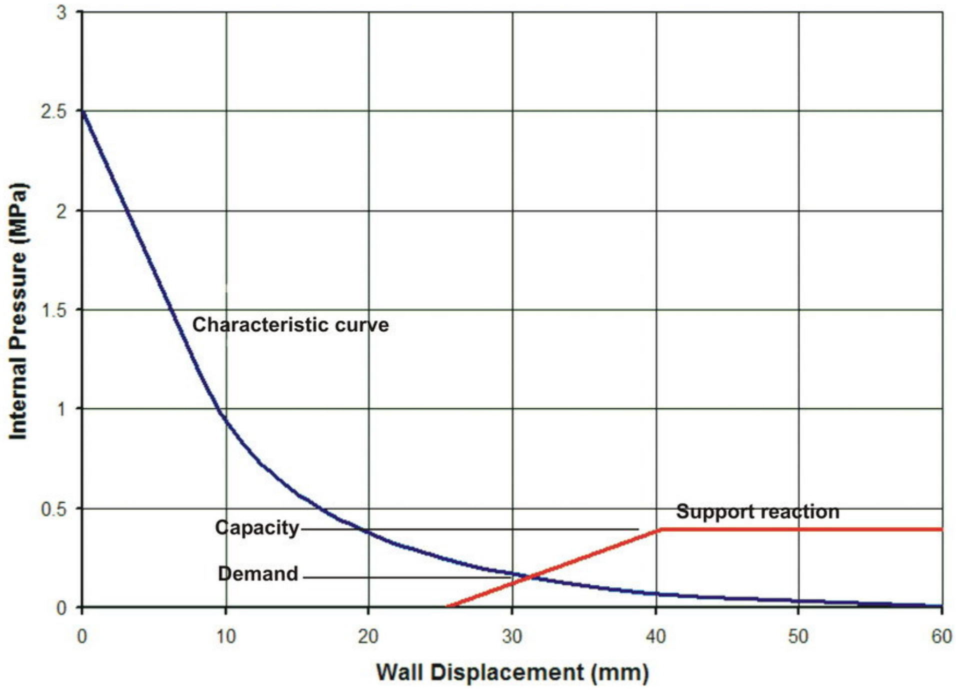

Figure 17: Rock support interaction diagram for a 10 m diameter tunnel subjected to a uniform in situ stress of 2.5 MPa.

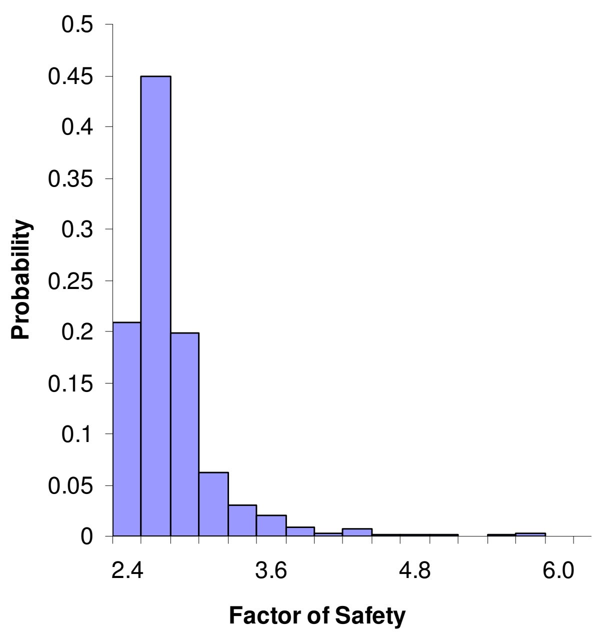

Figure 18: Distribution of the Factor of Safety for the tunnel discussed above.

Conclusions

The uncertainty associated with estimating the properties of in situ rock masses has a significant impact or the design of slopes and excavations in rock. The examples that have been explored in this section show that, even when using the 'best' estimates currently available, the range of calculated factors of safety are uncomfortably large. These ranges become alarmingly large when poor site investigation techniques and inadequate laboratory procedures are used.

Given the inherent difficulty of assigning reliable numerical values to rock mass characteristics, it is unlikely that 'accurate' methods for estimating rock mass properties will be developed in the foreseeable future. Consequently, the user of the Hoek-Brown procedure or of any other equivalent procedure for estimating rock mass properties should not assume that the calculations produce unique reliable numbers. The simple techniques described in this section can be used to explore the possible range of values and the impact of these variations on engineering design.

Practical examples of rock mass property estimates

The following examples are presented in order to illustrate the range of rock mass properties that can be encountered in the field and to give the reader some insight of how the estimation of rock mass properties was tackled in a number of actual projects.

Massive weak rock

Karzulovic and Diaz (1994) have described the results of a program of triaxial tests on a cemented breccia known as Braden Breccia from the El Teniente mine in Chile. In order to design underground openings in this rock, attempts were made to classify the rock mass in accordance with Bieniawski's RMR system. However, as illustrated in Figure 19, this rock mass has very few discontinuities and so assigning realistic numbers to terms depending upon joint spacing and condition proved to be very difficult. Finally, it was decided to treat the rock mass as a weak but homogeneous 'almost intact' rock, similar to a weak concrete, and to determine its properties by means of triaxial tests on large diameter specimens.

A series of triaxial tests was carried out on 100 mm diameter core samples, illustrated in Figure 20. The results of these tests were analysed by means of the regression analysis using the program RocLab[4]. Back analysis of the behaviour of underground openings in this rock indicate that the in-situ GSI value is approximately 75. From RocLab the following parameters were obtained:

---

[4] Available from www.rocscience.com as a free download

Intact rock strength	σ_{ci}	51 MPa	Hoek-Brown constant	m_b	6.675
Hoek-Brown constant	m_i	16.3	Hoek-Brown constant	s	0.062
Geological Strength Index	GSI	75	Hoek-Brown constant	a	0.501
			Deformation modulus	E_m	15000 MPa

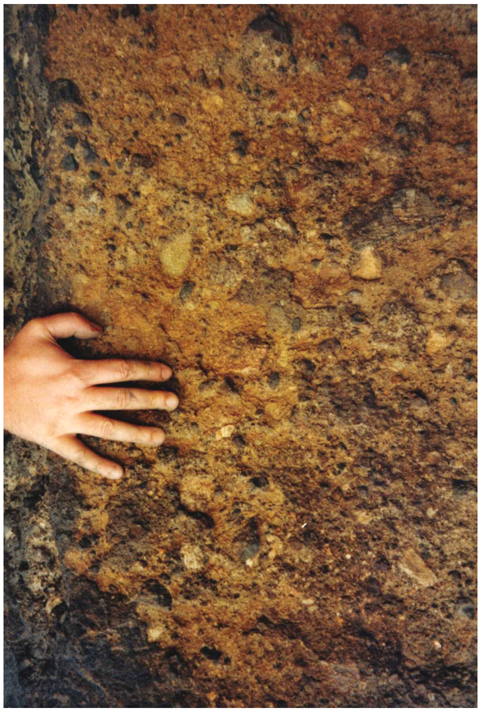

Figure 19: Braden Breccia at El Teniente Mine in Chile. This rock is a cemented breccia with practically no joints. It was dealt with in a manner similar to weak concrete and tests were carried out on 100 mm diameter specimens illustrated in Figure 20.

Fig. 20. 100 mm diameter by 200 mm long specimens of Braden Breccia from the El Teniente mine in Chile

Massive strong rock masses

The Rio Grande Pumped Storage Project in Argentina includes a large underground powerhouse and surge control complex and a 6 km long tailrace tunnel. The rock mass surrounding these excavations is massive gneiss with very few joints. A typical core from this rock mass is illustrated in Figure 21. The appearance of the rock at the surface was illustrated earlier in Figure 6, which shows a cutting for the dam spillway.

Figure 21: Excellent quality core with very few discontinuities from the massive gneiss of the Rio Grande project in Argentina.

Figure 21: Top heading of the 12 m span, 18 m high tailrace tunnel for the Rio Grande Pumped Storage Project.

The rock mass can be described as BLOCKY/VERY GOOD and the GSI value, from Table 5, is 75. Typical characteristics for the rock mass are as follows:

Intact rock strength	σ_{ci}	110 MPa	Hoek-Brown constant	m_b	11.46
Hoek-Brown constant	m_i	28	Hoek-Brown constant	s	0.062
Geological Strength Index	*GSI*	75	Constant	a	0.501
			Deformation modulus	E_m	45000 MPa

Figure 21 illustrates the 8 m high 12 m span top heading for the tailrace tunnel. The final tunnel height of 18 m was achieved by blasting two 5 m benches. The top heading was excavated by full-face drill and blast and, because of the excellent quality of the rock mass and the tight control on blasting quality, most of the top heading did not require any support.

Details of this project are to be found in Moretto et al (1993). Hammett and Hoek (1981) have described the design of the support system for the 25 m span underground powerhouse in which a few structurally controlled wedges were identified and stabilised during excavation.

Average quality rock mass

The partially excavated powerhouse cavern in the Nathpa Jhakri Hydroelectric project in Himachel Pradesh, India is illustrated in Figure 22. The rock is a jointed quartz mica schist, which has been extensively evaluated by the Geological Survey of India as described by Jalote et al (1996). An average GSI value of 65 was chosen to estimate the rock mass properties which were used for the cavern support design. Additional support, installed on the instructions of the Engineers, was placed in weaker rock zones.

The assumed rock mass properties are as follows:

Intact rock strength	σ_{ci}	30 MPa	Hoek-Brown constant	m_b	4.3
Hoek-Brown constant	m_i	15	Hoek-Brown constant	s	0.02
Geological Strength Index	*GSI*	65	Constant	a	0.5
			Deformation modulus	E_m	10000 MPa

Two and three dimensional stress analyses of the nine stages used to excavate the cavern were carried out to determine the extent of potential rock mass failure and to provide guidance in the design of the support system. An isometric view of one of the three dimensional models is given in Figure 23.

Figure 22: Partially completed 20 m span, 42.5 m high underground powerhouse cavern of the Nathpa Jhakri Hydroelectric Project in Himachel Pradesh, India. The cavern is approximately 300 m below the surface.

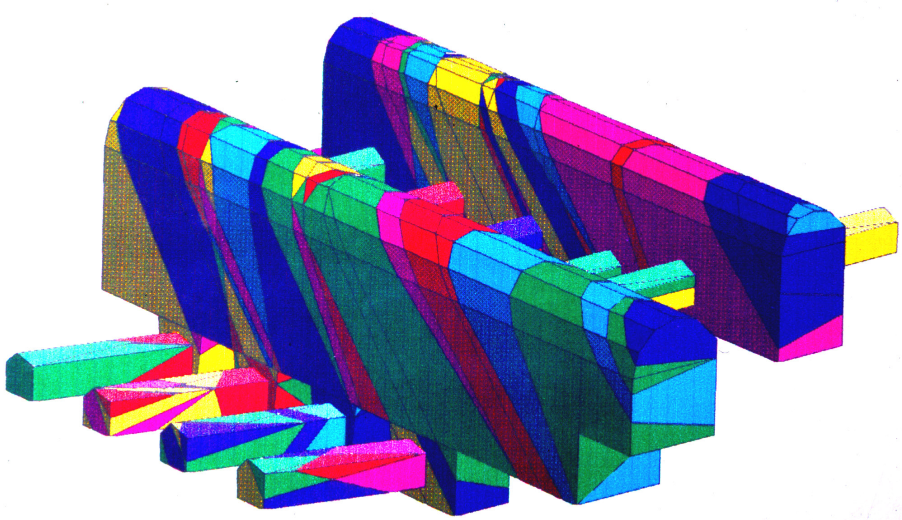

Figure 23: Isometric view of the 3DEC5 model of the underground powerhouse cavern and transformer gallery of the Nathpa Jhakri Hydroelectric Project, analysed by Dr. B. Dasgupta[6].

[5] Available from ITASCA Consulting Group Inc, 111 Third Ave. South, Minneapolis, Minnesota 55401, USA.

[6] Formerly at the Institute of Rock Mechanics (Kolar), Kolar Gold Fields, Karnataka.

The support for the powerhouse cavern consists of rockbolts and mesh reinforced shotcrete. Alternating 6 and 8 m long 32 mm diameter bolts on 1 x 1 m and 1.5 x 1.5 m centres are used in the arch. Alternating 9 and 7.5 m long 32 mm diameter bolts were used in the upper and lower sidewalls with alternating 9 and 11 m long 32 mm rockbolts in the centre of the sidewalls, all at a grid spacing of 1.5 m. Shotcrete consists of two 50 mm thick layers of plain shotcrete with an interbedded layer of weldmesh. The support provided by the shotcrete was not included in the support design analysis, which relies upon the rockbolts to provide all the support required.

In the headrace tunnel, some zones of sheared quartz mica schist have been encountered and these have resulted in large displacements as illustrated in Figure 24. This is a common problem in hard rock tunnelling where the excavation sequence and support system have been designed for 'average' rock mass conditions. Unless very rapid changes in the length of blast rounds and the installed support are made when an abrupt change to poor rock conditions occurs, for example when a fault is encountered, problems with controlling tunnel deformation can arise.

Figure 24: Large displacements in the top heading of the headrace tunnel of the Nathpa Jhakri Hydroelectric project. These displacements are the result of deteriorating rock mass quality when tunnelling through a fault zone.

The only effective way to anticipate this type of problem is to keep a probe hole ahead of the advancing face at all times. Typically, a long probe hole is percussion drilled during a maintenance shift and the penetration rate, return water flow and chippings are constantly monitored during drilling. Where significant problems are indicated by this percussion drilling, one or two diamond-drilled holes may be required to investigate these problems in more detail. In some special cases, the use of a pilot tunnel may be more effective in that it permits the ground properties to be defined more accurately than is possible with probe hole drilling. In addition, pilot tunnels allow pre-drainage and pre-reinforcement of the rock ahead of the development of the full excavation profile.

Poor quality rock mass at shallow depth

Kavvadas et al (1996) have described some of the geotechnical issues associated with the construction of 18 km of tunnels and the 21 underground stations of the Athens Metro. These excavations are all shallow with typical depths to tunnel crown of between 15 and 20 m. The principal problem is one of surface subsidence rather than failure of the rock mass surrounding the openings.

The rock mass is locally known as Athenian schist which is a term used to describe a sequence of Upper Cretaceous flysch-type sediments including thinly bedded clayey and calcareous sandstones, siltstones (greywackes), slates, shales and limestones. During the Eocene, the Athenian schist formations were subjected to intense folding and thrusting. Later extensive faulting caused extensional fracturing and widespread weathering and alteration of the deposits.

The GSI values range from about 15 to about 45. The higher values correspond to the intercalated layers of sandstones and limestones, which can be described as BLOCKY/DISTURBED and POOR (Table 5). The completely decomposed schist can be described as DISINTEGRATED and VERY POOR and has GSI values ranging from 15 to 20. Rock mass properties for the completely decomposed schist, using a GSI value of 20, are as follows:

Intact rock strength - MPa	σ_{ci}	5-10	Hoek-Brown constant	m_b	0.55
Hoek-Brown constant	m_i	9.6	Hoek-Brown constant	s	0.0001
Geological Strength Index	GSI	20	Hoek-Brown constant	a	0.544
			Deformation modulus MPa	E_m	600

The Academia, Syntagma, Omonia and Olympion stations were constructed using the New Austrian Tunnelling Method twin side drift and central pillar method as illustrated in Figure 25. The more conventional top heading and bench method, illustrated in Figure 26, was used for the excavation of the Ambelokipi station. These stations are all 16.5 m wide and 12.7 m high. The appearance of the rock mass in one of the Olympion station side drift excavations is illustrated in Figures 27 and 28.

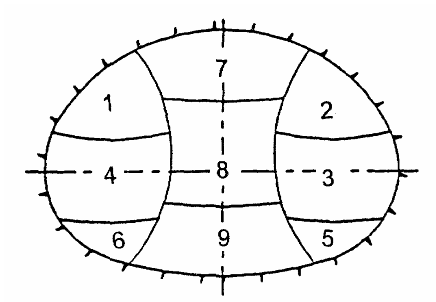

Figure 25: Twin side drift and central pillar excavation method. Temporary support consists of double wire mesh reinforced 250 - 300 mm thick shotcrete shells with embedded lattice girders or HEB 160 steel sets at 0.75 - 1 m spacing.

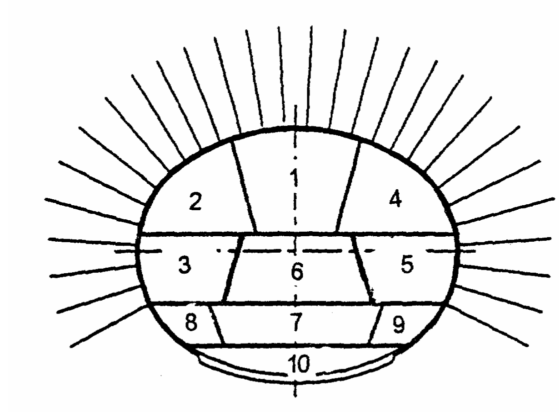

Figure 26: Top heading and bench method of excavation. Temporary support consists of a 200 mm thick shotcrete shell with 4 and 6 m long untensioned grouted rockbolts at 1.0 - 1.5 m spacing

Figure 27: Side drift in the Athens Metro Olympion station excavation that was excavated by the method illustrated in Figure 25. The station has a cover depth of approximately 10 m over the crown.

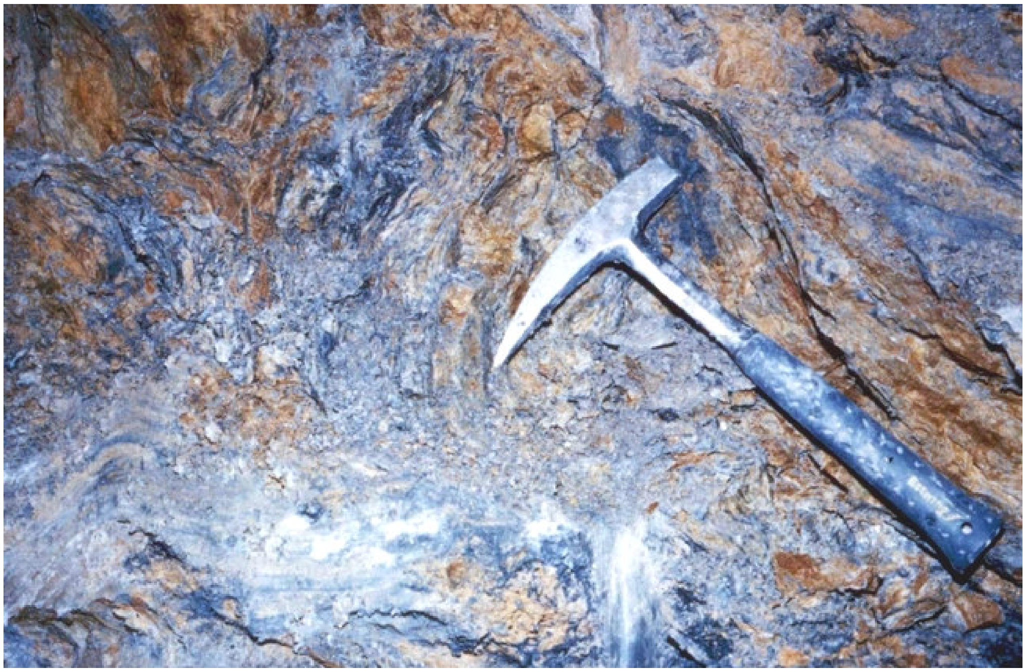

Figure 28: Appearance of the very poor quality Athenian Schist at the face of the side heading illustrated in Figure 27.

Numerical analyses of the two excavation methods showed that the twin side drift method resulted in slightly less rock mass failure in the crown of the excavation. However, the final surface displacements induced by the two excavation methods were practically identical.

Maximum vertical displacements of the surface above the centre-line of the Omonia station amounted to 51 mm. Of this, 28 mm occurred during the excavation of the side drifts, 14 mm during the removal of the central pillar and a further 9 mm occurred as a time dependent settlement after completion of the excavation. According to Kavvadas et al (1996), this time dependent settlement is due to the dissipation of excess pore water pressures which were built up during excavation. In the case of the Omonia station, the excavation of recesses towards the eastern end of the station, after completion of the station excavation, added a further 10 to 12 mm of vertical surface displacement at this end of the station.

Poor quality rock mass under high stress

The Yacambú Quibor tunnel in Venezuela is considered to be one of the most difficult tunnels in the world. This 25 km long water supply tunnel through the Andes is being excavated in sandstones and phyllites at depths of up to 1200 m below surface. The graphitic phyllite is a very poor quality rock and gives rise to serious squeezing problems which, without adequate support, result in complete closure of the tunnel. A full-face tunnel-boring machine was completely destroyed in 1979 when trapped by squeezing ground conditions.

The graphitic phyllite has an average unconfined compressive strength of about 50 MPa and the estimated GSI value is about 25 (see Figures 2 and 3). Typical rock mass properties are as follows:

Intact rock strength MPa	σci	50	Hoek-Brown constant	m_b	0.481
Hoek-Brown constant	mi	10	Hoek-Brown constant	s	0.0002
Geological Strength Index	GSI	25	Hoek-Brown constant	a	0.53
			Deformation modulus MPa	E_m	1000

Various support methods have been used on this tunnel and only one will be considered here. This was a trial section of tunnel, at a depth of about 600 m, constructed in 1989. The support of the 5.5 m span tunnel was by means of a complete ring of 5 m long, 32 mm diameter untensioned grouted dowels with a 200 mm thick shell of reinforced shotcrete. This support system proved to be very effective but was later abandoned in favour of yielding steel sets (steel sets with sliding joints) because of construction schedule considerations. In fact, at a depth of 1200 m below surface (2004-2006) it is doubtful if the rockbolts would have been effective because of the very large deformations that could only be accommodated by steel sets with sliding joints.

Examples of the results of a typical numerical stress analysis of this trial section, carried out using the program PHASE2[7], are given in Figures 29 and 30. Figure 29 shows the extent of failure, with and without support, while Figure 30 shows the displacements in the rock mass surrounding the tunnel. Note that the criteria used to judge the effectiveness of the support design are that the zone of failure surrounding the tunnel should lie within the envelope of the rockbolt support, the rockbolts should not be stressed to failure and the displacements should be of reasonable magnitude and should be uniformly distributed around the tunnel. All of these objectives were achieved by the support system described earlier.

Slope stability considerations

When dealing with slope stability problems in rock masses, great care has to be taken in attempting to apply the Hoek-Brown failure criterion, particularly for small steep slopes. As illustrated in Figure 31, even rock masses that appear to be good candidates for the application of the criterion can suffer shallow structurally controlled failures under the very low stress conditions which exist in such slopes.

[7] Avaialble from www.rocscience.com.

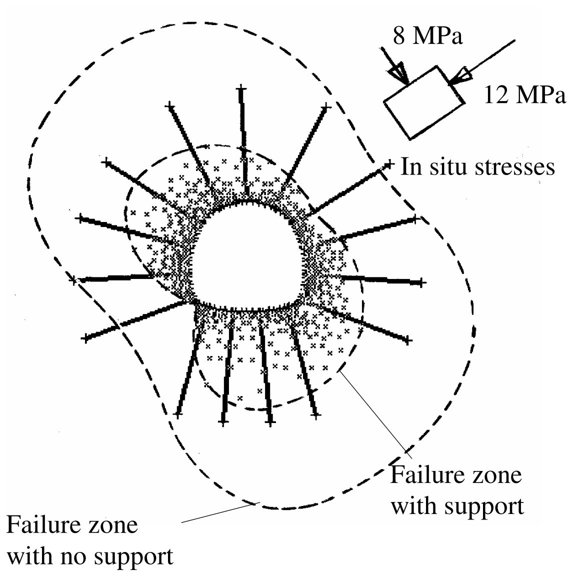

Figure 29: Results of a numerical analysis of the failure of the rock mass surrounding the Yacambu-Quibor tunnel when excavated in graphitic phyllite at a depth of about 600 m below surface.

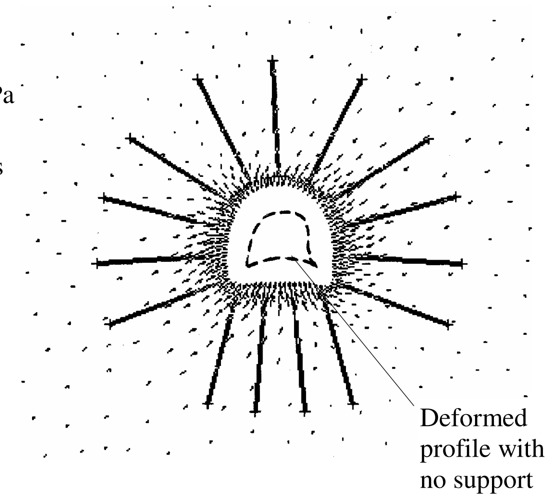

Figure 30: Displacements in the rock mass surrounding the Yacambu-Quibor tunnel. The maximum calculated displacement is 258 mm with no support and 106 mm with support.

As a general rule, when designing slopes in rock, the initial approach should always be to search for potential failures controlled by adverse structural conditions. These may take the form of planar failures on outward dipping features, wedge failures on intersecting features, toppling failures on inward dipping failures or complex failure modes involving all of these processes. Only when the potential for structurally controlled failures has been eliminated should consideration be given to treating the rock mass as an isotropic material as required by the Hoek-Brown failure criterion.

Figure 32 illustrates a case in which the base of a slope failure is defined by an outward dipping fault that does not daylight at the toe of the slope. Circular failure through the poor quality rock mass overlying the fault allows failure of the toe of the slope. Analysis of this problem was carried out by assigning the rock mass at the toe properties that had been determined by application of the Hoek-Brown criterion. A search for the critical failure surface was carried out utilising the program SLIDE which allows complex failure surfaces to be analysed and which includes facilities for the input of the Hoek-Brown failure criterion.

Figure 31: Structurally controlled failure in the face of a steep bench in a heavily jointed rock mass.

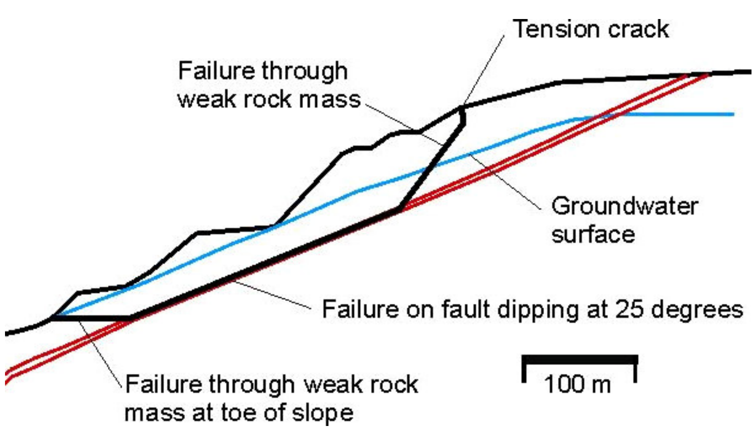

Figure 32: Complex slope failure controlled by an outward dipping basal fault and circular failure through the poor quality rock mass overlying the toe of the slope.

References

Balmer, G. 1952. A general analytical solution for Mohr's envelope. *Am. Soc. Test. Mat.* **52**, 1260-1271.

Bieniawski, Z.T. 1976. Rock mass classification in rock engineering. *In Exploration for rock engineering, proc. of the symp*., (ed. Z.T. Bieniawski) **1**, 97-106. Cape Town: Balkema.

Bieniawski, Z.T. 1989. *Engineering rock mass classifications*. New York: Wiley.

Deere D.U. 1968. Chapter 1: Geological considerations. *In Rock Mechanics in Engineering Practice* (eds. Stagg K.G. and Zienkiewicz, O.C.), 1-20. London: John Wiley and Sons.

Franklin, J.A. and Hoek, E. 1970. Developments in triaxial testing equipment. *Rock Mech*. **2**, 223-228. Berlin: Springer-Verlag.

Hammett, R.D. and Hoek, E. 1981. Design of large underground caverns for hydroelectric projects, with reference to structurally controlled failure mechanisms. *Proc. American Soc. Civil Engrs. Int. Conf. on recent developments in geotechnical engineering for hydro projects.* 192-206. New York: ASCE

Hoek, E. 1983. Strength of jointed rock masses, 23rd. Rankine Lecture. *Géotechnique* **33**(3), 187-223.

Hoek, E. 1994. Strength of rock and rock masses, *ISRM News J*, **2**(2), 4-16.

Hoek, E. and Brown, E.T. 1980a. *Underground excavations in rock*. London: Instn Min. Metall.

Hoek, E. and Brown, E.T. 1980b. Empirical strength criterion for rock masses. *J. Geotech. Engng Div*., ASCE **106**(GT9), 1013-1035.

Hoek, E. and Brown, E.T. 1988. The Hoek-Brown failure criterion - a 1988 update. In Rock engineering for underground excavations, proc. *15th Canadian rock mech. symp*., (ed. J.C. Curran), 31-38. Toronto: Dept. Civ. Engineering, University of Toronto.

Hoek, E., Marinos, P. and Benissi, M. 1998. Applicability of the Geological Strength Index (GSI) classification for very weak and sheared rock masses. The case of the Athens Schist Formation. *Bull. Engng. Geol. Env.* **57**(2), 151-160.

Hoek, E. and Brown, E.T. 1997. Practical estimates or rock mass strength. Int. *J. Rock Mech. Min.g Sci. & Geomech. Abstr.*. **34**(8), 1165-1186.

Hoek, E., Kaiser, P.K. and Bawden. W.F. 1995. *Support of underground excavations in hard rock*. Rotterdam: Balkema.

Hoek, E., Wood, D. and Shah, S. 1992. A modified Hoek-Brown criterion for jointed rock masses. Proc. *rock characterization, symp. Int. Soc. Rock Mech.: Eurock '92*, (ed. J.A. Hudson), 209-214. London: Brit. Geol. Soc.

Hoek E, Carranza-Torres CT, Corkum B. Hoek-Brown failure criterion-2002 edition. In*: Proceedings of the 5th North American Rock Mechanics Symp.*, Toronto, Canada, 2002: **1**: 267–73.

Hoek, E., Marinos, P., Marinos, V. 2005. Characterization and engineering properties of tectonically undisturbed but lithologically varied sedimentary rock masses. *Int. J. Rock Mech. Min. Sci.*, **42/**2, 277-285

Hoek, E and Diederichs, M. 2006. Empirical estimates of rock mass modulus*. Int. J Rock Mech. Min. Sci*., **43**, 203–215

Karzulovic A. and Díaz, A.1994. Evaluación de las Propiedades Geomacánicas de la Brecha Braden en Mina El Teniente. *Proc. IV Congreso Sudamericano de Mecanica de Rocas, Santiago* **1**, 39-47.

Kavvadas M., Hewison L.R., Lastaratos P.G., Seferoglou, C. and Michalis, I. 1996.Experience in the construction of the Athens Metro. *Proc. Int. symp. geotechical aspects of underground construction in soft ground.* (Eds Mair R.J. and Taylor R.N.), 277-282. London: City University.

Jalote, P.M., Kumar A. and Kumar V. 1996. Geotechniques applied in the design of the machine hall cavern, Nathpa Jhakri Hydel Project, N.W. Himalaya, India. *J. Engng Geol. (India)* XXV(1-4), 181-192.

Marinos, P, and Hoek, E. 2001 – Estimating the geotechnical properties of heterogeneous rock masses such as flysch. *Bull. Enginng Geol. & the Environment* (IAEG), **60**, 85-92

Marinos, P., Hoek, E., Marinos, V. 2006. Variability of the engineering properties of rock masses quantified by the geological strength index: the case of ophiolites with special emphasis on tunnelling. *Bull. Eng. Geol. Env.,* **65/**2, 129-142.

Moretto O., Sarra Pistone R.E. and Del Rio J.C. 1993. A case history in Argentina - Rock mechanics for underground works in the pumping storage development of Rio Grande No 1. *In Comprehensive Rock Engineering*. (Ed. Hudson, J.A.) **5**, 159-192. Oxford: Pergamon.

Palmstrom A. and Singh R. 2001.The deformation modulus of rock masses: comparisons between in situ tests and indirect estimates. *Tunnelling and Underground Space Technology*. **16**: 115-131.

Salcedo D.A.1983. Macizos Rocosos: Caracterización, Resistencia al Corte y Mecanismos de Rotura. *Proc. 25 Aniversario Conferencia Soc. Venezolana de Mecánica del Suelo e Ingeniería de Fundaciones*, Caracas. 143-172.